



Universidad  
del País Vasco Euskal Herriko  
Unibertsitatea

NAZIOARTEKO  
BIKAITASUN  
CAMPUSA  
CAMPUS DE  
EXCELENCIA  
INTERNACIONAL

# DEVELOPMENT AND EVALUATION OF NON-VIRAL GENE DELIVERY VECTORS AND THEIR COMBINATION WITH HYDROGEL SCAFFOLD TECHNOLOGY

# **GENE-GARRAIO EZ-BIRALERAKO BEKTOREEN GARAPENA ETA EBALUAZIOA ETA HORIEN KONBINAKETA HIDROGELEN TEKNOLOGIAREKIN**

# **DESARROLLO Y EVALUACIÓN DE VECTORES NO-VIRALES PARA TERAPIA GÉNICA Y SU COMBINACIÓN CON LA TECNOLOGÍA DE HIDROGELES**

ANE ILIA VILLATE BEITIA

NanoBioCel Group, Laboratory of Pharmaceutics

University of the Basque Country (UPV/EHU)

Vitoria-Gasteiz

June 2018



## **ACKNOWLEDGEMENTS / ESKERRAK / AGRADECIMIENTOS**

*Badira lau urte Bidarteko kongresu batean nire tesi-zuzendariak izango zirenak ezagutu nituela, eta orduan hasitako bidean zehar emandako laguntza eta konfiantza eskertu nahi nieke. José Luis, muchas gracias por brindarme la oportunidad de formar parte de este grupo de investigación. Jon, eskerrik asko zure aholkuengatik eta beti nire formakuntza aberasteko jardueretan parte hartzera animatzeagatik. Gustavo, mila esker bide guztian zehar nire ondoan egoteagatik eta edozein proiektu aurrera ateratzeko erakutsitako indarragatik. Asko ikasi dut hirurongandik eta oso pozgarria izan da zuekin lan egitea.*

*Jakina, eskerrik asko laborategiko jende guztiari elkarrekin pasatako une politengatik. Egindako barreek eta elkarri emandako laguntzak beti aurrera egiteko indarra eman didate.*

*Eta mila esker baita ere tesian zehar ezagutu ditudan ikertalde guztiei. Muchas gracias a los compañeros de la Universidad Miguel Hernández de Elche, siempre es un placer trabajar con vosotros. Thank you so much Prof. Tatiana Segura for giving me the opportunity to be part of your research group and to all members from Segura Lab for making my stay at UCLA an unforgettable experience.*

*Azkenik, eskerrik asko bihotzez nire ikerketa-ibilbide guztian zehar hor egon zaretenoi. Gurasoei, neure printzipioei eusten erakusteagatik. Kermani, beti nigan sinesteagatik. Eta, noski, Javiri, nire lanean eta etorkizunean konfiantza osoa izateagatik.*

## **ACKNOWLEDGEMENT FOR THE FINANCIAL SUPPORT**

*This thesis has been partially supported by the Basque Government (Department of Education, University and Research, predoctoral grant PRE\_2016\_2\_0302 and Consolidated Groups, IT907-16), the University of the Basque Country (UPV/EHU) (UFI 11/32) and the Spanish Ministry of Education (Grant SAF2013-42347-R). Authors wish to thank the intellectual and technical assistance from the ICTS “NANBIOSIS”, more specifically by the Drug Formulation Unit (U10) of the CIBER in Bioengineering, Biomaterials and Nanomedicine (CIBER-BBN) at the University of the Basque Country (UPV/EHU). Ane Ibia Villate Beitia gratefully acknowledges the support provided by the Basque Government for the fellowship grant.*

## **ACKNOWLEDGMENT TO THE EDITORIALS**

*Authors would like to thank the editorials for granting permission to reuse their previously published articles in this thesis.*

Have no fear of perfection,  
you'll never reach it.

*Marie Curie*



## TABLE OF CONTENTS

<b>Introduction / Sarrera / Introducción .....</b>	<b>15</b>
First Insights into Non-invasive Administration Routes for Non-viral Gene Therapy.....	17
Gene-terapia ez-birala eman-bide ez-inbaditzailak erabiliz .....	53
<b>Objectives / Helburuak / Objetivos .....</b>	<b>93</b>
<b>Experimental section / Atal experimentala / Sección experimental ..</b>	<b>107</b>
Chapter 1: Non-viral Vectors Based on Magnetoplexes, Lipoplexes and Polyplexes for VEGF Gene Delivery into Central Nervous System Cells .....	109
Chapter 2: Polysorbate 20 non-ionic surfactant enhances retinal gene delivery of non-viral vectors based on cationic niosomes after intravitreal and subretinal administration .....	135
Chapter 3: Non-viral vectors based on cationic niosomes and minicircle DNA technology enhance gene delivery efficiency for biomedical applications in retinal disorders .....	161
Chapter 4: Hyaluronic acid hydrogels loaded with cationic niosomes for efficient non-viral gene delivery.....	183
<b>Discussion / Eztabaidea/ Discusión .....</b>	<b>203</b>
<b>Conclusions / Ondorioak / Conclusiones .....</b>	<b>327</b>

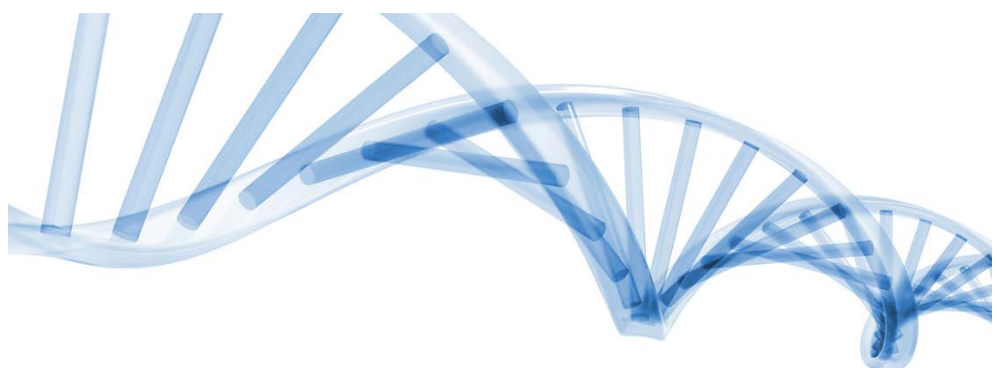
**Note:**

*For high quality images refer to the electronic version*

*Kalitate altuko irudietarako bertsio elektronikoa konsultatu*

*Para imágenes de alta calidad consultar la versión electrónica*





***Introduction***

**Sarrera**

***Introducción***



# **First Insights into Non-invasive Administration Routes for Non-viral Gene Therapy**

*Published in Gene Therapy. Principles and Challenges (InTech) (2015)*

*Ilia Villate-Beitia, Gustavo Puras, Jon Zarate, Mireia Agirre, Edilberto Ojeda and Jose Luis Pedraz (November 26th 2015). First Insights into Non-invasive Administration Routes for Non-viral Gene Therapy, Gene Therapy Doaa Hashad, IntechOpen, DOI: 10.5772/61060.*

*Available from: <https://www.intechopen.com/books/gene-therapy-principles-and-challenges/first-insights-into-non-invasive-administration-routes-for-non-viral-gene-therapy>*



## *Introduction*

# **First Insights into Non-invasive Administration Routes for Non-viral Gene Therapy.**

*Ilia Villate<sup>a,b</sup>, Gustavo Puras<sup>a,b</sup>, Jon Zarate<sup>a,b</sup>, Mireia Agirre<sup>a,b</sup>, Edilberto Ojeda<sup>a,b</sup>, Jose Luis Pedraz<sup>a,b,\*</sup>.*

*<sup>a</sup> NanoBioCel Group, Laboratory of Pharmaceutics, School of Pharmacy, University of the Basque Country (UPV/EHU), Paseo de la Universidad 7, 01006, Vitoria-Gasteiz, Spain*

*<sup>b</sup> Biomedical Research Networking Center in Bioengineering, Biomaterials and Nanomedicine (CIBER-BBN), Vitoria-Gasteiz, Spain*

---

**Abstract:** Gene delivery has attracted increasing interest as a highly promising therapeutic method to treat various diseases, including both genetic and acquired disorders. However, its clinical application is still hampered by the lack of safe and effective gene delivery techniques, as well as by the need of non-invasive routes of administration in gene delivery platforms. Among the different approaches used to transport nucleic acids into target cells, non-viral vectors represent promising and safer alternatives to viruses. Non-invasive administration routes are currently being studied, such as intranasal administration to target the brain, topical retinal administration for ocular diseases and aerosolized formulations for inhalation for the treatment of pulmonary diseases. Reasonable evidence suggests that future gene delivery systems might be based on effective non-viral vectors administered through non-invasive routes, which would constitute a safe, easy to produce, cheap and customizable alternative to the current viral gene delivery platforms. In this review, after briefly introducing the basis of gene therapy, we discuss the up-to-date and possible future strategies to improve DNA transfection efficiency using non-viral vectors and focusing on the non-invasive routes of administration.

**Keywords:** gene therapy, non-viral vector, intra- and extracellular barriers, non-invasive routes of administration.

## *Introduction*

### **INTRODUCTION**

#### **1.1 Concept and historical evolution of gene therapy**

Gene therapy can be broadly defined as the introduction of genetic material into target cells in order to modify and control protein expression for therapeutic or experimental purposes [1]. Nowadays, the culmination of the Human Genome Project along with recent advances on molecular biology have provided a better understanding of cellular and pathogenic processes, and several genes have been identified as targets for therapeutic approaches. Additionally, the constant advance in the development of gene carriers for the delivery of nucleic acids into target cells has led to conceiving new therapeutic strategies for the treatment of pathologies by genetic and cell-based approaches, collectively known as gene therapy [1].

Researchers have been working for decades to bring gene therapy to the clinic, but very few patients have received an effective gene-therapy treatment. The potential of gene therapy in medical applications was recognized soon after the discovery of DNA as genetic material, and the concept of gene therapy arose during the 1960s and 1970s [2]. The first success of gene therapy on humans arrived in 1990, it was performed by researchers at the National Institute of Health, and the treated disease was a form of severe combined immune deficiency (SCID) due to defects in the gene encoding adenosine deaminase (ADA) [3]. However, a fatal event in 1991 raised serious concerns about gene therapy. An eighteen-year-old boy died as a result of his voluntary participation in a gene therapy trial, becoming the first known human victim of this technology [4]. The Food and Drug Administration (FDA) investigation concluded that the scientists involved in the trial did not foresee serious side effects or fatality and that they did not follow the federal rules to ensure the safety of the participants [4]. This tragic case caused a severe setback in the research field of gene therapy.

According to data updated to June 2014 and presented by The Journal of Gene Medicine [5], since the onset of the first gene therapy clinical trial in 1989, more than 2000 new clinical trials for gene therapy have been approved globally (Figure 1). As shown in Figure 2, these trials address the most challenging diseases of today, that is, cancer (64.1% of approved trials), monogenic diseases (9.1%) such as cystic fibrosis, infectious diseases (8.2%) and cardiovascular diseases (7.8%). Although in a lesser extent, neurological diseases (1.8%) and ocular diseases (1.6%) are also subject to clinical trials with gene therapy. However, despite the intensive study

## *Introduction*

during the last few years, at present only 0.1% of all the gene therapy products approved for clinical trials have arrived to the phase IV (Figure 3). In 2012, the European Medicine Agency approved for the first time a gene therapy product, Glybera, an adeno-associated viral vector engineered to express lipoprotein lipase in the muscle for the treatment of lipoprotein lipase deficiency [5].

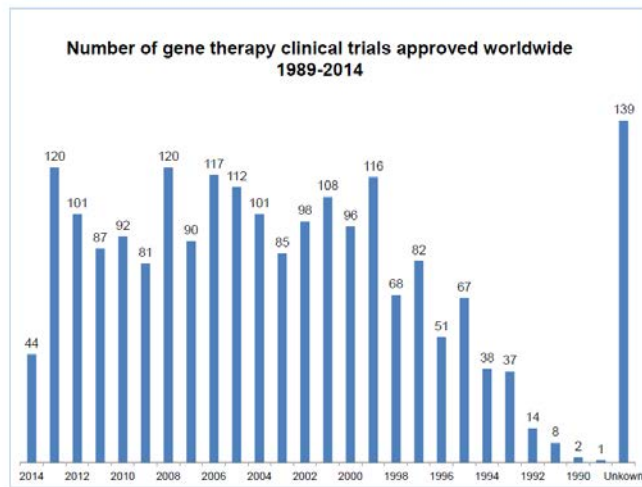


**Figure 1.** Number of gene therapy clinical trials approved worldwide 1989-2014.(adapted from <http://www.wiley.co.uk/genmed/clinical>).

### **1.2 The need of carriers**

One of the main reasons why gene therapy clinical trials are still few in number is the lack of suitable and safe approaches to deliver the genetic material to target cells. The success of gene therapy critically depends on suitable transfection vectors, which should be able to: (i) protect nucleic acids against degradation by blood and interstitial nucleases, (ii) promote internalization of the genetic material into target cells and (iii) release the nucleic acids once inside the cell to the correct site [1]. Furthermore, an ideal gene delivery system should be effective, specific, long lasting, safe, easy to use and as inexpensive as possible [6]. Broadly, gene delivery vectors are mainly classified into two categories: viral vectors and non-viral vectors. According to data updated to June 2014 and presented by The Journal of Gene

## *Introduction*

Medicine [7], among the over 2,000 clinical trials for gene therapy approved globally nowadays, 70% correspond to trials using viral vectors. As shown in Figure 4, there is a 17.7% of the gene therapy clinical trials that use naked DNA, and 5.3% of trials use lipofection [7].

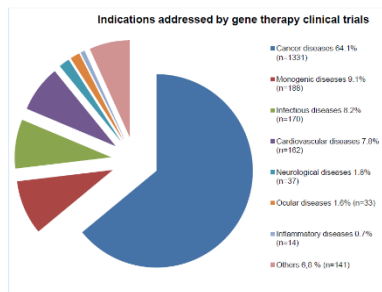


**Figure 2.** Indications addressed by gene therapy clinical trials. (adapted from <http://www.wiley.co.uk/genmed/clinical>).

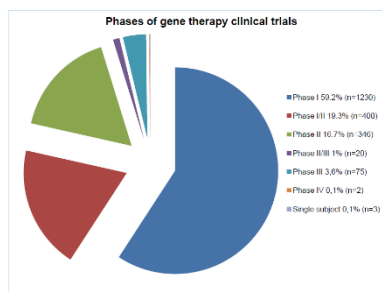


**Figure 3.** Phases of gene therapy clinical trials. (adapted from <http://www.wiley.co.uk/genmed/clinical>).

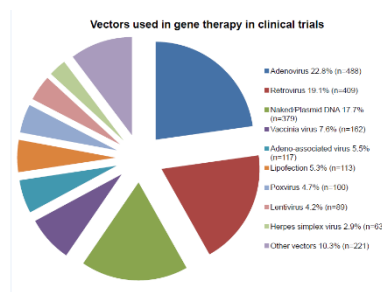


**Figure 4.** Vectors used in gene therapy in clinical trials (adapted from <http://www.wiley.co.uk/genmed/clinical>).

## *Introduction*

Despite the still absolute predominance of viral vector based gene delivery platforms – which is due to their higher transfection efficiency- in clinical trials, non-viral vectors represent promising and safer alternatives to viruses. In addition, non-invasive routes of administration for gene delivery systems are currently being studied, such as intranasal administration to target the brain, topical administration on the surface of the eye to treat retinal inherited diseases and aerosolized formulations for inhalation for the treatment of pulmonary diseases. There is reasonable hope to suggest that future gene delivery systems might be based on effective non-viral vectors administered through non-invasive routes and that they would constitute a safe, easy to produce, cheap and customizable alternative to gene delivery platforms. Moreover, it is increasingly accepted that future gene delivery platforms may be based on multifunctional vectors specifically tailored for different applications [1].

### **1.2.1 Viral vectors**

In this review we will focus on non-viral vector based strategies for gene delivery platforms, but we will briefly discuss the most relevant aspects of viral gene therapy. Viruses are highly evolved biological machines that efficiently gain access into host cells, deliver their genetic material to cells and exploit the cellular machinery to facilitate their replication [8]. Therefore, viruses represent an excellent platform for the development of recombinant vectors containing foreign genes for gene delivery purposes [1]. However, viral vectors also present many impediments such as the low carrying capacity, the expensive and complex production and, most importantly, safety issues, since they can induce oncogenesis when randomly integrated in the host genome. In addition, the human immune system recognizes and combats viruses, shortening their effectiveness [1]. Table 1 summarizes the principal viral vectors used in gene therapy, as well as their main utilities and impediments. Viral vectors are, therefore, powerful tools but present important drawbacks for clinical use in humans.

## *Introduction*

Viral vector	Integrative/ Episomal	Utility	Impediments
Adenovirus	Episomal	- Very efficient transfection in most tissues	- Induces inflammatory response
Adeno-associated virus (AAV)	Episomal (>90%)	- Not inducing inflammatory response	- Limited nucleic acid carrying capacity (<5 kb)
Retrovirus	Integrative	- Persistent gene expression	- Only transfets dividing cells - Risk of insertional mutagenesis
Lentivirus	Integrative	- Broad tropism - Persistent gene expression	- Risk of insertional mutagenesis
Herpes Simplex Virus-1 (HSV-1)	Episomal	- Large nucleic acid carrying capacity (up to 150 kb)	- Induces inflammatory response

**Table 1.** Principal viral vectors used in gene therapy, advantages and drawbacks. Based on [8].

### **1.2.2. Non-viral vectors**

Non-viral vectors have emerged as a safer, cheaper and easier to produce alternative to viral vectors. In fact, non-viral vectors can be produced on a large scale with high reproducibility and acceptable costs, they are relatively stable to storage, they can be administered repeatedly with no or little immune response and the dimension of the genetic material they can carry is practically unlimited [1,9]. Nevertheless, the employment of non-viral gene delivery vectors still strongly limited by their lower transfection efficiency as compared to viral vectors [1].

Non-viral vectors can be classified into two main categories depending on whether they are based on physical methods or on chemical methods. We will briefly review the most commonly employed non-viral DNA delivery systems for each category.

#### **1.2.1.1 Physical methods**

Physical methods for gene delivery purposes usually employ physical force to create transient membrane holes to cross the cell membrane and enhance gene transfer

## *Introduction*

[6,10]. No particulate system is used to introduce the genetic material into the target cells [6]. Needle injection, ballistic DNA injection, electroporation, sonoporation, photoporation, magnetofection and hydroporation are the most utilized physical methods at present [6,11].

### **1.2.1.2 Chemical methods**

Depending on the chemical feature, those methods can be classified into three groups: cationic lipids, cationic polymers and inorganic nanoparticles. Chemical vectors based on cationic lipids and cationic polymers form condensed complexes with negatively charged DNA through electrostatic interactions [10]. The complexes protect DNA and facilitate cell uptake intracellular delivery [10]. The principal characteristics of the non-viral chemical vectors are the following:

- Vectors based on cationic lipids

As shown in Figure 4, cationic lipid-mediated gene transfer or lipofection represents the most commonly used non-viral gene delivery system. Cationic lipids share four common functional domains: (i) a hydrophilic head-group – which is responsible for the interaction with the DNA-, (ii) a hydrophobic domain – which is usually derived from aliphatic hydrocarbon chains-, (iii) a linker structure – which influences the flexibility, stability and biodegradability of the cationic lipid- and (iv) a backbone domain – which separates the polar head-group from the hydrophobic domain and it is usually a serinol or a glycerol group- [12]. Changes in those domains can vary the transfection efficiency of different vectors elaborated with cationic lipids. The most employed cationic lipid formulations for gene delivery platforms are (i) **liposomes** –vesicles made up of phospholipids-, (ii) **niosomes** –non-ionic surfactant vesicles, with greater physic-chemical and storage stability than liposomes- and (iii) **solid lipid nanoparticles (SLN)** –particles with a solid lipid core, stabilized with surfactants- [13].

- Vectors based on cationic polymers

Vectors based on cationic polymers are mostly spherical particles ranging in the size of 1-1000nm and they condense DNA into polyplexes preventing DNA from degradation [6]. The DNA can be entrapped into the polymeric matrix or can be adsorbed or conjugated on the surface of the nanoparticles [6]. The most popular

## *Introduction*

cationic polymers employed for DNA delivery purposes are: (i) poly(ethylene imine) - PEI, which has an excellent buffering capacity-, (ii) chitosan – a linear polysaccharide derived from the deacetylation of the natural chitin-, (iii) cyclodextrins – a series of natural cyclic oligosaccharids-, (iv) dendrimers – tree-shaped synthetic molecules up to a few nanometers in diameter that are formed with a regular branching structure- and (vi) Poly(L-lysine) – PLL, which can form nanometer size complexes with polynucleotides thanks to the presence of protonable amine groups on the lysine moiety- [6,13,14].

- Vectors based on inorganic nanoparticles

Inorganic nanoparticles are nanostructures varying in size, shape and porosity, and calcium phosphate, silica, gold, and several magnetic compounds are the most studied [6,15]. Inorganic particles can be easily prepared and surface-functionalized. They exhibit good storage stability and are not subject to microbial attack [6,16].

In summary, non-viral vectors for gene delivery represent a safer alternative to conventional viral vectors. However, although tremendous progress has been made in this field in recent years, the clinical application of non-viral vector based gene therapy is still hampered by the lack of effective gene delivery techniques. In the present review, we will discuss the up-to-date and possible future strategies to improve DNA transfer efficacy using non-viral vectors and focusing on non-invasive routes of administration. First, the intracellular barriers that non-viral vectors have to overcome and the strategies to improve the transfection efficiency in this regard will be described. Second, we will review the extracellular barriers that hamper an efficient gene delivery, as well as the invasive and the alternative non-invasive routes of administration that elude those barriers. Finally, challenges for non-viral vectors to reach clinical trials will be discussed, focusing on the transfection efficiency, the targeting and the duration of the transfected gene expression.

## **2. INTRACELLULAR BARRIERS AND STRATEGIES TO IMPROVE TRANSFECTION EFFICIENCY**

A key factor conditioning transfection efficiency is the ability of the gene delivery system to overcome the intracellular and extracellular barriers. In this section we will describe the main intracellular barriers that gene delivery systems must overcome to reach an efficient transfection and the different strategies used for this purpose. Intracellular barriers involve all the obstacles that a gene delivery system must

## *Introduction*

overcome from cell surface association to nuclear entry in target cells. The knowledge of the molecular features that command all these processes for the non-viral vectors and the overcoming of these hurdles are mandatory issues that need to be deeply considered in order to design efficient gene delivery methods. In this section, we will review the cellular uptake pathways and intracellular trafficking of non-viral vectors and we will discuss the existing methods to enhance the endosomal escape and the nuclear entry, which are the principal strategies to achieve an efficient transfection.

### **2.1. Cellular uptake pathways**

Cell surface association is the first intracellular barrier that non-viral gene delivery platforms need to overcome and it can directly influence the next intracellular fates of the non-viral complexes [17]. Cell binding interactions of non-viral vectors can be receptor independent or receptor mediated. Receptor independent cell surface association occurs by electrophilic attraction between the positively charged non-viral complexes (i.e. cationic lipoplexes and cationic polyplexes) and the negatively charged cell surface proteoglycans [18]. This binding method can efficiently transfect many cell types *in vitro*, but therapeutic potential *in vivo* requires additional refinement. In fact, in order to specifically deliver a gene into a target tissue *in vivo*, non-specific cell binding would require very high and potentially toxic doses of the non-viral vector. The addition of cell-specific ligands or antibodies to the vectors reduces this problem, allowing the use of lower and safer vector doses and promoting tissue targeting [18]. For instance, transferrin (Tf), which is an iron transporting protein, has been used to achieve brain delivery in view that the Tf receptor is expressed in neurons and in the capillary endothelial cells of the brain-blood-barrier (BBB) [19]. Ligand choice not only depends on the cell type being targeted, but it is also important to consider the type of cell entry pathway that will be induced after ligation. As discussed in the following section, the endocytic pathway used by the vector can depend on the targeting ligand.

Once bound to the cell surface, non-viral vectors need to cross the plasma membrane to enter the cell and initiate the intracellular trafficking to enter the nucleus. The cellular uptake of macromolecules and solutes into membrane-bound vesicles derived by the invagination and pinching off of pieces of the plasma membrane is known as endocytosis [20]. There are four principal endocytic pathways: clathrin-mediated endocytosis (CME), caveolae-mediated endocytosis

## *Introduction*

(CvME), phagocytosis, and macropinocytosis [17,21]. These endocytic pathways are described below.

### **2.1.1 Clathrin-Mediated Endocytosis**

Clathrin-mediated endocytosis (CME) is a highly regulated and energy-dependent process, and it constitutes the major and best characterized endocytic pathway [20]. The first step in CME is the strong binding of a ligand to a specific cell surface receptor. This triggers the localized accumulation of clathrin structures on the cytoplasmic surface of the plasma membrane, which helps to deform the membrane into a coated pit with a size about 100-150 nm [22]. As the clathrin lattice formation continues, the coated pits become deeply invaginated and they finally pinch off from the plasma membrane to form intracellular clathrin-coated vesicles (CCVs) [20]. The clathrin coats then depolymerize, resulting in early endosomes. A kind of GTPase named dynamin is necessary for the vesicle fission from the plasma membrane [23]. Cholesterol seems to be also important for CCV formation because its depletion impedes the coated pits to pinch off from the plasma membrane [24].

In the next step of the CME pathway, the endocytosed vesicles internalized from the plasma membrane are integrated into late endosomes and those then deliver their cargos to lysosomes [25]. During maturation from early to late endosomes, proton pumps located on the endosome membrane produce the acidification of the compartment, and there is a further reduction to pH 5 in the progression from late endosomes to lysosomes [20]. The acid pH in endosomes seems to cause the dissociation of the ligands from their receptors. Most authors state that, in absence of an endosomal escape mechanism, non-viral vector/DNA complexes are retained and degraded in the lysosomes due to the acid environment and the enzymatic activity in these compartments. The final result is that DNA molecules have little or almost no access to the nucleus [20].

Some authors suggest that in some cases, depending on the formulation of the non-viral vector, the CME pathway might be the most suitable to achieve a high transfection efficiency because the lysosomal activity facilitates the cytosolic release of nanoparticles and enhances the nuclear entry of DNA [26]. Depending on the composition of the vector, the most appropriate internalization mechanism may be modulated [26]. Therefore, it is crucial to have a comprehensive understanding of the cellular internalization pathways of non-viral gene delivery systems.

## *Introduction*

### **2.1.2 Caveolae-Mediated Endocytosis**

Caveolae-mediated endocytosis (CvME) begins in membrane microdomains called caveolae, which are small, hydrophobic, and cholesterol- and sphingolipid-rich smooth invaginations [17,20]. As well as CME, CvME is a type of receptor-mediated and dynamin-dependent pathway in which cholesterol also plays an important role [27]. The main difference between the clathrin- and the caveolae-mediated pathways is that in CvME there are no endosomes. Instead, internalized molecules go into intracellular vesicles called caveosomes, which do not fuse with lysosomes and, therefore, the potential degradation process of the DNA is avoided in this pathway [17]. In fact, CvME is generally considered a non-acidic and non-digestive internalization pathway, meaning that the internalized molecules can be directly transported into their intracellular target sites without being degraded in lysosomes [17,28]. Nevertheless, this issue is still under debate because some authors have recently reported that sometimes caveosomes join the classical endocytic pathway, in which they eventually fuse with lysosomes [29]. Therefore, in this regard further evidence is needed in order to understand the relationship between caveosomes and lysosomes.

### **2.1.3 Phagocytosis**

Phagocytosis is a special type of endocytic pathway that is primarily used by professional phagocytes such as macrophages, monocytes, neutrophils and dendritic cells, although other cells might use it too [17]. Cup-like membrane extensions larger than 1 $\mu$ m mediate the phagocytic pathway, and it is usually employed by cells to internalize large particles such as bacteria or dead cells, although large lipoplexes and polyplexes can also be internalized through this pathway [17].

Phagocytosis usually involves three steps that are common for all molecules internalized through this pathway, including non-viral vectors. First, non-viral vector/DNA complexes are recognized by opsonins and, therefore, opsonized, in the bloodstream. Second, the opsonized complexes bind to the surface of macrophages through the interaction between macrophage receptors and the constant fragment of particle-adsorbed immunoglobulins [17]. Antibodies lacking the constant fragment can be employed in non-viral gene delivery systems to prevent their recognition and clearance by macrophages *in vivo* [30].

## *Introduction*

Finally, the union of the molecule or non-viral/DNA complex to the macrophage receptors activates Rho-family GTPases, which trigger actin assembly and cell surface extension formation [17]. The complexes are ingested by the macrophages when the surface extension zippers up around them [20]. The vesicles internalized in the cells through the phagocytic pathway are called phagosomes and they usually have a diameter of 0.5 – 1.0  $\mu\text{m}$  [20]. The phagosomes carrying the internalized complexes form mature phagolysosomes when they fuse with lysosomes, where the complexes undergo an acidification process [20]. In view that the intracellular fate of the phagocytic pathway is the fusion with lysosomes, the nucleic acids carried in the non-viral vector complexes will probably be degraded in this internalization pathway [31].

### **2.1.4 Macropinocytosis**

Macropinocytosis is an internalization pathway based on fluid-phase endocytosis, since it non-specifically takes up a large amount of fluid-phase contents [17]. Similarly to the phagocytic pathway, macropinocytosis also happens through the formation of actin-directed membrane protuberances. Nevertheless, here the protrusions do not zipper up the ligand-coated particle. Alternatively, as shown in Figure 5, in the macropinocytic pathway the protuberances fuse with the plasma membrane. Macropinosomes are also different from clathrin-coated vesicles (CCVs) and caveosomes, since macropinosomes have no coat structures and, even if they are heterogeneous in size, they tend to be larger than 0.2  $\mu\text{m}$  in diameter [32]. As well as the other endocytic pathways, macropinocytosis also depends on small GTPase proteins since they are necessary for the vesicle fission from the plasma membrane [17].

The connection between macropinosomes and lysosomes remains still unknown. In some studies, early macropinosomes have been reported to show the same markers as early endosomes, and late macropinosomes have been reported to present lysosome markers [17]. However, macropinosomes have been shown to present different intracellular fates depending on the cell type, even if the explanation of this event remains unclear, and they do not always fuse with lysosomes [17].

### **2.2. Endosomal escape mechanisms**

As mentioned before, most non-viral vectors are internalized in the cells mainly through the clathrin-mediated endocytic pathway. The major problem here is the intracellular fate of the endosomes, that fuse with lysosomes and this can potentially

## *Introduction*

lead to the degradation of the nucleic acids. In order to avoid this effect, while taking advantage of the CME pathway for cellular uptake, several attempts have been made to promote the early endosomal escape of non-viral gene delivery systems.

Many pathogens, mainly viruses and bacteria, have evolved different mechanisms to promote endosomal escape when internalized in cells. Several endosomal escape agents derive for virus (i.e. haemagglutinin protein of influenza virus) and bacteria (i.e. diphtheria toxin), and some derive from plants (i.e. ricin), human (i.e. fibroblast growth factors) or animals (i.e. melittin from bee venom) too [33]. The understanding of the mechanism used by pathogens allows to design and to ameliorate endosomal escape strategies applicable to non-viral gene delivery systems. Nowadays several synthetic peptides with specific sequences and length are designed (i.e. the amphiphatic Sweet Arrow Peptide), as well as specific chemical agents (i.e. the polymer polyethylenimine PEI) for endosomal escape induction [33]. In the following paragraphs the principal endosomal escape mechanisms are described.

### **2.2.1 Pore formation in the endosomal membrane**

Pore formation is based on the interplay between a membrane tension that enlarges the pore and a line tension that closes the pore. Some peptides have a high affinity for the edge of the pore, and binding of those peptides to the edge of the pore produces a reduction of the line tension [33].

Some studies have reported that the union of cationic amphiphilic peptides to the lipid bilayer produces a strong internal membrane tension able to create pores in the lipid membrane [33].

### **2.2.2 pH-buffering effect (the proton sponge effect)**

In this endosomal escape mechanism, the low pH of the endosomal environment leads to the protonation of the entrapped agents with a high buffering capacity. Protonation causes an influx of ions ( $H^+$  and  $Cl^-$ ) and water into endosomes, resulting in osmotic swelling and endosome rupture [33].

The proton-sponge effect has been observed in certain cationic polymers with a high  $H^+$  buffering capacity over a wide pH range [34]. These polymers usually contain protonable secondary or tertiary amine groups with  $pK_a$  close to endosomal/lysosomal pH. As explained before, during the maturation of endosomes, the membrane-bound ATPase proton pumps actively translocate protons from the cytosol into endosomes, causing the acidification of the endosomal compartments.

## *Introduction*

At this point, cationic polymers with high buffering capacity become protonated and resist the acidification of endosomes, which results in more protons pumped into the endosome in an attempt to decrease the pH [34]. The proton pumping action is followed by passive chloride ions entry, increasing ionic concentration and, consequently, water influx [34]. The high osmotic pressure produces the swelling and the rupture of endosomes, releasing their contents to the cytosol [34]. Histidine-rich molecules show a buffering effect upon protonation [33] and histidine can be included in non-viral vectors to enhance transfection efficiency by facilitating endosomal escape.

### **2.2.3 The *flip-flop* mechanism**

This endosomal escape mechanism can be useful for endocytosed lipoplexes. Lipoplexes are endocytosed and become entrapped inside the early endosomes. There is an electrostatic interaction between the cationic lipoplexes and the anionic lipids of the endosomal membrane [34]. The anionic lipids of the endosomal membrane laterally diffuse into the lipoplexes and form charge-neutralized ion pair with cationic lipids of the lipoplexes, resulting in the nucleic acids being displaced from the lipoplexes and released in the cytoplasm [34].

### **2.2.4 Fusion in the endosomal membrane**

This mechanism of endosomal escape is based on the destabilization of the endosomal membrane by water soluble and partly hydrophobic, and/or polybasic peptides known as cell-penetration peptides or CPPs. CPPs were originally derived from viruses, and they are constituted by short sequences of amino acids (10-30 residues) that used to be cationic and/or amphiphatic [34]. The main features of CPPs are their abilities to penetrate the cell membrane at low molecular concentrations without causing significant membrane damage and to internalize electrostatically or covalently bound biologically active cargoes (including proteins, peptides and nucleic acids) with high efficiency and low toxicity [35]. CPPs either form complexes with nucleic acids, through electrostatic interaction, or can be incorporated into polymeric and lipidic delivery systems [34]. To date, the internalization mechanism of CPPs still remains controversial, since there is evidence for both energy-independent and endocytic processes for cellular uptake of CPPs. Nowadays, it is generally accepted that endocytosis is the major internalization mechanism for most CPPs. However, it seems plausible that several CPPs utilize two or more cellular uptake pathways depending on the experimental conditions [35]. Further research would be needed in order to elucidate the exact uptake mechanisms and to identify the precise factors influencing these processes.

## *Introduction*

There are different criteria to categorize CPPs into different families. In general, CPPs can be classified into two categories [36]: (i) Cationic peptides that usually contain arginine and lysine residues; and (ii) amphiphatic peptides that consist of both hydrophobic and hydrophilic segments. Two examples of CPPs currently used to improve transfection efficiency of non-viral gene delivery platforms are the transcriptional activator protein or TAT (which belongs to the first category and was the first CPP identified, derived from the transcription activating factor of human immunodeficiency virus 1 (HIV-1)) [33,37] and the Sweet Arrow Peptide or SAP (which belongs to the second category and is a proline-rich amphiphatic peptide of synthetic origin) [38].

### **2.2.5 Photochemical disruption of the endosomal membrane**

Photochemical internalization (PCI) is a light-directed delivery technology that utilizes photosensitizers to facilitate the transport of membrane impermeable macromolecules from endocytic vesicles into the cytoplasm [34]. Photosensitizers that are used in PCI use to be amphiphilic compounds that can bind and localize in the plasma membrane. In this mechanism, photosensitizers bind to and localize in the plasma membrane, and they can be taken up by endocytosis together with the non-viral gene delivery systems. Photosensitizers are confined to the endosomal membrane and remain inactive until they are triggered by light with specific wavelengths matching their absorption spectra [39]. Once activated, they induce the formation of highly reactive oxygen species, causing the rupture of endosomes and lysosomes membrane. As a result, macromolecules that are trapped inside the endosomes/lysosomes can be liberated into the cytosol [34].

In general, the enhancement of endosomal escape is believed to be a crucial factor in non-viral vector based DNA delivery platforms. Different strategies for endosomal escape have different characteristics. A safe endosomal escape agent applicable in the clinic should have low immunogenicity and toxicity, high efficiency, ease of use and production, modular attachment of targeting ligands and the potential for cost-effective large-scale manufacture [33].

### **2.3 Nuclear import**

In the previous section we have seen several strategies suitable for non-viral gene delivery to avoid endosomal degradation of the DNA and to enhance its release to the cytoplasm. However, in order to achieve an effective transfection, the DNA

## *Introduction*

molecules have to enter the nucleus. Here, we will discuss the principal strategies to transport DNA to the nucleus once released in the cytoplasm.

To enter the nucleus, molecules must pass through nuclear pore complexes (NPCs), which are multimeric structures with a central channel of 9 nm that prevents molecules with a molecular weight higher than 45 kDa from passively diffusing into the nucleus [40]. In the case of naked DNA, molecules smaller than 300 bp can passively diffuse into the nucleus, but larger DNA molecules, even when condensed by a non-viral vector, are excluded from the nucleus except when cells are undergoing mitosis [40-42]. During cell division, the integrity of the nuclear membrane is lost, which allows the nuclear entry of DNA-vector complexes within the daughter cells [21,40]. This is the case in the *in vitro* transfection with dividing cells, but *in vivo* transfection often targets slow dividing or terminally differentiated cells [21,40]. Therefore, the nuclear envelope cannot be neglected in *in vivo* situations, and there is considerable interest in improving the nuclear import efficiency of non-viral vectors [21,40].

Classically, proteins that are destined for the nucleus contain a nuclear localization signal (NLS), which is abundant in basic amino acids and it can be recognized by cytoplasmic proteins known as importins [17], that mediate energy-dependent transport through the NPC [40,43]. The same approach can be used to enhance non-viral gene delivery to the nucleus [21]. A NLS containing vector can be added to the DNA-vector formulation or a NLS sequence can be directly bound to the DNA in order to promote its transport to the nucleus by the importins [40]. In addition, highly polymers such as polylysine and protamine, the highly basic sequence of which resemble typical NLS sequences, have been used as potential agents to enhance nuclear targeting when complexed with DNA [40].

Finally, it should be considered that, once inside the nucleus, the non-viral vector itself may constitute a barrier to transgene expression. In fact, the agent used to condense the DNA could potentially interfere with the access of the cellular transcription machinery to the transgene promoter, thereby reducing or preventing its expression [40]. Still, premature release of DNA from the vector may expose the DNA to enzymatic degradation before expression can occur [40,44]. For liposomal-based vectors, DNA displacement from the vector seems to be connected to endosomal escape, driven by the anionic lipids of the endosomal membrane that neutralize the charge of the cationic lipids in the liposomal formulation [40,45,46]. In contrast, polycation/DNA complexes appear to release from each other in the

## *Introduction*

nucleus through exchange of the polycations in the complexes with the protein components of the surrounding proteins [40,47,48]. However, it seems plausible that additional mechanisms other than competitive charge interactions may be involved in the dissociation of DNA from polycations, and a deeper understanding of chromatin remodelling mechanisms may shed further light on this issue.

In summary, non-viral vectors for DNA delivery systems must overcome several intracellular barriers from cell-surface association to nuclear entry and DNA release. Depending on the cell type and on the cellular internalization pathway, some intracellular barriers may differ. Most non-viral vectors are taken up in cells through the CME pathway, which presents some problems such as the acid environment of endosomal and lysosomal compartments and the risk of DNA degradation. Therefore, several endosomal escape agents and mechanisms are currently being studied to avoid DNA degradation and to enhance its cytosolic release. In addition, DNA molecules have to enter the nucleus for the transgene expression. The most employed strategy for this purpose is the incorporation of a NLS in the vector-DNA complex. Finally, once inside the nucleus or earlier during the endocytic pathway, the vector-DNA complex needs to dissociate in order to allow the transcriptional machinery of the cell to access the transgene promoter. Thus, Figure 5 summarizes the most relevant aspects described in this section.

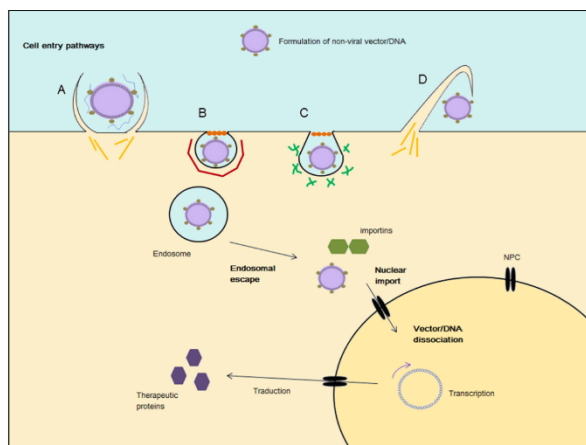


**Figure 5.** Cell entry pathways and intracellular trafficking of non-viral gene delivery systems. A) Phagocytosis. B) Clathrin-mediated endocytosis (CME). C) Caveolae-mediated endocytosis. D) Macropinocytosis. Internalized vector/DNA complexes following the CME pathway escape from endosomes and can be transported into the nucleus by the importins if they contain a NLS. When vector and DNA dissociate from each other, the transgene is

## *Introduction*

expressed in the target cells. Yellow filaments represent actin; red chain represents clathrin coat; green filaments represent caveolin dimers; orange little circles represent the small GTPase dynein; blue filaments represent opsonins. Adapted from [23; 24].

---

### **3. EXTRACELLULAR BARRIERS TO OVERCOME. NON-INVASIVE ROUTES OF ADMINISTRATION.**

Depending on the administration route and the target organ, gene delivery systems must overcome several extracellular barriers *in vivo* before reaching the target cells. As mentioned earlier, cancer diseases represent 60% of all clinical trials in gene therapy; yet other pathologies such as infectious, neurodegenerative, ocular and pulmonary diseases merit special attention, which, in sum, represent 10% of clinical trials in gene therapy. The principal and most studied route of administration of non-viral gene delivery systems for those diseases is the intravenous administration. Here, vectors need to be properly designed in order to overcome all the hurdles this route presents. Moreover, when specific tissues need to be targeted, such as the brain, the eye or the lungs, additional extracellular barriers appear and vectors have to be able to surpass them too. In this section, we will review the principal systemic barriers following the intravenous administration of non-viral gene delivery systems, as well as the additional tissue-specific barriers DNA/vector complexes have to overcome. We will also describe several attempts that have been made in order to overcome those barriers using invasive and alternative non-invasive routes of administration. Many efforts are being conducted to achieve effective strategies for safe non-viral gene delivery platforms based on non-invasive administration routes.

#### **3.1 Intravenous administration**

For many cancer forms, and specially disseminated cancer diseases, treatment needs to be administered systemically. Thus, intravenously administered current gene delivery systems to treat cancer should be able to transport and deliver the genetic cargo into cancerous cells.

The principal challenge of systemically administered DNA is to resist the extracellular enzymatic degradation, since DNA is subject to enzymatic degradation from the point of entry. However, it is possible to considerably dominate this hurdle by condensing the negatively charged DNA with the positively charged non-viral vectors [13].

## *Introduction*

Secondly, other major extracellular barrier in the systemic route is the non-specific binding of the non-viral vector/DNA complex –which has a net positive charge- with blood cells and serum proteins such as albumin, complements, immunoglobulins and fibronectin –which have a negative surface charge- [49]. These interactions could potentially end in aggregation or dissociation of vector/DNA complexes, resulting in their rapid clearance and elimination by the reticuloendothelial systems [49].

A third obstacle in systemic delivery might be the colloidal instability of non-viral vector/DNA complex formulations in the extracellular environment, which can also result in the aggregation of the complexes [49]. Fourth, vascular system is an extracellular barrier to be considered since it limits the size of the nanoparticles that can pass through the endothelial cells, which are relatively small and have tight junctions [49].

Finally, the activation of the immune system by the foreign vector/DNA complexes is an extracellular issue to be taken into consideration as well. In fact, foreign synthetic vectors can also induce an inflammatory response and/or complement activation, and hydrophobic particles can be eliminated by mononuclear phagocytic system through opsonisation [49].

In order to overcome all these systemic barriers, non-viral vectors should be structurally modified. Formulation of gene delivery vectors is a key factor in determining their bioavailability and transfection efficiency *in vivo* [49]. Some of the strategies that are being developed to improve the properties of nanoparticles in the extracellular environment are discussed below.

The most employed strategy to increase the stability of vector/DNA complexes is shielding the outer surface of complexes with poly(ethylene glycol) or PEG [50]. Because of its highly hydrophobic nature, PEG produces a steric barrier against nuclease degradation and aggregation of nanoparticles in blood circulation [49]. However, despite the promising results, some difficulties exist in conjugation of PEG to gene delivery systems. PEGylation could decrease binding ability of non-viral vectors to DNA causing instability of lipo- or polyplexes in blood circulation. It may also affect the binding of vector/DNA complexes to receptors on the cell membrane [51]. Moreover, PEGylation can induce accelerated blood clearance due to activation of splenic synthesis of anti-PEG IgM antibody after first injection, resulting in the opsonisation of the subsequent doses [49]. The length and the degree of PEGylation can also affect the ability of DNA condensation and biodistribution of gene carriers

## *Introduction*

*in vivo*, and the optimal PEG length and content depends on gene carrier systems [52].

Consequently, considerable research has been made with the aim of compensating the negative effect of PEGylation in non-viral gene delivery systems. As reported in a recent study, one possible solution is to replace PEG by some hydrophilic polymers such as poly(N-vinyl-2-pyrrolidone) (PVP), poly(4-acryloylmorpholine), or poly(N,N-dimethylacrylamide) [53]. Coating of nanoparticles with these polymers led to extended residence of the nanoparticles in blood circulation in rats, although they had a shorter half-life than the PEG-coated nanoparticles [53]. Other strategies include providing stability against serum compounds and enzymatic digestion using copolymers of poly(L-lysine) and poly(2-methyl-2-oxazoline) [54], the pH-sensitive shielding of DNA polyplexes or lipoplexes (e.g. with PEG-acetal-MAL or maleimide moiety) [55], the use of enzymatically cleavable PEG linkers (e.g. PEG-peptide-DOPE or PPD that is cleaved in a matrix metalloproteinase-rich environment) [56], or the production of reducible PEG nanoparticles (e.g. PEG and chitosan bound through disulphide bridges) [57].

Besides from PEGylation, other chemical and structural modifications can be applied to gene delivery agents in order to overcome the systemic barriers. In the case of cationic lipid-based non-viral vectors, incorporation of cholesterol can stabilize lipoplexes against binding to red blood cells [49]. In the case of cationic polymer-based non-viral vectors, conjugation of lactose to chitosan polyplexes has shown excellent DNA binding ability, good protection of DNA from nuclease, and the suppression of self-aggregation and serum-induced aggregation [58]. Therefore, current research has focused on multifunctional and diverse non-viral gene carriers that can be adjusted for each particular condition.

### **3.2 Targeting specific tissues: additional extracellular barriers**

When targeting specific tissues, vectors have to be able to surpass additional barriers as well. Here, we will focus on specific extracellular barriers present in gene delivery to the central nervous system (CNS), to the eye and to the lungs. The invasive and alternative non-invasive routes of administration that avoid those barriers will also be discussed.

#### **3.2.1. Gene delivery to CNS**

The CNS possesses particular anatomical and physiological properties that make gene delivery to CNS specially challenging. The CNS is protected by the blood-brain-

## *Introduction*

barrier (BBB), which consists of tightly joined capillary endothelial cells [19], and it is considered to be impermeable for almost 100% of the macromolecular drugs and over 98% of small molecule drugs [59]. The spinal cord is part of the CNS and it is protected by the blood-cerebrospinal fluid barrier (BCSFB), which is constituted of choroid plexus epithelial cells and restricts the free diffusion of molecules into the cerebrospinal fluid (CSF) [19]. Transport into the CNS of essential nutrients, such as glucose and amino acids, occurs through specific receptors present in the BBB and the BSCFB [19]. Within the CNS, distinct cell types exist including neurons and different types of glial cells; neurons are particularly challenging to transfect and it is thought this is attributable to their post-mitotic nature, their complex structure and the complexity of neuronal networking [19].

Most of the strategies to cross the BBB upon systemic administration of non-viral vector/DNA complexes exploit receptor-mediated uptake of molecules such as transferrin (Tf), lactoferrin and insulin, since receptors of those molecules are expressed on many cell types, including neurons and the capillary endothelial cells of the BBB [19]. By attaching a ligand for those receptors to the non-viral delivery system, one can enhance the transport of the vector/DNA complex towards the CNS. Other strategy known as “Molecular Trojan Horse” uses peptidomimetic monoclonal antibodies that are designed to target specific receptors on the BBB and induce receptor-mediated transcytosis of the non-viral delivery system into the CNS [60]. Other approaches investigated for CNS delivery of conventional pharmaceuticals upon systemic administration include transient mechanical disruption of the BBB and RNAi-mediated knockdown of tight junction proteins [19].

The ultimate goal for CNS gene therapeutics is delivery by systemic route, which is the most acceptable for clinical use. Nevertheless, in view of the high amount of extracellular barriers vectors must overcome, many studies have attempted different routes of administration. To date, several pre-clinical studies have essayed local administration to the brain, either by injection or by infusion. However, even if local administration to the brain eludes the extracellular barriers to access the CNS, the need for brain surgery to infuse a gene therapy vector clearly limits the clinical applicability for this approach.

Intranasal delivery offers a novel and non-invasive means by which non-viral gene delivery systems can gain access to the brain. The mechanisms by which intranasally delivered substances enter the CNS have not been fully elucidated, but an accumulating amount of evidence suggests that substances can reach the brain

## *Introduction*

through a combination of perineuronal, perivascular and lymphatic transport pathways. In addition, the prevailing nose-to-brain pathway will largely depend on the region where the delivered agent is placed within the nasal cavity and the physicochemical properties of the therapeutic being administered [61]. It is currently accepted that the intranasally administered substance can reach the CNS by three main pathways: (i) direct paracellular or transcellular transport via the olfactory neurons or olfactory epithelial cells (“olfactory neural pathway”), (ii) transport via the trigeminal nerves (“trigeminal pathway”) or (iii) indirectly, *via* blood vasculature and/or lymphatic system (“systemic pathway”) [62]. The nasal mucosa is highly vascularized, and the blood vessels allow passage of drugs following nasal administration in nano-drug delivery systems; however, the substance that has been absorbed into the systemic circulation has to cross the BBB in order to reach the CNS [61]. Following olfactory and trigeminal nerve pathways, drug is delivered to the olfactory bulbs and to more caudal brain areas, respectively [63]. Within the brain, pulsatile flow in perivascular spaces has been postulated to allow for widespread transport of molecules within interstitial fluid to sites deep in parenchyma [63,64].

Advantages of intranasal administration include ease of administration (non-invasive), rapid dose absorption via highly vascularized mucosa, large nasal mucosa surface area for dose absorption, avoidance of the gastrointestinal tract and first-pass metabolism and lower side effects among others [65]. Moreover, intranasal administration confers improved convenience and compliance compared to other more invasive routes and it allows self-administration [65]. Disadvantages of this route include that nasal congestion could interfere with dose absorption, that the amount of dose that reaches the CNS varies with each agent and that the frequent use of this route leads to mucosal damage [65]. In addition, the administered formulation can undergo rapid clearance from nasal cavity by the mucociliary system [59,66]. This latter drawback can be overcome by adding a mucoadhesive substance to the formulations. For non-viral vector based gene delivery systems, chitosan is an attractive excipient that can confer both bioadhesion and absorption properties, and it is the most widely investigated absorption enhancer material both in terms of efficiency and safety [63]. Chitosan is able to interact through its positively charged amino groups with the anionic counterpart present in the mucus layers, mainly sialic acid, and to affect permeability of the epithelial membrane by the transient opening of the tight junctions in the epithelial cells [67]. In a recent study, another substance, the non-ionic surfactant lauroate sucrose ester has been also reported to be an effective intranasal absorption enhancer [68].

## *Introduction*

Recently, the first report that intranasal delivery of DNA nanoparticles can bypass the BBB and transfect and express the encoded protein in rat brain has been published, thereby affording a non-invasive approach for gene therapy CNS disorders [63]. Authors demonstrated that intranasal delivery of unimolecularly compacted DNA nanoparticles, which consist of single molecules of plasmid DNA encoding enhanced green fluorescent protein (eGFP) compacted with 10kDa commercial peptide (PEG-substituted lysine 30mers or CK30PEG10k) successfully transfect cells and leads to the expression of the eGFP in the rat brain [63]. The results further suggest that the cells transfected within the brain are likely to be pericytes, and that the distribution of nasally administered substances occurs via perivascular transport [63]. Additionally, another recent study has reported brain (cortex and hippocampus) transfection upon intranasal administration of chitosan and polyethyleneimine (PEI)-coated magnetic micelles [69]. Even if those nanoparticles were able to reach the brain presumably because of a transient disruption of the BBB following mild traumatic brain injury, the results show that the intranasal route might be useful for targeting the brain. Although further optimization of the dose, dosing regimen and dose interval is needed to achieve appropriate levels of transgene expression [63], the promising results will certainly encourage the research in the field of intranasal administration of non-viral vector based gene delivery systems, which has clinical importance due to its non-invasive nature.

### **3.2.2 Gene delivery to the eye**

The eye is an attractive target organ for gene therapy because of its unique characteristics. The tissue volume to be treated is small, the therapeutic concentration to be administered is relatively low and the diffusion of active products from the eye to the circulation is minimal [70]. In addition, the eye benefits from a relative immune privilege, minimizing the potential immune and inflammatory reactions that may follow the intraocular injections of foreign agents [70].

In general, gene delivery systems for eye diseases range from simple eye drops and ointments to more advanced bio- and nanotechnology-based systems such as muco-adhesive systems, polymers, liposomes and ocular inserts. Most of these technologies were developed for front-of-the-eye ophthalmic therapies and are not applicable as back-of-the-eye delivery systems [71].

When the systemic administration is used to target the eye, non-viral vector/DNA complexes must cross the blood-ocular-barrier (BOB) to reach the ocular tissue. This

## *Introduction*

constitutes a real challenge, since the BOB is composed of tight epithelial junctions. Two principal strategies to overcome this barrier are the use of vectors smaller than 100 nm to allow intracellular passage across the BOB [72] and the use of ligand-equipped vectors that recognize specific receptors in the BOB [73]. Therefore, even if the intravenous route permits the delivery of larger volumes of the formulations as well as repeated administrations, the therapeutic effect achieved by this method is often limited by the factors restricting the access to the eye.

Invasive methods such as intravitreal injection, subconjunctival injection and subretinal injection can bypass some of those barriers, and intravitreal and subretinal injections are currently considered as the most effective and common methods of gene delivery to retinal ganglion cells and to inner layers of the retina, respectively. However, these methods are very invasive and repeated gene delivery to the eye using such methods can cause further damage of the eye like retinal detachment, haemorrhages, and sub- or pre-retinal fibrosis [71]. Therefore, non-invasive and effective methods for ocular gene delivery are needed. In this regard, topical administration in the form of eye drops is a non-invasive delivery method that can be performed repeatedly with minimal side effects [71].

However, the non-invasive route of administration is perhaps the most ambitious goal because the barriers associated with topical gene delivery to the posterior ocular tissue are the most challenging. First, vector/DNA complexes have to surpass the tear film, which is an aqueous layer covered by lipids and underlined by mucin that covers the corneal and conjunctival layers [71]. This tear film restricts the bioavailability of applied formulations because of the tear turnover rate and the lacrimal and nasolacrimal drainage [85]. Strategies to overcome this barrier include addition of viscosity enhancers –such as cellulose derivatives or thermoreversible poloxamer gels- [71] and, most importantly, the incorporation of muco-adhesive polymers –such as chitosan and hyaluronic acid derivatives- in gene delivery systems [74]. Second, ocular tissue barriers such as the cornea, conjunctiva, sclera and choroid, contain epithelial tight junctions, proteoglycan matrices and fibril collagen networks within their structures, which contribute to restrict the passage of vector/DNA complexes to the neuroretina [71]. Finally, the vitreous is an aqueous biogel composed of collagen, hyaluronan and proteoglycans that hinders transfection of the retinal cells [71]. Strategies to overcome those barriers include all the above-mentioned methods from the use of vectors of suitable dimensions to the use of specific ligands and muco-adhesive polymers [71].

## *Introduction*

The majority of success in ocular gene therapy research thus far was accomplished for applications involving the anterior part of the eye, using mainly viral-based delivery systems and invasive delivery methods. Interestingly, effective gene delivery to the retina and retinal pigment epithelium using non-viral vectors has been recently reported; however, in this study magnetic nanoparticles were administered invasively, through intravitreal and subretinal injections [75]. Rather than in gene delivery, significant advances have been made in drug delivery systems to target the posterior part of the eye using non-invasive administration routes. For instance, in a recent study, it was reported that surface-modified submicron-sized lipid emulsions could be promising vehicles of hydrophobic drug delivery to the ocular posterior segment [76]. In that study, researchers performed surface modification of the lipid emulsions using a positive charge inducer and the functional polymers chitosan and poloxamer 407. Authors suggested that poloxamer 407 increased the lipid emulsion retention time on the eye surface by its adhesive properties, therefore enhancing gene delivery to the ocular posterior segment. Additionally, another study has reported successful drug delivery to the posterior segment of the eye of rats and rabbits using annexin A5-associated liposomes [77]. Here, authors suggested that annexin A5 mediated endocytosis can enhance the delivery of associated lipidic drug delivery vehicles across biological barriers. Moreover, a novel study has reported the topical drug delivery to retinal pigment epithelium with microfluidizer produced small liposomes, which might be an attractive option for drug delivery to the posterior segment tissues of the eye [78]. It may be reasonable that some of the advances in drug delivery will be applicable for gene delivery systems as well, and they will probably inspire further strategies for non-invasive, non-viral gene therapy platforms aimed at targeting the posterior segment of the eye.

### **3.2.3 Gene delivery to the lungs**

Pulmonary gene therapy is considered for the treatment of a variety of lung diseases like cystic fibrosis, asthma, emphysema and lung cancer [79]. Depending on the respiratory disease to be treated, the target cells in the lung can vary from epithelial cells, alveolar cells, macrophages, respiratory stem cells or endothelial cells [79]. Besides, the nucleic acid cargo needs to be delivered to cells in the target region of the lung. Nevertheless, this is severely limited by the pulmonary architecture, the presence of mucus, the clearance mechanisms and the activation of the immune system [79]. Inhalation, intranasal instillation, intratracheal instillation, and intratracheal intubation are techniques that can be used to administer materials of interest to the lungs. Considering the interest of non-invasive administration routes

## *Introduction*

for clinical applications, aerosolized non-viral vector/DNA complexes for inhalation would be the ideal choice for lung gene therapy. There are many advantages to administering medications to the lungs as an aerosol, such as the high local concentration by delivery directly to the airways, and the pain- and needle-free delivery.

Respiratory secretions, which include mucus and alveolar fluid, are the most important extracellular barriers for lung gene delivery. Respiratory mucus is one of the most important defence mechanisms and it is mainly composed by a three-dimensional network of cross-linked mucin chains, which gives the mucus viscoelastic properties [79]. The major proteins in respiratory mucus are albumin, proteases, anti-proteases, immunoglobulins, lysozyme and lactoferrin, and the respiratory secretions of patients with cystic fibrosis or respiratory infections also contain huge amounts of DNA and actin [79]. The alveolar fluid is a thin continuous layer of pulmonary surfactant that covers the alveolar epithelium and it comprises phospholipids and specific surfactant-associated proteins [79].

Respiratory mucus can act as a barrier towards pulmonary gene delivery in several ways. The biopolymer network of mucus limits the diffusion of complexes by sterical obstruction or by binding the complexes [79]. Also, negatively charged and non-cross-linked macromolecules of mucus, as well as other components present in the mucus such as antibodies, can bind to the surface of vector/DNA complexes. These interactions may cause: (i) entrapment of the vector/DNA complexes in the mucus, (ii) aggregation of the complexes due to neutralization of their surface charges, (iii) release of the DNA cargo from the vector, and (iv) an inefficient cell binding of the complex due to shielding of their positive charges or their receptor binding ligands [79]. Finally, the mucus blanket is continuously removed via mucociliary transport or coughing. Therefore, the vector/DNA complex should be able to cross the mucus before they are cleared from the respiratory tract. The diffusion coefficient of the complexes in the mucus, the thickness of the mucus layer and the rate of mucus clearance will determine whether the vector/DNA complexes will reach the epithelial cells [79].

Regarding the alveolar fluid as a barrier towards pulmonary gene therapy, the presence of this surfactant layer can inhibit transfection of cationic lipid based vector/DNA complexes [79]. It has been suggested that this inhibitory effect results from disintegration of the lipoplexes by the negatively charged lipids present in the surfactant layer, leading to accessibility of nucleases to the DNA cargo and thus its

## *Introduction*

degradation and loss of function [80]. On the other hand, non-viral vectors based on cationic polymers such as PEI might be more resistant to detrimental effects by pulmonary surfactant [79].

Several strategies have been developed in order to overcome the extracellular barriers of lung gene delivery. Size and surface properties of non-viral vector/DNA complexes have a pivotal role in determining their behaviour in respiratory secretions. Most efforts have been conducted to increase the mobility of vector/DNA complexes in respiratory mucus and to avoid interactions of complexes with respiratory secretions.

There are different methods to increase non-viral vector/DNA complex mobility through the respiratory mucus. One straightforward mechanism consists of adding mucolytic agents that hydrolyze mucins present in the mucus [79]. Also, it has been demonstrated that N-acetylcysteine and its derivatives lower the viscosity and elasticity of mucus by reducing the disulphide bridges between the subunits of mucins [81]. As future directions, research is focusing on functionalized nanoparticles with mucolytic agents able to cut a way through the mucus, enhancing their transport across the extracellular matrix [79].

On the other hand, the principal strategy to avoid interactions between vector/DNA complexes and components of biological fluids is the shielding of the complexes by modification with biocompatible hydrophilic but biologically inert polymers [79]. Shielding of vector/DNA complexes may not only be important to reduce interaction with mucus and alveolar fluid components but also diminish clearance by alveolar macrophages. For instance, shielding the positive surface charges of vector/DNA complexes with neutral hydrophilic polymers such as polyethylene glycol (PEG) favours their physicochemical stability and their gene transfer capacity [79].

A number of challenges must be overcome before pulmonary gene therapy becomes a reality, such as the development of gene vectors that can more efficiently penetrate the mucus barrier [82]. However, real advances have been made in recent years, novel aerosol therapeutic modalities are currently being investigated for lung cancer, and inhaled gene therapy has already presented safety and effectiveness in cystic fibrosis [83].

## *Introduction*

As summarized in Figure 6, non-viral vector/DNA complexes have to overcome several extracellular barriers before binding the target cells and initiate the intracellular trafficking towards the nucleus, where transgene expression will occur. Intravenous injection is the most widely used administration route but it presents many hurdles that hamper effective gene delivery. Local administration routes are being explored in order to directly target the tissue of interest and avoid systemic barriers, but they often implicate invasive procedures (e.g. brain surgery). Many efforts are currently focused on the study of non-invasive routes of administration that can equally avoid the systemic barriers (e.g. intranasal administration). Besides, local administration into specific tissues such as the eye or the lungs, involve additional barriers that gene delivery systems have to elude. Surface modifications of the vector/DNA formulations are the most employed strategies to overcome both systemic and tissue-specific barriers. It is expected that future non-viral gene delivery systems will be based on multifunctional vectors and that they will allow a non-invasive administration of therapeutic genes into target tissues.

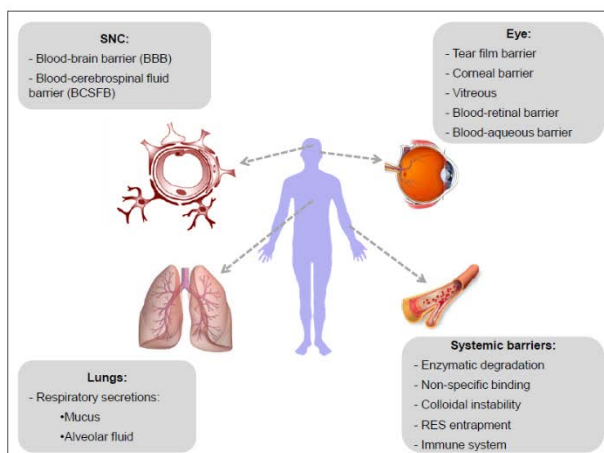


**Figure 6.** Overview of the systemic and tissue-specific (SNC, eye, lungs) extracellular barriers in non-viral gene therapy.

## **4. CHALLENGES OF NON-VIRAL GENE THERAPY AND FUTURE PROSPECTS**

Non-viral gene therapy has emerged as a promising therapeutic approach for gene delivery. Even if this field is still far from clinical practice, much progress has been made in the last few years regarding both the optimization of the non-viral vector formulations and the exploration of alternative routes of administration. For

## *Introduction*

transgene expression to occur, optimal non-viral vectors should not elicit an immune response and should be able, among other aspects, to protect the DNA cargo from degradation in circulation, to enable extravasation from the bloodstream, to traverse cellular membranes, to enhance endosomal escape and to facilitate DNA transport to the nucleus [84]. The comprehensive understanding of the extracellular and intracellular barriers vector/DNA complexes have to overcome in order to achieve an efficient transfection, has allowed the development of several strategies to surpass all those barriers, most of them based on formulation modifications of the complexes and on the use of local routes of administration. Regarding this latter aspect, considerable evidence suggests that the optimization of non-invasive routes of administration may provide safer and more effective gene delivery platforms in the future; therefore, it might be relevant to guide some efforts in this direction.

The major limitation of non-viral gene delivery, as mentioned repeatedly, is the low transfection efficiency. Several strategies discussed along the chapter increase transfection efficiency by providing to the nanoparticles the ability to overcome extra- and intracellular barriers. However, there are two other aspects that are also essential for developing optimal gene delivery platforms; those are *targeting* and *long-term expression* of the transgene. Both are crucial to bring non-viral gene delivery systems into the clinic, since they provide specificity and sustained effect of the treatment, respectively. Many efforts have been made in this regard; however, further research is still required. In addition, other aspects such as the toxicity of the nanoparticles and the manufacturing and regulatory issues have to be carefully considered. Here, we will briefly discuss the current strategies for targeting the desired cells or tissues and for achieving a long-term expression of the transgene. We will also highlight the importance of considering the toxicity, manufacturing and regulatory issues of the nanoparticle formulations.

### **4.1 Targeting**

Targeting to the desired cells or tissue can be achieved by modifying either the vehicle (the non-viral vector) or the cargo (the plasmid DNA). The most employed strategy is the attachment to the non-viral vector specific ligands (such as transferrin for targeting the SNC) that recognize particular receptors present in the target cells or tissues. As discussed earlier, this approach has proved effective in several studies. Also, in cancer gene therapy, some strategies are based on the exploitation of the tumour-specific physiological changes (the tumour microenvironment) to specifically conduct the nanoparticles to cancer cells [85].

## *Introduction*

On the other hand, another possibility is to introduce modifications in the DNA cargo (instead of the vector) to achieve targeted expression of the transgene, this approach is known as “transcriptional targeting”. This strategy is based on the use of DNA expression cassettes that contain regulatory regions that are recognized by transcription factors specifically present or selectively expressed by the target cell population [85]. In this strategy the DNA would, in theory, be delivered to all tissues, but the expression of the transgene would only occur in the cell populations where the particular transcription factors are present, that is, in the target cell populations [84]. The success of this method of targeting needs prior knowledge of a difference in transcription factor expression between the target and normal tissue [84].

Targeting is an essential requirement in gene delivery systems. Beneficial aspects of targeted gene delivery include, among others, increased bioavailability of the therapeutic product in the diseased tissue; reduced accumulation in healthy tissues and, hence, reduced side effects; reduction of drug dosage and reduced dosing frequency, which enhances patient compliance. All those aspects help to increase the therapeutic efficacy and permit to reduce treatment costs [86].

### **4.2 Duration of gene expression**

Long-term or sustained expression of the transgene delivery constitutes a real challenge in non-viral gene therapy, and it is a considerable limiting factor, since transient expression requires repeated dosing and makes the therapeutic effect unsustainable. Transgene expression can decrease in time due to several factors, including destruction by nucleases, loss by recombination, distribution to non-nuclear compartments and/or recognition and subsequent silencing of foreign DNA [85]. In addition, in dividing cells the percentage of transfected cells decreases at each division, because while cells replicate, plasmids do not.

Strategies to increase duration of transgene expression have focused on plasmid DNA modifications rather than on vector modifications. Some of those strategies are aimed to integrating the transgenes into the host genome using viral integrases, site-specific recombinases and transposases, which are enzymes with capacity of inserting foreign DNA into the host genome [85]. However, this approach cannot be clinically applicable in humans because of its associated risks, such as the induction of insertional mutagenesis in the host cells.

A different strategy to achieve sustained transgene expression is the use of autonomously replicating plasmids or episomes, which does not require integration

## *Introduction*

in the host genome and, hence, avoids insertional mutagenesis risks [85]. In addition, episomally replicating plasmids usually yield high levels of transgene expression. These strategies incorporate genes that encode necessary cofactors for transcription of the plasmid to the therapeutic plasmid DNA, making the transgene expression less dependent on host factors. Incorporation of viral DNA that allows the plasmid to replicate extrachromosomally is an efficient approach, but it presents a major drawback, since those replication-inducing viral DNA elements are associated with induction of immune response and risk of transformation and oncogenicity [85]. Alternatively, mammalian scaffold/matrix attachment regions (S/MARs) have been identified that can be incorporated to plasmid DNA instead of the aforementioned viral sequences. These sequences can also enhance episomal replication of the plasmids, probably by bringing the plasmids into contact with the host replication machinery [73]. Episomally replicating plasmids are especially important in cancer gene therapy, where maintenance and vertical transfer of the therapeutic plasmid will be essential because of the presence of dividing tumour cells [85].

Some other strategies for achieving sustained expression focus on the prevention of transgene silencing, since cellular gene silencing mechanisms can impede transgene expression [85].

Further modifications can be also applied to the therapeutic plasmid DNA in order to increase the strength or the specificity of the therapeutic transgene expression. For instance, positive feedback loops can be incorporated. To do this, a promoter that drives the expression of both the transgene and of a strong artificial transcriptional activator is used. This transcriptional activator is capable of interacting with appropriate binding sites within the promoter and, that way, upregulating transgene expression, as well as its own expression [85]. Technologies incorporating positive feedback loops are estimated to increase strength of weak but highly specific regulatory elements [85].

### **4.3 Toxicity, Manufacturing and Regulatory issues**

Besides from increasing transfection efficiency through targeting and other strategies, careful consideration of toxicity, manufacturing and regulatory issues of non-viral delivery systems is mandatory. Scalability and long-term storage requirements are essential factors to be taken into serious consideration when developing non-viral formulations for potential commercial application and introduction in clinical practice [19]. A generally accepted advantage of non-viral vectors is their ease of large-scale manufacture. However, this can become more

## *Introduction*

complex as formulations increase in complexity, incorporating stabilising components and bioactive targeting ligands.

Regarding toxicity of non-viral vectors, characteristics such as size, charge, surface functionalization, shape and architecture may contribute to the toxicity profile of nanoparticles. Non-viral vectors are thought to cause toxicity through different mechanisms, including membrane destabilisation and lysis, inducing oxidative stress, initiating inflammatory response, inducing global changes in gene expression profiles among others [85]. Also, the properties of the biomaterials used can influence toxicity, depending on the rate of degradation and persistence in organs [19]. Persisting and accumulating biomaterials are more likely to induce an inflammatory response; also, products of the degradation of nanoparticles could potentially cause toxicity. However, knowledge about how non-viral vectors are disassembled and metabolically processed is still very scarce and further research is necessary in this regard [19].

To conclude, the concept of a unique universal non-viral vector is nowadays abandoned, and it is increasingly accepted that future non-viral gene delivery platforms will be based on multifunctional vectors specifically tailored for different applications [1]. However, there are some generally assumed features that all non-viral vectors should accomplish for efficient gene delivery. In short, three main factors should be taken into consideration when developing non-viral gene delivery platforms: (i) formulation components (of both the vector and the DNA) – the nanoparticle should be able to protect DNA over extra- and intracellular barriers and deliver the cargo into the nucleus of target cells; once inside the nucleus, the plasmids can be addressed to the nuclear matrix for episomal replication and sustained expression–; (ii) manufacturing issues – non-viral vector formulations should have potential for scale up–; and (iii) safety and regulatory issues – formulations should be non-toxic, non-immunogenic and should have suitable storage conditions–. Although non-viral vectors are still far from clinical practice, they represent a safer alternative to conventional viral vectors. Several formulations and strategies are under investigation with the aim of overcoming extra- and intracellular barriers, enhancing targeted transfection and, in general, increasing transfection efficiency. In addition, those formulations would ideally be suitable for administration through non-invasive routes, such as the intranasal administration to target the brain, topical ocular administration for the retina and aerosols for pulmonary diseases. Finally, the inclusion of novel functional modules within both the carrier and the DNA molecule will produce a range of non-viral vectors tailored for specific applications,

## *Introduction*

including the safe and long-term expression of therapeutic genes in humans [40]. Therefore, reasonable hope suggests that next generation gene delivery systems may be based on non-viral vector systems tailored for specific applications and suitable for non-invasive administration routes, representing an ideal platform to effectively shuttle the genetic material to target cells in a safe and controlled way.

### **5. ACKNOWLEDGMENTS**

This project was partially supported by the University of the Basque Country UPV/EHU (UFI 11/32), the Basque Government (Department of Education, University and Research, predoctoral PRE\_2014\_1\_433 and BFI-2011-2226 grants), the National Council of Science and Technology (CONACYT), Mexico, Reg. # 217101 and the Spanish Ministry of Education (Grant SAF2013-42347-R). Authors also wish to thank the intellectual and technical assistance from the platform for Drug Formulation (NANOBIOSIS) CIBER-BBN.

***References are listed in pages 85 to 91.***



# **Gene-terapia ez-birala eman-bide ez-inbaditzailak erabiliz**

*Gene Therapy. Principles and Challenges (InTech) liburuan argitaratutako kapituluaren itzulpena (2015)*



Sarrera

## Gene-terapia ez-birala eman-bide ez-inbaditzailaileak erabiliz

*Ilia Villate<sup>a,b</sup>, Gustavo Puras<sup>a,b</sup>, Jon Zarate<sup>a,b</sup>, Mireia Agirre<sup>a,b</sup>, Edilberto Ojeda<sup>a,b</sup>, Jose Luis Pedraz<sup>a,b,\*</sup>.*

*<sup>a</sup> NanoBioCel Group, Laboratory of Pharmaceutics, School of Pharmacy, University of the Basque Country (UPV/EHU), Paseo de la Universidad 7, 01006, Vitoria-Gasteiz, Spain*

*<sup>b</sup> Biomedical Research Networking Center in Bioengineering, Biomaterials and Nanomedicine (CIBER-BBN), Vitoria-Gasteiz, Spain*

---

**Laburpena:** Gene-terapiak interes handia pitzu du azken aldian gaixotasun ezberdinei, genetikoak zein ez-genetikoak, aurre egiteko tratamendu itxaropentsu gisa. Hala ere, bektoreen eraginkortasun faltak eta eman-bide ez-inbaditzailleen beharrak gene-terapiaren erabilera klinikoa oztopatzentz dute oraindik ere. Material genetikoa garraiatzeko erabili daitezkeen molekulen artean, bektore ez-biralak birusak baino seguruagoak dira eta alternatiba egokia izan litezke. Eman-bide ez-inbaditzailleen ikerketek ere aurrera egin dute, esate baterako, sudur-barneko bidea garunera iristeko, eman-bide topiko okularra erretinara iristeko edota inhalazioz hartzeko aerosol erako formulazioak biriketara iristeko. Gaur egungo zantzuen arabera, datorren belaunaldiko gene-garraiorako sistemak bektore ez-biraletan oinarrituta egongo dira eta eman-bide ez-inbaditzaleetatik emateko egokiak eta seguruak izango dira. Errebisio-lan honetan, gene-terapiaren kontzeptua labur berrikusi ondoren, gene-transferentziaren eraginkortasuna hobetzeko gaur egungo eta etorkizuneko estrategiak deskribatuko ditugu.

**Hitz gakoak:** gene-terapia, bektore ez-birala, zelulaz kanpoko eta barneko hesiak, eman-bide ez-inbaditzailaileak.

## 1.SARRERA

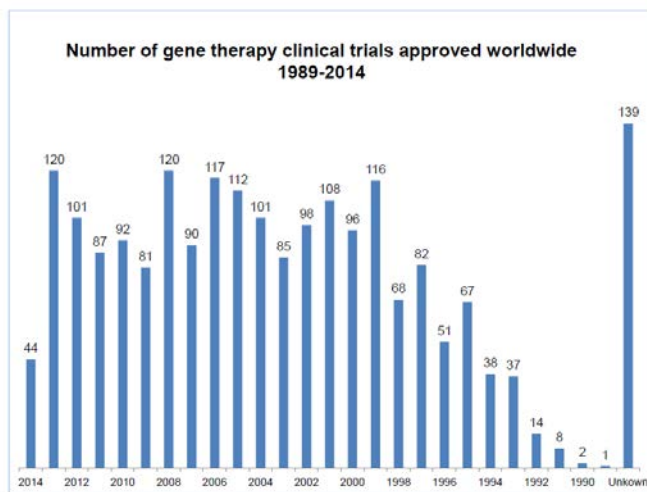
### 1.1. Gene-terapiaren kontzeptua eta eboluzio historikoa

Orohar, gene-terapia gisa ezagutzen da material genetiko arrotza zeluletan txertatzea horien proteina-espresioa aldatzeko edota kontrolatzeko, eta helburu esperimentalak zein terapeutikoak izan ditzake<sup>1</sup>. Gaur egun, Giza Genomaren Proiektuari eta biologia molekularrean egindako aurrerapenei esker, hobeto ulertzten dira prozesu zelularrak nahiz patologikoak, eta estrategia terapeutikoen jomuga izan litzkeen hainbat gene identifikatu ahal izan dira. Gainera, azido nukleikoen garraiatzaile gisa jarduten duten molekulak edo bektoreak etengabe garatzen eta hobetzen ari dira, eta horrek gene terapeutikoak modu eraginkorrean jomuga diren zeluletara garraiatzea ahalbidetzen du, gene-terapiaren oinarritutako estrategiak errealitate klinikora gero eta gehiago gerituratz.

Hala ere, oraindik gutxi dira entsegu klinikoetara edota merkatura iritsi diren gene-terapiaren oinarritutako produktuak. Metodo honen potentziala DNAREN egitura deskribatu eta denbora gutxira plazaratu zen eta gene-terapia kontzeptua 1960 eta 1970 hamarkaden artean sortu zen<sup>2</sup>. Gene-terapiaren oinarritutako lehen entsegu arrakastatsua 1990. urtean iritsi zen, *National Institute of Health* erakundearren eskuistik. Entsegu hartan, adenosina desaminasa (ADA) genearen mutazioak eragiten duen immunodefizientzia konbinatu larria (ingelesez SCID siglaz ezaguna) sendatzea lortu zen<sup>3</sup>. Zoritzarrez, 1991. urtean jazotako gertaera larri batek gene-terapiaren segurtasuna kolokan jarri zuen. Izan ere, hemezortzi urteko mutil bat hil egin zen gene-terapiaren entsegu kliniko batean boluntario gisa parte hartu eta gero<sup>4</sup>. *Food and Drug Administration* (FDA) erakundearren ikerketen arabera, entsegu kliniko hura aurrera eraman zuten ikertzaileek ez zituzten aurreikusi albo-ondorio larriak eta ez zituzten bete parte-hartzaleen segurtasuna bermatzeko neurriak<sup>4</sup>. Kasu tragiko horrek atzerapauso handia eragin zuen gene-terapiaren arloko ikerketan.

Gaur egun, *The Journal of Gene Medicine* aldizkariak 2014ko ekainean eguneratutako datuen arabera<sup>5</sup>, 1989. urtean lehen gene-terapiako entsegu klinikoa egin zenetik, beste 2.000 entsegu kliniko baino gehiago baimendu dira mundu-mailan (1. irudia). Entsegu horiek batez ere ondorengo gaixotasunen sendabideak lortzera zuzenduta daude (2. irudia): minbizia (baimendutako entseguen %64,1), eritasun monogenikoak (%9,1), gaixotasun infekziosoak (%8,2) eta bihotzko gaitzak (%7,8). Neurri txikiagoan bada ere, gaixotasun neurologikoak (%1,8) eta erretinakoak (%1,6) ere aztergai dira gene-terapia bidezko entsegu klinikoetan. Hala

eta guztiz ere, gutxi dira oraindik merkatura edota entsegu klinikoen laugarren fasera iritsi diren produktuak (3. irudia). 2012. urtean, Europako Medikutza Agentziak (EMA) lehenbiziko aldiz gene-terapiaren oinarritutako medikamentu bat merkaturatzea baimendu zuen Europan. Produktu horrek, Glybera® izenekoak, birus adeno-asoziatua darama bektore gisa eta ingeniaritza genetikoaren bidez lipoproteina lipasa entzimaren genea garraiatzeko diseinatua izan zen<sup>5</sup>.

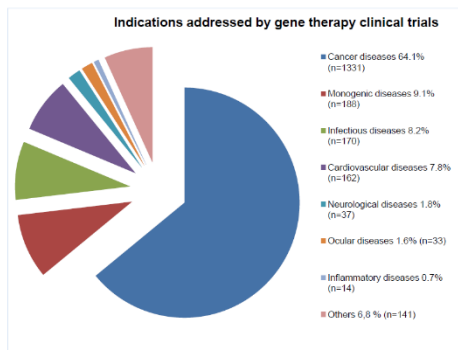


**1.Irudia:** Mundu-mailan 1989-2014 urteen artean baimendutako gene-terapia bidezko entsegu klinikoak. (Ondorengo estekatik moldatua: <http://www.wiley.co.uk/genmed/clinical>).

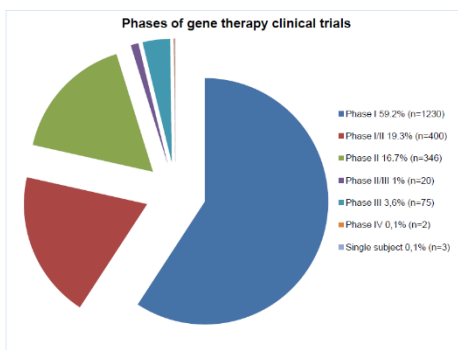
## 1.2. Gene-garraiatzaileen beharra

Gene-terapiaren erabilera mugatzen duen faktore nagusia gene-garraiatzaile eraginkor eta seguruuen eskasia da. Gene terapeutikoak zeluletara garraiatzen dituzten molekulak bektoreak dira, eta honako funtzioren hauetako betetzeko gai izan behar dira: (i) azido nukleikoak odoleko nukleasengandik babestea, (ii) material genetikoa zeluletan barneratzea eta (iii) azido nukleikoak zelula-barneko gune egokian askatzea<sup>1</sup>. Horrez gain, gene-garraio sistema idealak efizienteak, espezifikoak, iraunkorak, seguruak, erabilerrazak eta merkeak izan beharko lirateke [6]. Orokorrean, bektoreak bi multzo nagusitan sailkatzen dira: biralak eta ez-biralak. *The Journal of Gene Medicine* aldizkariak 2014an argitaratutako datuen arabera<sup>7</sup>, gaur egun baimendutako gene-terapia bidezko 2.000 entsegu klinikoen artean, %70ak bektore biralak erabiltzen ditu (4. irudia). Beste %17,7ak DNA biluzia edo askea erabiltzen du eta soilik %5,3ak lipofekzioa<sup>7</sup>.

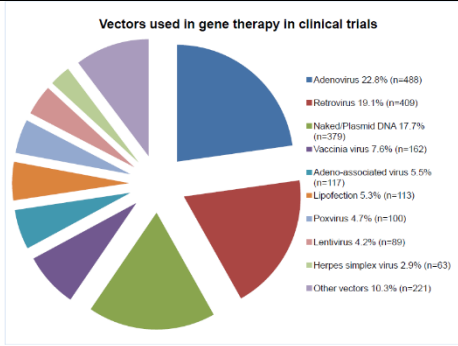
## Sarrera



2. Irudia. Gene-terapiako entsegu klinikoetan sendatu nahi diren gaixotasunak. (Ondorengo estekatik moldatua: <http://www.wiley.co.uk/genmed/clinical>).



3. Irudia. Gene-terapiako entsegu klinikoen fase klinikoak. (Ondorengo estekatik moldatua: <http://www.wiley.co.uk/genmed/clinical>).



4. Irudia. Gene-terapiako entsegu klinikoetan erabilitako bektoreak. (Ondorengo estekatik moldatua: <http://www.wiley.co.uk/genmed/clinical>).

## Sarrera

Beraz, gaur egun oraindik ere bektore biralak dira nagusi gene-terapia entseguetan, batez ere eraginkortasun handiena dutenak direlako. Hala ere, bektore ez-biralak alternatiba seguru eta merkeago gisa sortu dira, eta gero eta ikerketa talde gehiagok horien aldeko apustua egin dute. Horrez gain, eman-bide ez-inbaditzileen ikerketak ere pisu handia hartu du azken urteotan, adibidez, sudur-barneko administrazioa garunera iristeko, topikoa erretinarako edota aerosol erako formulazioak biriketarako. Zantzu askoren arabera, etorkizunean gene-garraioa eman-bide ez-inbaditzaietatik administratu daitezkeen bektore ez-biralen bidez egingo da, eta plataforma terapeutiko seguruak, eraginkorrik, erabilerrazak eta individualizatuak eskainiko dituzte. Bestalde, bektore ez-biralak multifuntzionalak eta aplikazio bakoitzerako modu espezifikoan moldatuak izan beharko dira<sup>1</sup>.

### 1.2.1. Bektore biralak

Errebisio honetan bektore ez-biralen gainean jardungo dugu, baina komeni da birusen ezaugarri nagusiak labur aipatzea ere. Birusak sistema biologiko konplexuak dira eta euren eboluzio-prozesua material genetikoa zeluletan ahalik eta modu eraginkorrenean txertatzera zuzenduta egon da, horretan oinarritzen baita euren ugaltzeko gaitasuna<sup>8</sup>. Beraz, alde horretatik, birusak erreminta ezin hobeak dira material genetiko terapeutikoa zeluletara bideratzeko gene-terapien<sup>1</sup>. Hala ere, bektore biralek hainbat desabantaila ere badituzte, adibidez, ezin dituzte tamaina handiko DNA molekulak garraiatu, euren produkzioa oso konplexua eta garestia da eta, gainera, ez dira guztiz seguruak giza-genoman modu aleatorioan txertatu ezkerro mutagenesia eragin dezakete eta. Horrez gain, gizakion sistema immunologikoak birusak identifikatu eta erasotu egiten ditu eta, horrek, bektore biralen eraginkortasuna gutxitu dezake<sup>1</sup>. Honenbestez, birusak erreminta sendoak izan daitezke geneen garraiorako, baina erabilera klinikorako mugak ere badituzte. Ondorengo taulan gehien erabiltzen diren bektore biralen ezaugarri nagusiak laburbiltzen dira, baita bakoitzaren abantaila eta desabantaila nagusiak ere.

BEKTORE BIRALA	INTEGRAZIOZKOA /EPISOMALA	ERABILERA	DESABANTAILAK
ADENO BIRUSA	<b>Episomala</b>	<b>Eraginkorra ehun gehienetan</b>	<b>Hantura erantzuna eragiten du</b>
ADENO- ASOZIATUA	<b>&gt;%90 episomala</b>	<b>Ez du hanturarik sortzen</b>	<b>Karga-gaitasun baxua (&lt;5 Kb)</b>

ERRETROBIRUSA	<b>Integraziozkoa</b>	Gene-espresio iraunkorra	Soilik zatitzen ari diren zelulen transfekzioa, mutagenesi arriskua
LENTIBIRUSA	<b>Integaziozkoa</b>	Tropismo zabala, expresio iraunkorra	Mutagenesi arriskua
HERPES SIMPLEX	<b>Episomala</b>	150 kb karga-gaitasuna	Hantura erantzuna eragiten du

**1.Taula.** Gene-terapien gehien erabiliak diren bektore biralak, abantailak eta desabantailak. (8. erreferentzian oinarrituta).

---

### 1.2.2. Bektore ez-biralak

Bektore ez-biralak birusak ordezkatu ditzaketen alternatiba seguruagoak, merkeagoak eta errazago ekoiztu daitezkeenak dira. Izan ere, bektore ez-biralak eskala industrialetan produzitu daitezke erreprodukzio handiarekin eta kostu onargarriekin, egonkorak dira biltegiratzean, behin eta berriro hartu daitezke erantzun immunerik eragiteko arriskurik gabe eta garraiatu dezaketen material genetikoaren tamaina mugagabea da<sup>1, 9</sup>. Hala ere, ez dira birusak bezain eraginkorrik dira eta horrek bektore ez-biralen erabilera mugatzen du<sup>1</sup>.

Bektore ez-biralak bi kategoria nagusitan sailkatu daitezke, metodo fisikoetan ala kimikoetan oinarritzen diren kontuan hartuta. Jarraian, bektore ez-biral nagusiak aipatuko ditugu.

#### 1.2.2.1. Metodo fisikoak

Gene-terapiarako metodo fisiko gehienek indar fisikoa erabiltzen dute zelula-mintzetan aldi baterako poroak sortzeko eta bertatik material genetiko arrotza zeluletan barneratzeko<sup>6, 10</sup>. Metodo hauetan, ez dira partikula-sistema erabiltzen azido nukleikoak garaiatzeko, baizik eta indar fisikoa aplikatuz burutzen da gene

transferentzia<sup>6</sup>. Horren adibide dira orratz bidezko injekzioa, injekzio balistikoa, elektroporazioa, fotoporazioa, magnetofekzioa eta hidroporazioa<sup>6, 11</sup>.

### 1.2.2.2. Metodo kimikoak

Ezaugarri kimikoaren arabera, metodo hauek hiru multzotan sailkatzen dira: lipido kationikoak, polimero kationikoak eta partikula inorganikoak. Lipido eta polimero kationikoetan oinarritutako bektore ez-biralek partikula kondentsatuak eratzen dituzte karga negatiboa duten DNA molekulekin indar elektrostatikoen bitartez<sup>10</sup>. Elkarrekintza horien ondorioz eratzen diren partikulek DNA molekulak babesten dituzte nukleasen eraginetik eta zeluletan barneratzea ahalbidetzen dute<sup>10</sup>. Ondorengoak dira bektore ez-biral kimiko ezberdinen ezaugarri nagusiak:

- Lipido kationikoetan oinarritutako bektoreak

Lipofekzioa edo lipido kationiko bidezko transfekzioa da gene-garraio ez-biral nagusia (4. irudia). Lipido kationiko guztiak lau domeinu funtzional dituzte: (i) buru hidrofilikoa –DNA molekulekin elkarrekintza elektrostatikoa ahalbidetzen dituena-, (ii) domeinu hidrofobikoa –normalean hidrokarburo kate alifatikoen eratorria-, (iii) egitura lotailua –lipido kationikoaren malgutasuna, egonkortasuna eta biodegradagarritasuna baldintzatzen dituena- eta (iv) *bizkarrezur* deritzon domeinua –buru hidrofilikoaren eta domeinu hidrofobikoaren artean kokatua, orokorrean glizerol edo serinol talde batez osatuta egoten da<sup>12</sup>. Domeinu horietan egindako aldaketek bektoreen transfekzio eraginkortasuna aldatu dezakete. Gene-terapien erabiltzen diren eta lipido kationikoetan oinarritutako formulazio nagusiak ondorengoak dira: (i) liposomak –fosfolipidoz osatutako besikulak-, (ii) niosomak –tentsoaktibo ez-ionikoz osatutako besikulak, liposomak baino egonkorragoak- eta (iii) nanopartikula lipidiko solidoa (SLN) –nukleo solidoa duten eta surfaktantez egonkortutako partikulak-.

- Polimero kationikoetan oinarritutako bektoreak

Orokorrean, polimero kationikoetan oinarritutako partikulak esferikoak izaten dira eta 1-1000 nm arteko tamaina izaten dute. DNA molekulak matrize polimerikoan txertatzen dira edota partikulen gainazalean konjugatzen dira, poliplexoak eratuz. Egitura horiek material genetikoa nukleasen degradaziotik babesten dute<sup>6</sup>. DNA garraiatzeko gehien erabiltzen diren polimero kationikoak ondokoak dira: (i) poli(etileno imina) edo PEI –tanpoi gaitasun handikoa-, (ii) kitosanoa –polisakarido lineala, kitina naturalaren desazetilaziotik eratorria-, (iii) ziklodextrinak –

oligosakarido zikliko naturalak-, (iv) dendrimeroak –zuhaitz itxurako molekula sintetikoak, adarkatze egitura erregularrak dituztenak- eta (v) poli(L-lisina) edo PLL –polinukleotidoekin nanometro tamainako egiturak osatu ditzakeena amina protonagarriei esker<sup>6, 13, 14</sup>.

- Nanopartikula inorganikoetan oinarritutako bektoreak

Nanopartikula inorganikoak tamaina, forma eta porositate ezberdineko nanoegiturak dira, eta erabilienak kaltzio fosfatoa, silizea, urea eta hainbat elementu magnetiko dira<sup>6, 15</sup>. Partikula inorganikoak erraz prestatu eta funtzionalizatu daitezke eta ez dute mikrobio-erasorik jasaten<sup>6, 16</sup>.

Beraz, gene-garraiorako bektore ez-biralak birusak baino alternatiba seguruagoa dira. Hala ere, nahiz eta arlo horretan asko aurreratu den azken urteotan, bektore ez-biralen erabilera klinikoa oraindik ere mugatuta dago eraginkortasun falta dela eta. Errebisio honetan, gene-transferentzia hobetzeko gaurko eta etorkizuneko estrategiak eztabaidatuko ditugu, betiere bektore ez-biralak eta eman-bide ez-inbaditzaileak oinarri hartuta. Lehenengo, bektore ez-biralek gainditu beharreko zelula-barneko hesiak deskribatuko ditugu. Jarraian, zelulaz kanpoko hesiak aipatuko ditugu, eta hesi horiek gainditzeko eman-bide inbaditzaile eta ez-inbaditzaileen gainean jardungo dugu. Azkenik, bektore ez-biralek klinikara iristeko dituzten erronkak eztabaidatuko ditugu, batez ere, transfekzio eraginkortasunari, jomugara zuzentzeari eta gene-espresioaren iraunkortasunari dagokionean.

## 2. ZELULA-BARNEKO HESIAK ETA TRANSFEKZIO ERAGINKORTASUNA HOBETZEKO ESTRATEGIAK

Transfekzio eraginkortasuna baldintzatzen duen faktore nagusia sistema ez-biralak zelula-barneko zein kanpoko hesiak gainditzeko duen gaitasuna da. Atal honetan, bektore ez-biralek gene-transferentzia eraginkorra lortzeko gainditu beharreko zelula-barneko hesi nagusiak eta horretarako estrategiak deskribatuko ditugu. Zelula-barneko hesiak dira zelula-mintzetik nukleorainoko bidean bektore ez-biralek gainditu beharreko oztopoak. Hesi horien ezaugarri molekularrak ezagutzea ezinbestekoa da horiek gainditzeko gai izango diren bektoreak diseinatu ahal izateko. Beraz, atal honetan zelulan barneratzeko eta nukleoraino iristeko bide ezberdinak deskribatuko ditugu, eta endosomatik ihesa zein nukleorako sarrera areagotzeko hainbat estrategia aipatuko ditugu, horiek baitira gene-transferentziaren eraginkortasuna handitzeko gako nagusiak.

## 2.1. Zelulan barneratzeko bideak

Zelula-mintzarekiko asoziazioa da lehen hesia, eta bektore ez-biralak DNA molekularekin osatzen duten partikulek jarraian hartuko duten zelula-barneko ibilbidea baldintzatuko duen faktore nagusia da<sup>17</sup>. Zelula-mintzarekin bertako errezeptoreen bitartez edota modu independentean lotu daitezke bektore ez-biralak. Errezeptoreekiko modu independentean gertatzen diren asoziazioak erakarpen elektrofilikoaren bitartez gauzatzen dira, karga positiboa duten partikulen (adibidez, poliplexo edota lipoplexo kationikoak) eta karga negatiboa duten zelula-mintzeko proteoglikanoen artean<sup>18</sup>. Lotura-modu horren bitartez zelula-mota ugariren transfekzioa gauzatu daiteke *in vitro*, baina *in vivo* egin ahal izateko prozesuak optimizazio handiagoa eskatzen du. Izan ere, gene terapeutiko bat ehun jakin batera transferitzeko, zelula-lotze ez-espezifikoak direla eta dosi oso altuak eta, ziurrenik, toxikoak beharko lirateke. Hori ekiditeko, estekatzaile zehatzak edota antigorputzak gehitu dakizkieke bektore ez-biralei ehun- edo zelula-espezifikotasuna lortzeko<sup>18</sup>. Esate baterako, transferrina (Tf) izeneko proteina burdin-garaiatzalea erabili daiteke bektore ez-biralak garunera bideratzeko, proteina horren errezeptorea neuronek eta hesi hematoentzefalikoko zelula endotelialek agertzen baitute<sup>19</sup>. Erabilitako estekatzailearen aukeraketa ez da soilik iritsi nahi den zelula-motaren araberakoa, baizik eta baita behin zelulari lotuta abiaraziko duen zelula-barneko ibilbidearen araberakoa ere. Hurrengo atalean aipatuko den bezala, bektore ez-biralak jarraituko duen ibilbide endozitikoa honi gehitutako estekatzaileak baldintzatuta egon daiteke.

Behin zelula-gainazalean lotuta, bektore ez-biralek mintz plasmatikoa zeharkatu behar dute zelulan sartzeko, trafiko intrazelularra abian jartzeko eta nukleoraino iritsi ahal izateko. Endozitosi deritzo partikulak zeluletan zelula-mintzaren inbaginazioaren bidez barneratzeari eta zelula barneko ibilbidea inbaginazio horretatik sortutako besikulen baitan egiteari<sup>20</sup>. Hori izaten da bektore ez-biralek jarraitzen duten bidea. Lau endozitosi mota nagusi daude: klatrina bidezko endozitosia (CME), kabeola bidezko endozitosia (CvME), fagozitosia eta makropinozitosia<sup>17, 21</sup>. Ibilbide endozitiko horiek jarraian azaltzen dira.

### 2.1.1. Klatrina bidezko endozitosia

Klatrina bidezko endozitosia (CME) oso prozesu erregulatua eta energia-dependentea da eta, gainera, hobekien ezagutzen den ibilbide endozitikoa da<sup>20</sup>. Lehen pausua CME ibilbidean partikuletako estekatzaile baten eta zelula-mintzeko errezeptore baten arteko lotura sendoa da. Horrek klatrina estrukturen metaketa

lokalizatua abiarazten du zelula-mintzaren alde zitoplasmaticoan, mintz plasmaticoaren deformazioa eraginez eta 100-150 nm arteko inbaginazio bat eratuz<sup>22</sup>. Klatrina pilaketak jarraitu ahala, inbaginazio horiek gero eta gehiago barneratzen dira zitoplasman, azkenean mintz plasmaticotik askatu arte eta klatrinaz bildutako besikula zitoplasmaticoak sortu arte<sup>20</sup>. Jarraian, klatrina desegin egiten da eta besikulak endosoma goiztiar bilakatzen dira. Besikula mintz plasmaticotik askatzeko beharrezkoa da GTPasa mota bat, dinamina izenekoa<sup>23</sup>. Horrez gain, dirudienez kolesterolak ere paper garrantzitsua jokatzen du besikularen eraketan, kolesterolik gabe besikulak ez baitira gai zelula-mintzetik askatzeko<sup>24</sup>.

Ibilbide honetako hurrengo pausuan, endosoma goiztiarrak heldu eta endosoma berantiar bilakatzen dira eta, jarraian, horiek lisosomekin bat egiten dute<sup>25</sup>. Endosoma goiztiarretatik endosoma berantiarretarako heltze prozesuan, protoi bonbek konpartimentuko azidifikazioa eragiten dute eta endosometatik lisosometarako trantsizioan pH-aren balioa are gehiago jaisten da 5era iritsi arte<sup>20</sup>. Endosometako pH azidoak, dirudienez, estekatzaile eta errezeptoreen arteko disoziazioa eragiten du. Autore gehienen esanetan, endosomatik ihes egiteko mekanismorik ez badago, bektore ez-biralek eta DNA molekulek osatutako partikulak harrapatuta geratzen dira lisosometan eta bertan degradatzen dira azidotasunaren eta aktibilitate entzimaticoaren eraginez, nukleora iristeko aukerarik gabe<sup>20</sup>.

Beste autore batzuen arabera, berriz, bektore ez-biralen konposizioaren arabera, kasu batzuetan CME ibilbidea egokiena litzateke transfekzio eraginkortasun altua lortzeko, lisosometako giroak bektore ez-biralen eta DNA molekulen arteko lotura askatzea ahalbidetzen duelako, DNA molekulak aske utzi nukleoraino iristeko<sup>26</sup>. Bektorearen ezaugarrien arabera, zelula barneko ibilbide bat edo bestea jarraitu dezake<sup>26</sup> eta beharrezkoa da bektore ez-biralek bide ezberdinak ezagutzea bektore eraginkorragoak diseinatu ahal izateko.

### **2.1.2. Kabeola bidezko endozitosia**

Kabeola bidezko endozitosia (CvME) kabeola izeneko zelula-mintzeko mikrodomeinuetan hasten da. Horiek zelula-mintzaren inbaginazio txikiak eta hidrofobikoak dira, kolesterol eta esfingolipido ugari dituztenak<sup>17, 20</sup>. Aurreko ibilbidea bezala, CvME ere estekatzaile bidezko eta dinamina proteinaren akzioa behar duen ibilbide endozitikoa da, kolesterolak ere paper garrantzitsua jokatzen duelarik<sup>27</sup>. Klatrina bidezko endozitosiarekin alderatuta, ezberdintasun nagusia da kabeola bidezkoan ez dela endosomarik sortzen, baizik eta kabeosoma izeneko besikulak

sortzen dira eta horiek, autore gehienen arabea, ez dira lisosomekin elkartzen<sup>17</sup>. Beraz, lisosoma barruko DNA molekulen degradaziorik ez da espero ibilbide honetan. Orokorean, CvME ibilbide ez-azidiko eta ez-digestibotzat hartzen da, alegia, degradaziorik gabeko ibilbidetzat<sup>17, 28</sup>. Hala ere, kontu hori ez dago erabat argi eta debatea zabalik dago, ikertzaile batzuek argitaratu baitute kasu batzuetan kabeosomek lisosomekin bat egiteko joera dutela<sup>29</sup>. Beraz, ikerketa sakonagoak beharrezkoak izango dira auzi hori argitzeko.

### 2.1.3. Fagozitosia

Fagozitosia endozitosi mota berezia da, gehienbat horretan espezializatutako zelula taldeek burutzen dutena, hala nola, makrofagoek, monozitoek, neutrofiloek eta zelula dendritikoek, nahiz eta beste zelula talde batzuk ere burutu dezaketen<sup>17</sup>. Zelula-mintzaren luzapenen bitartez (normalean 1 µm ingurukoak edo luzeagoak) bideratzen da fagozitosia eta batez ere partikula handiak irenstekeko balio du, besteak beste, bakterioak eta zelula hilak, eta baita tamaina handiko lipoplexo eta poliplexoak irensteke ere<sup>17</sup>.

Fagozitosiak normalean hiru fase izaten ditu, molekula guztientzat –bektore ez-biralak barne- berdinak direnak. Lehenbizi, opsoninek bektore ez-biralak eta DNA molekulak osatutako partikulak antzematen dituzte eta opsonizatu egiten dituzte odolean. Jarraian, partikula opsonizatuak makrofagoen gainazalari lotzen zaizkio antigorputzen atal konstantearen eta makrofagoen zelula-mintzeko errezeptoren arteko interakzioaren bidez<sup>17</sup>. Atal konstanterik gabeko antigorputzak bektore ez-biralei txerta dakizkie *in vivo* makrofagoek antzeman ez ditzaten eta beste zelula batzuetara iritsi daitezzen<sup>30</sup>.

Azkenik, makrofagoen errezeptoren aktibazioak Rho familiako GTPasak aktibatzen ditu, eta horiek aktinaren antolaketa eta zelula-mintzaren luzapenen eraketa abiarazten ditu<sup>17</sup>. Horrela, makrofagoek bektore ez-biralak eta DNA molekulak osatutako partikulak irensten dituzte<sup>20</sup>. Zelulan fagozitosi bidez barneratzen diren besikulei fagosoma deritze eta 0,5 – 1,0 µm arteko diametroa izaten dute<sup>20</sup>. Fagosomek, heltzean, lisosomekin bat egiten dute eta, beraz, azidifikazio prozesua jasaten dute<sup>20</sup>. Horrenbestez, litekeena da bide endozitiko honen bitartez zelulan barneratutako bektore ez-biralak eta DNA molekulak ere lisosometan degradatzea<sup>31</sup>.

#### **2.1.4. Makropinozitosia**

Makropinozitosia fase fluidoko endozitosi-mota da, eta era ez-espezifikoan elementu fluidoak barneratzen ditu zeluletan<sup>17</sup>. Fagozitosian bezala, makropinozitosian ere aktina filamentuek sortutako mintz-luzapenek hartzen dute parte. Hala ere, kasu honetan protuberantziek mintz plasmatikoarekin bat egiten dute azkenean (5. irudia). Makropinozitosian sortzen diren besikulei makropinosomak deritze eta, nahiz eta tamaina heterogeneoak ager ditzaketen, normalean 0,2 µm inguruko diametroa izaten dute<sup>32</sup>. Gainontzeko endozitosi-motak bezala, makropinozitosia ere GTPasa proteinen menpeko prozesua da eta proteina horiek beharrezkoak dira besikulak zelulen barnean mintz plasmatikotik askatzeko<sup>17</sup>.

Makropinosomen eta lisosomen arteko konexioa ez da oraindik ezagutzen. Ikerketa batzuek diotenez, makropinosoma goiztiarrek eta endosoma goiztiarrek markatzaile berdinak aurkezten dituzte eta gauza bera gertatzen omen da makropinosoma berantiarren eta lisosomen artean ere<sup>17</sup>. Hala ere, hainbat ikerketak erakutsi dute makropinosomek patu ezberdinak izan ditzaketela zelula motaren arabera eta ez dutela beti lisosomekin bat egiten, nahiz eta oraindik asko dagoen ikertzeko arlo horretan ere<sup>17</sup>.

#### **2.2. Endosomatik ihes egiteko mekanismoak**

Esan bezala, bektore ez-biral gehienak klatrina bidezko endozitosiz barneratzen dira zeluletan. Horren arazoa da endosomatik ihes egin ezean, lisosomara iritsiko direla eta bertan degradatuak izango direla. Hori ekiditeko, bektore ez-biralek endosomatik ihes egiteko hainbat estrategia garatu dira.

Patogeno askok, batez ere birusek eta bakterioek, endosomatik ihes egiteko mekanismoak garatu dituzte eboluzioan zehar. Endosomatik ihes egiteko gaitasuna duten molekula asko birusetan (adib. influenza birusaren hemaglutinina), bakterioetan (adib. difteria toxina), landareetan (adib. errizinoa), gizakian (adib. fibroblastoen hazkuntza faktorea) edota animalietan (adib. erleen pozoitik ateratako melitina) aurki daitezke<sup>33</sup>. Molekula horien funtzionamendua ulertzear ahalbidetzen du bektore ez-biralentzako endosomatik ihes egiteko estrategia berriak sortzea. Gaur egun, sekuentzia eta luzera jakineko peptido sintetikoak (adib. Sweet Arrow Peptide edo SAP anfipatikoa) eta agente kimiko espezifikoak (adib. poli(etileno imina) edo PEI polimeroa) erabiltzen dira endosomatik ihesa bultzatzeko<sup>33</sup>. Datozen paragrafoetan endosomatik ihes egiteko erabiltzen diren estrategia nagusiak deskribatzen dira.

### **2.2.1. Endosoma-mintzean poroak eratzea**

Poro-eraketa mintzaren tentsioaren eta tentsio linealaren arteko erlazioan oinarritzen da. Zenbait peptidok afinitate handia dute poroen ertzarekiko eta tentsio linearraren jaitsiera eragiten dute<sup>33</sup>. Hainbat ikerketaren arabera, peptido kationiko anifilikoak mintz plasmatikora lotzeak barne-tentsio handia eragiten du, poroak sortzeko gai dena<sup>33</sup>.

### **2.2.2. pH indargetzailea (protoi-esponja efektua)**

Endosomatik ihes egiteko mekanismo honetan, endosomako pH baxuak bertako elementuen protonazioa eragiten du, gaitasun indargetzaile handia izango dutenak. Protonazioak ioien ( $H^+$  eta  $Cl^-$ ) eta uraren barne-fluxua eragiten du, endosomaren hantura eta haustura eragiten dituena<sup>33</sup>.

Mekanismo hori protoiak indargetzeko gaitasuna duten hainbat polimero kationikorekin ikusi da pH tarte zabalean<sup>34</sup>. Polimero horiek protonatu daitezkeen amina binarioak edo tertziarioak izan ohi dituzte, pKa balioa endosomaren pH mailatik gertu dutenak. Esan bezala, endosomen heltze prozesuan ATPasa protoi bonbek protoiak barneratzen dituzte zitosomektik endosomara, barneko azidifikazioa eraginez. Une horretan, polimero kationikoak protonatu egiten dira endosomako pH-a mantentzeko, baina horrek protoi gehiagoren sarrera eragiten du, konpartimentua are gehiago azidotuz<sup>34</sup>. Presio osmotiko altuak endosomen hantura eta apurketa eragiten du, barruko elementuak zitoplasmara jaurtiz<sup>34</sup>. Histidina daukaten molekulek efektu indargetzailea dute<sup>33</sup> eta, beraz, bektore ez-biraletan txertatu daitezke hauek ere endosomatik ihes egiteko gai izan daitezzen.

### **2.2.3. *Flip-flop* mekanismoa**

Edozitosi bidez barneratutako lipoplexoentzat erabilgarria izan daitekeen mekanismoa da hau. Endosoma barruko lipoplexoetako lipido kationikoen eta endosomako mintzeko lipido anionikoen artean elkarrekintza elektrostatikoak sortzen dira, bi mintzen arteko interakzioa eta fusioa sortuz eta, horrela, material genetikoa zitoplasmara askatuz<sup>34</sup>.

### **2.2.4. Endosoma-mintzarekin fusioa**

Mekanismo hau zeluletan barneratzeko peptido edo CPP (*cell penetrating peptides*) izeneko molekulen erabileran oinarritzen da. CPP-ak uretan disolbagarriak eta partzialki hidrofobikoak dira eta birusetan aurki daitezke. CPP-en ezaugarri nagusia

## Sarrera

mintz plasmatikoan kalterik sortu gabe zeluletan barneratzeko gaitasuna da, eta elektrostatikoki edo kobalenteki lotutako molekulak barneratu ditzakete eurekin batera (proteinak, peptidoak eta azido nukleikoak) eraginkortasun handiarekin eta toxikotasun baxuarekin<sup>35</sup>. Hala ere, ez da oraindik ezagutzen CPP-ek zelulan barneratzeko erabiltzen duten mekanismo zehatza. Izen ere, ikerketa batzuen arabera, energiaren menpeko prozesua da eta, beste batzuen arabera, mekanismo energia-independentea da. Gaur egun uste da batez ere endozitosi bidez barneratzen direla zeluletan, baina baldintza esperimentalen arabera bide bat edo gehiago har ditzakete. Beraz, ikerketa sakonagoak behar dira prozesu horiek argitzeko.

Irizpide ezberdinak daude CPP-ak sailkatzea, baina, orokorrean, bi multzotan sailkatzen dira<sup>36</sup>: (i) arginina eta lisina aminoazidoak dituzten peptido kationikoak eta (ii) peptido anfipatikoak. Adibidez, bektore ez-biralen endosomatik ihes egiteko gaitasuna handitzeko birusetatik eratorritako TAT izeneko transkripzio aktibatzaila erabiltzen da<sup>33, 37</sup>. Bestalde, bigarren kategoriarri dagokion SAP peptidoa ere erabiltzen da<sup>38</sup>.

### 2.2.5. Endosoma-mintzaren haustura fotokimikoa

Barneratze fotokimikoa argiaren bitartez gauzatzen den mekanismoa da eta elementu fotosensibilizatzailak erabiltzen ditu molekulek mintza zeharkatu ahal izateko [34]. Fotosensibilizatzailak elementu anfifilikoak dira eta mintz plasmatikoan txertatu daitezke. Elementu horiek endozitosi bidez barneratzen dira bektore ez-biralekin batera eta egoera inaktiboan jarraitzen dute beren absorzio espektroko argi uhinek aktibatzen dituzten arte<sup>39</sup>. Orduan, oxigeno errektibo espezieak eratzen dituzte, endosomen haustura eraginez. Horrela, endosomako molekulak zitoplasmara askatzen dira<sup>34</sup>.

Orohar, uste da endosomatik ihes egiteko gaitasuna faktore oso garrantzitsua dela gene-transferentzia eraginkortasunez gauzatzeko. Hala ere, endosomatik ihes egiteko ahalmena duten molekula seguruak eta erabilerrazak behar dira klinikan erabiliko diren bektore ez-biraletan txertatzeko.

### 2.3. Nukleora sarrera

Aurreko atalean aipatu dugu zer mekanismoren bitartez egin dezaketen ihes bektore ez-biralek endosomatik transfekzio eraginkortasuna handiagotzeko. Hala ere, beste pausu bat ere beharrezkoa da gene-transferentzia egiteko: material genetikoa

## Sarrera

nukleoan sartzea. Horretarako ere hainbat estrategia daude eta atal honetan deskribatuko ditugu.

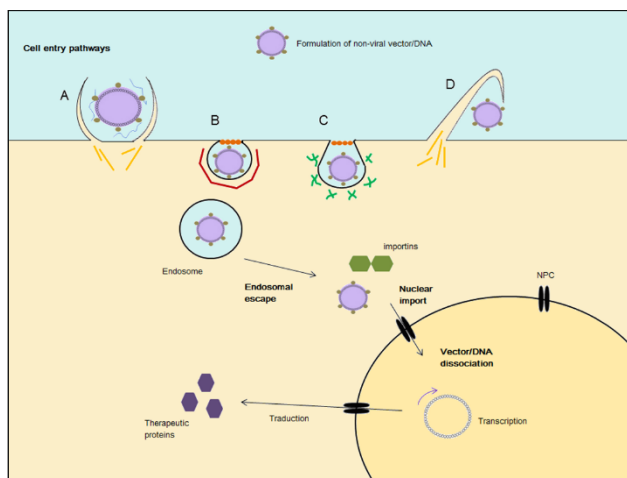
Nukleoan sartzeko, molekulek nukleo-poro konplexuak (NPC) zeharkatu behar dituzte. Horiek egitura multimerikoak dira eta 9 nm-ko kanal bat daukate erdian, 45 kDa baino gutxiago duten molekulei difusio pasiboz nukleoan sartzen uzten diena<sup>40</sup>. DNA molekula biluzien kasuan, 300 bp baino gutxiagoko molekulak ere difusio pasiboz pasatu daitezke, baina molekula handiagoak ezin dira sartu zelulak ez badira zatiketa mitotikoa egiten ari<sup>40-42</sup>. Zelularen zatiketa prozesuan edo mitosian, nukleo mintza desegiten da eta horrek bektore ez-biralak eta DNA molekulak osatutako partikulak barneratzeari ahalbidetzen du<sup>21, 40</sup>. Hori da hain zuzen zelulak *in vitro* transfektatzean gertatzen dena, *baina in vivo* kasuetan prozesua zailagoa da zelula batzuk ez direlako inoiz edo ia inoiz zatitzen<sup>21, 40</sup>. Beraz, nukleo-mintza ere kontuan hartu beharra dago bektore ez-biralak diseinatzeko orduan, DNA molekulak nukleora iritsiko badira.

Orohar, nukleora joan behar duten proteinek nukleora bideratzeko sekuentzia bat izaten dute, NLS (*nuclear localization signal*) izenekoa eta aminoazido basiko ugari dituena<sup>17</sup>. Sekuentzia hori importina izeneko zitoplasmako proteina batzuek antzematen dute eta nukleora bidaltzen dute seinale hori daraman proteina oro NPC-an barrena, energiaren menpeko garraioaren bitartez<sup>40, 43</sup>. Estrategia bera erabili daiteke bektore ez-biralak ere nukleora bideratzeko. Hau da, bektore ez-biralei NLS sekuentzia txertatuta, importinek ezagutu eta nukleora bidaliko lituzkete NPC-an zehar. Aminoazido basiko ugari dituzten beste sekuentzia batzuk ere erabili izan dira molekula ezberdinak nukleora bideratzeko, besteak beste, poli-lisina eta protamina<sup>40</sup>.

Azkenik, kontuan hartu behar da behin nukleoan egonda, bektore ez-biralak gai izan behar direla material genetikoa bertan askatzeko transkripzioa gertatu dadin. Halere, ez da komenigarria ere DNA azkarregi askatzea, degradazio entzimatikoa jasan lezake eta<sup>40, 44</sup>. Liposometan oinarritutako bektore ez-biraletan, DNAren garraioa endosomatik ihes egiteko *flip flop* mekanismoari lotuta dagoela dirudi eta, beraz, DNA molekulak bakarrik iritsiko lirateke zitoplasmatik nukleora, bektoreei lotuta heldu beharrean<sup>40, 45, 46</sup>. Aldiz, bektore polimerikoetan, DNA nukleoan askatzen da bektoretik nukleoko proteinen interakzioaren eta oraindik guztiz argitu gabeko beste prozesu batzuen bitartez<sup>40, 47, 48</sup>.

Beraz, bektore ez-biralek hainbat zelula-barneko hesi zeharkatu behar dituzte zelula-mintzean lotzen direnetik DNA molekulak nukleoraino iritsi arte. Zelula-

motaren arabera eta endozitosi motaren arabera, hesi intrazelularrak ezberdinak izan daitezke. Bektore ez-biral gehienak klatrina bidezko endozitosiz barneratzen dira zeluletan eta endosomatik ihes egin beharra izaten dute lisosometan degradaziorik ez jasateko. Gainera, DNA molekulak nukleoan sartu behar dira transgenearren espresioa gertatu ahal izateko eta horretarako NLS seinalea gehitu dakioke bektoreak eta material genetikoak osatutako partikulari. Behin nukleoan, DNA molekulak bektoretik askatu behar dira transkripzio prozesuan parte hartu ahal izateko. Prozesu hori guztia 5. irudian laburbilduta ageri da.



**5. Irudia.** Bektore ez-biralen zelulan barneratzeko eta zelula barneko ibilbide endozitikoak. A) Fagozitosia. B) Klatrina bidezko endozitosia (CME). C) Kabeola bidezko endozitosia (CvME). D) Makropinozitosia. Zelulan barneratutako bektore ez-birala/DNA partikulak klatrina bidezko bidea jarraituz, endosomatik ihes egin eta nukleora garraiatuak dira importinek NLS sekuentzia antzeman ostean. Horiz, aktina; gorri, klatrina; berdez, kabeolina dimeroak; laranjaz, dineina GTPasa txikia; urdinez, opsoninak. (23 eta 24 erreferentziatik moldatua).

### 3. ZELULAZ KANPOKO HESIAK. EMAN-BIDE EZ-INBADITZAILEAK.

Eman-bidearen eta iritsi nahi den ehunaren arabera, gene-garraiorako sistemek hainbat zelulaz kanpoko hesi gainditu behar dituzte zeluletara iritsi eta gene transferentzia egin ahal izateko. Lehenago aipatu bezala, gene-terapien oinarritutako entsegu klinikoen %60 inguru minbiziaren aurkako sendagaien ikerketari dagokio. Beste gaixotasun batzuk ere, hala nola infekziosoak, neurodegeneratiboak, ala begiari zein birikei eragiten dietenak, interes berezia piztu dute azken aldian eta entsegu klinikoen %10a osatzen dute. Bektore ez-biralen administraziorako gehien erabiltzen eta aztertu den eman-bidea zain barnekoa da.

Horretarako, bektore ez-biralak era egokian diseinatu behar dira eman-bide horretan zehar topatuko dituzten zelulaz kanpoko hesiak gainditu ahal izateko. Gainera, ehun zehatzetara iritsi nahi denean, esate baterako, garunera, begietara edo biriketara, beste hainbat zelulaz kanpoko hesi ere zeharkatu beharko dituzte bektoreek. Atal honetan, zain barneko eman-bidean ageri diren hesi sistemiko nagusiak aipatuko ditugu, eta baita garunean, begietan edota biriketan ageri diren hesi espezifikoak ere. Horrez gain, zelulaz kanpoko hesi horiek gainditzeko garatu diren estrategiak berrikusiko ditugu, eman-bide inbaditzale zein ez-inbaditzaleetan oinarritutakoak. Gaur egun, komunitate zientifikoa gogor ari da lanean bektore ez-biralak modu seguruan eta eman-bide ez-inbaditzaleen bitartez ehun espezifikoetara helarazteko.

### **3.1. Zain barneko eman-bidea**

Minbizi mota askotan eta, batez ere, minbizi hedatuetan, tratamendua odolaren bidez administratu beharra dago. Beraz, minbiziari aurre egiteko diseinatutako bektore ez-biralak gai izan behar zain barneko eman-bidean aurkituko dituzten oztopoei aurre egin eta minbizi-zeluletaraino iristeko.

Zain barnetik emandako DNA molekulenzat, erronka nagusia da zelulaz kanpoko degradazioa ekiditea, odolean azido nukleikoak erasotzen dituzten nukleasa ugari baitaude. Horretan laguntzen dute hain zuzen ere bektore ez-biralek, DNA molekulak kondentsatuz eta, horrela, aktibitate entzimatikotik babestuz<sup>13</sup>.

Odoleko nukleasez gain, bertako proteinek ere –albumina, immunoglobulinak, etab.- gainditu beharreko hesi bat osatzen dute. Izan ere, bektore ez-biralek eta DNA molekulek osatutako partikulak era ez-espezifikoan odoleko proteinekin elkartu daitezke, agregatuak sortuz eta jomuga diren minbizi zeluletara iristea oztopatuz<sup>49</sup>.

Hirugarren oztopoa zain barneko eman-bidean bektore ez-biralek eta DNA molekulak osatutako partikulen ezegonkortasun koloidalala litzateke. Ezegonkortasun horrek ere partikulen agregazioa eta helmugara ez iristea eragin ditzake<sup>49</sup>. Gainera, odol-hodien sistema bera ere hesi garrantzitsua da, endotelio-zeluletan barrena igaro daitezkeen partikulen tamaina baldintzatzen baitu<sup>49</sup>.

Azkenik, sistema immunologikoaren aktibazioa ere kontuan hartu beharreko faktorea da. Izan ere, bektore ez-biralek zein DNA molekula arrotzek hantura erantzuna piztu dezakete, partikulen deuseztapena eraginez<sup>49</sup>.

## Sarrera

Hesi sistemiko guzti horiei aurre egiteko, bektore ez-biralen egitura hobetu beharra dago. Bektoreen formulaziok baldintzatuko du *in vivo* horien bioerabilgarritasuna<sup>49</sup>. Ondorengo paragrafoetan, formulazioa optimizatzeko garatzen ari diren hainbat estrategia deskribatuko ditugu.

Bektore ez-biralek eta azido nukleikoek osatutako partikulak egonkortzeko, gehien erabiltzen den metodoa partikulen gainazala polietileno glikolez (PEG) estaltzea da<sup>50</sup>. Molekula hori oso hidrofobikoa denez, hesi moduko bat osatzen du bektore ez-birala/DNA partikularen inguruan, odoleko proteinekin interakzioak saihestuz eta, beraz, agregazioak ekidinez<sup>49</sup>. Hala ere, nahiz eta emaitza itxaropentsuak lortu diren estrategia hori erabilita, zenbait zailtasun ere badira PEG-aren erabilera. Iza ere, molekula horrek bektore ez-biralen eta DNAren arteko elkarrekintza ahaldu dezake, partikulen barne-ezegonkortasuna areagotuz. Gainera, erantzun immunea ere piztu dezake, antigorputzen produkzioa eraginez eta, beraz, bektore ez-birala/DNA partikulak zirkulaziotik kanporatuz<sup>51</sup>. PEG molekulen luzerak eta kantitateak baldintzatuko dute *in vivo* estrategia horren egokitasuna eta parametro horiek bektore ez-biralaren ezaugarrietara egokitutu beharko dira<sup>52</sup>.

Horren ondorioz, komunitate zientifikoan lanean ari da PEG molekulen desabantailak nola edo hala oreakatzeko. Ikerketa berri baten arabera, soluzioa izan daiteke PEG molekulen ordez polimero hidrofilikoak erabiltzea, adibidez poli(N-binil-2-pirrolidona) (PVP), poli(4-akriloilmorfolina) edo poli(N,N-dimetilakrilamida)<sup>53</sup>. Partikulen egonkortasuna handitzeko beste estrategia batzuk ko-polimeroen erabilera oinarritzen dira, adibidez, PLL<sup>54</sup>. Bestalde, pH-arekiko sentsibilitatea duten partikulak ere erabili izan dira<sup>55</sup>, baita entzimatikoki ebaki daitezkeen PEG molekulak<sup>56</sup> edota erreduzitu daitezkeenak<sup>57</sup> ere.

Gainera, beste aldaera kimiko eta estruktural batzuk ere egin daitezke bektore ez-biraletan zelulaz kanpoko hesiak gainditzen laguntzeko. Lipido kationikoak dituzten bektore ez-biraletan, esaterako, kolesterola gehitzeak odoleko globulu gorriekin elkartzea ekidin dezake<sup>49</sup>. Aldiz, polimero kationikoak dituzten bektore ez-biralen kasuan, esaterako, kitosanoa laktosarekin konjugatuz agregazioa ekiditea lortu da odol-hodietan<sup>58</sup>. Beraz, bektore ez-biralaren ezaugarrien arabera, estrategia ezberdinak erabil daitezke bektore ez-biralak eta DNA molekulak osatutako partikulek odoleko hesiak gainditu ditzaten.

### **3.2. Ehun zehatzetara bideratzea: zelulaz kanpoko hesi gehigarriak**

Ehun espezifikoetara iritsi nahi denean, bektoreak gai izan behar dira ehun bakoitzari dagozkion hesi gehigarriak ere zeharkatzeko. Atal honetan, hiru ehunetan jarriko dugu arreta: garuna, begia eta birikak. Ehun horietara iristeko erabiltzen diren eman-bide inbaditzaileak eta ez-inbaditzaileak ere berrikusiko ditugu.

#### **3.2.1. Gene-garraioa garunera**

Nerbio-sistema zentralak (NSZ) ezaugarri anatomiko eta fisiologiko bereziak ditu, garuneko gene-garraioa asko zaitzen dutenak. Hesi hematoentzefalikoak (HHE) babesten du NSZ, elkarri estu lotutako endotelio zelulez osatutakoak<sup>19</sup>, eta uste da farmako makromolekularren %100i sarrera galarazten diola, baita farmako txikien %98ri ere<sup>59</sup>. Bizkarrezur-muina ere NSZren parte da eta beste hesi batek babesten du, likido zefalorrakideoaren hesiak hain zuzen, epitelio-zelulez osatua eta molekula arrotzak likido zefalorrakideora hedatzea galarazten duena<sup>19</sup>. Nutrienteen garraioa NSZra, glukosa eta aminoazidoena kasu, HHEn ageri diren errezeptore espezifikoak bidez egiten da<sup>19</sup>. Zelula-mota ezberdinak daude NSZn, neuronak eta glia-zelulak barne, eta gehienbat neuronak oso zailak dira transfektatzen post-mitotikoak direlako eta euren egitura zein osatzen duten sarea oso konplexuak direlako<sup>19</sup>.

Bektore ez-biralak eta DNA molekulak osatutako konplexuek HHE zeharkatzeko hainbat estrategia garatu dira. Gehienak HHEko errezeptoreetan lotuko diren estekatzaileen erabilera oinarritzen dira, adibidez, transferrina, laktot ferrina eta insulina, horien errezeptore ugari baitaude bai HHEko zeluletan eta baita neuronetan ere<sup>19</sup>. Estekatzaile horietako bat bektore ez-biralari lotuta, bektore ez-birala/DNA konplexua HHEn barrena garraiatu ahal izango da NSZra iritsi arte. Beste estrategia bat “Troiako zaldia” gisa ezagutzen dena da eta antigorputz monoklonal peptido-mimetikoen erabilera oinarria. Antigorputz horiek HHEko errezeptoreak aktibatzeko gai dira eta bektore ez-birala/DNA konplexuaren garraioa ahalbidetzen dute NSZra<sup>60</sup>. Beste ildo batzuk HHEren aldi baterako ezegonkortze mekanikoa eragitea edota HHE osatzen duten endotelio-zelulen arteko loturak modu iragankorrean haustea dira<sup>19</sup>.

Garunera helarazi nahi diren farmakoentzat eman-bide sistemikoa da egokiena eta onargarriena erabilera klinikorako. Hala ere, kontuan izanda horrek zelulaz kanpoko hesi ugari igaro behar izatea dakarrela eta ez dela beti posible izaten, hainbat ikerketak beste eman-bide batzuk aztertu dituzte. Entsegu aurre-kliniko batzuetan injekzio bidez edo difusio bidez farmakoak modu lokalean garunean bertan

## Sarrera

administratzen saiatu dira, baina nahiz eta eman-bide horien bidez HHE eta beste zelulaz kanpoko hesiak gainditzen diren, askotan inbaditzaleegiak izaten dira eta bide horretatik eman beharreko farmakoek aukera gutxi dituzte erabilera klinikora iristeko.

Sudur-barneko eman-bidea ez-inbaditzalea eta itxaropentsua izan daiteke farmakoak garunera modu seguruan eta zelulaz kanpoko hesiak ekidinez iritsi ahal izateko. Oraindik ez dago erabat argi farmakoak sudurretik garunera zer mekanismoren bidez iristen diren, baina, dirudienez, garraio perineuronal, peribaskular eta linfatikoen bitartez gertatzen da. Dena dela, garraio horietako bata edo bestea gailenduko da bektore ez-biralaren ezaugarrien arabera<sup>61</sup>. Gaur egun, uste da sudur barnetik emandako substantzia bat hiru bide ezberdinatik heldu daitekeela NSZra: (i) garraio parazelular edo transzelular zuzena usaimen neuronetan edo zelula epitelialean barrena (“usaimen neurona bidea”), (ii) nerbio trigeminoan barrena (“trigeminoko bidea”) edo (iii) zeharka, odol-hodietan edo sistema linfatikoan barrena (“bide sistemikoa”)<sup>62</sup>. Sudurreko mukosak odol-kapilar ugari ditu eta horiek nano-farmakoei igarotzen uzten diente, baina zirkulazio sistemikora pasatzen diren farmakoek HHE zeharkatu beharko dute NSZra iristeko<sup>61</sup>. Nerbio trigeminoa jarraituz, farmakoak usaimen erraboiletan eta garuneko alde kaudaletan askatzen dira<sup>63</sup>. Behin garunean, espacio peribaskularretako fluxuak farmakoak garuneko eremu ezberdinetara iristea ahalbidetzen duela uste da<sup>63, 64</sup>.

Sudur-barneko eman-bideak hainbat abantaila ditu, besteak beste, administrazio erraza eta ez-inbaditzalea, dosiaren absorbio azkarra sudurreko mukosan barrena, azalera egokia dosia xurgatzeko eta albo-efektu gastrointestinalak zein lehen pausuko metabolismoa ekiditea<sup>65</sup>. Gainera, norberak har dezake farmakoa eman-bide honetatik eta beste bide inbaditzale batzuk baino onargarriagoa da<sup>65</sup>. Desabantailen artean, aipagarrienak dira sudurreko kongestioa dagoenean dosia ez dela behar bezala xurgatuko eta eman-bide hau behin eta berriro erabiliko balitz sudurreko mukosa kaltetu egingo litzatekeela<sup>65</sup>. Gainera, sistema mukoziliarrak farmakoa mukosatik bizkor kanporatu dezake<sup>59, 66</sup>, baina oztopo hori erraz gainditu daiteke farmakoari molekula muko-adesiboak gehituta. Bektore ez-biralentzat, kitosanoa eszipiente erakargarria da sudur-barneko eman-bidean erabiltzeko. Izen ere, absorbioa errazten du eta mukosako azido sialikoarekin elkarrekintzak mantentzeko gai da, zelula epitelialen arteko lotura estuetan zabaluneak sortuz eta, beraz, mintz epitelialaren iragazkortasuna handituz<sup>67</sup>. Beste ikerketa batean,

Iaureato sukrosa tentsoaktibo ez-ionikoa erabili dute sudur-barneko absortzioa areagotzeko<sup>68</sup>.

Azken aldian, HHE zeharkatu dezaketen lehen DNA nanopartikulak erabiltzea lortu da eta, gainera, arratoien garunean *in vivo* egindako entseguetan, transginea garuneko zeluletan espresatzea lortu da<sup>63</sup>. Ikerketa horren egileek erakutsi dutenez, proteina berde fluoreszentearen (eGFP) genea daraman DNA molekula 10 kDa-ko peptido komertzial batean kondentsatzean, zelulen transfekzioa egitea lortzen da eta eGFP proteinaren expresioa modu egokian ematen da. Emaitza horien arabera, garunean transfektatutako zelulak perizitoak dira, eta bektore ez-birala/DNA konplexuak garraio peribaskularra jasan du<sup>63</sup>. Gainera, duela gutxiko beste ikerketa batean lortu dute kortexta eta hipokanpoa transfekatzea sudur-barneko eman-bidea eta kitosanoz eta PEG molekulaz osatutako mizelak bektore ez-birala gisa erabilita<sup>69</sup>. Nahiz eta ematen duen partikula horiek HHERen behin behineko ezegonkortzearen bidez lortu zutela garunera iristea, sudur-barneko bidea egokia izan daitekeela iradokitzen dute emaitza horiek. Hala ere, oraindik dosia eta dosi-erregimena hobetu behar dira transgene expresio maila egokiak lortu ahal izateko<sup>63</sup>.

### 3.2.2. Gene-garraioa begietara

Begia oso ehun erakargarria gene-terapien bere ezaugarri bereziak direla eta. Izan ere, ehnaren tamaina txikia da, eman beharreko kontzentrazio terapeutikoa baxua da eta begin ematen diren farmakoak ez dira odol zirkulazio sistemikora igarotzen<sup>70</sup>. Gainera, begiak nolabaiteko immunitate-pribilegioa dauka eta, beraz, molekula arrotzak begin injektatzean gerta daitezkeen erantzun immune eta hanturazkoak ez dira horren larriak izaten<sup>70</sup>.

Orokorrean, begirako gene-garraio sistemek espektro zabala hartzen dute, begietako tanta arruntetatik hasita bio- eta nanoteknologian oinarritutako farmako aurreratuetaraino, adibidez, sistema muko-adesiboak, polimeroak, liposomak eta begiko inplanteak. Teknologia horiek gehienak begiaren aurreko atalerako terapia oftalmikoei zuzenduta daude eta ezin dira begiaren atzealdean aplikatu<sup>71</sup>.

Eman-bide sistemikoa erabiltzen denean farmakoak begira garaiatzeko, horiek hesi odol-ocularra zeharkatu behar dute begiaren atzeko aldera helduko badira. Hesi odol-ocularra ere elkarren artean estu lotutako zelula epitelialez osatuta dago, eta hori zeharkatzea erronka handia da bektore ez-birala eta DNA molekulak osatutako partikulentzat. Bi estrategia nagusi erabiltzen dira hesi hori gainditzeko: 100 nm baino gutxiago neurten duten partikulak diseinatzea<sup>72</sup> eta estekatzaileak dituzten

## Sarrera

bektore ez-biralak erabiltzea, hesiko errezeptore espezifikoak ezagutzen dituztenak<sup>73</sup>. Beraz, eman-bide sistemikoaren bidez bolumen handiak eta errepikatuak administratu badaitezke ere, horien begiko bioerabilgarritasuna hesi odol-okularrak baldintzatuko du.

Metodo inbaditzairen ere badira begiaren atzoko aldera iristeko, adibidez, bitreobarneko injekzioa, konjuntiba-azpikoa eta erretina-azpikoa. Horiek hesi odolokularra gainditzea eta erretinako geruza ezberdinetara iristea ahalbidetzen dute. Hala ere, metodo horiek oso inbaditzairen dira eta administrazio errepikatuek begiko kalte larriak eragingo lituzkete, esate baterako, erretina-askatzea, odoljarioak eta azpi-edo aurre-erretinako fibrosia<sup>71</sup>. Beraz, beharrezkoak dira begiaren atzoko aldera bektore ez-biralak garraiatzeko eman-bide ez-inbaditzairen eraginkor eta seguruak. Horri dagokionez, begiko tantak lirateke aukerarik onena eta alboefektu gutxien sortuko lituzketenak<sup>71</sup>.

Dena dela, begiko atzoko aldera iristeko eman-bide ez-inbaditzairen eraginkorrak lortzea erronka handia da, bektore ez-biralek begi barneko hesi ugari zeharkatu beharko lituzketelako haraino iristeko. Lehenik eta behin, malko-hesia gainditu behar dute, lipidoz estalitako geruza irtsua eta konjuntibako zein korneako geruzak estaltzen dituen muzinaz inguratua<sup>71</sup>. Malko-hesiak formulazioen bioerabilgarritasuna mugatzen du, malko jarioa eta drainatze lakrimala eta nasolakrimala direla eta<sup>85</sup>. Hesi hori gainditzeko estrategien artean, bektore ez-biralei biskositatea areagotzeko elementuak –zelulosa edo poloxamer gelak, kasu<sup>71</sup> eta polimero muko-adesiboak –kitosanoa edota azido hialuronikoaren eratorriak, esate baterako<sup>74</sup> gehitzea ditugu. Bigarren, ehun okularreko hesiak daude, besteak beste, korna, konjuntiba, esklera eta koroidea, eta egitura horiek zelula epitelialen arteko lotura estuak, proteoglikano matrizeak eta kolageno sareak dituzte, bektoreak igarotzea oztopatzenten dutenak<sup>71</sup>. Azkenik, humore beirakara biogel irtsua da eta bertako kolageno, azido hialuroniko eta proteoglikanoek erretinako zelulen transfekzioa oztopatzenten dute<sup>71</sup>. Hesi horiek gainditzeko ere, aurretik aipatutako estrategiak erabiltzen dira, alegia, tamaina egokiko partikulak eta polimero muko-adesiboak<sup>71</sup>.

Begiko gene-terapien, arrakastarik handiena begiko aurreko aldearen transfekzioan lortu da, batez ere bektore biralak eta eman-bide inbaditzairen erabilita. Duela gutxi, erretinako zelulak bektore ez-biralen bidez transfektatzea lortu da, baina kasu horretan ere partikula magnetikoak era inbaditzairen eman ziren, bitreobarneko eta erretina-azpiko injekzioen bidez<sup>75</sup>. Gene-garraioan baino, aurrerapen

garrantzitsuagoak egin dira farmakoen garraioan begiaren atzealdera eman-bide ez-inbaditzaileen bidez iristeko. Adibidez, ikerketa berri batean erakutsi dutenez, emulstio lipidikoak erabilita posible da farmako hidrofobikoak ehun okularren atzeko aldera bideratzea eman-bide ez-inbaditzaileen bitartez<sup>76</sup>. Lan horretan, ikertzaileek emulstio lipidikoen gainazalean aldaketa batzuk egin zituzten kitosanoa eta poloxamer 407 bezalako polimero funtzionalak gehituz. Egileen esanetan, poloxamer 407 elementuak emulstioaren atxikipen denbora luzatu zuen begiaren gainazalean bere propietate adesiboei esker. Gainera, beste ikerketa batean ere lortu dute farmakoak begiaren atzeko aldera bideratzea eman-bide ez-inbaditzaileak erabilita, A5 anexina daramaten liposomen bitartez<sup>77</sup>. Kasu horretan, egileen arabera, A5 anexinak partikulen endozitosia sustatzen du, gene-transferentziaren eraginkortasuna handituz. Azkenik, beste ikerlan batek erakutsi du mikrofluidika bidez eratutako liposoma txikiak era topikoan eman daitezkeela ehun okularrean eta erretinako geruzetara iritsi daitekeela horrela<sup>78</sup>. Pentsatzekoa da farmako-garraioan egindako ekarpenak eta aurrerapenak baliagarriak izatea gene-garraiorako bektore ez-biral egokien diseinuan ere aurrera egiteko.

### 3.2.3. Gene-garraioa biriketara

Biriketako gene-terapia egokia izan daiteke arnas-bideetako hainbat gaixotasunen tratamendurako, besteak beste, fibrosi kistikoa, asma, enfisema edota biriketako minbizia<sup>79</sup>. Gaixotasunaren arabera, biriketako zelula-mota ezberdinak izan daitezke jomuga gene-terapien, adibidez, albeolo zelulak, epitelialak, makrofagoak, endotelialak edota biriketako zelula-amak<sup>79</sup>. Bestalde, material genetikoa biriketako toki egokian askatu beharko da iritsi nahi den zelula-motaren arabera. Zoritzarrez, biriketako hainbat eremutara iristea oso zaila da ehun horren arkitektura, mukiaren presentzia, garbiketa mekanismoak eta sistema immunearen aktibazioa direla medio<sup>79</sup>. Inhalazioa, sudur-barneko instilazioa eta trakea-barneko intubazioa dira teknika erabilienak bektoreak biriketara bideratzeko. Erabilera klinikorako, inhalazioz har daitezkeen aerosoletan formulatutako bektore ez-biral/DNA partikulak izango lirateke egokienak, izan ere, horrek abantaila ugari eskainiko lituzke, besteak beste, eman-bide ez-inbaditzailea erabiltzea, arnas bideetan zuzenean eta lokalki kontzentrazio altuak lortzea eta albo-efektuak gutxitzea.

Arnas-bideko jariakinak, alegia, mukia eta albeolo-fluidoa, dira bektore ez-biralek biriketan gainditu beharreko hesi garrantzitsuenak. Arnas-bideko mukia defentsa mekanismo eraginkorra da eta batez ere muzinazko hiru dimensioko sareek osatzen dute, mukiaren propietate biskoelastikoen erantzule izanik<sup>79</sup>. Mukian ageri

## Sarrera

diren proteina nagusiak albumina, proteasak, anti-proteasak, antigorputzak, lisozima eta laktoferrina dira, eta fibrosi kistikoak jotako edo infekzioak dituzten gaixoen mukiak DNA eta aktina kantitate handiak ere izaten ditu bere konposizioan<sup>79</sup>. Albeolo-fluidoa fosfolipidoz eta beste proteina batzuez osatutako geruza surfaktante fina eta jarraia da eta albeolo-epitelioa biltzen du<sup>79</sup>.

Arnas-bideko mukiak hesi gisa jardun dezake era ezberdinan biriketako generapian. Mukiko biopolimero sareak konplexuen difusioa oztopatzeko du, bai modu esterikoan eta baita konplexuekin elkartuz ere<sup>79</sup>. Gainera, karga negatiboa duten eta elkarri lotuta ez dauden mukiko makromolekulak eta antigorputzak ere bektore ez-biralek eta DNA molekulek osatutako konplexuekin lotu daitezke. Interakzio horiek ondorio ezberdinak izan ditzakete: (i) konplexuak mukian harrapatuta geratzea, (ii) partikulen agregazioa gainazaleko kargen neutralizazioa dela eta, (iii) DNA konplexutik denbora baino lehen askatzea edota (iv) partikulak era ez-eraginkorrean lotzea zeluletan, karga positiboak partzialki neutralizatuta geratu direlako<sup>79</sup>. Azkenik, mukia etengabe garbitzen da garraio mukoziliarraren bitartez. Beraz, bektore ez-biralek mukia kanporatu baino lehen zeharkatu behar dute zeluletara garaiz iristeko. Partikulen difusio koefizienteak, mukiaren Iodierak eta muki-garbiketa abiadurak baldintzatuko dute partikulak zeluletaraino iritsi ahal izatea<sup>79</sup>.

Albeolo-fluidoari dagokionez, geruza surfaktante honek transfekzio eraginkortasuna kaltetzen du<sup>79</sup>. Uste da lipoplexoak degradatu egin daitezkeela geruza surfaktantearen eraginez eta horrek DNA babesgabe uzten duela nukleasen aurrean<sup>80</sup>. Bektore polimerikoei dagokienez, bektore lipidikoak baino sendoagoak lirateke albeolo-fluidoaren aurrean eta ez lieke kalte handirik eragingo<sup>79</sup>.

Estrategia ezberdinak garatu dira biriketako zelulaz kanpoko hesiak gainditzeko. Bektore ez-biralek eta DNA molekulek osatutako partikulen tamaina faktore garrantzitsua da, baina saiakera gehienak mukian zehar partikulen bizkortasuna areagotzera zuzenduta daude.

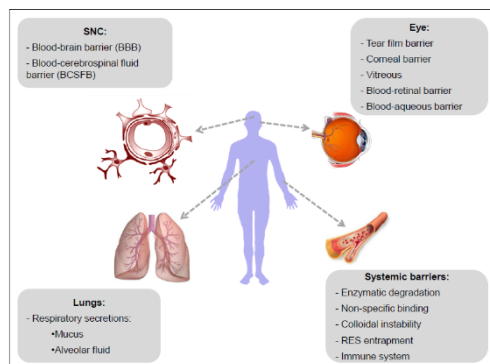
Metodo ezberdinak erabil daitezke partikulek mukia azkarrago zeharkatu dezaten. Errazena bektoreei agente mukolitikoak gehitzea da, horrela, inguruko mukia hidrolizatzeko eta bizkorago mugitzeko gaitasuna izan dezaten<sup>79</sup>. Baita, erakutsi da N-azetil zisteina eta eratorriek mukiaren biskositatea eta elastikotasuna gutxitzen dituztela, muzinen arteko disulfuro zubiak hausten dituztelako<sup>81</sup>. Etorkizunera begira, ikerketa-lerro gehienak saiatzen ari dira nanopartikulak elementu mukolitikoekin funtzionalizatzen, horrela mukian zehar bidea ebaki ahal izateko<sup>79</sup>.

## Sarrera

Bestalde, partikulen eta fluido biologikoetako proteinen arteko interakzioak ekiditeko, estrategia nagusia da partikulak biologikoki inerteak diren polimero biobateragarriekin estaltzea<sup>79</sup>. Horrek, interakzioak gutxitzeaz gain, makrofagoen garbiketa ere ekiditen du. Adibidez, polietileno glikola edo PEG aukera egokia izan liteke bektore ez-biralen egonkortasun fisiko-kimikoa eta gene-transferentzia gaitasuna hobetzeko<sup>79</sup>.

Erronka ugari gainditu behar dira oraindik biriketako gene-terapia klinikara iristeko eta, beharbada, garrantzitsuena bektoreak mukian zehar azkar eta era eraginkorrean igarotzea lortzea litzateke<sup>82</sup>. Hala ere, aurrerapen handiak egin dira alor horretan eta aerosol bidezko formulazioak ikertzen ari dira dagoeneko biriketako minbiziari aurre egiteko, besteak beste. Gainera, inhalazio bidezko gene-terapiak lehen emaitza onak lortu ditu fibrosi kistikorekin egindako entseguetan, eraginkorra eta segurua dela erakutsiz<sup>83</sup>.

Beraz, aurreko guztia kontuan hartuta, bektore ez-biralek eta DNA molekulek osatutako partikulak gai izan behar dira zelulaz kanpoko hesiak gainditzeko jomuga diren zelula eta ehunetara iritsi ahal izateko (6. irudia). Injekzio sistemikoa da eman-bide erabiliena, baina zenbait oztopo ditu gene-terapiaren eraginkortasuna baldintzatzen dutenak. Eman-bide lokalak eraginkorrik dira zelulaz kanpoko hesi gehienak gainditzeko, baina askotan inbaditzaileak dira eta ezin dira praktika klinikoan erabili. Gaur egun, ikerketa lerro askok eman-bide ez-inbaditzaileetan jarri dute arreta eta, horien bitartez, zelulaz kanpoko hesiak gainditzeko estrategiak garatzen ari dira. Izan ere, ehun zehatzetara bideratzean, hesi gehigarriak agertzen dira, esate baterako, HHE garunean edota hesi odol-okularra begian. Beraz, administrazio lokal eta ez-inbaditzaileak ehun horietan zaitasun gehiago dakartzza eta kontuan hartu behar dira bektore ez-biral eraginkorrik diseinatu ahal izateko. Espero da etorkizuneko gene-garraio sistema ez-birak eman-bide lokal eta ez-inbaditzaileen bitartez iritsiko direla sendatu beharreko ehunetara.



**6. irudia.** Zelulaz kanpoko hesi orokorrak (eman-bide sistemikoa) eta ehun-espezifikoak (garuna, begia, birikak) gene-terapia ez-biralean.

#### 4. GENE-TERAPIA EZ-BIRALAREN ERRONKAK ETA ETORKIZUNERAKO PERSPEKTIBAK

Bektore ez-biralak gene-terapiarako estrategia itxaropentsuak dira. Nahiz eta oraindik ere erabilera klinikotik urrun egon, aurrerapauso handiak egin dira azken urteetan bai bektoreen diseinuari dagokionean eta baita eman-bide ez-inbaditzailleei dagokienean ere. Transgenearren expresioa modu egokian eman dadin, hainbat baldintza bete behar dira. Horien artean, garrantzitsuenak erantzun immunerik ez eragitea, DNA degradazio entzimatikotik babestea, zelulaz kanpoko zein barneko hesiak gainditzea eta DNA molekulak nukleoraino helaraztea dira<sup>84</sup>. Zelulaz kanpoko zein barruko hesien ezagutza molekularak oztopo horiek gainditzen lagunduko duten estrategiak garatzea ahalbidetu du eta metodo gehienak formulazioaren diseinuaren aldaketetan edota eman-bide lokalen erabileran oinarritzen dira. Azken honi dagokionez, ematen du eman-bide ez-inbaditzailleen bitartez ere iritsi daitekeela jomuga diren ehun eta zeluletarra, eta etorkizuneko gene-terapiarako bektore ez-biralen garapena norabide horretan doa.

Gene-terapia ez-biralaren oztopo nagusia, behin eta berriro errepikatu dugun bezala, transfekzio-eraginkortasun baxua da. Metodologia ezberdinak erabili dira horri aurre egiteko, batik bat, bektoreei gorputzeko hesiak gainditzeko ahalmena emanez. Halere, beste estrategia batzuk ere garrantzizkoak dira transfekzio eraginkortasuna handitu ahal izateko: bektoreen bideratzea edo *targeting-a* eta transgenearren expresio iraunkorra lortzea. Biak ala biak ere nahitaezkoak dira bektore ez-biralak erabilera klinikora iristeko, espezifikotasuna eta epe luzerako tratamendua bermatzen dituztelako. Esfortzu handiak egin dira bi aspektu horiek

garatzeko, baina oraindik ikerketa sakonagoak falta dira zentzu horretan. Bestalde, erabilera klinikora iristeko beste faktore batzuk ere kontuan hartu behar dira, besteak beste, bektoreen toxikotasuna eta produkzioari zein produktuen erregulazioari lotutako auziak. Atal honetan, bektoreak ehun espezifikoetara bideratzeko eta transgene expresio iraunkorra lortzeko gaur egun existitzen diren estrategia nagusiak aipatuko ditugu. Halaber, bektoreen toxikotasunari, produkzioari eta erregulazioari dagozkien datuak ere berrikusiko ditugu.

#### **4.1. Ehun espezifikoetara bideratzea edo *targeting-a***

Bektore ez-biralak ehun zehazteta bideratzea bektorean bertan edota horiek garraiatzen duten DNA molekuletan aldaketak eginez lortu daiteke. Estrategia erabiliena bektore ez-biralari estekatzaile espezifikoak txertatzea da, jomuga diren organoetako zeluletako errezeptoreak ezagutuko dituztenak. Lehenago aipatu bezala, metodo horren eraginkortasuna frogatua izan da hainbat ikerketatan. Gainera, minbiziaren aurkako gene-terapien, minbizi-zelulen ezaugarri fisiologiko bereziak baliatzen dira bektoreak modu espezifikoan zelula horietara helarazteko<sup>85</sup>.

Bestalde, DNA molekularen ere aldaketak egin daitezke transfekzio espezifikoagoa lortze aldera. Estrategia horri “*transcriptional targeting*” edo bideratze transkripzionala deritzo, eta soilik jomuga den zelula-populazioak dituen transkripzio faktoreek ezagutuko dituzten DNA sekuentzien erabileran oinarritzen da<sup>85</sup>. Metodo honetan DNA molekula ehun guztietara iritsi arren, soilik tratatu nahi den zelula-populazioan gertatuko litzateke transgenearen edo gene terapeutikoaren expresioa<sup>84</sup>. Metodo hori arrakastaz gauzatzeko ezinbestekoa da zelula-populazioen transkripzio faktoreen arteko ezberdintasunak ondo ezagutzea<sup>84</sup>.

Gene-garraio sistemetan, partikulak ehun zehazteta bideratzea oso onuragarria da. Besteak beste, producto terapeutikoaren bioerabilgarritasuna igo egiten da, tratamendurik behar ez duten ehunetan ez da transgenearen expresiorik ematen eta, beraz, albo-efektuak gutxitu egiten dira eta eman beharreko dosiak ere baxuagoak dira. Aspektu guzti horiek eraginkortasun terapeutikoa areagotzen dute eta tratamenduaren kostua jaisten laguntzen dute<sup>86</sup>.

#### **4.2. Gene-expresioaren iraupena**

Epe luzeko transgenearen expresioa lortzea erronka zaila da gene-terapia ez-birarentzat eta klinikarako jauzia mugatzen duen faktore garrantzitsua da. Denboran zehar, arrazoi ezberdinek eragin dezakete transgenearen expresioaren

## Sarrera

jaitsiera, esate baterako, nukleasek eragindako degradazioak, errekonbinazioaren ondoriozko galerak, konpartimentu ez-nuklearretara lekualdatzeak edota DNA arrotza zeluletan isilarazteak<sup>85</sup>. Gainera, zatitzen diren zeluletan transfektatutako zelula-kopurua belaunaldi bakoitzean murriztu egiten da, zelulak ugaldu arren, plasmidoak ez direlako bikoizten.

Transgenearen espresioa denboran luzatzeko estrategia gehienek DNA molekulen aldaketetan jarri dute arreta guztia, eta ez bektorearen hobekuntzan. Metodo horietako batzuk integrasak erabiltzen dituzte material genetiko arrotza zeluletako genometan txertatzeko eta, horrela, transgenea belaunaldiz belaunaldi transmititzeko zelula-populazioetan<sup>85</sup>. Halabaina, metodo hori ezingo litzateke klinikan erabili arrisku handiak dakartzalako, horien artean larriena, mutagenesia sortzea transgenea modu aleatorioan zelulen genoman txertatzean.

Beste estrategia bat modu autonomoan bikoizten diren DNA plasmidoak erabiltzea da. Horiek ez dute zelulen genoman txertatzeko beharrik bikoizteko eta hurrengo zelula-belaunaldietara igarotzeko eta, beraz, mutagenesi arriskua ekiditen dute<sup>85</sup>. Gainera, mota horretako plasmidoek transfekcio maila altuak lortu ohi dituzte. Metodo horretan, plasmidoa bikoizteko beharrezkoak diren transkripcio ko-faktoreak gehitzen dira DNA sekuentzian, zelularen transkripcio makinariarekiko independenteago eginez. Horrez gain, hainbat birus sekuentzia ere gehitu daitezke are modu autonomoagoan bikoiztu dadin DNA molekula, baina horrek, besteak beste, immune-sistemaren aktibazioa eragin dezake<sup>85</sup>. Beste aukera bat da sekuentzia biralen ordez ugaztunen genomako S/MAR sekuentziak txertatzea. Sekuentzia horiek ere gai dira plasmidoen bikoizketa episomala abiarazteko zeluletako transkripcio makinaria DNA molekuletara hurbilduz<sup>73</sup>. Modu episomalean bikoizten diren plasmidoak bereziki garrantzitsuak dira minbiziaren aurkako generatieran, bertan ezinbestekoa baita produktu terapeutikoa zelula-belaunaldi batetik hurrengora igarotzea<sup>85</sup>. Transgenearen espresio iraunkorra lortzeko beste estrategia batzuk zeluletan DNA molekula arrotzen isilaraztea saihesten saiatzen dira, hori delako transgeneen espresioa oztopatzen duen faktore nagusietako bat<sup>85</sup>.

Gainera, aldaketa gehiago ere egin daitezke DNA molekuletan transgenearen espresioaren indarra edota espezifikotasuna handitzeko. Horretarako, transgenearen zein transkripcioaren aktibatzaile gisa jarduten duen genearen espresioa abiarazten dituen promotorea erabili behar da. Transkripcioaren aktibatzaile hori gai da promotorearen gune zehatzetan lotu eta promotorearen kontrolpean dauden transgenearen eta aktibatzailearen beraren transkripzioa behin

eta berriro abian jartzeko<sup>85</sup>. Atzeraelikatze positiboko mekanismo horiek egokiak izan daitezke oso espezifikoak baina expresio ahulekoak diren elementu erregulatzaileak kontrolatzeko<sup>85</sup>.

#### **4.3. Toxikotasuna, produkzioa eta erregulazioa**

Gene-transferentziaren eraginkortasuna handitzeaz gain, gene-terapiarako produktuak merkatura iristeko beste aspektu batzuk ere kontuan hartu behar dira. Horien artean, bektoreen toxikotasuna zehaztasun handiz ikertu beharreko atala da, eta baita bektoreen produkzioari eta erregulazioari dagozkien auziak ere. Produktua kantitate industrialetan ekoitzu ahal izatea eta epe luzera biltegiratu ahal izatea ezinbesteko baldintzak dira merkatura iritsi nahi bada<sup>19</sup>. Bektore ez-biralen kasuan, orokorrean onartuta dago horien abantaila nagusietako bat eskala industrialen ekoizteko erraztasuna dela. Halere, gaur egun hori gero eta zailagoa bihurtzen ari da, bektoreen konplexutasun-maila handituz doan heinean.

Toxikotasunari dagokionez, nanopartikulen tamainak, kargak, gainazaleko funtzionalizazioak, morfologiak eta arkitekturak segurtasun profilean eragina izan dezakete. Uste da bektore ez-biralek modu ezberdinetan sortu dezaketela toxikotasuna, adibidez, zelula-mintzaren ezegonkortzearen, estres oxidatzailearen edota hantura-erantzunen bidez, baita gene-expresioan aldaketa globalak eraginez ere<sup>85</sup>. Metatzeko joera duten biomaterialek errazago sortzen dituzte hantura-erantzunak eta partikulen degradazioan sortutako molekulak ere toxikoak izan daitezke. Hala ere, oraindik ez dago argi zer prozesuk hartzen duten parte bektore ez-biralen metabolizazioan eta ikerketa sakonagoak beharrezkoak dira auzi horiek argitzeko<sup>19</sup>.

Amaitzeko, esan dezakegu bektore ez-biral bakar eta unibertsalaren kontzeptua gaur egun baztertuta dagoela eta gero eta onartuago dagoela komunitate zientifikoan bektore ez-biralak anitzak eta aplikazio bakoitzerako espezifikoki egokituak izan behar direla<sup>1</sup>. Dena den, badira bektore ez-biral guztiekin bete behar dituzten gutxieneko baldintza baztuk gene-transferentzia modu seguru eta eraginkorrean gauzatu ahal izateko. Laburbilduz, hiru faktore nagusi hartu behar dira kontuan bektore ez-biraletan oinarritutako gene-garraiorako sistemak diseinatzean: (i) formulazioaren osagaiak, bai bektoreari eta baita DNA molekulari dagokionean – partikula gai izan behar da DNA babesteko, zelulaz kanpoko zein barneko hesiak gainditzezko eta, behin nukleoan, DNA modu autonomoan bikoiztea komeni da epe luzeko transgene expresioa lortzeko-, (ii) ekoizpenari dagokionez, maila industrialean produzitzea posible izan behar da eta (iii) segurtasun eta erregulazioari

## Sarrera

lotutako neurriak, hau da, formulazioak ez-toxicoak, ez-immunogenikoak eta biltegiratze egonkorrekoak izan behar dira. Nahiz eta oraindik aplikazio klinikotik urrun egon, bektore ez-biralak birusak baino seguruagoak dira. Formulazio eta estrategia ezberdinak ikertzen ari dira gene-transferentziaren eraginkortasuna igotzeko, hala nola, bektore ez-biralei zelulaz kanpoko zein barneko hesiak gainditzeko gaitasuna emanez, ehun espezifikoetara bideratuz eta gene-expresio iraunkorragoak bilatuz. Gainera, formulazio horitako asko eman-bide ez-inbaditzaleetatik emateko diseinatzen dira, esate baterako, sudur-barnetik garunera iristeko, administrazio topiko okularra erretinara iristeko edota inhalazioz hartzeko aerosolak biriketara iristeko. Azkenik, modulu funtzional berriak txertatzeak, bai bektorean eta baita DNA molekuletan ere, espezifikotasuna eta gene terapeutikoen iraunkortasuna bermatu ahal izango dute<sup>40</sup>. Beraz, zantzu horien arabera, etorkizuneko gene-terapia sistemak aplikazio bakoitzera egokitutako eta eman-bide ez-inbaditzaleetatik hartu ahal izango diren bektore ez-biraletan oinarrituta egongo dira, gene terapeutikoak ehun zehatzetara modu seguru eta eraginkorrean helarazteko.

## 5. ESKERRAK

Proiektu honen babesleak Euskal Herriko Unibertsitatea (UPV/EHU) (UFI 11/32), Eusko Jaurlaritza (Hezkuntza Saila, PRE\_2014\_1\_433 eta BFI-2011-2226 laguntzak), Mexikoko Gobernua (CONACYT) eta Espainiako Hezkuntza Ministerioa (SAF2013-42347-R laguntza) dira. Lan honen egileek CIBER-BBNko Drug Formulation Unit (NANBIOSIS) saileko laguntza tekniko eta intelektuala eskertzen dute.

## **6. REFERENCES / ERREFERENTZIAK**

- [1] Pezzoli D, Chiesa R, De Nardo L, Candiani G. We still have a long way to go to effectively deliver genes!. *J Appl Biomater Funct Mater* 2012;10(2) 82-91.
- [2] Gene Therapy Net. <http://www.genetherapy.net/patient-information.html> (accessed 7 January 2015).
- [3] Kohn DB. Gene therapy for XSCID: the first success of gene therapy. *Pediatr Res* 2000;48(5) 578.
- [4] Actionbioscience. <http://www.actionbioscience.org/biotechnology/kolehmainen.html#primer> (accessed 7 January 2015).
- [5] European Medicines Agency, EMA. <http://www.ema.europa.eu/ema/> (accessed 8 January 2015).
- [6] Rodríguez-Gascón A, del Pozo-Rodríguez A, Solinis MA (2013). Non-Viral Delivery Systems in Gene Therapy. In: Martin F. (ed.), *Gene Therapy - Tools and Potential Applications*. ISBN: 978-953-51-1014-9, InTech, DOI: 10.5772/52704. Available from: <http://www.intechopen.com/books/gene-therapy-tools-and-potential-applications/non-viral-delivery-systems-in-gene-therapy> (accessed 07 January 2015).
- [7] The Journal of Gene Medicine. Gene Therapy Clinical Trials Worldwide. <http://www.wiley.com/legacy/wileychi/genmed/clinical/> (accessed 7 January 2015).
- [8] Thomas CE, Ehrhardt A, Kay MA. Progress and problems with the use of viral vectors for gene therapy. *Nat Rev Genet* 2003;4(5) 346-358.
- [9] Davis ME. Non-viral gene delivery systems. *Curr Opin Biotechnol* 2002;13(2) 128-131.
- [10] Al-Dosari MS, Gao X. Nonviral gene delivery: principle, limitations, and recent progress. *AAPS J* 2009;11(4) 671-681.
- [11] Kamimura K, Suda T, Zhang G, Liu D. Advances in Gene Delivery Systems. *Pharmaceut Med* 2011;25(5) 293-306.
- [12] Ojeda E, Puras G, Agirre M, Zarate J, Grijalvo S, Pons R, et al. Niosomes based on synthetic cationic lipids for gene delivery: the influence of polar head-groups on the transfection efficiency in HEK-293, ARPE-19 and MSC-D1 cells. *Org Biomol Chem* 2015;13(4) 1068-1081.
- [13] Agirre M, Zarate J, Puras G, Rojas LA, Alemany R, Pedraz JL. Strategies for Improving the Systemic Delivery of Oncolytic Adenoviruses and Plasmids: Potential Application of Non-Viral Carriers. In: Atta-ur-Rahman M, Choudhary I. (ed.) *Frontiers in Anti-Cancer Drug Discovery*. Bentham Science; 2013.

- [14] Chawla V, Saraf SA, Saraf SK. Gene Delivery: The Non-Viral Vector Advantage. ACT-Biotechnology Research Communications 2011;1(1) 1-7.
- [15] Perez-Martinez FC, Carrion B, Cena V. The use of nanoparticles for gene therapy in the nervous system. J Alzheimers Dis 2012;31(4) 697-710.
- [16] Guo X, Huang L. Recent advances in nonviral vectors for gene delivery. Acc Chem Res 2012;45(7) 971-979.
- [17] Xiang S, Tong H, Shi Q, Fernandes JC, Jin T, Dai K, et al. Uptake mechanisms of non-viral gene delivery. J Control Release 2012;158(3) 371-378.
- [18] Medina-Kauwe LK, Xie J, Hamm-Alvarez S. Intracellular trafficking of nonviral vectors. Gene Ther 2005;12(24) 1734-1751.
- [19] O'Mahony AM, Godinho BM, Cryan JF, O'Driscoll CM. Non-viral nanosystems for gene and small interfering RNA delivery to the central nervous system: formulating the solution. J Pharm Sci 2013;102(10) 3469-3484.
- [20] Khalil IA, Kogure K, Akita H, Harashima H. Uptake pathways and subsequent intracellular trafficking in nonviral gene delivery. Pharmacol Rev 2006;58(1) 32-45.
- [21] Hillaireau H, Couvreur P. Nanocarriers' entry into the cell: relevance to drug delivery. Cell Mol Life Sci 2009;66(17) 2873-2896.
- [22] Xu L, Huang CC, Huang W, Tang WH, Rait A, Yin YZ, et al. Systemic tumor-targeted gene delivery by anti-transferrin receptor scFv-immunoliposomes. Mol Cancer Ther 2002;1(5) 337-346.
- [23] Rappoport JZ. Focusing on clathrin-mediated endocytosis. Biochem J 2008;412(3) 415-423.
- [24] Subtil A, Gaidarov I, Kobylarz K, Lampson MA, Keen JH, McGraw TE. Acute cholesterol depletion inhibits clathrin-coated pit budding. Proc Natl Acad Sci U S A 1999;96(12) 6775-6780.
- [25] Luzio JP, Parkinson MD, Gray SR, Bright NA. The delivery of endocytosed cargo to lysosomes. Biochem Soc Trans 2009;37(Pt 5) 1019-1021.
- [26] Delgado D, del Pozo-Rodriguez A, Solinis MA, Rodriguez-Gascon A. Understanding the mechanism of protamine in solid lipid nanoparticle-based lipofection: the importance of the entry pathway. Eur J Pharm Biopharm 2011;79(3) 495-502.
- [27] Nichols B. Caveosomes and endocytosis of lipid rafts. J Cell Sci 2003;116(Pt 23) 4707-4714.
- [28] Bengali Z, Rea JC, Shea LD. Gene expression and internalization following vector adsorption to immobilized proteins: dependence on protein identity and density. J Gene Med 2007;9(8) 668-678.

- [29] Kiss AL, Botos E. Endocytosis via caveolae: alternative pathway with distinct cellular compartments to avoid lysosomal degradation? *J Cell Mol Med* 2009;13(7) 1228-1237.
- [30] Ikeda Y, Taira K. Ligand-targeted delivery of therapeutic siRNA. *Pharm Res* 2006;23(8) 1631-1640.
- [31] Wattiaux R, Laurent N, Wattiaux-De Coninck S, Jadot M. Endosomes, lysosomes: their implication in gene transfer. *Adv Drug Deliv Rev* 2000;41(2) 201-208.
- [32] Swanson JA, Watts C. Macropinocytosis. *Trends Cell Biol* 1995;5(11) 424-428.
- [33] Varkouhi AK, Scholte M, Storm G, Haisma HJ. Endosomal escape pathways for delivery of biologicals. *J Control Release* 2011;151(3) 220-228.
- [34] Liang W, Lam J. Endosomal Escape Pathways for Non-Viral Nucleic Acid Delivery Systems. In: Ceresa B (ed.), ISBN: 978-953-51-0662-3, InTech;2012. DOI: 10.5772/46006. Available from: <http://www.intechopen.com/books/molecular-regulation-of-endocytosis/endosomal-escape-pathways-for-non-viral-nucleic-acid-delivery-systems> (accessed 27 January 2015)
- [35] Madani F, Lindberg S, Langel U, Futaki S, Graslund A. Mechanisms of cellular uptake of cell-penetrating peptides. *J Biophys* 2011;2011:414729.
- [36] Patel LN, Zaro JL, Shen WC. Cell penetrating peptides: intracellular pathways and pharmaceutical perspectives. *Pharm Res* 2007;24(11) 1977-1992.
- [37] Gupta B, Levchenko TS, Torchilin VP. Intracellular delivery of large molecules and small particles by cell-penetrating proteins and peptides. *Adv Drug Deliv Rev* 2005;57(4) 637-651.
- [38] del Pozo-Rodriguez A, Pujals S, Delgado D, Solinis MA, Gascon AR, Giralt E, et al. A proline-rich peptide improves cell transfection of solid lipid nanoparticle-based non-viral vectors. *J Control Release* 2009;133(1) 52-59.
- [39] Selbo PK, Weyergang A, Hogset A, Norum OJ, Berstad MB, Vikdal M, et al. Photochemical internalization provides time- and space-controlled endolysosomal escape of therapeutic molecules. *J Control Release* 2010;148(1) 2-12.
- [40] Glover J, Glouchkova L, Lipps H, Jans D. Overcoming barriers to achieve safe, sustained and efficient non-viral gene therapy. In: Teixeira da Silva J.A., Shima K. (ed.) *Advances in Gene, Molecular and Cell Therapy*. Global Science Books; 2007. p126-140.
- [41] Ludtke JJ, Zhang G, Sebestyen MG, Wolff JA. A nuclear localization signal can enhance both the nuclear transport and expression of 1 kb DNA. *J Cell Sci* 1999;112 ( Pt 12)(Pt 12) 2033-2041.

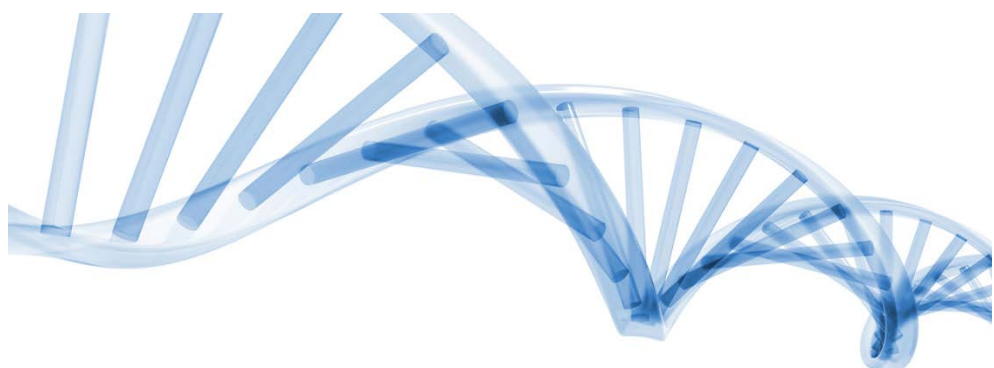
- [42] Lukacs GL, Haggie P, Seksek O, Lechardeur D, Freedman N, Verkman AS. Size-dependent DNA mobility in cytoplasm and nucleus. *J Biol Chem* 2000;275(3) 1625-1629.
- [43] Jans DA, Hubner S. Regulation of protein transport to the nucleus: central role of phosphorylation. *Physiol Rev* 1996;76(3) 651-685.
- [44] Lechardeur D, Sohn KJ, Haardt M, Joshi PB, Monck M, Graham RW, et al. Metabolic instability of plasmid DNA in the cytosol: a potential barrier to gene transfer. *Gene Ther* 1999;6(4) 482-497.
- [45] Xu Y, Szoka FC,Jr. Mechanism of DNA release from cationic liposome/DNA complexes used in cell transfection. *Biochemistry* 1996;35(18) 5616-5623.
- [46] Zelphati O, Szoka FC,Jr. Intracellular distribution and mechanism of delivery of oligonucleotides mediated by cationic lipids. *Pharm Res* 1996;13(9) 1367-1372.
- [47] Cereghini S, Yaniv M. Assembly of transfected DNA into chromatin: structural changes in the origin-promoter-enhancer region upon replication. *EMBO J* 1984;3(6) 1243-1253.
- [48] Masuda T, Akita H, Harashima H. Evaluation of nuclear transfer and transcription of plasmid DNA condensed with protamine by microinjection: The use of a nuclear transfer score. *FEBS Lett* 2005;579(10) 2143-2148.
- [49] Parhiz H, Hashemi M, Ramezani M. Non-biological gene carriers designed for overcoming the major extra- and intracellular hurdles in gene delivery, an updated review. *Nanomed J* 2015;2(1) 1-20.
- [50] Mishra S, Webster P, Davis ME. PEGylation significantly affects cellular uptake and intracellular trafficking of non-viral gene delivery particles. *Eur J Cell Biol* 2004;83(3) 97-111.
- [51] Khargharia S, Kizzire K, Ericson MD, Baumhover NJ, Rice KG. PEG length and chemical linkage controls polyacridine peptide DNA polyplex pharmacokinetics, biodistribution, metabolic stability and in vivo gene expression. *J Control Release* 2013;170(3) 325-333.
- [52] Amoozgar Z, Yeo Y. Recent advances in stealth coating of nanoparticle drug delivery systems. *Wiley Interdiscip Rev Nanomed Nanobiotechnol* 2012;4(2) 219-233.
- [53] Ishihara T, Maeda T, Sakamoto H, Takasaki N, Shigyo M, Ishida T, et al. Evasion of the accelerated blood clearance phenomenon by coating of nanoparticles with various hydrophilic polymers. *Biomacromolecules* 2010;11(10) 2700-2706.
- [54] von Erlach T, Zwicker S, Pidhatika B, Konradi R, Textor M, Hall H, et al. Formation and characterization of DNA-polymer-condensates based on poly(2-methyl-2-oxazoline) grafted poly(L-lysine) for non-viral delivery of therapeutic DNA. *Biomaterials* 2011;32(22) 5291-5303.

- [55] Knorr V, Allmendinger L, Walker GF, Paintner FF, Wagner E. An acetal-based PEGylation reagent for pH-sensitive shielding of DNA polyplexes. *Bioconjug Chem* 2007;18(4) 1218-1225.
- [56] Hatakeyama H, Akita H, Ito E, Hayashi Y, Oishi M, Nagasaki Y, et al. Systemic delivery of siRNA to tumors using a lipid nanoparticle containing a tumor-specific cleavable PEG-lipid. *Biomaterials* 2011;32(18) 4306-4316.
- [57] Jia L, Li Z, Zhang D, Zhang Q, Shen J, Guo H, et al. Redox-responsive cationomer based on PEG-ss-chitosan oligosaccharide-ss-polyethylenimine copolymer for effective gene delivery. *Polym Chem* 2013;4 156-165.
- [58] Hashimoto M, Morimoto M, Saimoto H, Shigemasa Y, Sato T. Lactosylated chitosan for DNA delivery into hepatocytes: the effect of lactosylation on the physicochemical properties and intracellular trafficking of pDNA/chitosan complexes. *Bioconjug Chem* 2006;17(2) 309-316.
- [59] Kozlovskaya L, Abou-Kaoud M, Stepensky D. Quantitative analysis of drug delivery to the brain via nasal route. *J Control Release* 2014;189 133-140.
- [60] Pardridge WM. Re-engineering biopharmaceuticals for delivery to brain with molecular Trojan horses. *Bioconjug Chem* 2008;19(7) 1327-1338.
- [61] Dhuria SV, Hanson LR, Frey WH,2nd. Intranasal delivery to the central nervous system: mechanisms and experimental considerations. *J Pharm Sci* 2010;99(4) 1654-1673.
- [62] Casettari L, Illum L. Chitosan in nasal delivery systems for therapeutic drugs. *J Control Release* 2014;190 189-200.
- [63] Harmon BT, Aly AE, Padegimas L, Sesenoglu-Laird O, Cooper MJ, Waszcak BL. Intranasal administration of plasmid DNA nanoparticles yields successful transfection and expression of a reporter protein in rat brain. *Gene Ther* 2014;21(5) 514-521.
- [64] Hadaczek P, Yamashita Y, Mirek H, Tamas L, Bohn MC, Noble C, et al. The "perivascular pump" driven by arterial pulsation is a powerful mechanism for the distribution of therapeutic molecules within the brain. *Mol Ther* 2006;14(1) 69-78.
- [65] Parvathi M. Intranasal delivery to the brain: an overview. *IJPRC* 2012;2(3) 889-895.
- [66] Illum L. Nasal drug delivery - recent developments and future prospects. *J Control Release* 2012;161(2) 254-263.
- [67] Migliore MM, Vyas TK, Campbell RB, Amiji MM, Waszcak BL. Brain delivery of proteins by the intranasal route of administration: a comparison of cationic liposomes versus aqueous solution formulations. *J Pharm Sci* 2010;99(4) 1745-1761.
- [68] Li Y, Li J, Zhang X, Ding J, Mao S. Non-ionic surfactants as novel intranasal absorption enhancers: in vitro and in vivo characterization. *Drug Deliv* 2014;27 1-8.

- [69] Das M, Wang C, Bedi R, Mohapatra SS, Mohapatra S. Magnetic micelles for DNA delivery to rat brains after mild traumatic brain injury. *Nanomedicine* 2014;10(7) 1539-1548.
- [70] Andrieu-Soler C, Bejjani RA, de Bizemont T, Normand N, BenEzra D, Behar-Cohen F. Ocular gene therapy: a review of nonviral strategies. *Mol Vis* 2006;12 1334-1347.
- [71] Alqawlaq S, Huzil JT, Ivanova MV, Foldvari M. Challenges in neuroprotective nanomedicine development: progress towards noninvasive gene therapy of glaucoma. *Nanomedicine (Lond)* 2012;7(7) 1067-1083.
- [72] Zhang Y, Schlachetzki F, Li JY, Boado RJ, Pardridge WM. Organ-specific gene expression in the rhesus monkey eye following intravenous non-viral gene transfer. *Mol Vis* 2003;9 465-472.
- [73] Glover DJ, Lipps HJ, Jans DA. Towards safe, non-viral therapeutic gene expression in humans. *Nat Rev Genet* 2005;6(4) 299-310.
- [74] Wadhwa S, Paliwal R, Paliwal SR, Vyas SP. Chitosan and its role in ocular therapeutics. *Mini Rev Med Chem* 2009;9(14) 1639-1647.
- [75] Prow TW, Bhutto I, Kim SY, Grebe R, Merges C, McLeod DS, et al. Ocular nanoparticle toxicity and transfection of the retina and retinal pigment epithelium. *Nanomedicine* 2008;4(4) 340-349.
- [76] Ying L, Tahara K, Takeuchi H. Drug delivery to the ocular posterior segment using lipid emulsion via eye drop administration: effect of emulsion formulations and surface modification. *Int J Pharm* 2013;453(2) 329-335.
- [77] Davis BM, Normando EM, Guo L, Turner LA, Nizari S, O'Shea P, et al. Topical delivery of Avastin to the posterior segment of the eye in vivo using annexin A5-associated liposomes. *Small* 2014;10(8) 1575-1584.
- [78] Lajunen T, Hisazumi K, Kanazawa T, Okada H, Seta Y, Yliperttula M, et al. Topical drug delivery to retinal pigment epithelium with microfluidizer produced small liposomes. *Eur J Pharm Sci* 2014;62 23-32.
- [79] Sanders N, Rudolph C, Braeckmans K, De Smedt SC, Demeester J. Extracellular barriers in respiratory gene therapy. *Adv Drug Deliv Rev* 2009;61(2) 115-127.
- [80] Ernst N, Ulrichskotter S, Schmalix WA, Radler J, Galneder R, Mayer E, et al. Interaction of liposomal and polycationic transfection complexes with pulmonary surfactant. *J Gene Med* 1999;1(5) 331-340.
- [81] King M, Rubin BK. Pharmacological approaches to discovery and development of new mucolytic agents. *Adv Drug Deliv Rev* 2002;54(11) 1475-1490.

- [82] Laube BL. The expanding role of aerosols in systemic drug delivery, gene therapy and vaccination: an update. *Transl Respir Med* 2014;2:3-0802-2-3. eCollection 2014.
- [83] Zarogouldis P, Karamanos NK, Porpodis K, Domvri K, Huang H, Hohenforst-Schmidt W, et al. Vectors for inhaled gene therapy in lung cancer. Application for nano oncology and safety of bio nanotechnology. *Int J Mol Sci* 2012;13(9) 10828-10862.
- [84] McCrudden CM, McCarthy HO. Cancer Gene Therapy – Key Biological Concepts in the Design of Multifunctional Non-Viral Delivery Systems. In: Martín F. (ed.) *Gene Therapy - Tools and Potential Applications*. InTech; 2013. ISBN: 978-953-51-1014-9, InTech, DOI: 10.5772/54271. Available from: <http://www.intechopen.com/books/gene-therapy-tools-and-potential-applications/cancer-gene-therapy-key-biological-concepts-in-the-design-of-multifunctional-non-viral-delivery-syst> (accessed 17 February 2015)
- [85] van Gaal EV, Hennink WE, Crommelin DJ, Mastrobattista E. Plasmid engineering for controlled and sustained gene expression for nonviral gene therapy. *Pharm Res* 2006;23(6) 1053-1074.
- [86] Aneja MK, Geiger JP, Himmel A, Rudolph C. Targeted gene delivery to the lung. *Expert Opin Drug Deliv* 2009;6(6) 567-583.





***Objectives***

***Helburuak***

***Objetivos***



### *Objectives*

Nanotechnology-based non-viral vectors have emerged as promising alternatives to viruses to carry genetic material into target cells due to their ability to overcome many limitations of viral vectors. Although very efficient, viruses present low carrying capacity, expensive and complex production and safety issues related to immunogenic responses and even oncogenesis when randomly integrated in the host genome. In this regard, non-viral vectors present lower immunogenicity, higher nucleic acid packing capacity and ease of fabrication compared to their viral counterparts. In addition, continuous advances in the fields of material science and nano-engineering as well as the diversity of available nanosized material allows the design of multifunctional vectors specifically tailored for different applications. Although most conventional gene therapy strategies based on gene addition use viral vectors, nowadays non-viral vectors are predominant in new investigations based on gene editing due to their favorable characteristics. To date, a wide variety of nanosized non-viral gene delivery vectors have been developed, including cationic lipids, polymers and magnetic nanoparticles. These molecules can be nanoengineered to pass over several extracellular and intracellular barriers and to transport therapeutic genes into specific organs or cell types, including cells in the central nervous system (CNS), one of the most challenging organs for both viral and non-viral gene delivery systems.

Among the wide plethora of non-viral vectors, recently emerged niosomes are biocompatible, synthetic, non-ionic surfactant vesicles with a closed bilayer structure. Niosomes have been demonstrated to be effective for retinal gene transfer, an important target organ in many gene therapy strategies due to the existence of several well characterized monogenic retinal disorders. Niosome formulations are based on three principal components -cationic lipids, helper lipids, and non-ionic surfactants. The global chemical properties of these components influence on the physicochemical characteristics of niosomes, such as size, surface charge and morphology, which in turn determine their ability to enter the cells, follow a particular endocytic pathway, deliver the DNA cargo into the nucleus and, therefore, their transfection efficiency. Although the roles of cationic lipids and helper lipids in the transfection process and efficiency mediated by niosomes have been thoroughly studied in rat retina and brain, there is still an important margin for transfection efficiency improvement. Thus, the influence of the non-ionic surfactant component also needs to be well characterized in order to optimize the design of niosome formulations for retinal gene delivery and be able to achieve persistent and high levels of transgene expression, necessary for their biomedical application.

### *Objectives*

Until recently, most efforts have focused on improving nucleic acid delivery strategies either by modifying non-viral vectors or by employing physical methods such as electroporation. However, successful gene transfer not only depends on the carrier, but the properties of the vectored genetic material are also important. With respect to the enhancement of transfection efficiency it can also be achieved by modifying the composition and conformation of the genetic material in order to improve its bioavailability, biocompatibility, durability and safety. In this regard, minimized expression units devoid of bacterial backbone and that only contain the gene of interest and regulatory sequences such as minicircle (MC) DNA vectors emerge as an attractive alternative to conventional plasmid DNA vectors. In fact, MC DNA vectors offer several advantages over their larger parental plasmid DNA vectors, including enhanced transfection efficiency with sustained transgene expression as well as improved immunocompatibility and safety profiles. High levels of transgene expression mediated by MC DNA vectors have been demonstrated in a variety of organ systems *in vivo* including the liver, heart and skeletal muscle, but MC DNA technology has not yet been assessed for retinal gene delivery in complex with niosome formulations.

Finally, in addition to the optimization of the carrier and the genetic material, a new trend in non-viral gene therapy is to explore novel combined strategies between delivery systems and tissue-engineered scaffolds or matrix design. In fact, these combined approaches may offer relevant advantages such as enhanced stability and reduced toxicity. Moreover, complementing gene transfer with matrix design would allow for an effective, targeted and local DNA delivery, which would promote the applicability of gene therapy in many therapeutic fields such as tissue regeneration. Hyaluronic acid (HA) hydrogels have been widely studied for their biocompatibility as well as their ability to incorporate a wide variety of molecules, including nucleic acids. In addition, polymeric non-viral vectors based poly(ethylene imine) (PEI) have been encapsulated into HA hydrogels with successful local transgene expression, but the biomedical application of PEI derivatives is often restricted due to immunogenicity and cytotoxicity issues. In this regard, niosomes offer several advantages due to their high compatibility with biological systems and low toxicity, but the combination between niosome gene delivery systems and HA hydrogel scaffolds has not yet been explored.

In view of these considerations, the main objective of the present work is to evaluate key factors that determine the transfection process and efficiency of non-viral vectors, including the composition and physicochemical properties of non-viral

### *Objectives*

vectors, the composition and conformation of the genetic material and the combination of delivery systems with other technologies such as matrix design. To accomplish that purpose, four specific objectives are considered:

1. To evaluate and compare the transfection efficiency of different commercial non-viral vectors based on cationic lipids, polymers and magnetic nanoparticles carrying a therapeutic plasmid containing the vascular endothelial growth factor gene into central nervous system cells.
2. To understand the role of the non-ionic tensioactive component of niosome formulations in the transfection process and efficiency in retinal cells *in vitro* and *in vivo*.
3. To analyze the interaction between DNA and niosome formulations and to study the influence of the genetic material of nioplexes in retinal gene delivery *in vitro* and *in vivo* comparing plasmid DNA vectors of different sizes and minicircle DNA vectors.
4. To explore new combinations between niosome-based gene delivery systems and hyaluronic acid hydrogel scaffolds for 3D transfection and local gene delivery.



## *Helburuak*

Nanoteknologian oinarritutako bektore ez-biralak birusen alternatiba itxaropentsu gisa sortu dira material genetikoa zeluletarra garraiatzeko, bektore biralek dituzten desabantaila ugari gainditu ditzaketelako. Nahiz eta oso eraginkorrik diren, birusak ez dira gai DNA molekula handiak garraiatzeko, euren ekoizpena oso konplexua eta garestia da eta, gainera, segurtasun arazoak dituzte, hantura erantzuna eta mutagenesia eragin ditzaketelako, besteak beste. Zentzu horretan, bektore ez-biralek ez dute erantzun immunerik sortzen, garraiatu ditzaketen DNA molekulen tamainan ez daukate mugarik, eta birusekin alderatuta, ekoizpen errazagoa eta merkeagoa daukate. Gainera, materialen zientzian zein nano-ingeniaritzan egiten diren etengabeko aurrerapenek, eskuragarri dugun biomaterialen aukera zabalarekin batera, aplikazio bakoitzera espezifikoki egokitutako bektore ez-biralak diseinatzea ahalbidetzen du. Nahiz eta entsegu klinikoetara iritsi diren gene-terapien oinarritutako ikerketa gehienetan birusak erabiltzen diren, gene-edizioan oinarritutako entsegu berrietan ohikoagoa da jada bektore ez-biralak erabiltzea beren ezaugarri onuragarriei esker. Gaur egun, nano-eskalako bektore ez-biral ezberdinak garatu dira eta material ezberdinez osatuta egon daitezke, ohikoenak lipido kationikoak, polimero kationikoak edota partikula magnetikoak direlarik. Molekula horiei nano-ingeniaritza aplikatuta, zelulaz kanpoko zein barneko hesiak gainditzeko gaitasuna eman dokieke, horrela, material genetikoa zelulen nukloetaraino garraiatzeko gai izan daitezen.

Bektore ez-biralen aukera zabalaren artean, niosoma izenekoak lipido kationikoz eta surfaktante ez-ionikoz osatutako besikula biobateragarriak dira. Niosomak gai dira erretinako zelulak modu eraginkorrean transfektatzeko eta ehun horri eragiten gaixotasun monogenikoen tratamendurako potentziala erakutsi dute. Niosoma formulazioek hiru osagai nagusi dituzte: lipido kationikoa, lipido laguntzailea eta tentsoaktibo ez-ionikoa. Osagai horien ezaugarri kimikoek niosomen ezaugarri fisiko-kimikoak –tamaina, karga, morfologia, etab.- baldintzatzen dituzte eta horiek, aldi berean, zeluletan barneratzeko eta DNA molekulak nukleoraino garraiatzeko gaitasuna baldintzatzen dute, gene-transferentziaren eraginkortasunean eraginez. Niosoma formulazioetan lipido kationikoeak eta lipido laguntzaileek jokatzen dituzten rolak sakonki aztertu dira arratoi erretinan eta garunean eginiko transfekzio entseguetan. Hala ere, oraindik aukera handiak daude formulazioak are gehiago optimizatzeko. Beraz, tentsoaktibo ez-ionikoak transfekzio prozesuan eta eraginkortasunean jokatzen duen papera aztertzea ezinbestekoa da niosoma formulazioen hobekuntzan aurrera egiteko.

## *Helburuak*

Dena dela, gene-transferentziaren arrakasta ez dago soilik bektorearen ezaugarrien menpe. Izan ere, bektoreek garaiatzen dituzten DNA molekulen ezaugarriak ere oso garrantzitsuak dira transfekzio prozesuan eta orain arte estrategia gehienek bektoreetan arreta jarri badute ere, gaur egun funtsezko da material genetikoaren propietateak ere ikertzea. Material genetikoaren osaerak eta konformazioak eragina dauka bere bioerabilgarritasunean, biobateragarritasunean, segurtasunean eta transgene-espresioaren irupenean. Zentzu horretan, plasmido konbentzionalen alternatiba gisa sortu dira *minicircle* (MC) izeneko DNA egitura berriak, alegia, expresio unitate minimoak, soilik transgenea eta sekuentzia erregulatzaleak dituztenak eta bakterioetatik eratorritako sekuentziak ezabatu zaizkienak. Izan ere, MC egiturek abantaila ugari aurkezten dituzte plasmido konbentzionalekin alderatuta, esate baterako, transfekzio-maila altuagoak, denboran gehiago irauten duten transgene-espresioak, immunobateragarritasun hobea eta segurtasun profil egokiagoak. DNA egitura berri horiekin transfekzio-maila altuak lortu dira hainbat ehunetan, besteak beste, gibelean, ehun kardiakoan eta muskuluetan, baina MC teknologiaren eraginkortasuna ez da oraindik ikertu erretinako zeluletan eta bektore ez-biral gisa niosomak erabilita.

Azkenik, bektorearen eta material genetikoaren hobekuntzez gain, gaur egun joera berriak sortu dira, adibidez, gene-garraio sistemak ehun-ingeniaritzarekin uztartzea. Izan ere, konbinaketa horiek zenbait onura ekar ditzakete, esate baterako, sistemen egonkortasuna hobetzea eta toxikotasuna jaistea. Gainera, gene-garraioa jomuga diren ehun edota zeluletan modu lokal, espezifiko eta eraginkorrean egitea ahalbidetuko luke eta horrek, aldi berean, klinikaroko jauzia erraztuko luke. Azido hialuronikoz (HA) osatutako hidrogelak asko ikertu dira dituzten propietate biobateragariak direla eta, baita molekula ezberdinak barneratzeko gai direlako ere. Gainera, polimeroz osatutako bektore ez-birala eta HAz osatutako hidrogelak konbinatu dira gene-garraioa bideratzeko eta emaitza onak lortu dira. Dena dela, entsegu horiek ez dute aplikazio klinikorik izan, erabilitako polimeroek zelulatoxikotasuna eta erantzun immuneak eragiten zituztelako. Zentzu horretan, interesgarria litzateke polimero horien ordez niosomak erabiltzea, sistema biologikoekin bateragarritasun handia dutelako eta ez dutelako ia erantzun immunerik sortzen. Gainera, oraindik ez da ikertu HA hidrogelen eta niosomen arteko elkarrekintzak zer ondorio izango lituzkeen gene-garraio lokala egiteko.

Aurreko guztia kontuan hartuta, tesi honen helburu nagusia da bektore ez-biralen bidezko transfekzio prozesua eta eraginkortasuna baldintzatzen dituzten faktore gakoak aztertzea, horretarako bektoreen zein material genetikoaren ezaugarriak

## *Helburuak*

kontuan hartuz eta bektore ez-biralen eta hidrogelen teknologiaren arteko uztartzea bilatuz. Helburu hori betetzeko, honako helburu espezifiko hauek mahaigaineratu ditugu:

1. Lipido kationikoz, polimero kationikoz eta partikula magnetikoz osatutako bektore ez-biral komertzialen transfekzio eraginkortasuna ebaluatzea eta konparaketa egitea, material genetiko gisa endotelio baskularraren hazkuntza faktorea daraman DNA plasmidoa eta entseguetarako nerbio sistema zentraleko zelulak erabilita.
2. Niosoma formulazioen osagai diren tentsoaktibo ez-ionikoeek transfekzio eraginkortasunean eta prozesuan jokatzen duten papera ulertzea, horretarako proteina berde fluoreszentearen genea daraman DNA plasmidoa erabilita erretinako zeluletan, *in vitro* zein *in vivo*.
3. Material genetikoaren eta bektore ez-biralen arteko elkarrekintza aztertzea eta material genetikoaren ezaugarriek erretinako zelulen transfekzio eraginkortasunean jokatzen duten rola aztertzea, plasmido konbentzionalen eta *minicircle* egituren arteko konparaketa eginez eta bektore ez-biral gisa niosomak erabilita.
4. Niosoma bektore ez-biralen eta HA hidrogelen teknologiak uztartzea genegarraio lokala bideratzeko, transfekzio eraginkortasunaren ebaluazioa hiru dimentsiotako zelula-kultiboetan eginez.



## *Objetivos*

Los vectores no-virales basados en la nanotecnología han surgido en los últimos años como alternativa a los virus para transportar genes terapéuticos a células diana, debido a su gran capacidad para superar varias limitaciones de los vectores virales. Aunque son capaces de llevar a cabo la transfección de manera eficiente, los virus presentan una baja capacidad de carga, una producción compleja y costosa y, además, conllevan problemas de seguridad relacionados con respuestas inmunes en el huésped y mutagénesis insercional. En este sentido, los vectores no-virales son menos inmunogénicos, tienen alta capacidad de carga y presentan una fabricación sencilla en comparación con los virus. Además, los continuos avances en los campos de la ciencia de materiales y la nano-ingeniería han propiciado el diseño de vectores no-virales multifuncionales específicos para cada aplicación. A pesar de que hoy en día la mayoría de estrategias de terapia génica convencional utilizan vectores virales, en las nuevas estrategias de terapia génica de edición o corrección genómica, el uso de sistemas no-virales predomina frente a los virales. Hasta la fecha, se han desarrollado vectores no-virales compuestos de diversos materiales, entre los que destacan los lípidos catiónicos, los polímeros o las nanopartículas magnéticas. Estas moléculas pueden ser diseñadas de modo que puedan atravesar barreras extra- e intracelulares para poder llevar a cabo la transfección en células u órganos diana, incluyendo las células del sistema nervioso central (NSC) que a día de hoy siguen siendo de las más difíciles de transfectar tanto para los vectores no-virales como los virales.

Entre la amplia variedad de vectores no-virales, los niosomas son vesículas de surfactante no-iónico sintéticas y biocompatibles, y forman una bicapa lipídica cerrada. Se ha demostrado que los niosomas son eficaces en la transferencia génica en retina, un órgano diana relevante en varias estrategias de terapia génica debido a la existencia de un gran número de enfermedades monogénicas bien caracterizadas que afectan a este tejido. Las formulaciones de niosomas se basan en tres componentes: el lípido catiónico, el lípido *helper* y el tensioactivo no-iónico. Las características químicas y moleculares de esos compuestos determinan en gran medida las propiedades físico-químicas de las formulaciones, como el tamaño de las partículas, la morfología o la carga superficial. A su vez, esas características determinan la habilidad de los niosomas de ser captados por las células diana, de seguir una particular ruta de tráfico intracelular y de liberar el ADN terapéutico en el compartimento intracelular correcto. En última instancia, todo ello condiciona la eficiencia de transfección de las formulaciones de niosomas. El rol del lípido catiónico y del lípido *helper* en el proceso y eficiencia de transfección en cerebro y retina de rata se han estudiado en detalle, pero aún existe un amplio margen de

## *Objetivos*

mejora en la eficiencia de transfección de los niosomas. Es por ello que es importante determinar también el papel que desempeña el tensioactivo no-iónico en el proceso de transfección de los niosomas, ya que esto permitiría diseñar formulaciones más eficientes y mejor adaptadas a cada aplicación terapéutica.

El éxito de la transferencia génica no solo depende del vector, sino que las características del material genético transportado son también relevantes. Hasta hace poco, la mayoría de estrategias para incrementar la eficiencia de transfección se basaban en las modificaciones del vector no-viral o en el uso de métodos físicos como la electroporación. Sin embargo, se puede mejorar la eficiencia de transfección a través de la modificación de la composición y la conformación del material genético con el fin de incrementar su biodisponibilidad, biocompatibilidad, duración de la expresión génica y seguridad. En este sentido, las unidades minimizadas de expresión génica como la tecnología *minicircle* (MC) constituyen una alternativa atractiva a los plásmidos convencionales. Las estructuras MC son secuencias de ADN a las que se les han eliminado los elementos bacterianos como los orígenes de replicación o los genes de resistencia a antibióticos, y que únicamente contienen el gen de interés y las secuencias reguladoras. Estas estructuras ofrecen ventajas importantes frente a los plásmidos convencionales, ya que consiguen mayor eficiencia de transfección y expresión génica prolongada, así como una mejora en el perfil de seguridad y mayor biocompatibilidad. El incremento en la expresión génica a través del uso de la tecnología MC se ha demostrado en varios órganos *in vivo*, incluyendo el hígado, el corazón o el músculo esquelético. Sin embargo, aún no se ha estudiado su eficiencia en terapia génica ocular y utilizando los niosomas para su vehiculización.

Por último, además de la optimización del vector y del material genético, una nueva tendencia en terapia génica no-viral es buscar sinergias complementarias con otras tecnologías como, por ejemplo, la ingeniería tisular. Estas estrategias combinadas pueden ofrecer ciertas ventajas, entre otras, proporcionan una mayor estabilidad al sistema no-viral de liberación génica y producen menos toxicidad. Además, la combinación de transferencia génica con el diseño de matrices tridimensionales ofrecería la posibilidad de liberar el ADN de manera local, prolongada y efectiva de manera específica en los tejidos diana, lo cual facilitaría su aplicabilidad en estrategias terapéuticas dirigidas al tratamiento del cáncer o la regeneración tisular. Los hidrogeles de ácido hialurónico (HA) son de gran interés en ese campo debido a su bicompatibilidad y a su capacidad para incorporar diferentes moléculas, incluyendo los ácidos nucleicos. Asimismo, los vectores poliméricos basados en

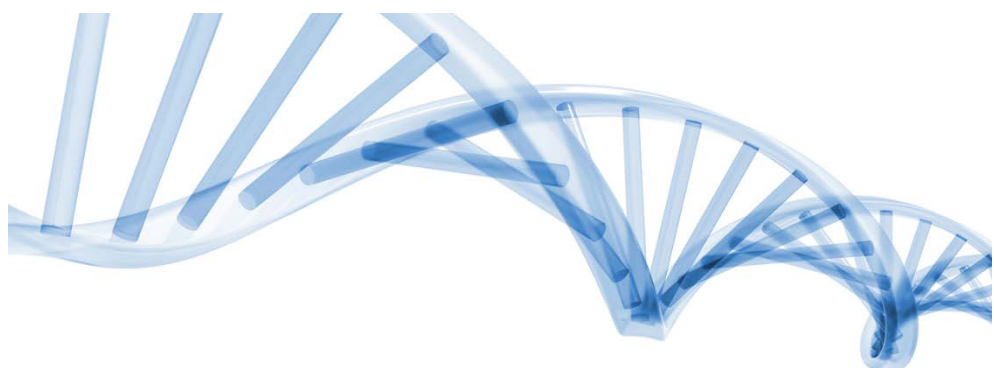
## *Objetivos*

derivados de la poli(etileno imina) o PEI han sido incorporados en hidrogeles de HA de manera exitosa, consiguiendo altas eficiencias de transfección. Sin embargo, la aplicabilidad clínica de los derivados de PEI está limitada por su elevada citotoxicidad. En este sentido, los niosomas pueden constituir una alternativa interesante, ya que ofrecen ventajas importantes como una elevada compatibilidad con sistemas biológicos y baja toxicidad, aunque su combinación con los hidrogeles de HA no se ha estudiado aún para terapia génica no-viral.

Tomando en cuenta las consideraciones anteriores, el principal objetivo de esta tesis doctoral es evaluar los factores clave que determinan la eficiencia de transfección de los sistemas no-virales de liberación génica, incluyendo la composición y las propiedades físico-químicas de los vectores no-virales, la composición y conformación del material genético y la combinación de la liberación génica no-viral con otras tecnologías como el diseño de matrices tridimensionales. Para ello, planteamos cuatro objetivos específicos:

1. Evaluar y comparar la eficiencia de transfección de distintos vectores no-virales basados en lípidos catiónicos, polímeros y nanopartículas magnéticas que vehiculizan un plásmido terapéutico que codifica el factor de crecimiento del endotelio vascular a células del sistema nervioso central.
2. Comprender el rol del tensioactivo no-iónico de las formulaciones de niosomas en el proceso y la eficiencia de transfección en retina tanto *in vitro* como *in vivo*.
3. Analizar la interacción entre el ADN y las formulaciones de niosomas y evaluar la influencia de la composición del material genético en la eficiencia de transfección en retina *in vitro* e *in vivo*.
4. Explorar nuevas combinaciones entre sistemas de liberación génica no-viral basadas en niosomas e hidrogeles de ácido hialurónico para transfectar cultivos celulares en 3D y conseguir una liberación local y efectiva de ADN.





***Experimental section***

***Atal esperimentala***

***Sección experimental***



## ***Chapter 1***

### **Non-viral Vectors Based on Magnetoplexes, Lipoplexes and Polyplexes for VEGF Gene Delivery into Central Nervous System Cells**

*Published in International Journal of Pharmaceutics (2017)*

*Villate-Beitia I, et al. Non-viral vectors based on magnetoplexes, lipoplexes and polyplexes for VEGF gene delivery into central nervous system cells. Int J Pharm. 2017 Apr 15;521(1-2):130-140. doi: 10.1016/j.ijpharm.2017.02.016.*

Nanoteknologian oinarritutako bektore ez-biralek itxaropen handia piztu dute gene terapeutikoak nerbio sistema zentralera (NSZ) modu seguru eta kontrolatuan garraiatzeko. Endotelio baskulararen hazkuntza faktorea (VEGF) hautagai terapeutiko egokia izan liteke NSZri eragiten dioten gaitzen tratamendurako, angiogenesian eta neuro-babesean jokatzen dituen rol garrantzitsuak kontuan hartuta. Lan horretan, hiru bektore ez-biral ezberdin prestatu genituen, partikula magnetikoak, lipido kationikoak edo polímero kationikoak erabiliz. Formulazio horiei phVEGF165a/RESGFP plasmidoa gehitu genien, VEGF proteina –zelulaz kanpoko- eta GFP proteina –zelula barneko- kodifikatzen dituena. Nanopartikulak eta dagozkien nanoplexoak –magnetoplexoak, lipoplexoak eta poliplexoak- fisiko-kimikoki karakterizatu ziren, tamainari, zeta potentzialari, polidispersio indizari, morfologiari eta DNA eusteko, babesteko eta askatzeko gaitasunari dagokionez. Nanoplexoen transfekzio eraginkortasuna neurteko, hainbat parametro aztertu ziren: GFP proteina espresatzen zuen zelulen ehunekoa, batezbesteko fluoreszentzia intentsitatea (MFI) eta VEGF proteinaren ekoizpena (ng/ml-tan) HEK293, C6 eta neurona kultibo primarioetako zeluletan. Magnetoplexoekin lortu ziren transfekzio-mailarik altuenak, lipoplexoak atzetik zitztela C6 zeluletan eta, aldiz, poliplexoak atzetik zitztela neurona kultibo primarioetan. Lipoplexoak izan ziren HEK293 zelulen transfekzioan eraginkorrenak, atzetik magnetoplexoak zitztela. VEGF proteinaren aktibitate biologikoa HUVEC zeluletan neurtu zen, horiengan eragiten zuen ugaltze-efektuaren arabera. Orohar, emaitza horiek ikuspegi berriak zabaltzen dituzte VEGF faktore terapeutikoak bektore ez-birala erabilita garunera bideratzeko

Los vectores no-virales basados en la nanotecnología poseen gran potencial para vehiculizar genes terapéuticos al sistema nervioso central (SNC) de manera segura y controlada. El factor de crecimiento del endotelio vascular (VEGF) es un prometedor gen terapéutico candidato para alteraciones del SNC debido a su rol específico en angiogénesis cerebral y neuroprotección. En este trabajo, elaboramos tres vectores no-virales distintos basados en nanopartículas magnéticas, lipídicas y poliméricas unidos al plásmido phVEGF165a/RESGFP, que codifica la proteína VEGF –extracelular- y la proteína verde fluorescente (GFP) –intracelular-. Las nanopartículas y los correspondientes nanoplexes –magnetoplexes, lipoplexes y poliplexos- fueron caracterizados según su tamaño de partícula, potencial zeta, índice de polidispersión (PDI), morfología y habilidad para condensar, proteger y liberar el ADN. Las eficiencias de transfección de los nanoplexes se determinaron a través de tres parámetros: el porcentaje de células que expresa GFP, la intensidad de fluorescencia media (MFI) y la producción de VEGF (ng/ml) en células HEK293, C6 y cultivo primario de neuronas. Los magnetoplexes presentaron la mayor eficiencia de transfección en C6, seguidos de los lipoplexes, y en células de cultivo primario de neurona, seguidos de los poliplexos. Los lipoplexes fueron los más eficaces en células HEK293, seguidos por los magnetoplexes. La actividad biológica de la proteína VEGF se confirmó por su efecto proliferativo en células HUVEC. En general, estos resultados proporcionan nuevo conocimiento para la vehiculización del gen VEGF a células del SNC mediante vectores no-virales.

*Experimental section: Chapter 1*

## **Non-viral Vectors Based on Magnetoplexes, Lipoplexes and Polyplexes for VEGF Gene Delivery into Central Nervous System Cells**

Ilia Villate-Beitia<sup>1,2</sup>, Gustavo Puras<sup>1,2</sup>, Cristina Soto-Sánchez<sup>2,3</sup>, Mireia Agirre<sup>1,2</sup>, Edilberto Ojeda<sup>1,2</sup>, Jon Zarate<sup>1,2</sup>, Eduardo Fernández<sup>2,3</sup> and José Luis Pedraz<sup>1,2\*</sup>.

<sup>1</sup> NanoBioCel Group, University of the Basque Country (UPV/EHU), Vitoria-Gasteiz, Spain

<sup>2</sup> Biomedical Research Networking center in Bioengineering, Biomaterials and Nanomedicine (CIBER-BBN), Spain

<sup>3</sup> Neuroprothesis and Neuroengineering Research Group, Miguel Hernandez University, Elche, Spain

---

### **Abstract**

Nanotechnology based non-viral vectors hold great promise to deliver therapeutic genes into the central nervous system (CNS) in a safe and controlled way. Vascular endothelial growth factor (VEGF) is a potential therapeutic gene candidate for CNS disorders due to its specific roles in brain angiogenesis and neuroprotection. In this work, we elaborated three different non-viral vectors based on magnetic, cationic lipid and polymeric nanoparticles complexed to the phVEGF165aIRESGFP plasmid, which codifies the VEGF protein –extracellular- and the green fluorescent protein (GFP) –intracellular-. Nanoparticles and their corresponding nanoplexes – magnetoplexes, lipoplexes and polyplexes- were characterized in terms of size, zeta potential, PDI, morphology and ability to bind, release and protect DNA. Transfection efficiencies of nanoplexes were measured in terms of percentage of GFP expressing cells, mean fluorescent intensity (MFI) and VEGF (ng/ml) production in HEK293, C6 and primary neuronal culture cells. Magnetoplexes showed the highest transfection efficiencies in C6, followed by lipoplexes, and in primary neuronal culture cells, followed by polyplexes. Lipoplexes were the most efficient in HEK293 cells, followed by magnetoplexes. The biological activity of VEGF was confirmed by its proliferative effect in HUVEC cells. Overall, these results provide new insights for VEGF gene delivery into CNS cells using non-viral vectors.

### **Keywords**

Non-viral vectors, gene delivery, VEGF, CNS.

*Experimental section: Chapter 1*

## **1. INTRODUCTION**

Nanotechnology-based gene delivery has gained interest in recent years. Continuous advances in the fields of material science and nano-engineering - along with a better understanding of the multiple possibilities for genome editing - have motivated the synthesis, characterization, and functionalization of biocompatible nanomaterials for gene delivery purposes (Keles et al., 2016). In addition, the diversity of available nanosized material allows the design of multifunctional vectors specifically tailored for different applications (Srikanth and Kessler, 2012; Pezzoli et al., 2012).

Non-viral vectors are characterized by their potential to overcome many of the limitations of viral vectors, especially those related to safety and vector production. Although viral vector based gene delivery platforms are still predominant in clinical trials due to their higher transfection efficiencies (Yin et al., 2014), non-viral vectors have emerged as a promising alternative because of their lower immunogenicity, higher nucleic acid packing capacity and ease of fabrication (Jin et al., 2014). Additionally, non-viral formulations can be produced on a large scale with high reproducibility and acceptable costs, and they are relatively stable to storage (Pezzoli et al., 2012). To date, a wide variety of nanosized non-viral gene delivery vectors have been developed, including cationic lipids (Yin et al., 2014; Ojeda et al., 2015; Jubeli et al., 2016), polymers (Pack et al., 2005; Agirre et al., 2015a) and magnetic nanoparticles (Soto-Sanchez et al., 2015). These molecules can be nanoengineered to transport therapeutic genes into specific organs or cell types and to pass over several extracellular and intracellular barriers.

Central nervous system (CNS) cells are one of the most challenging to transfet for both viral and non-viral gene delivery systems, due to the numerous protective barriers enclosing the CNS and its complex cellular organization. Therefore, the discovery of an effective approach to afford the wide range of neurodegenerative disorders remains a huge dare, where nanotechnologies are expected to play an important role. Most neurodegenerative disorders, although presenting diverse clinical manifestations, share some common traits such as vast neuronal loss, synaptic failures and aggregates of misfolded proteins (Spuch et al., 2012). Additionally, accumulating evidence suggests that aging-related vascular alterations of the brain make it vulnerable to cognitive dysfunction, leading to neurodegeneration and dementia (Kalaria, 2010). In Alzheimer's disease (AD) – the most prevalent adult-onset dementia –reductions in the cerebral blood flow and dysfunction of the blood-brain barrier (BBB) have been related to amyloid-beta (A $\beta$ )

## *Experimental section: Chapter 1*

accumulation in brain (Zlokovic, 2011). In this regard, vascular endothelial growth factor (VEGF) is a physiological regulator mainly involved in brain angiogenesis and BBB integrity, and it also plays specific roles in neuroprotection (Carmeliet and Ruiz de Almodovar, 2013a). Recently, it has been shown that administration of VEGF encapsulated in poly(lactic-co-glycolic acid) (PLGA) nanospheres to animal models of AD increases vascularisation and reduces neuronal loss and A $\beta$  deposits in brain (Herran et al., 2013a). Also, it has been reported that, in a mouse model of AD, administration of encapsulated VEGF-secreting cells enhances proliferation of neuronal progenitor cells in the hippocampus (Antequera et al., 2012).

Based on these considerations, we present a nanoformulation based approach for VEGF gene delivery into CNS cells. For that purpose, three different nanoformulations –ultrapure oligochitosan (UOC), *Lipofectamine* cationic lipid and *NeuroMag* magnetic nanoparticles– were complexed to the phVEG165aIRESGFP plasmid, which codifies for the human VEGF165a protein and for the green fluorescent protein (GFP). Nanoformulations and resulting nanoplexes – nanoformulations complexed to DNA– were physicochemically characterized in terms of size, superficial charge, polydispersity index (PDI), morphology and capacity to condense, release and protect DNA. *In vitro* transfection studies were carried out in C6 glial cells and in primary neuronal culture cells as CNS cell models, and in HEK293 cells, as a general transfection model. Transfection efficiencies were evaluated in terms of percentage of GFP expressing cells, mean fluorescent intensity (MFI) and VEGF protein expression. Cell viability upon exposition to nanoplexes was also evaluated. Bioactivity of the VEGF protein secreted by transfected primary neuronal culture cells was assessed by a proliferation assay in human umbilical vein endothelial cells (HUVEC).

## **2. MATERIALS AND METHODS**

### *2.1. Materials*

Ultrapure Oligochitosan (UOC) O15 (MWs of 5.7, DDA  $\geq$ 97% and endotoxin levels  $\leq$ 0.05 EU/mg) was purchased from NovaMatrix/FMC (Sandvika, Norway). Human embryonic kidney 293 (HEK293) cells, Rattus Norvegicus glial cells (C6), human umbilical vein endothelial cells (HUVEC), Eagles's Minimal Essential Medium with Earle's BSS and 2mM 1-glutamine (EMEM, ATCC 30-2003) and Kaighn's Modification of Ham's F-12 Medium (F-12K, ATCC 30-2004) were obtained from the American Type Culture Collection (ATCC, Teddington, UK). Endothelial Cell Growth Medium (EGM-2 Bullekit, CC-3162) was purchased from Lonza Group Ltd. (Basel,

## *Experimental section: Chapter 1*

Switzerland). Opti-MEM I reduced medium, Antibiotic/Antimicotic solution, Penicillin/Streptomycin solution and Lipofectamine 2000 were purchased from Invitrogen (Life Technologies, Paisley, UK). The phVEGF165aIRESEGFP plasmid was purchased from PlasmidFactory (Bielefeld, Germany). The Human VEGF ELISA Development Kit and the recombinant hVEGF165 protein were provided by Peprotech EC Ltd. (London, UK). Phosphate buffer saline (PBS), fetal bovine serum (FBS), horse serum (HS), Cell Counting Kit-8 (CCK-8), DNase I, sodium dodecyl sulfate (SDS) and propidium iodide were acquired from Sigma-Aldrich (Madrid, Spain). Gel electrophoresis materials were obtained from Bio-Rad (Madrid, Spain). NeuroMag Transfection Reagent was acquired from OZ Biosciences (Marseille, France). TECAN infiniteM200 spectrophotometer was acquired from TECAN Ibérica Instrumentación S.L., Madrid, Spain.

### *2.2. Preparation of nanoplexes*

Lipoplexes were prepared at a Lipofectamine/DNA ratio of 2:1 (w/w) by mixing gently Lipofectamine 2000 solution (1mg/mL) and the plasmid solution (1 mg/mL) at appropriate volumes. Magnetoplexes were prepared at a NeuroMag/DNA ratio of 2:1 (w/w) by mixing gently NeuroMag solution (1mg/mL) and plasmid solution (1 mg/mL) at appropriate volumes. Polyplexes based on UOC were prepared by the self-assembly method. Briefly, a determined value of plasmid solution (1 mg/ml) was added under vortex agitation to a stock solution of UOC (2 mg/ml) to obtain a final UOC/DNA ratio of 13:1 (w/w). In all cases, the formulations were incubated for 25 min at room temperature to allow the correct formation of the complexes.

### *2.3. Nanoformulation characterization: size, zeta potential, PDI, morphology*

The hydrodynamic diameter and the zeta potential of nanoparticles and their corresponding nanoplexes were determined by Dynamic Light Scattering (DLS) and by Lasser Doppler Velocimetry (LDV), respectively, using a Zetasizer Nano ZS (Malvern Instrument, UK) as previously described (Ojeda et al., 2015). Briefly, 50 µl of the formulations were resuspended into 950 µl of 0.1 mM NaCl solution. All measurements were carried out in triplicate. The particle size reported as hydrodynamic diameter was obtained by cumulative analysis. The Smoluchowski approximation was used to support the calculation of the zeta potential from the electrophoretic mobility.

The morphologies of cationic lipid and magnetic nanoparticles were characterized by transmission electron microscopy (TEM) and Cryo-TEM was used to characterize

## *Experimental section: Chapter 1*

the morphology of UOC polymeric nanoparticles as previously described (Ojeda et al., 2015).

### *2.4. Agarose gel electrophoresis assay*

For DNA release assay, 12 µl of a 7% SDS solution were added to the samples. For DNA protection assay, 3 µl of DNase I enzyme and 12 µl of a 7% SDS solution were added to the samples. For DNA binding assay, no SDS neither DNase I enzyme were added to the samples. The amount of DNA per well was 100 ng in all cases. Samples with DNase I were incubated at 37°C for 30 min. 4 µl of loading buffer were added to all samples before running the gel. Agarose gel (0.8% w/w) was immersed in a Tris-acetate-EDTA buffer and exposed for 30 min to 120 V. GelRed was used to stain the DNA bands and images were obtained with a ChemiDocTM MP Imaging System and analyzed by Image LabTM Software (BioRad, USA). Naked DNA was used as control at each condition.

### *2.5. Cell culture and in vitro transfection*

HEK293 and C6 cells were maintained in complete medium. For HEK293 cells, Eagles's Minimal Essential medium with Earle's BSS and 2mM 1-glutamine (EMEM, ATCC 30-2003) supplemented with 10% FBS and Antibiotic/Antimycotic solution was used. For C6 cells, Kaighn's Modification of Ham's F-12 Medium (F-12K, ATCC 30-2004) supplemented with 2.5% FBS, 15% HS and Penicillin/Streptomycin solution was used. Both cell cultures were kept at 37°C under a humidified atmosphere containing 5% CO<sub>2</sub>. Before transfection, HEK293 and C6 cells were seeded in 24-well plates at an initial density of 1.2 x 10<sup>5</sup> cells per well with 250 µl of complete medium and without the corresponding antibiotic solutions. All cells were incubated overnight to achieve 70-90% of confluence at the time of transfection.

Experimental procedures for *in vitro* primary neuronal cultures were carried out conformed to the directive 2010/63/EU of the European Parliament and of the Council, and the RD 53/2013 Spanish regulation on the protection of animals use for scientific purposes and was approved by the Miguel Hernandez University Committee for Animal use in Laboratory. Dissociated cultures from cortical tissue were obtained from E17-E18 rat embryos (Sprague Dawley) and preserved in DMEM (32430-027, GIBCO®, Thermo Fisher Scientific, MA, USA) containing 10% FBS, during extraction. Subsequently cells were transferred to FBS-free DMEM and trypsin was added and incubated at 37°C for chemical dissociation. The cell density was determined using a hemocytometer and seeded at an initial density of

## *Experimental section: Chapter 1*

approximately 3x10<sup>5</sup> cells per well in a 12-well plates on glass coverslips in Neurobasal (12348-017, GIBCO®) / FBS (S181B-500, Biowest, Nuaillé, France) medium supplemented with B27 (17504-044, GIBCO®), Glutamax (35050-038, GIBCO®) and Penicillin-Streptomycin (15-40-122, GIBCO®) and maintained in an incubator at 37 °C and 5% CO<sub>2</sub>

For transfection, antibiotic free complete mediums were replaced with serum-free Opti-MEM medium, and cells were exposed to nanoplexes resuspended in Opti-MEM at their corresponding nanoparticle/DNA ratios (w/w). The amount of plasmid per well was 1.25 µg, each formulation was tested in triplicate. Additionally, in the case of polyplexes, Opti-MEM containing 270 mM mannitol was used to obtain a final isotonic medium and pH was adjusted to 7.0 using HCl 0.1 M (Agirre et al., 2015b). After 3h of incubation at 37°C, nanoplexes were removed from wells and 250 µl of complete medium were added. HEK293, C6 and primary neuronal culture cells were allowed to grow 48 h at 37 °C under a humidified atmosphere containing 5% CO<sub>2</sub> for analysis of cell viability and transfection efficiencies.

### *2.6. Flow cytometry assay*

Flow cytometry analysis was conducted using a FACSCalibur system flow cytometer (Becton Dickinson Bioscience, San Jose, USA). The supernatant mediums of the plated cell samples were removed and kept at -80°C for later analysis of VEGF production. Plated cells were washed twice with PBS and detached from the microplate with 200 µl of trypsin/EDTA. 400 µl of complete growth mediums were added and cells were transferred to specific flow cytometer tubes. Cell viability was evaluated using 5 µL of propidium iodide (dilution 1:10) reagent in each sample, and dead cells were excluded from the GFP expression analysis. The fluorescent signal corresponding to dead cells was measured at 650 nm (FL3). Transfection efficiency was expressed as the percentage of live GFP positive cells at 525 nm (FL1). MFI data were obtained from live positive cells at 525 nm (FL1). Control samples (non-transfected cells) were displayed on a forward scatter (FSC) versus side scatter (SSC) dot plot to establish a collection gate and exclude cells debris. For each sample 10,000 events were collected. Each formulation was analyzed in triplicate.

### *2.7. Immunocytochemistry assay*

For analysis of GFP expression, primary neuronal cultures seeded onto coated coverslips were fixed with 4% paraformaldehyde (in 0.1M PBS) for 20 min at room temperature and incubated in blocking buffer (10% normal donkey serum, PBS,

## *Experimental section: Chapter 1*

0.5% Triton X-100) for 1 hour. Then incubated with primary antibody chicken anti-GFP (Invitrogen, 1:100, diluted in PBS, 0.5% Triton X-100) overnight at room temperature. Subsequently, cells were washed in PBS and incubated in secondary antibody Alexa Fluor 555-conjugated goat anti-chicken IgG (Invitrogen, 1:100, diluted in PBS, 0.5% Triton X-100) for 1 hour. Hoechst 33342 was used to label all the nuclei. The cells were finally washed in PBS and the coverslips mounted in fluoromount Vectashield (Vector Laboratories) for viewing by laser-confocal microscopy (Leica TCS SPE Microsystems GmbH, Germany). Alexa Fluor 555 was pseudocolored in green to visualize GFP expression. Immunocytochemistry controls were performed by omission of antibodies (data not shown).

### *2.8. VEGF production assay*

VEGF concentration (ng/ml) of transfected cell supernatants was analyzed using Human VEGF Standard ABTS ELISA Development Kit according to the manufacturer's instructions at 48 h post-transfection. Each measurement was performed in triplicate. The absorbance was measured at 405 nm with wavelength correction set at 650 nm using the Tecan i-Control 1.7 software and the TECAN spectrophotometer.

### *2.9. VEGF bioactivity assay*

HUVEC cells were maintained in Endothelial Cell Growth Medium (EGM-2 Bullekit, CC-3162) supplemented with a supplement kit, and cultured at 37°C in humidified air with 5% CO<sub>2</sub>. HUVEC cells between passages 1 and 2 were seeded into 96-well poly-L-lysine-coated culture plates at a density of 5 x 10<sup>3</sup> cells/well. After 24 h, the culture medium was removed, and 100 µl of fresh medium (without the supplement kit) were added and supplemented with 200 µl of transfected primary neuronal culture cells supernatant, containing VEGF secreted by transfected cells. HUVEC cells treated with secreted VEGF and non-treated control HUVEC cells were incubated for 72 h at 37°C in humidified air with 5% CO<sub>2</sub>. Cell proliferation was measured using a Cell Counting Kit-8 (CCK-8) according to the manufacturer's instructions.

### *2.10. Statistical analysis*

Statistical analyses were carried out using IBM SPSS Statistics software. Normal distribution of samples was assessed by the Kolmogorov–Smirnov test, and the homogeneity of the variance by the Levene test. Student's *t*-test was used to

*Experimental section: Chapter 1*

compare differences between groups. In all cases, P values < 0.05 were regarded as significant. Data were presented as mean  $\pm$  SD, unless stated otherwise.

### **3. RESULTS**

#### *3.1. Nanoformulation characterization: size, zeta potential, PDI, morphology*

Physicochemical characterization of nanoparticles and nanoplexes is represented in Fig. 1a-c. The mean particle size of magnetic nanoparticles was  $182.37 \pm 0.29$  nm and, when complexed to phVEGF165aIRESGFP plasmid DNA, mean size of magnetoplexes increased to  $384.97 \pm 21.57$  nm. Mean particle size of cationic lipid based nanoformulations was  $643.27 \pm 125.26$  nm, and lipoplexes exhibited mean particle size of  $476.17 \pm 98.65$  nm. UOC based polymeric nanoformulations showed a mean particle size of  $337.77 \pm 68.35$  nm, which increased to  $546.3 \pm 11.35$  nm when they formed polyplexes (Fig. 1a, bars). Size distributions of nanoformulations ranged from narrow –magnetic nanoparticles with a PDI of 0.15- to large –cationic lipid nanoparticles with a PDI of 0.635- (Fig.1b, table). Zeta potential values of magnetic, cationic lipid and polymeric nanoparticles were  $20.77 \pm 2.00$  mV,  $18.57 \pm 5.19$  mV and  $4.49 \pm 0.71$  mV, respectively. Upon complexing to DNA, mean zeta potential values of magnetoplexes, lipoplexes and polyplexes decreased to  $-16 \pm 2.01$  mV,  $-22.2 \pm 1.51$  mV and  $-2.05 \pm 0.39$ , respectively (Fig. 1a, lines). When observed magnetic nanoparticles under transmission electron microscopy (TEM) and polymeric nanoparticles under cryogenic transmission electron microscopy (Cryo-TEM), both appeared spherical. Cationic lipid nanoparticles observed under TEM showed an irregular morphology (Fig. 1c).

*Experimental section: Chapter 1*

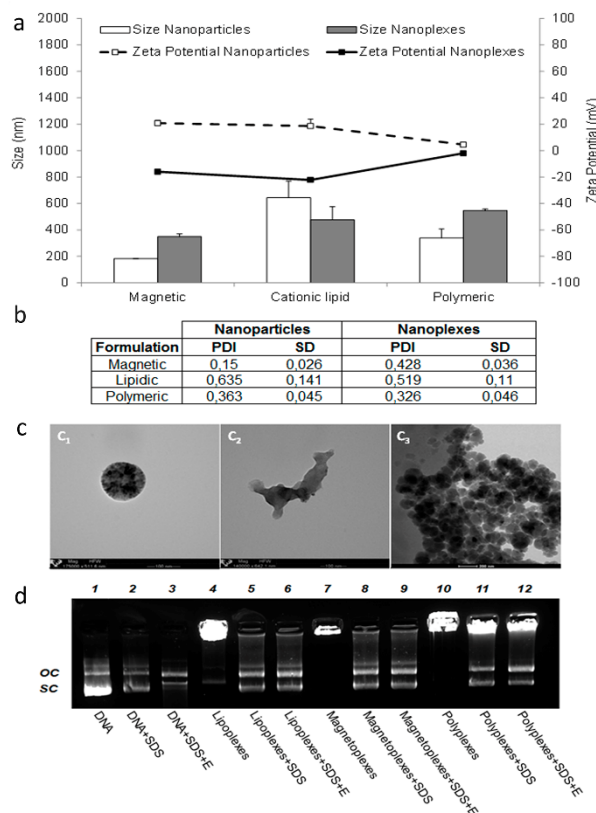


**Figure 1.** Physicochemical characterization of nanoparticles and nanoplexes. (a) Size (white and grey bars, which correspond to nanoparticles and nanoplexes, respectively) and zeta potential values (dotted and continuous lines, which correspond to nanoparticles and nanoplexes, respectively). Each value represents the mean  $\pm$  SD, n=3. (b) PDI values. Each value represents the mean  $\pm$  SD, n=3. (c) TEM images of cationic lipid (c<sub>1</sub>) and magnetic (c<sub>2</sub>) nanoparticles and Cryo-TEM images of polymeric (c<sub>3</sub>) nanoparticles. Original magnification 140,000x for cationic lipid nanoparticles, 175,000x for magnetic nanoparticles and 25,000x for polymeric nanoparticles. (d) Binding, protection, and SDS-induced release of DNA from nanoparticles visualized by agarose electrophoresis. Lanes 1–3 correspond to free DNA; lanes 4–6, lipoplexes; lanes 7–9, magnetoplexes; lanes 10–12, polyplexes. Free DNA and nanoplexes were treated with SDS (lanes 2, 5, 8 and 11) and DNase I + SDS (lanes 3, 6, 9, and 12). OC: open circular form, SC: supercoiled form.

## *Experimental section: Chapter 1*

### *3.2. phVEGF165aIRESGFP plasmid binding, releasing and protecting assay of nanoformulations*

Figure 1d shows the capacity of the three different nanoformulations to bind, release and protect the phVEGF165aIRESGFP plasmid against enzymatic degradation, evaluated by agarose gel electrophoresis. DNA was retained without migration in lanes 4, 7 and 10 (contrary to lane 1, where control naked DNA completely migrated). DNA partially migrated when SDS was added to the nanoplexes as indicated by the intense SC signal observed on lanes 5, 8 and 11 (similar to the control, on lane 2). Intensive SC bands observed in lanes 6, 9 and 12 indicate that DNA was not degraded by DNase I enzyme and was partially released after the addition of SDS. DNA signals observed in wells 6, 9 and 12 indicate that DNA was protected from enzymatic degradation and did not migrate upon SDS addition.

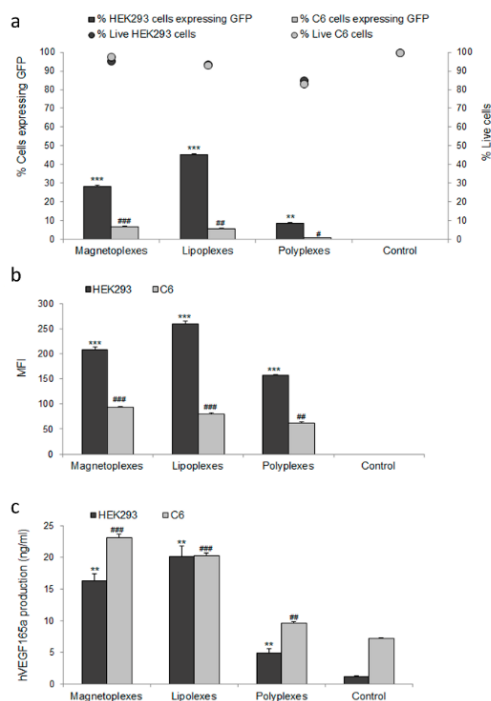
### *3.3. Cell viability and transfection efficiency assays*

Figure 2 represents cell viability and transfection efficiency –in terms of GFP expression, MFI and VEGF expression- of nanoplexes in HEK293 and C6 cell lines. The percentages of live HEK293 and C6 cells were above 90% upon transfection with magnetoplexes and lipoplexes; this value was lower –around 85% – when using polyplexes for transfection (Fig. 2a, dots). Regarding percentages of GFP expressing cells (Fig. 2a) and MFI (Fig. 2b), values in HEK293 cells (black bars) were higher than in C6 cells (light grey bars). GFP expressing HEK293 cell percentages were  $28.43 \pm 0.49\%$  with magnetoplexes,  $45.47 \pm 0.07\%$  with lipoplexes and  $8.54 \pm 0.55\%$  with polyplexes. In C6 cells, percentages of GFP expressing cells were  $6.87 \pm 0.35\%$  with magnetoplexes,  $5.51 \pm 0.38\%$  with lipoplexes and  $0.68 \pm 0.02\%$  with polyplexes (Fig. 2a, bars). MFI values in HEK293 and C6 cells transfected with magnetoplexes, lipoplexes and polyplexes, respectively, were  $208.33 \pm 5.51$  and  $93.23 \pm 2.27$ ;  $260.00 \pm 5.00$  and  $79.89 \pm 2.25$ ; and  $157 \pm 1.73$  and  $61.77 \pm 2.63$  (Fig. 2b).

VEGF expression levels (ng/ml) in transfected HEK293 and C6 cell lines are represented in Fig. 2c. After transfection with magnetoplexes, VEGF production in HEK293 cells was  $16.32 \pm 1.03$  ng/ml and in C6 cells  $23.11 \pm 0.48$  ng/ml. With lipoplexes, we obtained  $20.15 \pm 1.63$  ng/ml VEGF in HEK293 cells and  $20.21 \pm 0.48$  ng/ml VEGF in C6 cells. When transfected with polyplexes, HEK293 produced  $4.9 \pm 0.63$  ng/ml VEGF and C6 cells produced  $9.60 \pm 0.24$  ng/ml VEGF (Fig. 2c). Control non-transfected HEK293 cells produced  $1.16 \pm 0.13$  ng/ml VEGF and C6 cells  $7.19 \pm 0.09$  ng/ml VEGF.

## Experimental section: Chapter 1

Statistical differences were found in all cases when comparing GFP expression levels, MFI values and VEGF expression levels of cells transfected with nanoplexes and non-transfected control cells.



**Figure 2.** Cell viability and transfection efficiencies in HEK293 and C6 cells. (a) Cell viability (HEK293 cells, dark grey dots; C6 cells, light grey dots) 48h after transfection with magnetoplexes, lipoplexes and polyplexes. Control cells were not treated with nanoplexes. Percentages of GFP expressing cells (HEK293 cells, dark grey bars; C6 cells, light grey bars) 48 h after transfection with nanoplexes. Control cells were not treated with nanoplexes. Each value represents the mean  $\pm$ SD, n=3. (b) Mean Fluorescent Intensity (MFI) values 48h post-transfection with nanoplexes (HEK293 cells, dark grey bars; C6 cells, light grey bars). Each value represents the mean  $\pm$ SD, n=3. (c) VEGF production (ng/ml) values 48h post-transfection with nanoplexes (HEK293 cells, dark grey bars; C6 cells, light grey bars). Control cells were not treated with nanoplexes. Each value represents the mean  $\pm$ SD, n=3. Statistical significance: \*p<0.05, \*\*p<0.01, \*\*\*p<0.001 compared to control HEK293 cells; #p<0.05, ##p<0.01, ###p<0.001 compared to control C6 cells.

mean  $\pm$ SD, n=3. Statistical significance: \*p<0.05, \*\*p<0.01, \*\*\*p<0.001 compared to control HEK293 cells; #p<0.05, ##p<0.01, ###p<0.001 compared to control C6 cells.

### 3.4. Correlation between GFP expression, MFI and VEGF production values

Figure 3a shows the correlation between the levels of VEGF production and the percentage of GFP expressing cells in HEK293 cells transfected with the three different nanoplexes. Lipoplexes (white dot) exhibited the highest values in both variables, followed by magnetoplexes (grey dot) and then polyplexes (black dot). At higher percentage of GFP positive cells, higher VEGF production levels were obtained ( $R^2 = 0.9456$ ). As shown in Figure 3b, a similar correlation pattern was found between VEGF production and MFI values ( $R^2 = 0.9226$ ). FL1 histograms in

## Experimental section: Chapter 1

Fig. 3c illustrate HEK293 cells distribution 48h after transfection with the nanoplexes. FL1 positive cells represent cells expressing the GFP protein.

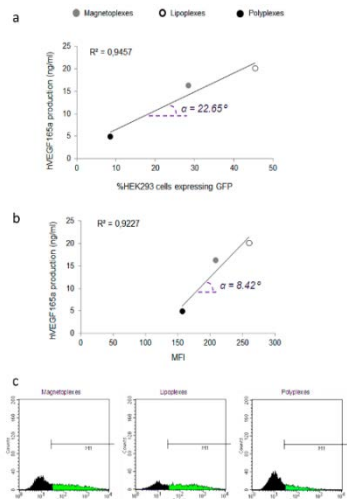


**Figure 3.** Correlations between the transfection efficiency parameters in HEK293 cells. (a) Correlation between VEGF production (ng/ml) and percentage of GFP expressing live cells in HEK293 cells 48h post-transfection with magnetoplexes (grey dot), lipoplexes (white dot) and polyplexes (black dot). Each value represents the mean  $\pm$  SD, n=3.  $\alpha$  represents the angle of the slope. (b) Correlation between VEGF production (ng/ml) and MFI values in HEK293 cells 48h post-transfection with nanoplexes. Each value represents the mean  $\pm$  SD, n=3.  $\alpha$  represents the angle of the slope. (c) GFP histograms of HEK293 cells 48h post-transfection with nanoplexes. M1 represents the threshold for GFP positive signal.

Figure 4a shows the correlation the levels of VEGF production and the percentage of GFP expressing cells in C6 cells transfected with the three different nanoplexes. In this case, magnetoplexes (grey dot) exhibited the highest values in both variables, followed by lipoplexes (white dot) and then polyplexes (black dot). Again, a robust correlation was found between the production levels of VEGF and the percentage of GFP expressing cells ( $R^2 = 0.999$ ). Figure 4b illustrates an analogous correlation pattern between VEGF production and MFI values ( $R^2 = 0.9474$ ) (Fig. 4b). FL1 histograms in Fig. 4c depict C6 cells distribution 48h after transfection with the nanoplexes. FL1 positive cells represent cells expressing the GFP protein.

## Experimental section: Chapter 1

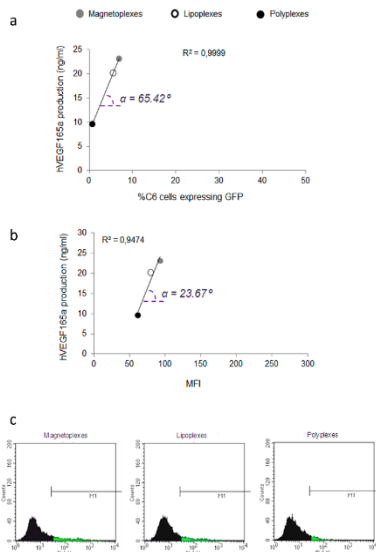


**Figure 4.** Correlations between the transfection efficiency parameters in C6 cells. (a) Correlation between VEGF production (ng/ml) and percentage of GFP expressing live cells in C6 cells 48h post-transfection with magnetoplexes (grey dot), lipoplexes (white dot) and polyplexes (black dot). Each value represents the mean  $\pm$  SD, n=3.  $\alpha$  represents the angle of the slope. (b) Correlation between VEGF production (ng/ml) and MFI values in C6 cells 48h post-transfection with nanoplexes. Each value represents the mean  $\pm$  SD, n=3.  $\alpha$  represents the angle of the slope. (c) GFP histograms of C6 cells 48h post-transfection with nanoplexes. M1 represents the threshold for GFP positive signal.

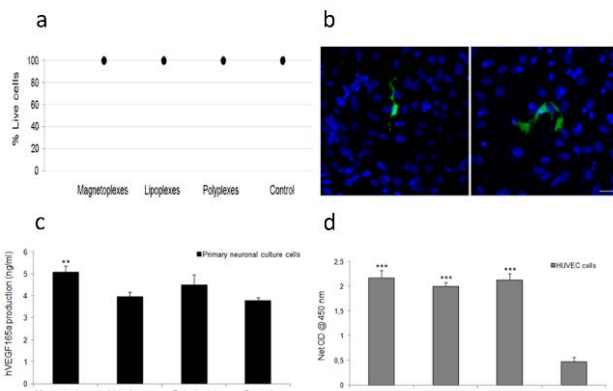
### 3.5. Cell viability and VEGF production in primary neuronal culture cells

Figure 5a-c shows cell viability and transfection efficiency of nanoplexes in primary neuronal culture cells. Upon transfection with nanoplexes, percentages of cell viability in primary neuronal culture were around 100% in all cases (Fig. 5a). In the immunocytochemistry images (Fig. 5b) a few disperse cells expressing GFP were observed upon transfection with magentoplexes. Regarding VEGF production levels, transfection with magnetoplexes obtained  $5.06 \pm 0.28$  ng/ml, lipoplexes  $3.94 \pm 0.21$  ng/ml and polyplexes  $4.47 \pm 0.47$  ng/ml (Fig. 5c). Control non-transfected cells secreted  $3.77 \pm 0.12$  ng/ml VEGF. Significant differences in VEGF secretion levels were found between magnetoplexes transfected cells and control cells ( $**p<0.01$ ).

### 3.6. Transfected primary neuronal culture cells released VEGF bioactivity assay

Figure 5d shows HUVEC cell proliferation in response to VEGF secreted by the primary neuronal culture cells transfected with the nanoplexes. Proliferation of HUVEC cells in medium supplemented with VEGF from primary neuronal culture cells transfected with magentoplexes, polyplexes and lipoplexes was significantly higher than the one of HUVEC cells maintained in medium without supplements ( $***p<0.001$ ).

*Experimental section: Chapter 1*



**Figure 5.** Primary neuronal culture cells viability, efficiencies of transfection with nanoplexes in those cells and bioactivity of VEGF protein secreted by the transfected cells. (a) Cell viability in primary neuronal culture cells 48h post-transfection with nanoplexes. Each value represents the mean  $\pm$  SD, n=3. (b) Immunocitochemistry images of transfected primary neuronal culture cells. Green, Anti-GFP. Blue, Hoechst. Scale: 25  $\mu$ m. (c) VEGF production (ng/ml) by primary neuronal culture cells 48h after transfection with nanoplexes. Control cells were not treated with nanoplexes. Each value represents the mean  $\pm$  SD, n=3. (d) HUVEC cell proliferation in response to VEGF secreted by primary neuronal culture cells transfected with nanoplexes. Control HUVEC cells were not treated with VEGF. Each value represents the mean  $\pm$  SD, n=6. Statistical significance: \* $p$ <0.05, \*\* $p$ <0.01, \*\*\* $p$ <0.001 compared to control HUVEC cells.

#### 4. DISCUSSION

Nucleic acid based therapies hold great promise but demand effective and safe carriers. Moreover, efficient transfection of CNS is still a challenge, which retards the development of therapeutic gene delivery strategies for the wide variety of neurodegenerative disorders. In recent years, biocompatible nanomaterials have emerged as potential candidates for that purpose. In fact, different nanosized non-viral vectors have been recently reported to efficiently transfect CNS cells *in vitro* and *in vivo*, such as chitosans (Puras et al., 2013a; Puras et al., 2013b), cationic lipids (Ojeda et al., 2016) and magnetic nanoparticles (Soto-Sanchez et al., 2015). Besides, VEGF may be a potential therapeutic gene candidate for CNS disorders (Ruiz de Almodovar et al., 2009), due to the strong relationship between vascular alterations in brain and neurodegenerative diseases (Fournier et al., 2012) and its specific roles in brain angiogenesis and neuronal survival (Herran et al., 2013a; Carmeliet and Ruiz de Almodovar, 2013b).

### *Experimental section: Chapter 1*

In this work we used non-viral nanocarriers for VEGF gene delivery into CNS cells. For that purpose, three different nanoparticles – magnetic, cationic lipid and polymeric - were complexed to the phVEGF165aIRESGFP plasmid to obtain the corresponding nanoplexes – magnetoplexes, lipoplexes and polyplexes-. Nanoformulations were fully characterized in terms of size, zeta potential, PDI, morphology and ability to bind, release and protect DNA. All formulations presented particle sizes in the nanoscale range (Fig. 1a, bars), which is related to higher cellular uptake values (Bivas-Benita et al., 2004), and exhibited positive surface charge values (Fig. 1a, lines), which is necessary to bind to the negatively charged DNA molecules by electrostatic interactions (Hosseinkhani and Tabata, 2006). Once complexed to DNA, surface charge switched to negative values in all cases. However, magnetoplexes and lipoplexes surface charge values changed from around +20 mV to around -20 mV, whereas polyplexes presented zeta potential values near the zero. It has been described that particles with surface charge values between -20mV and +20 mV form aggregates along the time (Caracciolo and Amenitsch, 2012). Therefore, to avoid aggregation, particularly in the case of polyplexes, all formulations employed in this work were used freshly prepared. PDI values were almost in all cases below 0.5, which is considered acceptable for comparative purposes of nanoparticles sizes measured by cumulative analysis (Reed et al., 2016). The exception was cationic lipids, where high PDI values could be attributed to the irregular morphology of these particles (Fig. 1c). In order to further analyze the ability of nanoparticles to bind, release and protect DNA, an agarose gel electrophoresis assay was performed (Fig.1d). Nanoparticles protected DNA from enzymatic degradation, but most of the plasmid was retained in the well, suggesting strong binding to DNA. However, all formulations showed a delicate balance between DNA binding and releasing abilities, necessary for efficient transfection mediated by non-viral vectors (Alatorre-Meda et al., 2011).

Once nanoplexes were physicochemically characterized, *in vitro* studies were carried out in three cell lines: HEK293 –a general transfection model-, C6 cells –a CNS transfection model- and primary neuronal culture cells –the most relevant cellular model of CNS-. Before performing assays in primary neuronal culture cells, we analyzed cell viability and transfection efficiency of the nanoplexes in HEK293 and in C6 cells, due to the challenge that represents primary neuronal culture cells transfection with non-viral vectors. Nanoplexes were well tolerated by both cell types, since cell viability was above 90% with magentoplexes and lipoplexes and above 80% with polyplexes (Fig. 2a, dots). The analysis of transfection efficiency was studied through three different parameters: percentage of GFP expressing cells (Fig.

### *Experimental section: Chapter 1*

2a, bars), MFI of those transfected cells (Fig. 2b) and the amount of VEGF (ng/ml) secreted by transfected cells (Fig. 2c). The phVEGF165aIRESGFP plasmid codifies for both proteins, VEGF –which is extracellular and, therefore, secreted to the extracellular medium by transfected cells- and GFP –which is intracellular and remains in the cytoplasm of transfected cells-. Therefore, parameters related to GFP were analyzed by flow citometry, while the concentration of VEGF present in cellular supernatants was measured by ELISA. Regarding percentages of GFP expressing cells and MFI values, transfection efficiencies with all nanoplexes were higher in HEK293 cells compared to C6 cells. However, regarding expression of VEGF (ng/ml), comparable values were obtained in HEK293 and C6 cells 48 h after transfection with nanoplexes. Indeed, when transfecting with magnetoplexes, the amounts of secreted VEGF were higher in the supernatant of C6 cells compared to HEK293 cells. It has been reported that non-viral vector mediated transfection processes are cell-dependent, meaning that the transfection efficiency of the same non-viral vector can diverge depending on the transfected cell type (Ojeda et al., 2015). Our results are consistent with this idea, since we found that in HEK293 cells highest transfection was achieved with lipoplexes, while in C6 cells magnetoplexes were more efficient. Polyplexes are in the third position in both cell lines, probably due to their surface charge values near zero, which may affect cellular uptake.

Interestingly, a clear correlation is observed in both cell lines between the three parameters used to analyze transfection efficiencies. At higher percentages of GFP expressing cells, higher levels of secreted VEGF were detected (Fig. 3a and Fig. 4a). Also, at higher MFI values, higher levels of secreted VEGF were observed (Fig. 3b and Fig. 4b). However, when comparing the angles of the slope in those graphs, differences were detected between cell lines, since the gradients were more pronounced in C6 than in HEK293 cells in both correlations –in Figs. 3a and 4a,  $\alpha=22.65^\circ$  in HEK293 vs.  $\alpha=65.42^\circ$  in C6; in Figs. 3b and 4b,  $\alpha=8.42^\circ$  in HEK293 and  $\alpha=23.67^\circ$  in C6 . These data support the fact that although GFP expression and MFI values were lower in C6, VEGF expression levels were comparable in both cell lines transfected with nanoplexes. This effect could in part be explained by the higher basal expression of VEGF protein in C6 cells (Fig. 2c, control bars). Therefore, even at lower transfection efficiencies, transfected C6 cells could be able to secrete as much VEGF protein as the more efficiently transfected HEK293 cells. Still, the big differences observed suggest that other factors may also be involved, specifically those related to the *Internal Ribosome Entry Site* (IRES) sequence of the plasmid. IRES sequences are translational enhancers that allow the co-expression of two genes of interest under the same promoter and with a constant ratio of the proteins

### *Experimental section: Chapter 1*

(Fussenegger et al., 1998; Allera-Moreau et al., 2007). However, it has been described that cellular IRES often exhibit low efficiencies in transiently transfected cells, which has been attributed to the cell and tissue specificity of the cellular IRES activities (Ngoi et al., 2004; Renaud-Gabardos et al., 2015). In those cases, the expression of the gene downstream of the IRES element is usually lower, while the expression of the gene upstream the IRES sequence is not affected (Jopling and Willis, 2001). In our scenario, the VEGF gene is located upstream the IRES element in the phVEGF165aIRESGFP plasmid, and the GFP gene is located downstream that sequence. Therefore, we hypothesized that the IRES sequence of the phVEGF165aIRESGFP plasmid may be working less efficiently in neural cells such as the C6 cell line, and that consequently, the expression of the GFP gene could be affected in those cells, while the VEGF gene is normally expressed.

Once the capacity of nanoplexes to transfect HEK293 and C6 cells was analyzed, we performed transfection assays in primary neuronal culture cells, which represent a more challenging scenario for non-viral gene delivery. Cell viabilities (Fig. 5a) were excellent in this case –near 100% with all nanoplexes-, but transfection efficiencies (Fig. 5a-b) were lower than in the previous cell lines, due to the difficulty of transfecting neuronal cells. GFP expression was only detectable by immunocitochemistry assay –Fig. 5b shows a few scattered fluorescent cells-. This supports the hypothesis of the tissue specificity of the IRES element in the phVEGF165aIRESGFP plasmid. Regarding VEGF expression, we found that these cells presented a high basal production of VEGF, probably due to the glial cells present in the primary culture, which secret angiogenic (Egervari et al., 2016) and neurotrophic (Du et al., 2014) factors to support the CNS cells. However, after transfection with nanoplexes, levels of secreted VEGF increased respect to the control in all cases, although statistically significant differences were only found in magnetoplexes transfected cells (Fig. 5c). Next, we analyzed the bioactivity of transfected cells secreted VEGF in HUVEC cells, since these cells are known to respond with increased proliferation to the effect of VEGF (Herran et al., 2013a; Bai et al., 2014). Compared to the proliferation control group –HUVEC cells not treated with VEGF-, HUVEC cells exposed to VEGF secreted by primary neuronal culture cells transfected with nanoplexes presented a statistically significant increase in proliferation, which validates that VEGF induced HUVEC cell proliferation. Furthermore, the increase of proliferation in HUVEC cells was proportional to the increase of VEGF production in primary neuronal culture cells, magnetoplexes obtaining the highest levels of VEGF expression in primary neuronal culture cells and their supernatants achieving the highest levels of proliferation in HUVEC cells,

### *Experimental section: Chapter 1*

followed in both cases by polyplexes and, finally, lipoplexes. It is remarkable that magnetoplexes transfected CNS cell models more efficiently than their counterparts and that, unexpectedly, polyplexes were more efficient than lipoplexes in primary neuronal culture cells.

Considering these results, non-viral vectors and, in particular, magnetoplexes might constitute a promising approach to deliver the VEGF gene into CNS cells in a safe and controlled way, which is consistent with previous reports (Soto-Sanchez et al., 2015). Strong relationships described between vascular alterations and neurodegeneration (Ruiz de Almodovar et al., 2009), along with reported beneficial effects of VEGF protein in animal models of neurodegenerative diseases such as AD (Herran et al., 2013a; Herran et al., 2015) and Parkinson's Disease (Herran et al., 2014; Herran et al., 2013b), suggest that VEGF may be a potential therapeutic candidate for CNS disorders. Besides, compared to drug delivery, VEGF gene delivery would demand fewer doses and would allow long-lasting effects. To date, administration of non-viral vectors to SNC is still a challenge for the scientific community, principally due to the invasive nature of the currently available approaches to target the brain, including craniotomy. A recent study has shown that intranasally administered plasmid DNA nanoparticles circumvented the BBB to target the CNS and have successfully transfected rat brain (Harmon et al., 2014). Therefore, the intranasal route, a safer and non-invasive alternative, merits special attention for non-viral gene delivery into the CNS.

### **ACKNOWLEDGEMENTS**

This project was supported by the University of the Basque Country UPV/EHU (UII 11/32), the Basque Government (Department of Education, University and Research, predoctoral grants PRE\_2015\_2\_0151 and BFI-2011-2226), the National Council of Science and Technology (CONACYT), Mexico, Reg. # 217101, the Spanish Ministry of Education (Grant CTQ2010-20541, CTQ2010-14897), and by Spanish grants MAT2012-39290-C02-01, IPT-2012-0574-300000 and MAT2015-69967-C3-1-R from the Spanish Government. Authors wish to thank the intellectual and technical assistance from the ICTS "NANBIOSIS", more specifically by the Drug Formulation Unit (U10) of the CIBER in Bioengineering, Biomaterials & Nanomedicine (CIBER-BBN) at the University of the Basque Country (UPV/EHU). Technical and human support provided by SGIker (UPV/EHU) is also gratefully acknowledged. I.V.B. thanks the Basque Country Government (Departamento de Educación, Universidades e Investigación) for the granted fellowship.

*Experimental section: Chapter 1*

**Conflicts of interest**

The authors declare that they have no conflict of interest.

**REFERENCES**

- Agirre, M., Ojeda, E., Zarate, J., Puras, G., Grijalvo, S., Eritja, R., García del Caño, G., Barrondo, S., González-Burguera, I., López de Jesús, M., Sallés, J., Pedraz, J.L., 2015b. New Insights into Gene Delivery to Human Neuronal Precursor NT2 Cells: A Comparative Study between Lipoplexes, Nioplexes, and Polyplexes. *Mol. Pharm.* 12(11):4056-66. doi: 10.1021/acs.molpharmaceut.5b00496.
- Agirre, M., Zarate, J., Puras, G., Ojeda, E., Pedraz, J.L., 2015a. Improving transfection efficiency of ultrapure oligochitosan/DNA polyplexes by medium acidification. *Drug Deliv.* 22(1):100-10. doi: 10.3109/10717544.2013.871373.
- Alatorre-Meda, M., Taboada, P., Hartl, F., Wagner, T., Freis, M., Rodriguez, J.R., 2011. The influence of chitosan valence on the complexation and transfection of DNA: the weaker the DNA–chitosan binding the higher the transfection efficiency. *Colloids Surf. B. Biointerfaces* 82:54–62. doi: 10.1016/j.colsurfb.2010.08.013.
- Allera-Moreau, C., Delluc-Clavières, A., Castano, C., Van den Berghe, L., Golzio, M., Moreau, M., Teissié, J., Arnal, J.F., Prats, A.C., 2007. Long term expression of bicistronic vector driven by the FGF-1 IRES in mouse muscle. *BMC Biotechnol.* 28;7:74.
- Antequera, D., Portero, A., Bolos, M., Orive, G., Hernández, R.M., Pedraz, J.L., Carro, E., 2012. Encapsulated VEGF-secreting cells enhance proliferation of neuronal progenitors in the hippocampus of AβPP/Ps1 mice. *J. Alzheimers Dis.* 2012;29(1):187-200. doi:10.3233/JAD-2011-111646.
- Bai, Y., Leng, Y., Yin, G., Pu, X., Huang, Z., Liao, X., Chen, X., Yao, Y., 2014. Effects of combinations of BMP-2 with FGF-2 and/or VEGF on HUVECs angiogenesis in vitro and CAM angiogenesis in vivo. *Cell Tissue Res.* 356(1):109-21. doi:10.1007/s00441-013-1781-9.
- Bivas-Benita, M., Romeijn, S., Junginger, H.E., Borchard, G., 2004. PLGA-PEI nanoparticles for gene delivery to pulmonary epithelium. *Eur. J. Pharm. Biopharm.* 58(1):1-6.

*Experimental section: Chapter 1*

- Caracciolo, G., Amenitsch, H., 2012. Cationic liposome/DNA complexes: from structure to interactions with cellular membranes. *Eur. Biophys. J.* 41(10):815-29. doi:10.1007/s00249-012-0830-8.
- Carmeliet, P., Ruiz de Almodovar, C., 2013a. VEGF ligands and receptors: implications in neurodevelopment and neurodegeneration. *Cell. Mol. Life Sci.* 70(10):1763-78. doi: 10.1007/s00018-013-1283-7.
- Carmeliet, P., Ruiz de Almodovar, C., 2013b. VEGF ligands and receptors: implications in neurodevelopment and neurodegeneration. *Cell. Mol. Life Sci.* 70:1763-1778. doi: 10.1007/s00018-013-1283-7.
- Du, J., Gao, X., Deng, L., Chang, N., Xiong, H., Zheng, Y., 2014. Transfection of the glial cell line-derived neurotrophic factor gene promotes neuronal differentiation. *Neural Regen. Res.* 9(1):33-40. doi: 10.4103/1673-5374.125327.
- Egervari, K., Potter, G., Guzman-Hernandez, M.L., Salmon, P., Soto-Ribeiro, M., Kastberger, B., Balla, T., Wehrle-Haller, B., Kiss, J.Z., 2016. Astrocytes spatially restrict VEGF signaling by polarized secretion and incorporation of VEGF into the actively assembling extracellular matrix. *Glia* 64(3):440-56. doi: 10.1002/glia.22939.
- Fournier, N.M., Lee, B., Banasr, M., Elsayed, M., Duman, R.S., 2012. Vascular endothelial growth factor regulates adult hippocampal cell proliferation through MEK/ERK and PI3K/Akt-dependent signaling. *Neuropharmacology* 63:642–652. doi:10.1016/j.neuropharm.2012.04.033.
- Fussenegger, M., Moser, S., Bailey, J.E., 1998. pQuattro vectors allow one-step multigene metabolic engineering and auto-selection of quattrocistronic artificial mammalian operons. *Cytotechnology* 28(1-3):229-235. doi: 10.1023/A:1008014706196.
- Harmon, B.T., Aly, A.E., Padegimas, L., Sesenoglu-Laird, O., Cooper, M.J., Waszczak, B.L., 2014. Intranasal administration of plasmid DNA nanoparticles yields successful transfection and expression of a reporter protein in rat brain. *Gene Ther.* 21(5):514-21. doi: 10.1038/gt.2014.28.
- Herrán, E., Pérez-González, R., Igartua, M., Pedraz, J.L., Carro, E., Hernández, R.M., 2013a. VEGF-releasing biodegradable nanospheres administered by craniotomy: a novel therapeutic approach in the APP/Ps1 mouse model of Alzheimer's disease. *J. Control. Release* 170(1):111-9. doi: 10.1016/j.jconrel.2013.04.028.
- Herran, E., Perez-Gonzalez, R., Igartua, M., Pedraz, J.L., Carro, E., Hernandez, R.M., 2015. Enhanced Hippocampal Neurogenesis in APP/Ps1 Mouse

*Experimental section: Chapter 1*

- Model of Alzheimer's Disease After Implantation of VEGF-loaded PLGA Nanospheres. *Curr. Alzheimer Res.* 12(10):932-40.
- Herrán, E., Requejo, C., Ruiz-Ortega, J.A., Aristieta, A., Igartua, M., Bengoetxea, H., Ugedo, L., Pedraz, J.L., Lafuente, J.V., Hernández, R.M., 2014. Increased antiparkinson efficacy of the combined administration of VEGF- and GDNF-loaded nanospheres in a partial lesion model of Parkinson's disease. *Int. J. Nanomedicine* 9:2677-87. doi: 10.2147/IJN.S61940.
- Herrán, E., Ruiz-Ortega, J.Á., Aristieta, A., Igartua, M., Requejo, C., Lafuente, J.V., Ugedo, L., Pedraz, J.L., Hernández, R.M., 2013b. In vivo administration of VEGF- and GDNF-releasing biodegradable polymeric microspheres in a severe lesion model of Parkinson's disease. *Eur. J. Pharm. Biopharm.* 85(3 Pt B):1183-90. doi: 10.1016/j.ejpb.2013.03.034.
- Hosseinkhani, H., Tabata, Y., 2006. Self assembly of DNA nanoparticles with polycations for the delivery of genetic materials into cells. *J. Nanosci. Nanotechnol.* 6(8):2320-8.
- Jin, L., Zeng, X., Liu, M., Deng, Y., He, N., 2014. Current progress in gene delivery technology based on chemical methods and nano-carriers. *Theranostics* 4(3):240-55. doi: 10.7150/thno.6914.
- Jopling, C.L., Willis, A.E., 2001. N-myc translation is initiated via an internal ribosome entry segment that displays enhanced activity in neuronal cells. *Oncogene* 20(21):2664-70.
- Jubeli, E., Maginty, A.B., Khalique, N.A., Raju, L., Nicholson, D.G., Larsen, H., Pungente, M.D., Goldring, W.P., 2016. Cationic lipids bearing succinic-based, acyclic and macrocyclic hydrophobic domains: Synthetic studies and in vitro gene transfer. *Eur. J. Med. Chem.* 125:225-232. doi: 10.1016/j.ejmec.2016.09.027.
- Kalaria, R.N., 2010. Vascular basis for brain degeneration: faltering controls and risk factors for dementia. *Nutr. Rev.* 68 Suppl. 2:S74-87. doi: 10.1111/j.1753-4887.2010.00352.x.
- Keles, E., Song, Y., Du, D., Dong, W.J., Lin, Y., 2016. Recent progress in nanomaterials for gene delivery applications. *Biomater. Sci.* 4(9):1291-309. doi: 10.1039/c6bm00441e.
- Ngoi, S.M., Chien, A.C., Lee, C.G., 2004. Exploiting internal ribosome entry sites in gene therapy vector design. *Curr. Gene Ther.* 4(1):15-31.
- Ojeda, E., Puras, G., Agirre, M., Zarate, J., Grijalvo, S., Eritja, R., Martinez-Navarrete, G., Soto-Sánchez, C., Diaz-Tahoces, A., Aviles-Trigueros, M., Fernández, E., Pedraz, J.L., 2016. The influence of the polar head-group of synthetic cationic lipids on the transfection efficiency mediated by niosomes

*Experimental section: Chapter 1*

- in rat retina and brain. *Biomaterials* 77:267-79. doi: 10.1016/j.biomaterials.2015.11.017.
- Ojeda, E., Puras, G., Agirre, M., Zárate, J., Grijalvo, S., Pons, R., Eritja, R., Martínez-Navarrete, G., Soto-Sánchez, C., Fernández, E., Pedraz, J.L., 2015. Niosomes based on synthetic cationic lipids for gene delivery: the influence of polar head-groups on the transfection efficiency in HEK-293, ARPE-19 and MSC-D1 cells. *Org. Biomol. Chem.* 13(4):1068-81. doi: 10.1039/c4ob02087a.
- Pack, D.W., Hoffman, A.S., Pun, S., Stayton, P.S., 2005. Design and development of polymers for gene delivery. *Nat. Rev. Drug Discov.* 4(7):581-93.
- Pezzoli, D., Chiesa, R., De Nardo, L., Candiani, G., 2012. We still have a long way to go to effectively deliver genes! *J. Appl. Biomater. Funct. Mater.* 10(2):82-91. doi: 10.5301/JABFM.2012.9707.
- Puras, G., Zarate, J., Díaz-Tahoces, A., Avilés-Trigueros, M., Fernández, E., Pedraz, J.L., 2013a. Oligochitosan polyplexes as carriers for retinal gene delivery. *Eur. J. Pharm. Sci.* 48:323–331. doi: 10.1016/j.ejps.2012.11.009.
- Puras, G., Zarate, J., Díaz-Tahoces, A., Avilés-Trigueros, M., Fernández, E., Pedraz, J.L., 2013b. Low molecular weight oligochitosans for non-viral retinal gene therapy. *Eur. J. Pharm. Biopharm.* 83:131–140. doi:10.1016/j.ejpb.2012.09.010.
- Reed, B.E., Grainger, R.G., Peters, D.M., Smith, A.J., 2016. Retrieving the real refractive index of mono- and polydisperse colloids from reflectance near the critical angle. *Opt. Express* 24(3):1953-72. doi: 10.1364/OE.24.001953.
- Renaud-Gabardos, E., Hantelys, F., Morfoisse, F., Chaufour, X., Garmy-Susini, B., Prats, A.C., 2015. Internal ribosome entry site-based vectors for combined gene therapy. *World J. Exp. Med.* 5(1):11-20. doi: 10.5493/wjem.v5.i1.11.
- Ruiz de Almodovar, C., Lambrechts, D., Mazzone, M., Carmeliet, P., 2009. Role and therapeutic potential of VEGF in the nervous system. *Physiol. Rev.* 89:607–648. doi: 10.1152/physrev.00031.2008.
- Soto-Sánchez, C., Martínez-Navarrete, G., Humphreys, L., Puras, G., Zarate, J., Pedraz, J.L., Fernández, E., 2015. Enduring high-efficiency in vivo transfection of neurons with non-viral magnetoparticles in the rat visual cortex for optogenetic applications. *Nanomedicine* 11(4):835-43. doi: 10.1016/j.nano.2015.01.012.
- Spuch, C., Saida, O., Navarro, C., 2012. Advances in the treatment of neurodegenerative disorders employing nanoparticles. *Recent Pat. Drug Deliv. Formul.* 6(1):2-18.

*Experimental section: Chapter 1*

- Srikanth, M., Kessler, J.A., 2012. Nanotechnology-novel therapeutics for CNS disorders. *Nat. Rev. Neurol.* 8(6):307-18. doi: 10.1038/nrneurol.2012.76.
- Yin, H., Kanasty, R.L., Eltoukhy, A.A., Vegas, A.J., Dorkin, J.R., Anderson, D.G., 2014. Non-viral vectors for gene-based therapy. *Nat. Rev. Genet.* 15(8):541-55. doi: 10.1038/nrg3763.
- Zlokovic, B.V., 2011. Neurovascular pathways to neurodegeneration in Alzheimer's disease and other disorders. *Nat. Rev. Neurosci.* 12(12):723-38. doi: 10.1038/nrn3114.



## ***Chapter 2***

### **Polysorbate 20 non-ionic surfactant enhances retinal gene delivery efficiency of cationic niosomes after intravitreal and subretinal administration**

*Published in International Journal of Pharmaceutics (2018)*

*Villate-Beitia I, et al. Polysorbate 20 non-ionic surfactant enhances retinal gene delivery efficiency of cationic niosomes after intravitreal and subretinal administration. Int J Pharm. 2018 Oct 25;550(1-2):388-397. doi: 10.1016/j.ijpharm.2018.07.035*

*Erretinako gene-terapiarako bektore ez-biralen arrakasta transgene espresio altuak eta iraunkorrik lortzearen menpe dago, batik bat hori lortzeko dosi bakarra ematea nahikoa izanda. Lan honetan, niosoma formulazioetako osagai diren tentsoaktibo ez-ionikoeak transfekzio prozesuan eta eraginkortasunean duten eragina aztertu dugu arratoi-erretinan. Horretarako, hiru niosoma formulazio prestatu ditugu, soilik tentsoaktibo ez-ionikoa aldatuta kasu bakoitzean. Niosomen osagaia izan ziren 1,2-di-O-oktadenilo-3-trimetilamonio propano (DOTMA) lipido kationikoa, eskualeño lipido laguntzailea eta Tween 20, 80 edo 85 tentsoaktibo ez-ionikoa. Niosomak eta dagozkien nioplexoak fisiko-kimikoki karakterizatu ziren tamainari, zeta potentzialari, polidispersio indizeari, morfologiari eta DNA babesteko eta askatzeko duten gaitasunaren arabera. In vitro esperimentuen bidez, formulazioen transfekzio gaitasuna eta bakoitzak jarraitutako zelula-barneko endozitosi-bideak aztertu ziren. Tween 20 tentsoaktibo ez-ionikoz osatutako nioplexoekin lortu ziren transfekzio-maila altuenak in vitro. Gainera, erretina-azpiko eta bitreo-barneko injekzioak eginda arratoiien erretinan transfekzio-maila altuak lortu ziren in vivo formulazio horrekin. Emaitzak horiek erakusten dutenez, niosomen formulazioan Tween 20 tentsoaktibo ez-ionikoa erabiltzeak erretinako transfekzioa hobetzen du. Beraz, formulazio berri hau hautagai egokia izan daiteke gene terapeutikoak erretinara garraiatzeko ehun horri eragiten dioten gaixotasunei aurre egiteko tratamenduetan.*

*El éxito de la liberación génica en retina mediante vectores no-virales basados en niosomas catiónicos depende de la habilidad de lograr niveles elevados y persistentes de expresión génica, idealmente tras una única administración. En este trabajo, estudiamos el efecto del tensioactivo no-iónico de las formulaciones de niosomas en su eficiencia de transfección en retina de rata. Para ello, se elaboraron tres formulaciones de niosomas que sólo diferían en el componente de tensioactivo no-iónico. Los niosomas contenían: el lípido catiónico 1,2-di-O-octadecenil-3-trimetilamonio propano (DOTMA), el lípido helper eskualeño y uno de los siguientes tensioactivos no-iónicos: polisorbato 20, 80 o 85. Los niosomas y correspondientes nioplexos se caracterizaron en términos de tamaño de partícula, índice de polidispersión (PDI), potencial zeta, morfología y habilidad para proteger y liberar el ADN. Se llevaron a cabo experimentos in vitro para evaluar la eficiencia de transfección, viabilidad celular y rutas de tráfico intracelular de las formulaciones. Los nioplexos que contenían polisorbato 20 fueron los más eficientes para transfectar células retinianas in vitro. Además, la administración intravítreo y subretiniana de esos nioplexos in vivo mostró elevados niveles de expresión génica en retina de rata. Estos resultados demuestran que la incorporación del polisorbato 20 en niosomas catiónicos mejora la transferencia génica en retina. Por tanto, esta formulación constituye un candidato prometedor como vector no-viral para transferir genes terapéuticos específicos al ojo con fines biomédicos.*

*Experimental section: Chapter 2*

## **Polysorbate 20 non-ionic surfactant enhances retinal gene delivery efficiency of cationic niosomes after intravitreal and subretinal administration**

*Ilia Villate-Beitia<sup>a,b,1</sup>, Idoia Gallego<sup>a,c,1</sup>, Gema Martínez-Navarrete<sup>b,d</sup>, Jon Zárate<sup>a,b</sup>, Tania López-Méndez<sup>a,b</sup>, Cristina Soto-Sánchez<sup>b,d</sup>, Edorta Santos-Vizcaíno<sup>a,b</sup>, Gustavo Puras<sup>a,b,\*</sup>, Eduardo Fernández<sup>b,d</sup>, José Luis Pedraz<sup>a,b,\*</sup>*

*<sup>a</sup>NanoBioCel Group, University of the Basque Country (UPV/EHU), Vitoria-Gasteiz, Spain*

*<sup>b</sup>Biomedical Research Networking Center in Bioengineering, Biomaterials and Nanomedicine (CIBER-BBN), Spain*

*<sup>c</sup>Ikerbasque, Basque Foundation for Science, Bilbao, Spain*

*<sup>d</sup>Neuroprothesis and Neuroengineering Research Group, Miguel Hernández University, Elche, Spain*

*<sup>1</sup>Ilia Villate-Beitia and Idoia Gallego contributed equally to this work.*

---

**Abstract:** The success of non-viral vectors based on cationic niosomes for retinal gene delivery applications depends on the ability to achieve persistent and high levels of transgene expression, ideally from a single administration. In this work, we studied the effect of the non-ionic surfactant component of niosomes in their transfection efficiency in rat retina. For that purpose, three niosome formulations that only differed in the non-ionic tensioactives were elaborated. Niosomes contained: cationic lipid 1,2-di-O-octadecenyl-3-trimethylammonium propane (DOTMA), helper lipid squalene and polysorbate 20, polysorbate 80 or polysorbate 85. Niosomes and corresponding nioplexes were fully characterized in terms of size, polydispersity index, zeta potential, morphology and ability to protect and release DNA. *In vitro* experiments were carried out to evaluate transfection efficiency, cell viability and intracellular trafficking pathways of the formulations. Nioplexes based on polysorbate 20 niosomes were the most efficient transfecting retinal cells *in vitro*. Moreover, subretinal and intravitreal administration of those nioplexes *in vivo* showed also high levels of transgene expression in rat retinas. Our results demonstrate that the incorporation of polysorbate 20 in cationic niosomes enhances retinal gene delivery. Thus, this formulation emerges as a potential non-viral candidate to efficiently transfer specific therapeutic genes into the eye for biomedical purposes.

**Keywords:** non-viral vector, gene therapy, retina; non-ionic surfactants, niosomes.

## *Experimental section: Chapter 2*

### **1. Introduction**

Several monogenic retinal disorders are well characterized, with identified mutations that most often affect specific genes in retinal pigment epithelium (RPE) cells<sup>1</sup>. RPE cells perform pivotal functions required for the maintenance of the neural retina, such as protecting the photoreceptor cells and secreting growth factors<sup>2</sup>. In many retinal diseases, including Leber's congenital amaurosis (LCA), retinitis pigmentosa (RP) and age-related macular degeneration (AMD) blindness occurs due to RPE degeneration, which results in photoreceptor loss or dysfunction<sup>1</sup>. Therefore, RPE cells constitute the main target of most ocular gene therapy strategies. Tight junctions between RPE cells form the blood retina barrier, which is responsible of the low ocular bioavailability of systemically administered drugs<sup>3</sup>. However, the same barriers that make ocular administration difficult also help the eye maintain its immune privilege, making intraocularly-delivered molecules less likely to induce severe immune responses than their systemically-delivered counterparts<sup>4</sup>. The success of retinal gene transfer strategies depends on the ability to achieve persistent and high levels of transgene expression in RPE cells, ideally from a single administration.

Nucleic acids can be delivered into the retina both through viral or non-viral vectors. Some clinical trials using viral vectors have shown encouraging results<sup>5,6</sup>. However, some limitations of viral vectors such as safety concerns, expensive production costs<sup>7</sup> and that many disease genes of the RPE and retina are too large to fit into viral vectors<sup>1</sup> have motivated the development of non-viral vectors for ocular gene delivery. Non-viral vectors present low immunogenicity, high nucleic acid packing capacity, ease of fabrication, high reproducibility and acceptable costs compared to their counterparts<sup>8</sup>. Among the wide plethora of non-viral vectors, recently emerged niosomes are biocompatible, synthetic, non-ionic surfactant vesicles with a closed bilayer structure<sup>9,10</sup> and they are based on three principal components: cationic lipids, helper lipids and non-ionic tensioactives<sup>11,12</sup>. The global chemical properties of these components influence on the physicochemical characteristics of niosomes, such as size, surface charge and morphology, which in turn determine their ability to enter the cells, follow a particular endocytic pathway and deliver the DNA cargo into the nucleus<sup>13,14</sup>. Our research group has previously evaluated the effect of cationic lipids<sup>15</sup> and helper lipids<sup>16</sup> in retinal transfection, and has reported transgene expression in retinal cells both *in vitro*<sup>16</sup> and *in vivo*<sup>16,17</sup>. In order to optimize the design of niosome formulations for retinal gene delivery applications, in this work we evaluated the effect of the non-ionic surfactant of niosomes on the retinal transfection process and efficiency.

## *Experimental section: Chapter 2*

For that purpose, we elaborated three niosome formulations that only differed in the non-ionic surfactant component. Niosomes used in this work contained the cationic lipid 1,2-di-O-octadecenyl-3-trimethylammonium propane (DOTMA), combined with the helper lipid squalene and one of the following non-ionic surfactants: polysorbate 20, polysorbate 80 or polysorbate 85, differing in their chemical structure and hydrophile-lipophile balance (HLB) values (Figure 1). The cationic lipid DOTMA has been successfully used in niosome formulations for gene delivery to the retina<sup>18</sup>. Squalene is a natural lipid belonging to the terpenoid family<sup>19</sup> that enhances the stability of niosome formulations<sup>20</sup>. Polysorbate 80 has been used combined with squalene obtaining effective transgene expression in rat retina *in vivo*<sup>17</sup>, but the effect of other non-ionic tensioactives such as polysorbate 20 and 85 combined with squalene and DOTMA has not been studied for retinal gene delivery. The three niosome formulations elaborated in this work were named DST20, DST80 and DST85, according to their composition. Niosomes were complexed to the pCMS-EGFP reporter plasmid or to a fluorescein isothiocyanate (FITC) labeled pCMS-EGFP plasmid to form nioplexes. Niosomes and nioplexes were characterized in terms of size, polydispersity index (PDI), zeta potential, morphology and ability to protect and release DNA. *In vitro* experiments were carried out in human embryonic kidney cells (HEK-293) and retinal pigment epithelial cells (ARPE-19) to evaluate cell viability and transfection efficiency. In order to examine the cell entry and intracellular trafficking process of the three formulations in ARPE-19 cells, co-localization analysis were performed between the nioplexes (niosomes/FITC stained DNA) and the stained endocytic pathways. The pathways under study were the clathrin mediated endocytosis (CME), caveolae-mediated endocytosis (CvME) and late endosomal compartments (Lys). The best of those formulations was used to transfet primary cultures of rat retinal cells and was administered into rat eyes in order to evaluate the capacity of the formulation to deliver genetic material into the retina after subretinal and intravitreal injections.

*Experimental section: Chapter 2*

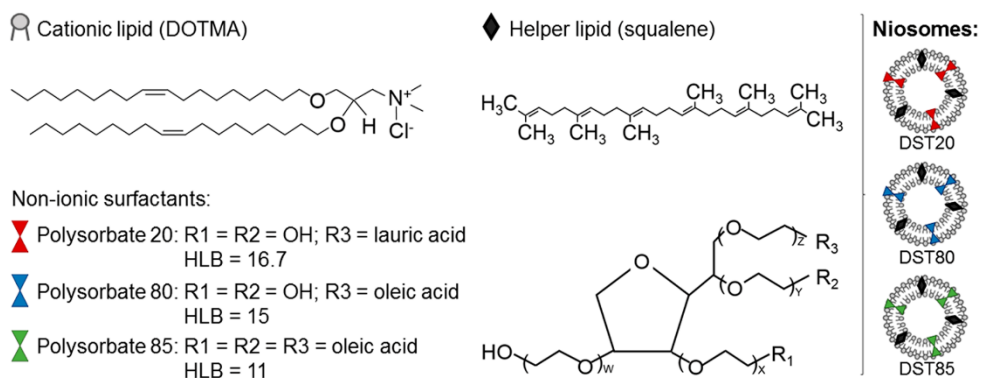


**Figure 1.** General scheme of niosomes and chemical structures of niosome components.

## 2. Materials and Methods

### 2.1. Preparation of niosomes and nioplexes

Niosomes based on cationic lipid DOTMA (Avanti Polar Lipids, Inc., Alabama, USA), helper lipid squalene (Sigma-Aldrich, Madrid, Spain) and polysorbates 20, 80 and 85 (Sigma-Aldrich, Madrid, Spain) were prepared using the o/w emulsification technique, as previously described<sup>12</sup>. Three different niosome formulations were prepared to a molar ratio of 2 mM cationic lipid – 8 mM helper lipid – 4 mM tensioactive. Briefly, 6.70 mg of the cationic lipid were gently ground with 19 µl of squalene. Then, 1 ml of dichloromethane (DCM) (Panreac, Barcelona, Spain) was added and emulsified with 5 ml of the non-ionic surfactant aqueous solution –at different w/v percentages to obtain the final molar relation- containing either polysorbate 20 (0.49% w/v), 80 (0.52% w/v) or 85 (0.17% w/v). The emulsion was obtained by sonication (Branson Sonifier 250, Danbury) for 30 s at 50 W. The organic solvent was removed from the emulsion by evaporation under magnetic agitation for 3 h at room temperature, obtaining niosome solutions DST20, DST80 and DST85.

The nioplexes were elaborated by mixing an appropriate volume of a stock solution of either a pCMS-EGFP plasmid (0.5 mg/ml) (Clontech Laboratories, Inc., USA) or a fluorescein isothiocyanate (FITC) labeled pCMS-EGFP plasmid (0.5 mg/ml) (DareBio, Elche, Spain), with different volumes of DST20, DST80 and DST85 niosomes to obtain cationic lipid/DNA (w/w) mass ratios 2/1, 5/1 and 10/1. The mixture was left for 30 min at room temperature to enhance electrostatic interactions between the cationic lipid and the DNA.

## *Experimental section: Chapter 2*

### *2.2. Plasmid propagation*

The pCMS-EGFP plasmid was propagated in *Escherichia coli* DH5- $\alpha$  and purified using the Qiagen endotoxin-free plasmid purification Maxi-prep kit (Qiagen, Santa Clarita, CA, USA) according to manufacturer's instructions. The concentration of pDNA was quantified by measuring the absorbance at 260 nm with a SimpliNano™ device (GE Healthcare, Buckinghamshire, UK).

### *2.3. Size, polydispersity index, zeta potential and morphology*

The intensity mean diameter (Z-average) and the zeta potential of niosomes and nioplexes were determined by dynamic light scattering and by lasser Doppler velocimetry, respectively, using a Zetasizer Nano ZS (Malvern Instrument, UK). Briefly, 50  $\mu$ l of the formulations were resuspended into 950  $\mu$ l of 0.1 mM NaCl solution. All measurements were carried out in triplicate. The particle size reported as hydrodynamic diameter was obtained by cumulative analysis. The Smoluchowski approximation was used to support the calculation of the zeta potential from the electrophoretic mobility. The morphology of niosomes was determined by transmission electron microscopy (TEM) as previously described<sup>17</sup>.

### *2.4. Agarose gel electrophoresis assay*

Naked DNA and nioplexes at different mass ratios were subjected to a 0.8 % agarose (Sigma-Aldrich, Madrid, Spain) gel electrophoresis assay. For DNA protection and release assay, 3  $\mu$ l of DNase I enzyme (Sigma-Aldrich, Madrid, Spain) were added and incubated at 37°C for 30 min. then, 12  $\mu$ l of 7 % sodium dodecyl sulfate (SDS) (Sigma-Aldrich, Madrid, Spain) were added to the samples and incubated at room temperature for 10 minutes. Before running the gel, 4  $\mu$ l of loading buffer (BioRad, USA) were added to all samples. The agarose gel was immersed in a Tris-acetate-EDTA buffer and exposed for 45 min at 100 V. Once DNA bands were stained with GelRed™ (Biotium, Hayward, California, USA), they were observed with a ChemiDoc™ MP Imaging System and analyzed with ImageLab™ Software (BioRad, USA). Naked DNA was used as control. The amount of DNA per well was 200 ng in all cases.

### *2.5. Cell culture and transfection assays*

Human embryonic kidney cells 293 (HEK-293) (ATCC® CRL1573TM) were grown in Eagles's Minimal Essential Medium (EMEM, ATCC 30-2003) supplemented with 10 % of fetal bovine serum (FBS) (Sigma-Aldrich, Madrid, Spain) and with 1 % of antibiotic-antimycotic solution (Life Technologies, Paisley, UK). Human retinal pigment epithelium cells (ARPE-19) (ATCC® CRL2302TM) were grown in

## *Experimental section: Chapter 2*

Dulbecco's Modified Eagle Medium: Nutrient Mixture F-12 (F-12K, ATCC 30-2006) supplemented with 10 % of FBS and 1 % of penicillin-streptomycin solution (Life Technologies, Paisley, UK). Cells were incubated at 37°C and 5 % CO<sub>2</sub> atmosphere, and were split every 3-4 days to maintain monolayer coverage.

For transfection efficiency in HEK-293 and ARPE-19 cell lines, cells were seeded in 24 well plates at a density of 10 x 10<sup>4</sup> cells per well in a total volume of 250 µl per well, and incubated overnight to achieve 70 % of confluence at the time of transfection with nioplexes. Both cell types were transfected with DST20, DST80 and DST85 nioplexes at cationic lipid/DNA mass ratio 2/1. For that purpose, electrostatic interactions between the cationic lipid and the pcMS-EGFP plasmid were left to occur for 30 min at room temperature in OptiMEM (Gibco, San Diego, CA, USA) transfection medium. Once removing the growth medium from the plate, cells were exposed for 4 h to nioplexes for transfection. After the incubation, nioplexes were removed and fresh medium was added to the cells. Transfection efficiency was analyzed by fluorescence microscopy and flow cytometry 48 h after the exposure to nioplexes. Lipofectamine 2000™ (Invitrogen, Carlsbad, CA, USA) was used as positive control. Transfection negative control cells were not exposed to nioplexes, but were incubated in OptiMEM for 4 h. Each condition was performed in triplicate.

### *2.6. Analysis of EGFP expression and cell viability*

Qualitative analysis of EGFP expression was conducted using an inverted microscope equipped with an attachment for fluorescent observation (EclipseTE2000-S, Nikon). For quantitative determination of EGFP expression and cell viability, flow cytometry analysis was conducted using a FACSCalibur system flow cytometer (Becton Dickinson Bioscience, San Jose, USA). DST20, DST80 and DST85 nioplex-transfected cells were washed twice with PBS (Sigma-Aldrich, Madrid, Spain) and detached with 200 µl of trypsin/EDTA (Gibco, San Diego, CA, USA) per well. 400 µl of complete growth medium were added and cells were transferred to specific flow cytometer tubes. Cell viability was evaluated using propidium iodide (Sigma-Aldrich, Madrid, Spain) at 1:10 dilution in each sample. The fluorescent signals corresponding to dead cells and to EGFP positive cells were measured at 650 nm (FL3) and 525 nm (FL1), respectively. Non-transfected cells, used as control samples, were displayed on a forward scatter (FSC) versus side scatter (SSC) dot plot to establish a collection gate and exclude cells debris. Positive control samples transfected with Lipofectamine 2000™ were used to establish cytometer settings and channel compensations. Cell viability data were normalized in relation to the value of non-treated control cells. Transfection data were

## *Experimental section: Chapter 2*

normalized in relation to the value of the positive control Lipofectamine 2000™ transfection. The experiments were carried out in triplicate for each condition. For each sample 10,000 events were collected. FlowJo software (Becton Dickinson, Mountain View, CA, USA) was employed to analyze the data.

### *2.7. Endocytic trafficking*

For cellular internalization assays, ARPE-19 cells were seeded on coverslips on 24 well plates and transfected with nioplexes containing the FITC-labeled pCMS-EGFP plasmid for 3 h. Then the following endocytic vesicle markers were added and incubated for 1 h with either AlexaFluor546-Transferrin (50 µg/mL), AlexaFluor555-Cholera toxin B (10 µg/mL) or Lysotracker (140 nM), which are markers for CME, CvME and late endosomal compartment, respectively. Cells were fixed with 4 % formaldehyde and mounted with DAPI-Fluoromount-GTM (Fisher Scientific SL, Madrid, Spain) for examination by confocal laser scanning microscopy (CLSM) (Zeiss Axiobserver, Germany). Co-localization of the green and red signal was analyzed by ImageJ software and quantified by a cross-correlation analysis as previously described by van Steensel et al.<sup>21</sup>. Briefly, the green signal image was shifted in the x-direction pixel per pixel relative to the red signal image and the respective Pearson's coefficient was calculated, which was then plotted as the function of the pixel shift ( $\delta x$ ) obtaining a cross-correlation function (CCF). Co-localizing structures peaked at  $\delta x = 0$  and presented a bell-shaped curve. 3D plots to relate HLB, transfection efficiency and co-localization values were built using MATLAB® R2017b.

### *2.8. Animals and anesthetics*

Adult male Sprague–Dawley rats were used as experimental animals in this study. All experimental procedures were carried out in accordance with the Spanish and European Union regulations for the use of animals in scientific research and the Association for Research in Vision and Ophthalmology (ARVO) statement for the use of animals in ophthalmic and vision research. Procedures were supervised by the Miguel Hernandez University Standing Committee for Animal Use in Laboratory.

Rats were housed in temperature and light controlled rooms with a 12 h light/dark cycle and had food and water ad libitum. All the experimental manipulations were carried under general anesthesia induced with an intraperitoneal (i.p.) injection of a mixture of ketamine (70 mg/kg, Ketolar, Parke–Davies, S.L., Barcelona, Spain) and xylazine (10 mg/kg, Rompún, Bayer, S.A., Barcelona, Spain).

## *Experimental section: Chapter 2*

### *2.9. Transfection assays in rat primary retinal cell culture and immunocytochemistry*

Embrionary rat retinal primary cells were extracted from E17.5 rat embryos from n = 4 Sprague Dawley rats. During the extraction of retina, the tissue was maintained in cold Hank's Balanced Salt Solution (Gibco, California, USA). After enzymatic digestion with trypsin (Sigma), the retina was mechanically dissociated in Dulbecco's modified Eagle medium (DMEM) (Thermo Fisher Scientific) and maintained in DMEM supplemented with 10 % FBS (Life Technologies, Paisley, UK), 2 % of B27 (Thermo Fisher Scientific), 0.4 % of Glutamax (Thermo Fisher Scientific) and 0.4 % of penicillin-streptomycin solution (Life Technologies, Paisley, UK). Cells were incubated at 37°C under 5 % CO<sub>2</sub> atmosphere.

For transfection assays, cells were seeded on poly-D-lysine-coated coverslips in 12 well plates at a density of 2x10<sup>5</sup> cells per well. The composition nioplexes and transfection conditions were the same as the previously mentioned for *in vitro* assays. Lipofectamine™ 2000 (Invitrogen, California, USA) was used as positive control.

Transfection efficiency was analyzed qualitatively 96 h after the exposure to nioplexes by immunocytochemistry. Cellular phenotypes were assessed using specific antibody markers. For that, cells were washed twice with PBS, fixed with 4% paraformaldehyde for 30 min and permeabilized by 0.5% triton X-100 (Sigma-Aldrich, St Louis, MO, USA), followed by 10% bovine serum albumin block to reduce non-specific bindings. Cover slips were incubated overnight with rabbit polyclonal anti-rabbit microtubule associated protein-2 (MAP2) (Millipore; 1:400 dilution) as a neuronal marker and with secondary antibody donkey anti-rabbit IgG Alexa Fluor 555 (Thermo Fisher Scientific; 1:200 dilution) previous wash with PBS. Nuclei were stained with Hoechst 33342 (Thermo Fisher Scientific). Cover slips were mounted on glass slides and analyzed for fluorescence by a Zeiss AxioObserver Z1 (Carl Zeiss) microscope equipped with an ApoTome system and different fluorescence filters.

### *2.10. Intravitreal and subretinal administration of nioplexes*

Adult male Sprague–Dawley rats of 6–7 weeks old and 150–200 g body weight (n = 6) were employed as experimental animals in this study. The injection solution consisted of 4 µl of nioplexes suspension containing 100 ng of the pCMS-EGFP plasmid. Nioplexes were injected in the left eyes of animals intravitreally (n = 3) or subretinally (n = 3) under an operating microscope (Zeiss OPMI® pico; Carl Zeiss

## *Experimental section: Chapter 2*

Meditec GmbH, Jena, Germany) with the aid of a Hamilton microsyringe (Hamilton Co., Reno, NV). A bent 34-gauge needle was used to inject nioplexes into the vitreous, immediately adjacent to the ora serrata without touching the lens. For subretinal administration of nioplexes, the needle was introduced through a sclerotomy 2 mm posterior to ora serrata and in a tangential direction toward the posterior retinal pole along the subretinal space. Successful administration was confirmed by the appearance of a partial retinal detachment by direct ophthalmoscopy of the eye fundus. The untreated right eyes served as negative control. Lipofectamine™ 2000 was used as positive control.

### *2.11. Evaluation of EGFP expression in rat retinas*

EGFP expression was evaluated qualitatively 96 h after the injection of nioplexes in wholmount and sagital sections of the retina. For that, rats were sacrificed and perfused with 0.9% saline followed by 4% paraformaldehyde in 0.1M phosphate buffer (pH 7.2-7.4) at 4°C. Then, both eyes were enucleated and the anterior segments, including the lens, were removed. The eyes were washed with PBS and retinas were dissected out for flat mount. For cryoprotection of frozen sections, retina and eyecups were immersed in a graded series of 15%, 20% and 30% sucrose solutions in PBS overnight at 4 °C. Eyecups were embedded and oriented in optimal cutting temperature (O.C.T.™) compound (Tissue-Tek®, Sakura Finetek Europe B.V., Alphen and den Rijn, Netherlands) and frozen. Radial sections of 16 µm thick were cut with a cryostat (HM 550; Microm International GmbH, Walldorf, Germany) and mounted on SuperFrost® Plus microscope slides (VWR International BVBA, Leuven, Belgium). Nuclei were stained with Hoechst 33342 (Thermo Fisher Scientific) in frozen sections and wholmount retinas. Images of EGFP signal were acquired using a Leica TCS SPE spectral confocal microscope (Laica Microsystems GmbH, Wetzlar, Germany). Images were processed, montaged and composed digitally using ImageJ (NIH, Bethesda, MD) and Adobe® Photoshop® CS5.1 software (Adobe Systems Inc., CA, USA).

### *2.12. Statistical analysis*

To analyze the differences among the different formulations DST20, DST80 and DST85, a multiple comparison Kruskal-Wallis test followed by a Mann-Whitney U test was performed. Normal distribution was determined by a Shapiro-Wilks test and homogeneity of variance by the Levene test. Data were expressed as mean ± SD, unless stated otherwise. A *P* value <0.05 was considered statistically significant. The analysis was performed using the IBM SPSS Statistics 22.Ink statistical package.

### **3. Results**

#### *3.1. Size, polydispersity index, zeta potential and morphology of niosomes and nioplexes*

The physicochemical analysis of formulations revealed that the mean particle size of DST20, DST80 and DST85 niosomes were  $159 \pm 1$  nm,  $145 \pm 1$  nm and  $173 \pm 2$  nm, respectively (Fig. 2A, bars). When complexed to plasmid DNA (pCMS-EGFP), the mean particle size of nioplexes remained similar, except for DST80 nioplexes, which increased to  $217 \pm 4$  nm at cationic lipid/DNA ratio 2/1 and decreased to  $128 \pm 2$  nm at cationic lipid/DNA ratio 10/1 (Fig. 2A, bars). All formulations showed low values of PDI (Fig. 2B). Zeta potential values of DST20, DST80 and DST85 niosomes were  $+48.0 \pm 2.3$  mV,  $+50.7 \pm 2.2$  mV and  $+52.8 \pm 1.5$  mV, respectively. When complexed to pCMS-EGFP, zeta potential values declined moderately, but with augmenting cationic lipid/DNA mass ratios, zeta potential values showed a clear tendency to rise again (Fig. 2A, lines). The three niosome formulations showed a clear spherical morphology when observed under TEM (Fig. 2C-E).

#### *3.2. Ability of nioplexes to protect and release DNA*

The capacity of DST20, DST80 and DST85 nioplexes to protect and release the pCMS-EGFP plasmid was determined by agarose gel electrophoresis (Fig. 2D). Lanes 1-2 correspond to control naked DNA; lanes 3-11 correspond to DST20, DST80 and DST85 nioplexes at cationic lipid/DNA (w/w) ratios 2/1, 5/1 and 10/1. The supercoiled (SC) DNA band on lane 1 indicated that the plasmid completely migrated, and the lack of DNA signals on lane 2 indicated total degradation of the plasmid. The SC DNA bands observed on lanes 3-11 indicated that DNA was protected against enzymatic degradation and effectively released in all conditions.

*Experimental section: Chapter 2*

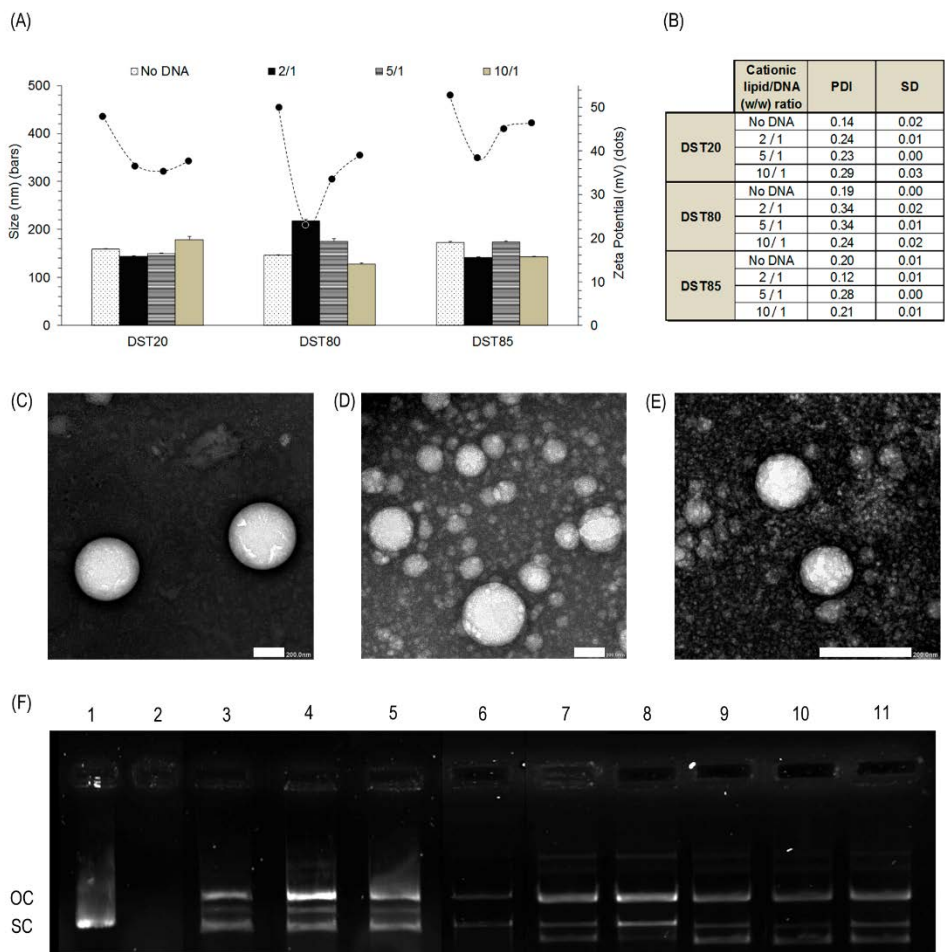


**Figure 2.** Physicochemical characterization of DST20, DST80 and DST85 niosomes and their corresponding nioplexes at cationic lipid/DNA (w/w) ratios 2/1, 5/1 and 10/1. (A). Size values are represented with bars and zeta potential values with dots. Each value represents the mean  $\pm$  SD, n=3. (B). PDI values. Each value represents the mean  $\pm$  SD, n=3. (C-E). TEM images of niosomes. Scale bars: 200.0 nm. (C) DST20 niosomes at 20,000x magnification, (D) DST80 niosomes at 20,000x magnification and (E) DST85 niosomes at 40,000x magnification. (F). Agarose gel electrophoresis assay for analyzing the ability of DST20, DST80 and DST85 nioplexes at different cationic lipid/DNA (w/w) ratios to protect the pCMS-EGFP plasmid. DNase I enzyme and SDS were added in lanes 2-11. Lanes 1-2 correspond to naked DNA. Lanes 3, 4 and 5 correspond to DST20 nioplexes at cationic lipid/DNA mass ratios 2/1, 5/1 and 10/1 respectively. Lanes 6-11 correspond to DST80 and DST85 nioplexes at cationic lipid/DNA mass ratios 2/1, 5/1 and 10/1 respectively. OC and SC lanes are also shown.

## *Experimental section: Chapter 2*

and 10/1, respectively. Lanes 6, 7 and 8 correspond to DST80 nioplexes at cationic lipid/DNA mass ratios 2/1, 5/1 and 10/1, respectively. Lanes 9, 10 and 11 correspond to DST85 nioplexes at cationic lipid/DNA mass ratios 2/1, 5/1 and 10/1, respectively. OC: open circular form, SC: supercoiled form.

---

### *3.3. Cell viability and transfection efficiency of nioplexes in HEK-293 and ARPE-19 cells*

Cell viability and transfection assays were performed with nioplexes at cationic lipid/DNA mass ratio 2/1. In HEK-293 cells, normalized cell viability percentages with DST20, DST80 and DST85 nioplexes were  $100.16 \pm 0.49\%$ ,  $99.87 \pm 0.56\%$  and  $99.43 \pm 0.31\%$ , respectively. In HEK-293 cells transfected with Lipofectamine 2000<sup>TM</sup>, the normalized cell viability value was  $95.37 \pm 0.56\%$ . In ARPE-19 cells, normalized cell viability percentages with DST20, DST80 and DST85 nioplexes were  $87.99 \pm 0.59\%$ ,  $97.27 \pm 1.17\%$  and  $96.68 \pm 3.67\%$ , respectively. In ARPE-19 cells transfected with Lipofectamine 2000<sup>TM</sup>, the normalized cell viability value was  $54.49 \pm 3.60\%$ .

Transfection efficiency data were normalized in each cell line in relation to the EGFP expression values obtained with the positive control Lipofectamine 2000<sup>TM</sup>. In HEK-293, the percentage of EGFP expressing cells with the positive control Lipofectamine 2000<sup>TM</sup> was  $40.26 \pm 1.95\%$ . The normalized percentages of EGFP expressing cells obtained with nioplexes DST20, DST80 and DST85 were  $18.62 \pm 3.90\%$ ,  $4.12 \pm 0.5\%$  and  $69.22 \pm 2.64\%$ , respectively (Figure 3A<sub>1</sub>). Differences in transfection efficiencies between the three nioplexes were statistically significant ( $p < 0.05$ ). In ARPE-19 cells, the percentage of EGFP expressing cells with the positive control Lipofectamine 2000<sup>TM</sup> was  $43.62 \pm 5.79\%$ . The normalized percentages of EGFP expressing cells obtained with nioplexes DST20, DST80 and DST85 were  $24.57 \pm 3.83\%$ ,  $14.19 \pm 3.16\%$  and  $14.13 \pm 1.09\%$ , respectively (Figure 3B<sub>1</sub>). Statistical differences ( $p < 0.05$ ) in transfection efficiency were found between DST20 and DST80 and between DST20 and DST85 nioplexes in ARPE-19 cells. Therefore, DST20 nioplexes were selected for further gene delivery assays in primary rat retinal cells and *in vivo* studies. Figures 3A<sub>2</sub> and 3B<sub>2</sub> show representative images of EGFP green fluorescent signal in HEK-293 cells transfected with DST85 nioplexes and in ARPE-19 cells transfected with DST20 nioplexes, respectively.

*Experimental section: Chapter 2*

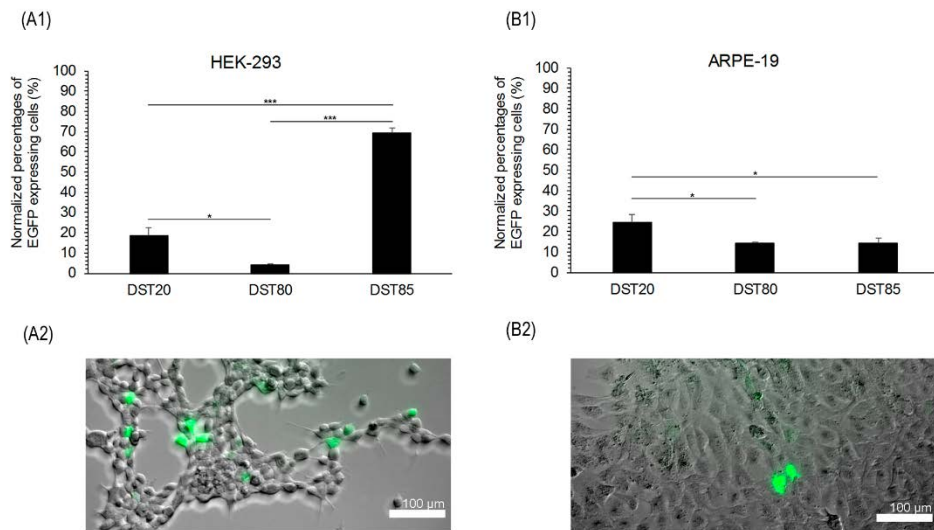


**Figure 3.** Transfection efficiency and cell viability assay in HEK-293 and ARPE-19 cells 48 h post-addition of DST20, DST80 and DST85 nioplexes vectoring the pCMS-EGFP plasmid at cationic lipid/DNA mass ratio 2/1. **(A<sub>1</sub>)**. Normalized percentages of EGFP expressing HEK-293 cells evaluated by flow cytometry. Each value represents the mean  $\pm$  SD, n = 3. Statistical significance: \*  $p < 0.05$ , \*\* $p < 0.01$ , \*\*\* $p < 0.001$ . **(A<sub>2</sub>)**. Representative fluorescence microscope image of EGFP expression in HEK-293 cells transfected with DST85 nioplexes captured at 20x magnification. Scale bar: 100  $\mu$ m. **(B<sub>1</sub>)**. Normalized percentages of EGFP expressing ARPE-19 cells evaluated by flow cytometry. Each value represents the mean  $\pm$  SD, n = 3. Statistical significance: \*  $p < 0.05$ , \*\* $p < 0.01$ , \*\*\* $p < 0.001$ . **(B<sub>2</sub>)**. Representative fluorescence microscope image of EGFP expression in ARPE-19 cells transfected with DST20 nioplexes captured at 20x magnification. Scale bar: 100  $\mu$ m.

### 3.4. Cellular internalization and trafficking of nioplexes in ARPE-19 cells

Figure 4 represents the cellular internalization and intracellular trafficking of DST20, DST80 and DST85 nioplexes at cationic lipid/DNA mass ratio 2/1 in ARPE-19 cells. DST20 nioplexes showed mean CCF peak values of  $0.33 \pm 0.04$  with CME,  $0.54 \pm 0.05$  with CvME and no co-localization with the late endosome compartment. In the case of DST80 nioplexes, mean CCF peak values were near zero with all endocytic pathways. DST85 nioplexes presented mean CCF peak values of  $0.58 \pm 0.23$ ,  $0.29 \pm 0.01$  and  $0.40 \pm 0.09$  with CME, CvME and late endosomes, respectively (Fig. 4B<sub>1-3</sub>). Differences in mean CCF peak values between the three formulations were statistically significant ( $p < 0.05$ ) in the case of CvME and late endosomes. 3D plots

## Experimental section: Chapter 2

in Figures 4C<sub>1-3</sub> relate the HLB values of the polysorbates of each formulation with their corresponding transfection efficiency and co-localization values.

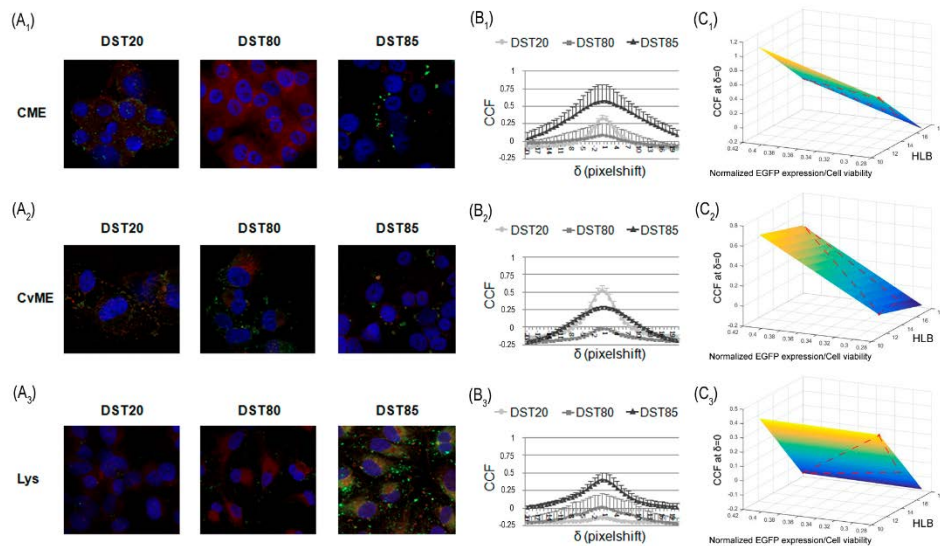


**Figure 4.** Endocytic and intracellular trafficking pathways detection assay of DST20, DST80 and DST85 nioplexes in ARPE-19 cells. (A1-3). Confocal microscopy merged images showing ARPE-19 cells co-incubated with nioplexes containing the FITC-labeled pCMS-EGFP plasmid (green) and with the endocytic vesicle marker (red): AlexaFluor546-Transferrin for CME, AlexaFluor555-Cholera toxin B for CvME and Lysotracker (Lys) for late endosomal compartment. (B1-3). Co-localization values of red and green signals determined by cross-correlation analysis in each case. Data are represented as mean  $\pm$  SEM, n=3. (C1-3). 3D plots relating HLB values and the corresponding transfection efficiency and co-localization with intracellular pathways CME (C1), CvME (C2) and late endosomes (C3).

**3.5. Transfection efficiency of DST20 nioplexes in primary culture of rat retinal cells**  
Transfection assays with DST20 nioplexes at cationic lipid/DNA mass ratio 2/1 showed EGFP expression in retinal primary cells (Fig. 5A). Figure 5B shows transgene expression in cells exposed to the positive control Lipofectamine 2000™. In both conditions, EGFP fluorescence signal was observed mainly in glial cells. Importantly, DST20 nioplexes were well tolerated by retinal primary cells whereas

*Experimental section: Chapter 2*

cell damage was observed in their counterpart positive controls (Fig. 5B, white arrows).

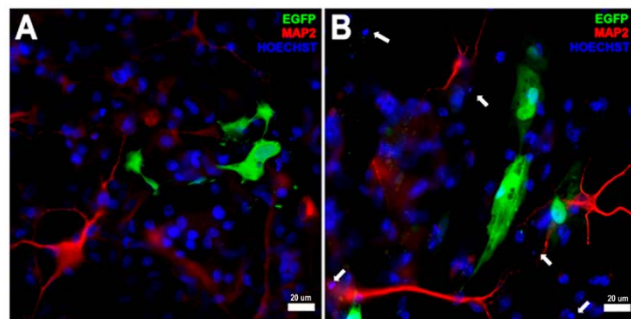
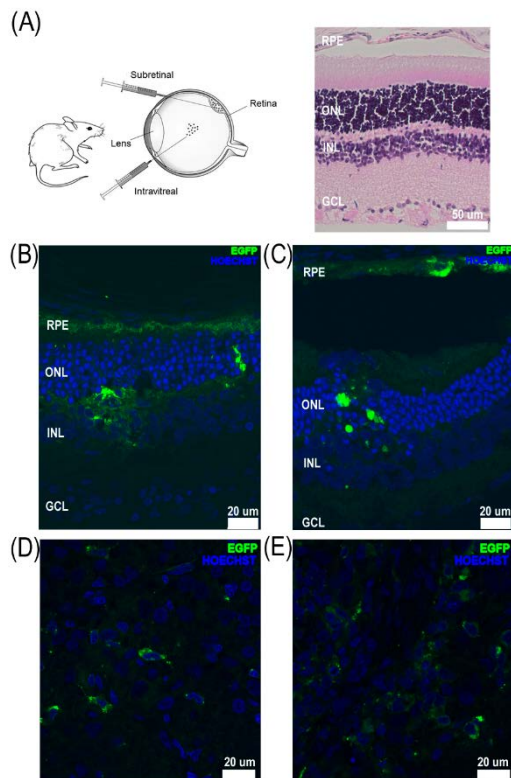


**Figure 5.** EGFP expression in embryonal rat retinal primary cells analyzed by fluorescence immunocytochemistry 96 h post-addition of DST20 nioplexes at cationic lipid/DNA mass ratio 2/1. (A). EGFP expression in cells exposed to DST20 nioplexes. (B). EGFP expression in cells exposed to Lipofectamine 2000<sup>TM</sup>. Red: MAP2 neuronal dendrite marker; Blue: Hoechst 33342 (cell nuclei); Green: EGFP. Scale bar: 20  $\mu$ m.

### 3.6. Transfection efficiency of DST20 nioplexes in rat retina *in vivo*

DST20 nioplexes were administered to the rat eye through subretinal (SR) and intravitreal (IV) injections and transgene expression was found after 72h (Fig. 6). Sagital retinal sections for the analysis of SR administration of DST20 nioplexes allowed detecting fluorescence signal in different retinal cell layers. The highest EGFP expression was observed in the inner nuclear layer (INL), both in retinal cells transfected with DST20 nioplexes (Fig. 6B) and with the positive control (Fig. 6C). Some diffused fluorescence signal in the outer nuclear layer (ONL) and even in the RPE cells could also be observed in both conditions. Regarding IV administration of the formulations, the analysis of whole-mount preparations showed fluorescence signal in the ganglion cell layer (GCL) both in the case of DST20 nioplexes (Fig. 6D) and the positive control Lipofectamine 2000<sup>TM</sup> (Fig. 6E). Qualitative analysis of cell viability suggested that DST20 nioplexes were well tolerated in rat retina.

*Experimental section: Chapter 2*



showing EGFP positive signal located in the ganglion cell layer after intravitreal administration of the positive control Lipofectamine 2000<sup>TM</sup>. Blue: Hoechst 33342 (cell nuclei); Green: EGFP. Scale bars: 20 µm.

**Figure 6.** *In vivo* expression of EGFP after subretinal and intravitreal injection of DST20 niosomes at cationic lipid/DNA mass ratio 2/1. **(A)**. General schema of intravitreal and subretinal injections and complete structure of rat retina with identified layers visualized by hematoxylin and eosin staining of tissue sections. Scale bar: 50 µm. RPE (retinal pigment epithelium), ONL (outer nuclear layer), INL (inner nuclear layer), GCL (ganglion cell layer). **(B)**. Confocal fluorescence micrographs of retinal cross sections showing EGFP signal after subretinal administration of DST20 niosomes. **(C)**. Confocal fluorescence micrographs of retinal cross sections showing EGFP signal after subretinal administration of the positive control Lipofectamine 2000<sup>TM</sup>. **(D)**. Fluorescence immunohistochemistry whole mount showing EGFP positive signal located in the ganglion cell layer after intravitreal administration of DST20 niosomes. **(E)**. Fluorescence immunohistochemistry whole mount

#### 4. Discussion

Chronic and degenerative diseases of the retina still lack curative treatments, and their blinding effect can seriously limit the quality of life<sup>3</sup>. Non-viral gene delivery offers reasonable hope to transfer specific therapeutic genes into the eye. Niosomes have been effectively used for gene delivery to retinal cells both *in vitro* and *in vivo*, and the effect of cationic lipids and helper lipids has been well studied in transfection processes mediated by those formulations<sup>16,17</sup>. To date, niosome formulations containing the cationic lipid DOTMA<sup>18</sup> or the non-ionic surfactant polysorbate 80 combined with the helper lipid squalene<sup>17</sup> have shown effective gene delivery to the retina. However, the use of other non-ionic surfactants with different chemical

## *Experimental section: Chapter 2*

properties such as polysorbate 20 and polysorbate 85 for retinal gene transfer has not been explored. Therefore, in this work we elaborated and characterized, in terms of physicochemical properties and transfection efficiency into retinal cells, three niosome formulations that only differed in their non-ionic tensioactives. These niosomes named DST20, DST80 and DST85 were based on the cationic lipid DOTMA, combined with squalene as helper lipid and polysorbates 20, 80 or 85 as non-ionic surfactants.

Non-ionic tensioactives in niosome formulations act as emulsifiers creating a steric barrier that avoids aggregation<sup>14</sup>. Polysorbates 20 and 85 share the same chemical root structure as polysorbate 80, but the three molecules differ in their hydrophyilic parts and number of hydroxyl groups, therefore presenting different (HLB) values (Figure 1). The HLB parameter determines the oil (HLB < 9) or water (HLB > 11) solubility of the non-ionic surfactants<sup>22</sup>. Among the three non-ionic surfactants tested, polysorbate 20 is the most hydrophilic, due to the presence of 2 hydroxyl groups and a lauric acid, with a HLB value of 16.7. Polysorbate 80 is next with HLB = 15 and polysorbate 85 is the less hydrophilic of the three non-ionic surfactants, due to the presence of three oleic acids in its chemical structure, with a HLB value of 11.

The physicochemical parameters of formulations are key factors that determine transfection efficiency. DST20, DST80 and DST85 niosomes revealed mean particle sizes between 100 nm and 225 nm (Fig. 2A, bars), suitable for gene delivery purposes<sup>23</sup>. Little oscillations in particle sizes upon the addition of plasmid DNA at cationic lipid/DNA ratios 2/1, 5/1 and 10/1 were probably due to the balance between the larger space demanded by the lipid and the higher DNA condensation when increasing mass ratios<sup>17</sup>. In all conditions, formulations showed narrow size distributions as indicated by the low PDI values (Fig. 2B). The surface charge of the formulations has an impact on their stability, and zeta potential values under -30 mV and over +30 mV avoid particle aggregation<sup>24</sup>. In addition, positive zeta potential values promote electrostatic interactions with negatively charged DNA to form nioplexes<sup>25</sup>. The three niosome formulations presented suitable zeta potential values over +40 mV (Fig. 2A, dots). As expected, at low cationic lipid/DNA mass ratios surface charge values of nioplexes clearly declined, demonstrating that the amine groups of the niosomes electrostatically interacted with the phosphate groups of the DNA resulting in partial neutralization of surface charges<sup>26</sup>. In order to determine the morphology of our formulations, niosomes were examined under a TEM microscope at different magnifications, corroborating that all formulations presented a clear

## *Experimental section: Chapter 2*

spherical shape (Fig. 2C-E). The ability of nioplexes to protect and release plasmid DNA at different cationic lipid/DNA mass ratios was evaluated by a gel retardation assay. We found that all formulations were able to protect plasmid DNA even at the lowest cationic lipid/DNA mass ratio 2/1 (Fig. 2F). The exception were DST80 nioplexes, which showed higher ability to protect DNA at higher cationic lipid/DNA mass ratios. However, since our purpose was to develop efficient niosome formulations for retinal gene delivery *in vivo*, in all formulations we selected the lowest cationic lipid/DNA mass ratio for posterior transfection assays, which allows increasing the amount of DNA to administer *in vivo* and reduces cellular toxicity associated to cationic lipids<sup>27</sup>.

Once the formulations were fully characterized, we performed *in vitro* transfection studies at cationic lipid/DNA mass ratio 2/1 in the well-known transfection model HEK-293 cell line and with the retinal model ARPE-19 cell line in accordance to the aim of our study. In both cell lines, nioplexes showed excellent cell viabilities above 95% in HEK-293 and above 85% in ARPE-19 cells, demonstrating that they were well tolerated by both types of cells. This was further confirmed by the healthy appearance of HEK-293 and ARPE-19 under the microscope 48 h after transfection (Fig. 3A<sub>2</sub> and 3B<sub>2</sub>). In contrast, transfection positive control Lipofectamine 2000™ showed lower cell viability values than nioplexes in both cells, around 90% in HEK-293 cells and around 55% in ARPE-19 cells, which in accordance with previous reports<sup>17</sup>, indicates that in retinal cells nioplexes are much better tolerated. In fact, Lipofectamine 2000™ is not considered suitable for retinal gene delivery due to its high toxicity to photoreceptor cells even at low concentrations<sup>28</sup>. Regarding transfection efficiency, we found that DST85 niosomes were the most efficient transfecting HEK-293 cells (Fig. 3A<sub>1</sub>), while DST20 nioplexes showed the highest transfection values in ARPE-19 cells (Fig. 3B<sub>1</sub>). It is generally accepted that non-ionic surfactants with low HLB values and high liposolubility enhance the cellular uptake of the formulations<sup>29,30</sup>. This is consistent with results in HEK-293 cells, since polysorbate 85 presents the lowest HLB value among the three non-ionic surfactants tested. Interestingly, in ARPE-19 cells, polysorbate 20 containing niosomes seemed to be the most efficient for gene transfer. As previously mentioned, polysorbate 20 has the highest HLB value and therefore, the lowest lipophilicity. All together suggests that other cell-dependent mechanisms such as the cell internalization mechanisms and endocytic pathways could explain the higher efficiency of DST20 nioplexes to transfect retinal cells.

## *Experimental section: Chapter 2*

In this regard, in order to further understand the transfection process with DST20, DST80 and DST85 nioplexes in ARPE-19 cells, we analyzed the cell entry mechanisms and intracellular trafficking pathways followed by the formulations. Non-viral vectors usually enter the cells via endocytosis, being CME and CvME the most common and well-studied endocytic pathways<sup>31</sup>. The CvME route has been generally considered a non-acidic and non-digestive endocytic pathway<sup>32</sup>, while the CME pathway is believed to integrate the endocytosed vesicles into late endosomes, which then deliver their cargos to lysosomes<sup>33</sup>. However, controversial data exist in this regard, since it has also been described that caveosomes can join the classical endocytic pathway, eventually fusing with lysosomes<sup>34,35</sup>. In addition, the acid pH in lysosomes is believed to cause the dissociation of the DNA from the non-viral vector<sup>36</sup> which, according to some authors, facilitates the cytosolic release of nanoparticles and enhances the nuclear entry of DNA<sup>37</sup>. Nevertheless, other studies reported that in absence of endosomal escape mechanisms, the acid environment and the enzymatic activity of lysosomes causes the degradation of nioplexes, impeding the access of DNA molecules into the nucleus<sup>38</sup>. In our study, we found that when nioplexes entered predominantly through CME, which was the case of DST85 nioplexes, they also co-localized with late endosome lysosomal compartments which apparently resulted in a lower transfection efficiency (Figure 4). In contrast, when nioplexes entered through CvME, as in the case of DST20 nioplexes, they seemed to avoid late endosomes and transfection efficiency increased. Therefore, our results are in accordance with the lysosomal degradation hypothesis upon CME-mediated cell entry, which in turn would explain the higher transfection efficiency of DST20 nioplexes in ARPE-19 cells. DST80 nioplexes showed very low co-localization values in ARPE-19 cells with both CME and CvME pathways, which might be explained by the presence of other cellular internalization pathways. In fact, a recent study reported that niosomes based on polysorbate 80, squalene and 1-(2-dimethylaminoethyl)-3-[2,3-di(tetradecyloxy) propyl] urea showed higher tendency to enter the cells through macropinocytosis than through CME or CvME<sup>16</sup>.

Based on these results, we selected the formulation DST20 for retinal gene delivery. Before moving on to *in vivo* assays, we performed a preliminary *in vitro* transfection assay in a primary culture of rat retinal cells with DST20 nioplexes, and we observed effective transgene expression (Figure 5). Encouraged by those findings, we carried out an *in vivo* study to assess whether the DST20 nioplexes were able to transfect the rat retinas after SR (Fig. 6B-C) and IV injections (Fig. 6D-E). In most cases, efficient transfection of ganglion cells of the retina can be achieved by IV injections,

## *Experimental section: Chapter 2*

whereas transfecting cells in the outer retina, such as photoreceptor and the RPE, requires the more invasive SR injection<sup>28,39</sup>. In accordance, our results show that IV administration of DST20 nioplexes was successful to transfet predominantly ganglion cells of the retina (Figure 6D), while with SR administration efficient transgene expression was observed in the inner layers of the retina, with clear diffusion to the outer layers including RPE cells (Figure 6B). Considering that many blinding diseases are associated to mutations in specific genes of the RPE, achieving transfection at this level is highly desirable for therapeutic purposes. Unfortunately, SR injection is one of the most invasive methods and implies significant risk of complications such as inflammation, damage to the lens and retinal detachment<sup>40</sup>. Although many efforts are conducted to increasing RPE transgene expression after IV injection, at present the SR administration remains more efficient for RPE cells transfection. Additionally, research is also being directed towards ocular topical instillation of drugs. In fact, efficient topical drug delivery to the RPE layer of the retina with microfluidizer produced small liposomes has been recently reported<sup>41</sup>. This method does not imply any risks of retinal damage and it would be the ideal administration method for non-viral vectors carrying nucleic acids. However, in the field of gene therapy more research is still needed to improve the efficiency of gene delivery through this approach and become clinically relevant for retinal diseases.

### **Conclusions**

In summary, we have elaborated and characterized three niosome formulations that only differed in the non-ionic tensioactives. We found that the novel DST20 niosome formulation, based on polysorbate 20 combined with cationic lipid DOTMA and helper lipid squalene, efficiently transfected rat retina both *in vitro* and *in vivo* at the low cationic lipid/DNA mass ratio 2/1. Targeted cells strongly depended on the administration route. SR injection transfected the inner layers of the retina and showed clear diffusion to outer layers including the RPE, while IV injection transfected predominantly the ganglion cell layer. With the advancement of DNA compaction technology and vector engineering strategies, efficient transfection through less invasive administration routes and prolonged transgene expression may be achievable goals.

### **Acknowledgements**

This project was supported by the Basque Country Government (Department of Education, University and Research, Predoctoral Grant PRE\_2016\_2\_0302 and

## *Experimental section: Chapter 2*

Consolidated Groups, IT907-16), by the Ikerbasque Foundation for Science from the Basque Country, by the Spanish Grants MAT 2015 -69976-C3-1 and SAF2013-42347-R, and by Research Chair “Bidons Egara”. Authors wish to thank the intellectual and technical assistance from the ICTS “NANBIOSIS”, more specifically by the Drug Formulation Unit (U10) of the CIBER in Bioengineering, Biomaterials and Nanomedicine (CIBER-BBN) at the University of the Basque Country (UPV/EHU). The authors thank for technical and human support provided by SGIker of UPV/EHU and European funding (ERDF and ESF). The authors also wish to thank A. Rujas for his intellectual and technical assistance. I.V.B. thanks the Basque Country Government for the granted fellowship.

### **References**

- (1) Koirala, A.; Conley, S.M.; Naash, M.I. A review of therapeutic prospects of non-viral gene therapy in the retinal pigment epithelium. *Biomaterials* **2013**, *34*(29), 7158-7167.
- (2) Strauss, O. The retinal pigment epithelium in visual function. *Physiol Rev.* **2005**, *85*(3), 845-881.
- (3) Conley, S.M.; Naash, M.I. Nanoparticles for retinal gene therapy. *Prog Retin Eye Res.* **2010**, *29*(5), 376-397.
- (4) Andrieu-Soler, C.; Bejjani, R.A.; de Bizemont, T.; Normand, N.; BenEzra, D.; Behar-Cohen, F. Ocular gene therapy: a review of nonviral strategies. *Mol Vis.* **2006**, *12*, 1334-1347.
- (5) Bainbridge, J.W.; Smith, A.J.; Barker, S.S.; Robbie, S.; Henderson, R.; Balaggan, K.; Viswanathan, A.; Holder, G.E.; Stockman, A.; Tyler, N.; Petersen-Jones, S.; Bhattacharya, S.S.; Thrasher, A.J.; Fitzke, F.W.; Carter, B.J.; Rubin, G.S.; Moore, A.T.; Ali, R.R. Effect of gene therapy on visual function in Leber's congenital amaurosis. *N. Engl. J. Med.* **2008**, *358*(21), 2231–2239.
- (6) Maguire, A.M.; Simonelli, F.; Pierce, E.A.; Pugh Jr., E.N.; Mingozzi, F.; Bennicelli, J.; Banfi, S.; Marshall, K.A.; Testa, F.; Surace, E.M.; Rossi, S.; Lyubarsky, A.; Arruda, V.R.; Konkle, B.; Stone, E.; Sun, J.; Jacobs, J.; Dell'Osso, L.; Hertle, R.; Ma, J.X.; Redmond, T.M.; Zhu, X.; Hauck, B.; Zeleniaia, O.; Shindler, K.S.; Maguire, M.G.; Wright, J.F.; Volpe, N.J.; McDonnell, J.W.; Auricchio, A.; High, K.A.; Bennett, J. Safety and efficacy of gene transfer for Leber's congenital amaurosis. *N. Engl. J. Med.* **2008**, *358*(21) 2240–2248.
- (7) Pezzoli, D.; Chiesa, R.; De Nardo, L.; Candiani, G. We still have a long way to go to effectively deliver genes!. *J. Appl. Biomater. Funct. Mater.* **2012**, *10*(2), 82–91.

*Experimental section: Chapter 2*

- (8) Jin, L.; Zeng, X.; Liu, M.; Deng, Y.; He, N. Current progress in gene delivery technology based on chemical methods and nano-carriers. *Theranostics* **2014**, 4(3), 240–255.
- (9) Choi, W.J.; Kim, J.K.; Choi, S.H.; Park, J.S.; Ahn, W.S.; Kim, C.K. Low toxicity of cationic lipid-based emulsion for gene transfer. *Biomaterials* **2004**, 25(27), 5893-903.
- (10) Grimaldi, N.; Andrade, F.; Segovia, N.; Ferrer-Tasies, L.; Sala, S.; Veciana, J.; Ventosa, N. Lipid-based nanovesicles for nanomedicine. *Chem. Soc. Rev.* **2016**, 45(23), 6520-6545.
- (11) Ojeda, E.; Puras, G.; Agirre, M.; Zárate, J.; Grijalvo, S.; Pons, R.; Eritja, R.; Martínez-Navarrete, G.; Soto-Sánchez, C.; Fernández, E.; Pedraz, J.L. Niosomes based on synthetic cationic lipids for gene delivery: the influence of polar head-groups on the transfection efficiency in HEK-293, ARPE-19 and MSC-D1 cells. *Org. Biomol. Chem.* **2015**, 13(4), 1068-1081.
- (12) Ojeda, E.; Puras, G.; Agirre, M.; Zarate, J.; Grijalvo, S.; Eritja, R.; Martínez-Navarrete, G.; Soto-Sánchez, C.; Diaz-Tahoces, A.; Aviles-Trigueros, M.; Fernández, E.; Pedraz, J.L. The influence of the polar head-group of synthetic cationic lipids on the transfection efficiency mediated by niosomes in rat retina and brain. *Biomaterials* **2016**, 77, 267-79.
- (13) Dabkowska, A.P.; Barlow, D.J.; Campbell, R.A.; Hughes, A.V.; Quinn, P.J.; Lawrence, M.J. Effect of helper lipids on the interaction of DNA with cationic lipid monolayers studied by specular neutron reflection. *Biomacromolecules* **2012**, 13(8), 2391-2401.
- (14) Liu, F.; Yang, J.; Huang, L.; Liu, D. Effect of non-ionic surfactants on the formation of DNA/emulsion complexes and emulsion-mediated gene transfer. *Pharm. Res.* **1996**, 13(11), 1642-1646.
- (15) Ojeda, E.; Puras, G.; Agirre, M.; Zarate, J.; Grijalvo, S.; Eritja, R.; DiGiacomo, L.; Caracciolo, G.; Pedraz, J.L. The role of helper lipids in the intracellular disposition and transfection efficiency of niosome formulations for gene delivery to retinal pigment epithelial cells. *Int. J. Pharm.* **2016**, 503(1-2), 115-26.
- (16) Ojeda, E.; Agirre, M.; Villate-Beitia, I.; Mashal, M.; Puras, G.; Zarate, J.; Pedraz, J.L. Elaboration and Physicochemical Characterization of Niosome-Based Nioplexes for Gene Delivery Purposes. *Methods Mol. Biol.* **2016**, 1445, 63-75.
- (17) Puras, G.; Mashal, M.; Zárate, J.; Agirre, M.; Ojeda, E.; Grijalvo, S.; Eritja, R.; Diaz-Tahoces, A.; Martínez Navarrete, G.; Avilés-Trigueros, M.; Fernández, E.; Pedraz, J.L. A novel cationic niosome formulation for gene delivery to the retina. *J. Control. Release* **2014**, 174, 27-36.

*Experimental section: Chapter 2*

- (18) Mashal, M.; Attia, N.; Puras, G.; Martínez-Navarrete, G.; Fernández, E.; Pedraz, J.L. Retinal gene delivery enhancement by lycopene incorporation into cationic niosomes based on DOTMA and polysorbate 60. *J Control Release* **2017**, *254*, 55-64.
- (19) Reddy, L.H.; Couvreur, P. Squalene: a natural triterpene for use in disease management and therapy. *Adv. Drug Deliv. Rev.* **2009**, *61*(15), 1412–1426.
- (20) Kim, Y.J.; Kim, T.W.; Chung, H.; Kwon, I.C.; Sung, H.C.; Jeong, S.Y. The effects of serum on the stability and the transfection activity of the cationic lipid emulsion with various oils. *Int. J. Pharm.* **2003**, *252*(1–2), 241–252.
- (21) van Steensel, B.; van Binnendijk, E.P.; Hornsby, C.D.; van der Voort, H.T.; Krozowski, Z.S.; de Kloet, E.R.; van Driel, R. Partial colocalization of glucocorticoid and mineralocorticoid receptors in discrete compartments in nuclei of rat hippocampus neurons. *J. Cell Sci.* **1996**, *109*(Pt 4), 787-792.
- (22) Moghassemi, S.; Hadjizadeh, A. Nano-niosomes as nanoscale drug delivery systems: an illustrated review. *J. Control. Release* **2014**, *185*, 22-36.
- (23) Andar, A.U.; Hood, R.R.; Vreeland, W.N.; Devoe, D.L.; Swaan, P.W. Microfluidic preparation of liposomes to determine particle size influence on cellular uptake mechanisms. *Pharm. Res.* **2014**, *31*(2), 401-413.
- (24) Caracciolo, G.; Amenitsch, H. Cationic liposome/DNA complexes: from structure to interactions with cellular membranes. *Eur. Biophys. J.* **2012**, *41*(10), 815-829.
- (25) Hosseinkhani, H.; Tabata, Y. Self assembly of DNA nanoparticles with polycations for the delivery of genetic materials into cells. *J. Nanosci. Nanotechnol.* **2006**, *6*(8), 2320-2328.
- (26) Paecharoenchai, O.; Niyomtham, N.; Ngawhirunpat, T.; Rojanarata, T.; Yingyongnarongkul, B.E.; Opanasopit, P. Cationic niosomes composed of spermine-based cationic lipids mediate high gene transfection efficiency. *J. Drug Target.* **2012**, *20*(9), 783–792.
- (27) Shao, X.R.; Wei, X.Q.; Song, X.; Hao, L.Y.; Cai, X.X.; Zhang, Z.R.; Peng, Q.; Lin, Y.F. Independent effect of polymeric nanoparticle zeta potential/surface charge, on their cytotoxicity and affinity to cells. *Cell Prolif.* **2015**, *48*(4), 465-474.
- (28) Kachi, S.; Oshima, Y.; Esumi, N.; Kachi, M.; Rogers, B.; Zack, D.J.; Campochiaro, P.A. Nonviral ocular gene transfer. *Gene Ther.* **2005**, *12*, 843–851.
- (29) Huang, Y.Z.; Gao, J.Q.; Chen, J.L.; Liang, W.Q. Cationic liposomes modified with non-ionic surfactants as effective non-viral carrier for gene transfer. *Colloids Surf. B Biointerfaces* **2006**, *49*(2), 158-164.

*Experimental section: Chapter 2*

- (30) Huang, Y.; Rao, Y.; Chen, J.; Yang, V.C.; Liang, W. Polysorbate cationic synthetic vesicle for gene delivery. *J. Biomed. Mater. Res. A.* **2011**, *96*(3), 513-519.
- (31) Rejman, J.; Oberle, V.; Zuhorn, I.S.; Hoekstra, D. Size-dependent internalization of particles via the pathways of clathrin- and caveolae-mediated endocytosis. *Biochem. J.* **2004**, *377*(Pt 1), 159-169.
- (32) Nichols, B. Caveosomes and endocytosis of lipid rafts. *J. Cell Sci.* **2003**, *116*(Pt 23), 4707-4714.
- (33) Luzio, J.P.; Parkinson, M.D.; Gray, S.R.; Bright, N.A. The delivery of endocytosed cargo to lysosomes. *Biochem. Soc. Trans.* **2009**, *37*(Pt 5), 1019-1021.
- (34) Kiss, A.L.; Botos, E. Endocytosis via caveolae: alternative pathway with distinct cellular compartments to avoid lysosomal degradation?. *J. Cell. Mol. Med.* **2009**, *13*(7), 1228-1237.
- (35) Agirre, M.; Ojeda, E.; Zarate, J.; Puras, G.; Grijalvo, S.; Eritja, R.; García del Caño, G.; Barrondo, S.; González-Burguera, I.; López de Jesús, M.; Sallés, J.; Pedraz, J.L. New Insights into Gene Delivery to Human Neuronal Precursor NT2 Cells: A Comparative Study between Lipoplexes, Nioplexes, and Polyplexes. *Mol. Pharm.* **2015**, *12*(11), 4056-4066.
- (36) Villate-Beitia, I.; Puras, G.; Zarate, J.; Agirre, M.; Ojeda, E.; Pedraz, J.L. First insights into non-invasive administration routes for non-viral gene therapy. In: Gene therapy – principles and challenges. D. Hashad, Ed.; InTech: Croatia, 2015; pp 145–177.
- (37) Delgado, D.; del Pozo-Rodríguez, A.; Solinís, M.Á.; Rodríguez-Gascón, A. Understanding the mechanism of protamine in solid lipid nanoparticle-based lipofection: the importance of the entry pathway. *Eur. J. Pharm. Biopharm.* **2011**, *79*(3), 495-502.
- (38) Khalil, I.A.; Kogure, K.; Akita, H.; Harashima, H. Uptake pathways and subsequent intracellular trafficking in nonviral gene delivery. *Pharmacol. Rev.* **2006**, *58*(1), 32-45.
- (39) Farjo, R.; Skaggs, J.; Quiambao, A.B.; Cooper, M.J.; Naash, M.I. Efficient non-viral ocular gene transfer with compacted DNA nanoparticles. *PLoS One* **2006**, *1*, e38.
- (40) Adjianto, J.; Naash, M.I. Nanoparticle-based technologies for retinal gene therapy. *Eur J Pharm Biopharm.* **2015**, *95*(Pt B), 353-367.
- (41) Lajunen, T.; Hisazumi, K.; Kanazawa, T.; Okada, H.; Seta, Y.; Yliperttula, M.; Urtti, A.; Takashima, Y. Topical drug delivery to retinal pigment epithelium with microfluidizer produced small liposomes. *Eur J Pharm Sci.* **2014**, *62*, 23-32.

## ***Chapter 3***

### **Non-viral vectors based on cationic niosomes and minicircle DNA technology enhance gene delivery efficiency for biomedical applications in retinal disorders**

*Under review in Nanomedicine: Nanotechnology, Biology and Medicine  
(2018)*

*Transfekzio-maila egokiak lortzea da bektore ez-biralek erabilera klinikora iristeko gainditu beharreko erronka nagusia. Gure helburua gene-terapia ez-biralaren eraginkortasuna areagotzeko estrategia berriak garatzea izan da, betiere erretinari eragiten dioten gaitzei aurre egiteko tratamenduak lortze aldera. Nioplexoak lortzeko, niosoma kationiko bakoitzari ondorengo hiru material genetiko ezberdinak bat lotu genien: minicircle-a (2,3 kb), bere jatorrizko plasmidoa (3,5 kb) eta plasmido handiago bat (5,5 kb). Karakterizazio fisiko-kimiko osoa egin ondoren, in vitro entseguak egin genituen ARPE-19 erretinako zeluletan. Gure emaitzen arabera, minicircle material genetikoa zeramaten niosomekin lortutako transfekzio-maila plasmidoak zeramatzenetan lortutakoaren bikoitza izan zen, kasu guzietan zelulen biziraupen-maila egokiak mantenduz. Erretinako zelula primarioen kultiboetan zein in vivo arratoi erretinetan egindako transfekzio entseguak ere gauza bera erakutsi zuten, minicircle-a zeramaten niosomen transfekzio-mailak altuenak ziren kasu guzietan. Beraz, niosoma kationikoz eta minicircle material genetikoz osatutako bektore ez-birala aukera aparta izan daitezke erretinarako gaitzen aurkako aplikazio biomedikoetan erabiltzeko.*

*Superar la baja eficiencia de transfección para llegar a la práctica clínica sigue siendo uno de los mayores retos de la terapia génica no-viral. Nuestro objetivo fue explora nuevas estrategias para obtener estrategias de transferencia de genes no-virales más eficientes que pudieran tener aplicaciones biomédicas en el tratamiento de enfermedades que afectan a la retina. Se combinaron niosomas catiónicos y tres tipos de material genético que codificaban la proteína verde fluorescente (GFP) que consistían en un minicircle (2,3 kb), su plásmido parental (3,5 kb) y un plásmido de mayor tamaño (5,5 kb) para formar los nioplexos. Una vez completamente caracterizados, se llevaron a cabo experimentos de transfección in vitro en la línea celular ARPE19 y se observó que la eficiencia de transfección de los nioplexos que contenían el minicircle doblaba la de los nioplexos que contenían los plásmidos, manteniendo excelentes porcentajes de viabilidad celular en todos los casos. Las transfecciones en células de cultivo primario de retina y las inyecciones de los nioplexos en retina de rata confirmaron la mayor capacidad de transfección de los nioplexos que vehiculizaban el minicircle frente a los que vehiculizaban plásmidos. Por lo tanto, los nioplexos basados en niosomas catiónicos y ADN minicircle representan una herramienta prometedora para el tratamiento de enfermedades retinianas genéticas.*

*Experimental section: Chapter 3*

## **Non-viral vectors based on cationic niosomes and minicircle DNA technology enhance gene delivery efficiency for biomedical applications in retinal disorders**

Idoia Gallego, PhD<sup>a,b,1</sup>, Ilia Villate-Beitia, MSc<sup>a,c,1</sup>, Gema Martínez-Navarrete, PhD<sup>c,d</sup>, Margarita Menéndez, PhD<sup>e,f</sup>, Tania López-Méndez, MSc<sup>a,c</sup>, Cristina Soto-Sánchez, PhD<sup>c,d</sup>, Jon Zárate, PhD<sup>a,c</sup>, Gustavo Puras, PhD<sup>a,c,\*</sup>, Eduardo Fernández, PhD<sup>c,d</sup>, José Luis Pedraz, PhD<sup>a,c,\*</sup>

<sup>a</sup> *NanoBioCel Group, University of the Basque Country (UPV/EHU), Vitoria-Gasteiz, Spain*

<sup>b</sup> *Ikerbasque, Basque Foundation for Science, Bilbao, Spain*

<sup>c</sup> *Biomedical Research Networking Center in Bioengineering, Biomaterials and Nanomedicine (CIBER-BBN), Spain*

<sup>d</sup> *Neuroprothesis and Neuroengineering Research Group, Miguel Hernández University, Elche, Spain*

<sup>e</sup> *Rocasolano Physical Chemistry Institute, Superior Council of Scientific Investigations (IQFR-CSIC), Madrid, Spain*

<sup>f</sup> *Biomedical Research Networking Center in Respiratory Diseases (CIBERES), Spain*

<sup>1</sup> *Idoia Gallego and Ilia Villate-Beitia contributed equally to this work.*

---

### **Abstract**

Low transfection efficiency is a major challenge to overcome in non-viral approaches to reach clinical practice. Our aim was to explore new strategies to achieve more efficient non-viral gene therapies for clinical applications and in particular, for retinal diseases. Cationic niosomes and three GFP-encoding genetic materials consisting on minicircle (2.3 kb), its parental plasmid (3.5 kb) and a larger plasmid (5.5 kb) were combined to form nioplexes. Once fully physicochemically characterized, *in vitro* experiments in ARPE-19 retina epithelial cells showed that transfection efficiency of minicircle nioplexes doubled that of plasmids ones, maintaining good cell viability in all cases. Transfections in retinal primary cells and injections of nioplexes in rat retinas confirmed the higher capacity of cationic niosomes vectoring minicircle to deliver the genetic material into retina cells. Therefore, nioplexes based on cationic niosomes vectoring minicircle DNA represent a potential tool for the treatment of inherited retinal diseases.

**Keywords:** Non-viral vector, niosomes, minicircle, transfection, gene therapy, retina.

## *Experimental section: Chapter 3*

### **1. Background**

The pathogenesis of several blinding retinal disorders such as retinitis pigmentosa, Leber's congenital amaurosis, macular dystrophies and age-related degeneration of the macula among others, have a genetic background<sup>1, 2</sup>. Currently, there is no an effective treatment for these kind of disorders and, to date, gene therapy strategies seem to be one of the most promising field of research<sup>3, 4</sup>. Non-viral gene delivery approaches have key safety advantages over viral vectors and their use in clinical trials has gained importance since 2004, meanwhile the viral vectors ones have significantly decreased<sup>5</sup> due to their risk of oncogenesis, immunogenicity, mutagenicity and even the persistence of viral vectors in the brain after intravitreal injection<sup>6-8</sup>. Particularly, cationic lipids are actually among the most commonly used non-viral vectors<sup>5, 9</sup>.

Niosomes are drug delivery systems able to bind genetic material, forming complexes known as nioplexes, with the ability to protect the DNA from enzymatic digestion and to introduce it into the cell with controlled release kinetics. Furthermore, they present low toxicity due to their biocompatibility and biodegradability, are osmotically active, chemically stable formulations, and easy handling<sup>10, 11</sup>, establishing as a better alternative than the common liposomes. Niosomes are composed by cationic lipids to form complexes with the negatively charged DNA by electrostatic interactions<sup>12</sup>, helper lipids to promote the physico-chemical and biological properties of the complex<sup>13, 14</sup>, and non-ionic surfactants to enhance the stability<sup>15</sup>. Recently, it has been reported their capacity to transfect *in vivo* brain and retinal cells in rats<sup>16-19</sup>. Even though the low toxicity of nioplexes preserve cell viability when transfected, the major challenge to reach the clinical practice is the limited transfection efficiency<sup>20</sup>. Therefore, more research efforts are required for the successful implementation of niosomes as optimal gene delivery carriers.

Currently, minicircle (MC) DNA technology offers a potential solution to the reduced transfection efficiency translational barrier for gene therapy. MCs are small circular DNA vectors with no antibiotic resistant genes or bacterial backbone sequences, which make them superior to regular plasmids. MC-DNA has a reduced size compared with conventional plasmid DNA with the same expression cassette and the content of unmethylated CpG dinucleotides is considerably reduced. Thus, their use results in sustained transgene expression due to lower activation of nuclear transgene silencing mechanisms, and reduced immunogenic responses *in vivo*<sup>21-26</sup>. Our goal is to provide as far as we are concerned, the first evidence that niosome based non-viral vectors combined with the MC technology is an effective technique for future clinical applications in the retinal gene therapy field. We employed DST20

## *Experimental section: Chapter 3*

formulation comprised of cationic lipid 1,2-di-O-octadecenyl-3-trimethylammonium propane (DOTMA), the helper lipid Squalene and the non-ionic surfactant polysorbate Tween 20<sup>17-19</sup>. The resulting niosomes were combined with three different DNA materials consisting on MC-GFP of 2257 bp, pGFP of 3487 bp and pEGFP of 5541 bp, to form the corresponding nioplexes. Niosomes and nioplexes were characterized in terms of particle size, polydispersity index (PDI), zeta potential, morphology and stability. The capacity of niosomes to protect and release these DNA materials as well as the binding interactions between cationic niosomes and DNAs at molecular level was also analyzed. *In vitro* experiments were performed to evaluate both the efficiency and cell viability of transfection over time and at different temperatures with the three DNA materials complexed to DST20 niosomes in human ARPE-19 retinal pigment epithelium cells. Additionally, the transfection capacity of these nioplexes was assessed by *ex vivo* experiments in embryonal rat retinal primary cells and by *in vivo* administration of nioplexes to rat eyes via intravitreal (IV) and subretinal (SR) injections.

## **2. Methods**

### **2.1. Production of cationic niosomes**

Niosomes based on cationic lipid DOTMA (Avanti Polar Lipids, Inc., Alabama, USA), helper lipid squalene (Sigma-Aldrich, Madrid, Spain) and the polysorbate Tween 20 (Sigma-Aldrich, Madrid, Spain) were prepared using the o/w emulsification technique to a molar ratio of 2 mM cationic lipid/ 8 mM helper lipid/ 4 mM tensioactive. The emulsion was obtained by sonication (Branson Sonifier 250, Danbury) for 30 s at 50 W. The dichloromethane organic solvent was removed from the emulsion by evaporation under magnetic agitation for 3 h at room temperature, obtaining the niosome DST20 solution.

### **2.2 DNA material: plasmids and minicircle technology**

The 5541 bp pCMS-EGFP plasmid (Clontech laboratories, Inc, USA) (Figure 1), here named as pEGFP 5.5 kb, was propagated in *Escherichia coli* DH5- $\alpha$  and purified using the Qiagen endotoxin-free plasmid purification Maxi-prep kit (Qiagen, California, USA) according to manufacturer's instructions. The concentration of the purified pDNA was quantified by measuring the absorbance at 260 nm in a SimpliNano™ spectrophotometer device (GE Healthcare, Buckinghamshire, UK). The 3487 bp pCMV-GFP plasmid (PlasmidFactory, Bielefeld, Germany) was employed as the parental plasmid of the 2257 bp MC.CMV-GFP minicircle (PlasmidFactory, Bielefeld, Germany) (Figure 1), which was devoid of any selection markers such as antibiotic resistance genes and bacterial origin of replication (ori).

### *Experimental section: Chapter 3*

Here we abbreviated as pGFP 3.5 kb for the parental plasmid and MC-GFP for the resulting minicircle.

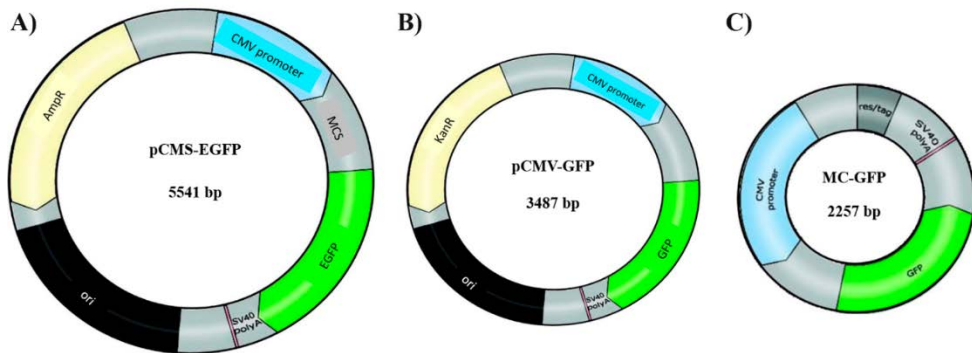


**Figure 1: DNA material composition.**

(A) pEGFP 5.5 kb, (B) pGFP 3.5 kb, (C) MC-GFP 2.3 kb. MC: minicircle; GFP: green fluorescent protein; EGFP: enhanced green fluorescent protein; pCMS: plasmid containing Cytomegalovirus promoter, Multiple cloning site and SV40 promoter; pCMV: cytomegalovirus promoter plasmid; bp: base pairs.

#### **2.3. Preparation of nioplexes**

The nioplexes were prepared by mixing an appropriate volume of a stock solution of either MC-GFP (1 mg/ml), pGFP 3.5 kb (1 mg/ml) or pEGFP 5.5 kb (0.5 mg/ml), with a volume of the niosome DST20 suspension (1 mg DOTMA/ml) to obtain a DOTMA/DNA ratio (w/w) of 2/1. The mixture was incubated for 30 min at room temperature before use to enhance electrostatic interactions between the cationic lipid and the negatively charged DNAs.

#### **2.4. Physicochemical characterization of niosomes and nioplexes**

Z-average particle size and PDI were determined by dynamic light scattering, and zeta potential was measured by laser Doppler velocimetry in a Zetasizer Nano ZS (Malvern Instruments, UK) previous resuspension of the samples into NaCl 1 mM solution. The particle size, reported as hydrodynamic diameter, was achieved by cumulative analysis. The Smoluchowski approximation supported the calculation of the zeta potential from the electrophoretic mobility. All measurements were carried out in triplicate.

The morphology of niosomes was assessed by transmission electron microscopy (TEM) as previously described<sup>17</sup>. The capacity of niosomes to protect and release

### *Experimental section: Chapter 3*

the genetic material from enzymatic digestion was analyzed by a gel retardation assay as previously described<sup>27</sup>. Naked DNA was used as control at each condition, being the amount of DNA per well 100 ng in all cases.

Niosome-DNA interactions for nioplexes formation were analyzed by isothermal titration calorimetry (ITC) using a MicroCal PEAQ-ITC microcalorimeter (Malvern Instruments, UK). The assay was executed at 25°C by stepwise injection of DST20 (0.25 mg/ml DOTMA) into the reaction cell loaded with an aqueous solution of the DNA material (0.0166 mg/ml). Typically, 1 × 0.4 µl injection followed by 13 × 3 µl injections was carried out automatically under 750 rpm stirring. In selected experiments, a second set of injections followed the first one after refilling the injection pipette with the same DST20 solution. The heat contributed by niosome dilution was measured in separate runs and subtracted from the total heat produced following each injection prior to the data analysis. The full set of experiments achieved at a given condition was carried out with the same dilution of niosomes in order to minimize errors.

#### **2.5. Stability assays**

DST20 niosomes were evaluated for stability at day 0 and after their storage for 30 days at 4°C and 25°C. Stability test consisted of the analysis of niosomes and nioplexes at day 0 and after the aforementioned storage in terms of particle size, PDI, zeta potential, TEM, gel retardation assay and ITC, as previously mentioned. Additionally, biological stability of niosomes in terms of transfection efficiency and cell viability were assessed *in vitro* at the aforementioned storage conditions.

#### **2.6. Cell culture and *in vitro* transfection assays**

Human retinal pigment epithelium cells ARPE-19 (ATCC, CRL-2302™) were transfected with nioplexes at the day 0 of the DST20 niosomes preparation and after the storage of niosomes for 30 days at 4°C and 25°C. Cells were seeded without antibiotics in the medium in 24 well plates at 12 × 10<sup>4</sup> cells per well and incubated overnight to achieve 70 % of confluence at the time of transfection. The formation of DST20:DNA complexes composed of DST20 niosomes and 1.25 µg DNA of either MC-GFP, pGFP 3.5 kb or pEGFP 5.5 kb at 2/1 (w/w) DOTMA/DNA ratio, were left to occur through electrostatic interactions for 30 min at room temperature. Medium was removed and cells were washed with serum-free OptiMEM solution (Gibco, California, USA). Next, cells were exposed to nioplexes diluted in serum-free OptiMEM solution for 4 h at 37°C for transfection. After incubation, the transfection medium was removed and fresh medium was added to the cells.

### *Experimental section: Chapter 3*

Transfection efficiency was analyzed qualitatively and quantitatively by fluorescence microscopy imaging (EclipseTE2000-S, Nikon) and by flow cytometry (FACSCalibur, BD Biosciences), respectively, 48 h after the exposure to nioplexes. To analyze cell viability, cells were stained with ethidium homodimer-1 (Life Technologies, Paisley, UK) prior to flow cytometry. A minimum of 10,000 events were collected and analyzed for each sample. Lipofectamine™ 2000 (Invitrogen, California, USA) was used as positive control, and corresponding lipoplexes were prepared according to the manufacturer's protocol. Non-transfected cells but incubated with OptiMEM for 4 h were employed as negative control. Each condition was performed in triplicate.

#### **2.7. Animal model**

Adult male Sprague–Dawley rats were used as experimental animal model. All experimental procedures were carried out in accordance with the Spanish and European Union regulations for the use of animals in scientific research and the Association for Research in Vision and Ophthalmology (ARVO) statement for the use of animals in ophthalmic and vision research. Procedures were supervised by the Miguel Hernández University Standing Committee for Animal Use in Laboratory.

#### **2.8. Transfection assays in rat primary retinal cell culture and immunocytochemistry**

Embrionary rat retinal primary cells were extracted from E17.5 rat embryos from n = 4 Sprague Dawley rats. Transfection assays with nioplexes were performed at the day 0 of the DST20 niosomes preparation. Cells were seeded on poly-D-lysine-coated coverslips in 12 well plates at 2x10<sup>5</sup> cells per well. The composition of DST20:DNA nioplexes and transfection conditions were the same as the previously mentioned ones for *in vitro* assays. Lipofectamine™ 2000 was used as positive control.

Transfection efficiency was analyzed qualitatively 96 h after the exposure to nioplexes by immunocytochemistry. Cellular phenotypes were assessed using specific antibody markers. For that, coverslips were incubated overnight with rabbit polyclonal anti-rabbit microtubule associated protein-2 (MAP2) (1:400 dilution; Millipore) as neuronal marker and with secondary antibody donkey anti-rabbit IgG Alexa Fluor 555 (1:200 dilution; Thermo Fisher Scientific), previous wash with PBS. Nuclei were stained with Hoechst 33342 (Thermo Fisher Scientific). Fluorescence analysis was performed with a Zeiss AxioObserver Z1 (Carl Zeiss) microscope equipped with an ApoTome system and different fluorescence filters.

#### **2.9. Intravitreal and subretinal administration of nioplexes**

### *Experimental section: Chapter 3*

The injection solution consisted of 4 µl of nioplexes suspension containing 100 ng of either the plasmids or MC. Nioplexes were injected in the left eyes of adult male Sprague–Dawley rats (6–7 weeks old and 150–200 g body weight) intravitreally (n = 3) or subretinally (n = 3) under an operating microscope (Zeiss OPMI® pico; Carl Zeiss Meditec GmbH, Jena, Germany) with the aid of a Hamilton microsyringe (Hamilton Co., Reno, NV), as previously described<sup>17</sup>. The untreated right eyes served as negative control. Lipofectamine™ 2000 was used as positive control of gene delivery.

#### **2.10. Evaluation of GFP expression in rat retina**

GFP expression was evaluated qualitatively 96 h after the injection of nioplexes in whole-mount and sagittal sections of the retina, as previously described<sup>17</sup>. Images of GFP signal were acquired using a Leica TCS SPE spectral confocal microscope (Leica Microsystems GmbH, Wetzlar, Germany). Images were processed, montaged and composed digitally using ImageJ (NIH, Bethesda, MD) and Adobe® Photoshop® CS5.1 software (Adobe Systems Inc., CA, USA). GFP expression in the different layers of the retina was quantitatively evaluated in 7 to 10 retinal vertical sections from each group after subretinal injection. The percentage of the fluorescence in every layer was calculated with ImageJ software (<http://imagej.nih.gov/ij/>; provided in the public domain by the National Institutes of Health, Bethesda, MD, USA) using a self-developed macro for analysis of acquired image. The same procedure was followed for retinal whole mounts fluorescent measurements after intravitreal injections.

#### **2.11. Statistical analysis**

Differences between groups were evaluated using a Student's *t* test for unpaired data or a Mann–Whitney *U* test, as appropriate after evaluating normality (Shapiro–Wilks test) and the homogeneity of the variance (Levene test). Data are expressed as mean ± SD. A *P* value < 0.05 was considered statistically significant. Analyses were performed with the IBM SPSS Statistics 22.0 statistical package.

### **3. Results**

#### **3.1. Physicochemical characterization and stability of niosomes and nioplexes**

The physicochemical characteristics of niosomes and nioplexes at the day 0 of the formulation and after 30 days of storage at 4°C and 25°C are summarized in Figure 2A. The mean diameter size of niosomes was around 125 nm and remained constant over time and temperature. PDI was lower than 0.20 and zeta potential values increased up to 63.4 mV after 30 days of incubation at 25°C. In nioplexes, as

### *Experimental section: Chapter 3*

expected, mean diameter sizes increased when complexing DST20 niosomes with the corresponding DNA material, reaching almost the double of its original diameter (from 123 nm to 239–255 nm), and zeta potential values diminished (from 63.4 mV to 22.7–5.1 mV). As all nioplexes were at the same 2/1 ratio, only slight differences in size were found among nioplexes, ranging from 228 nm to 255 nm. Furthermore, nioplexes maintained proper characteristics for gene therapy applications, with values under 0.3 for PDI and positive zeta potential after 30 days of incubation. Regarding stability of nioplexes, pEGFP 5.5 kb and specially MC-GFP nioplexes kept their size over time independently of the temperature of storage. In contrast, pGFP 3.5 kb nioplexes increased their size specially when stored at 25°C, which consequently caused a more drastic reduction of its zeta potential value to 5 mV<sup>28</sup>. TEM images (Figure 2B), revealed that DST20 niosomes at day 0 had clear spherical morphology and no aggregations were formed (Figure 2B, i), meanwhile a loss of the spherical shape was observed after 30 days of storage (Figure 2B, ii and iii) and, additionally, a high proportion of aggregates when stored at 25°C (Figure 2B, iii). The gel retardation assay (Figure 2C) showed that DNA was properly protected from DNase I enzymatic digestion and released after the addition of sodium dodecyl sulfate (SDS) on lanes 3, 6 and 9 corresponding to MC-GFP, pGFP 3.5 kb and pEGFP 5.5 kb nioplexes, respectively. Of note, the signal of these bands was lower in the nioplexes formed with DST20 niosomes stored for 30 days at 4°C and 25°C (Figure 2C, ii and iii, respectively) compared with the ones formed with day 0 DST20 niosomes (Figure 2C, i). The absence of bands on lanes 2, 5 and 8 demonstrated that free DNA was completely digested by the DNase I enzyme. In addition, in Figure 2C, i, minicircle nioplexes (lane 3) showed better stability under enzymatic digestion, since intensity of lane 6 (pGFP 3.5 kb plasmid) is clearly inferior, and lane 9 (pEGFP 5.5 kb plasmid) shows a long smear. This fact could account for better transfection efficiency of minicircle nioplexes.

ITC data (Figure 2D) represents the heat evolved per injection (normalized per mg of DOTMA injected) as a function of the DOTMA/DNA ratio. At day 0 of niosome formulation (black circles), there was an abrupt change in the titration curves of pGFP 3.5 kb and pEGFP 5.5 kb at values of around 1.25 and 2.0, respectively. As more niosomes were added, the heat released during the injection decreased approaching to zero (Supplementary Figure S1). In addition, a slow process was observed in the raw injection peaks of pGFP 3.5 kb data at ratios 0.9–1.4, meanwhile the formation of MC-GFP and pGFP 5.5 kb nioplexes proceeded through fast kinetics (Supplementary Figure S2). Remarkably, both the abrupt change in the tendency of the titration profile and the slow process were sensitive to DST20

### *Experimental section: Chapter 3*

storage, as evidenced their shift toward lower DOTMA/DNA ratios when day 30 niosomes were used.

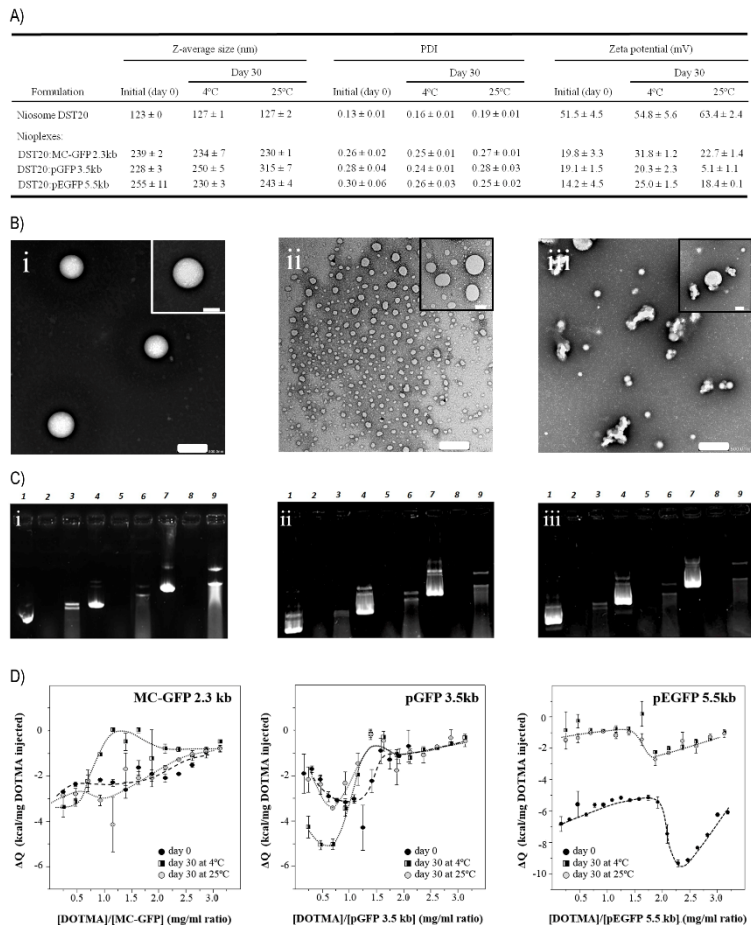


**Figure 2: Physicochemical characterization and stability measurements of niosomes and nioplexes.** (A) Physicochemical characterization of DST20 niosomes at day 0 and at day 30 of storage at 4°C and 25°C, and corresponding nioplexes. Each value represents the mean ± SD from three measurements. (B) TEM images of DST20 niosomes at day 0 (i), at day 30 of storage at 4°C (ii) and 25°C (iii). Scale bars: 500 nm (outer images) and 200 nm (inner images). (C) Gel retardation assay to analyze the capacity of DST20 niosomes to protect and release the DNA material at day 0 (i), at day 30 of storage at 4°C (ii) and 25°C (iii). DNase I enzyme and SDS were added in lanes 3, 6 and 9 to evaluate both protection and release in

### *Experimental section: Chapter 3*

MC-GFP, pGFP 3.5 kb and pEGFP 5.5 kb nioplexes, respectively. As controls, lanes 1, 4 and 7 correspond to control naked MC-GFP, pGFP 3.5 kb and pEGFP 5.5 kb, respectively, and lanes 2, 5 and 8 to those naked DNAs after adding DNase I enzyme, respectively. (D) ITC study of DNA titration with DST20 niosomes. Corresponding variation of heat evolved per mg of DOTMA injected vs. the ratio of DOTMA/DNA concentrations expressed in mg/ml. Symbols represent the experimental data whereas the discontinuous line illustrate the tendency of the ITC profiles.

---

### **3.2. In vitro studies for transfection efficiency and cell viability over time and storage conditions**

The higher rate of transfection observed *in vitro* in ARPE-19 cell line was obtained with MC-GFP and pGFP 3.5 kb Lipofectamine positive controls, with a normalized value of 1 representing a 52% of GFP expression in live cells (Figure 3A, bars). All data were normalized in relation to this value. For DST20 formulation at day 0, there were no significant differences in GFP expression between MC-GFP nioplexes ( $0.8 \pm 0.03$ ) and its positive control ( $1.0 \pm 0.15$ ). In contrast, GFP expression of nioplexes carrying plasmid material was lower than their respective positive controls ( $P < 0.05$ ). In addition, significant differences were found among nioplexes depending on the DNA material complexed to the niosome, thus, DST20 nioplexes containing MC presented higher transfection efficiency than those containing plasmids (MC-GFP:  $0.8 \pm 0.03$ ; pGFP 3.5 kb:  $0.4 \pm 0.02$ ; pEGFP 5.5 kb:  $0.1 \pm 0.01$ ;  $P < 0.05$ ).

Upon DST20 storage for 30 days, transfection efficiency of nioplexes was lower ( $P < 0.05$ ) for every DNA material when compared to that at day 0, reaching the lowest values when stored at  $25^\circ\text{C}$  except for pEGFP 5.5 kb where no differences were found between  $4^\circ\text{C}$  and  $25^\circ\text{C}$  storage (Figure 3B, bars). Of note, DST20 niosomes stored for 30 days at  $4^\circ\text{C}$  vectoring MC remained exhibiting a higher gene delivery capacity compared with plasmid nioplexes (MC-GFP:  $0.35 \pm 0.02$ , pGFP 3.5 kb:  $0.26 \pm 0.01$ , pEGFP 5.5 kb:  $0.05 \pm 0.01$ ;  $P < 0.05$ ). Qualitative analysis of *in vitro* transfection efficiency is reflected in the fluorescence microscopy images shown in Supplementary Figure S3.

### Experimental section: Chapter 3

Regarding cell viability, DST20 at day 0 nioplexes presented higher rates ( $P < 0.05$ ) of living cells compared with their counterpart positive controls in all cases, reaching values above 90% (Figure 3A, dots). This cell viability remained stable over time when DST20 was stored for 30 days at 4°C and decreased to 80% values when stored at 25°C (Figure 3B, dots).

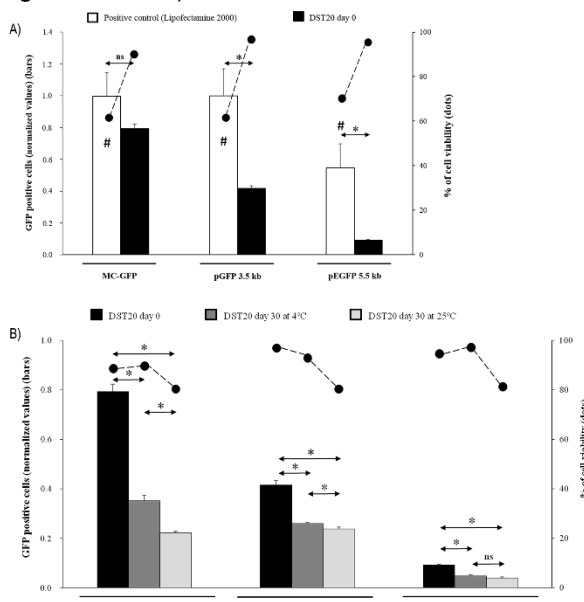


**Figure 3: Transfection efficiency of nioplexes and cell viability in ARPE-19 cell line.**

Flow cytometry evaluation of GFP positive live cells (bars) and viability (dots) after transfection employing (A) DST20 niosomes at day 0 and (B) after 30 days of storage at 4°C and 25°C, bound to either MC-GFP, pGFP 3.5 kb or pEGFP 5.5 kb. Data are presented as mean  $\pm$  SD,  $n = 3$ . \* $P < 0.05$  for transfection efficiency groups, # $P < 0.05$  for cell viability relative to its respective Lipofectamine™ 2000; ns means no statistically significant differences.

### 3.3. Immunofluorescence analysis of GFP expression in embryonic rat retinal primary cells

Transfection assays showed GFP expression in retinal primary cells exposed to DST20 at day 0 nioplexes for every DNA material (Figure 4). In general terms, fluorescence signal emitted due to MC-GFP, pGFP 3.5 kb and pEGFP 5.5 kb transfected vectored by DST20 niosomes was observed mainly in glial cells (Figure 4A-C, respectively). Accordingly, glial morphology like cells too showed transgene

### *Experimental section: Chapter 3*

expression when vectored by their counterpart positive control (Figure 4D-F, respectively). Of note, many apoptotic cells could be observed in the Lipofectamine™ 2000 positive controls (Figure 4, white arrows).

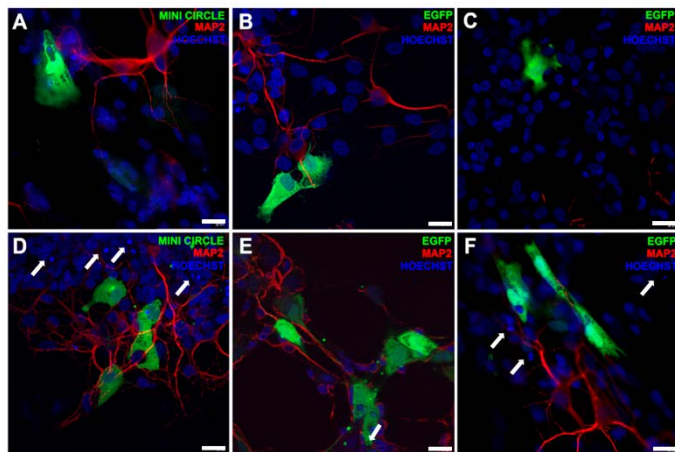


**Figure 4: GFP expression in embryonic rat retinal primary cells.**

Fluorescence immunocytochemistry showing GFP positive signal located mainly in glial cells after transfection with DST20 nioplexes, carrying either (A) MC-GFP, (B) pGFP 3.5 kb or (C) pEGFP 5.5 kb. (D-F) images of their counterpart positive controls exposed to Lipofectamine™ 2000. Cell nuclei were counterstained with Hoechst 33342 (pseudocolored blue) and neuronal dendrites with MAP2 (red color). White arrows indicate apoptotic nuclei. Scale bars: 20  $\mu$ m.

#### **3.4. Analysis of GFP expression *in vivo***

GFP expression was found in rat retinas 72 hours upon IV and SR administration of DST20 nioplexes vectoring any of the three DNA materials (Figures 5 and 6), whereas no fluorescence signal was detected in control retinas (data not shown). The analysis of whole-mount preparations after IV administration of DST20 nioplexes showed in all cases GFP expression in the ganglion cell layer (GCL) (Figure 5). SR administration of DST20 nioplexes vectoring either MC-GFP, pGFP 3.5 kb or pEGFP 5.5 kb (Figure 6 A-C, respectively) was analyzed in sagittal retinal sections, showing GFP expression located in different retinal cell layers. Some fluorescence signal was located in the inner nuclear layer (INL), especially for MC which showed also GFP expression in the ganglion cell layer (GCL). In all cases, GFP signal was mainly observed in the outer segments (OS) of the photoreceptors and, importantly, at the retinal pigment epithelium level (RPE). Qualitative analysis

*Experimental section: Chapter 3*

after both IV and SR injections showed that MC-GFP nioplexes resulted in the higher rate of GFP expression, diminishing progressively with pGFP 3.5 kb and pEGFP 5.5 kb nioplexes.

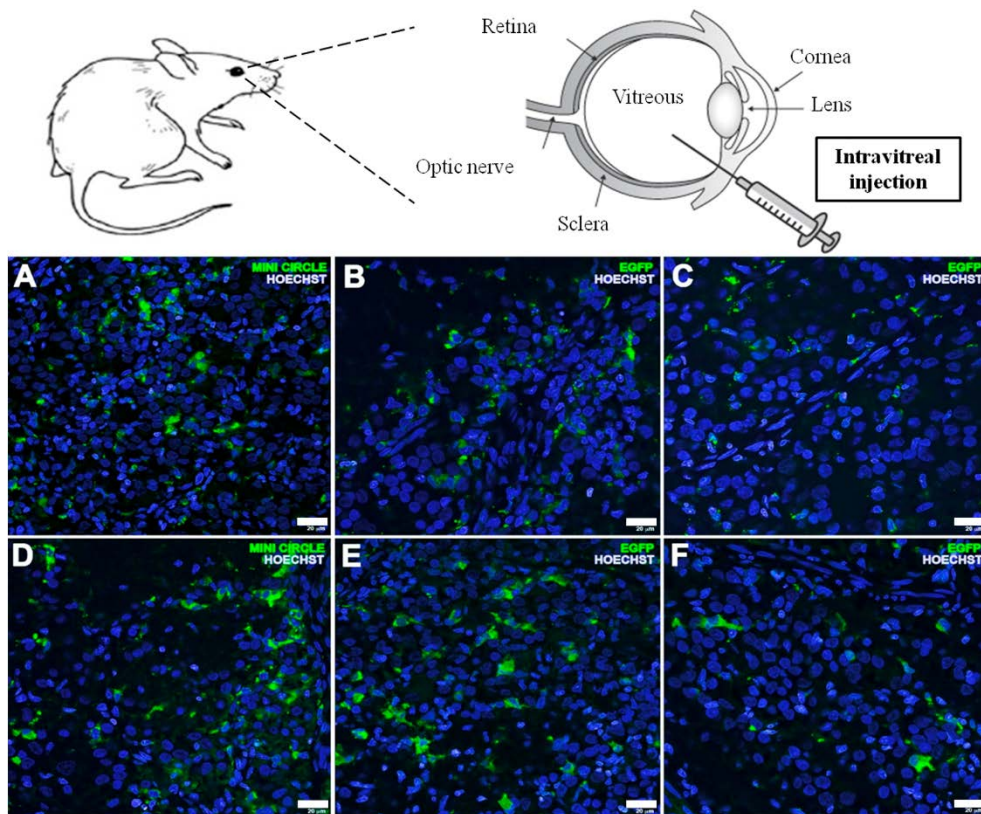


**Figure 5: *In vivo* expression of GFP after intravitreal injection of nioplexes.**

Fluorescence immunohistochemistry in a whole-mounted vitreous side-up retinal section showing GFP positive signal located in the ganglion cell layer after intravitreal administration of DST20 nioplexes carrying either (A) MC-GFP, (B) pGFP 3.5 kb or (C) pEGFP 5.5 kb. (D-F) images of their counterpart positive controls. Cell nuclei were counterstained with Hoechst 33342 (pseudocolored blue). Scale bars: 20  $\mu$ m.

*Experimental section: Chapter 3*

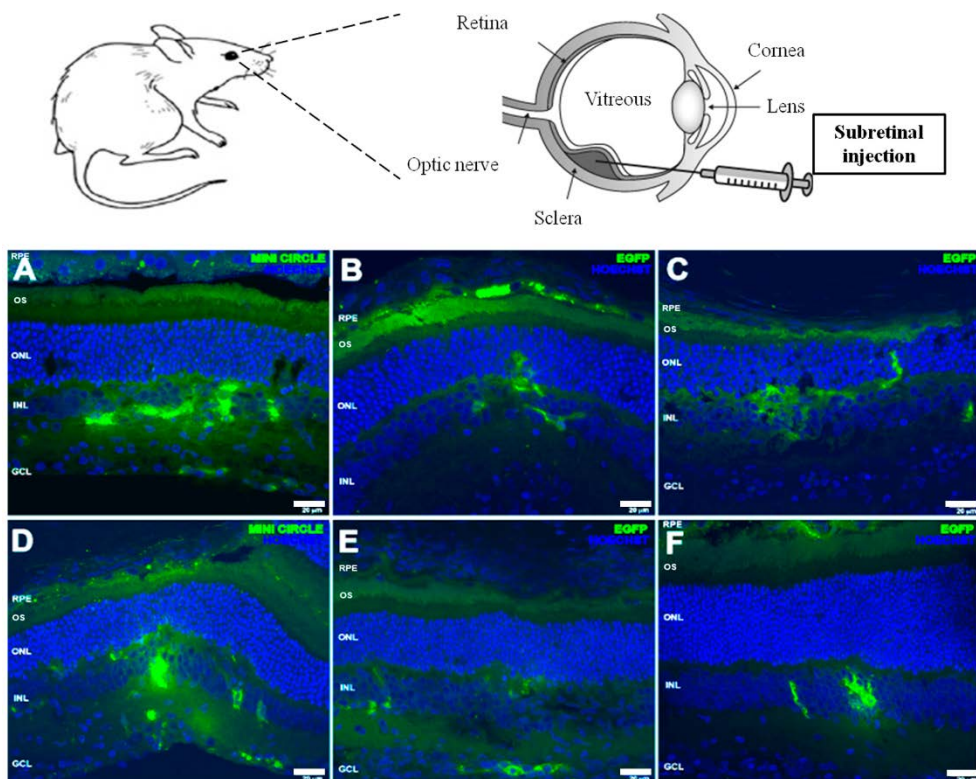


**Figure 6: *In vivo* expression of GFP after subretinal injection of nioplexes.**

Confocal fluorescence micrographs of retinal cross sections showing GFP signal after subretinal administration of DST20 nioplexes carrying either (A) MC-GFP, (B) pGFP 3.5 kb or (C) pEGFP 5.5 kb. (D-F) images of their counterpart positive controls. RPE (retinal pigment epithelium), OS (outer segments), ONL (outer nuclear layer), INL (inner nuclear layer), GCL (ganglion cell layer). Cell nuclei were counterstained with Hoechst 33342 (pseudocolored blue). Scale bars: 20  $\mu$ m.

#### 4. Discussion

The main findings of this study are the following: (1) DST20 niosomes is a non-viral vector able to protect genetic material and release it with controlled kinetics; (2) the capacity of niosomes to protect and interact with DNA material is affected over time and temperature of storage; (3) DST20 niosomes complexed with different genetic material, varying in terms of size and composition, present similar size and zeta

### *Experimental section: Chapter 3*

potential but have different transfection efficiencies *in vitro*, meanwhile cell viability is not affected; (4) DST20 nioplexes containing MC-DNA present higher transfection efficiency than those containing plasmids in *in vitro* assays, even after DST20 storage for 30 days; and (5) DST20 nioplexes are able to transfer the genetic material not only in *ex vivo* primary retinal cell cultures but also after *in vivo* injection in rat retinas regardless the via of administration, being those carrying MC-DNA the ones that present the higher rate of GFP signal. Therefore, DST20 niosomes vectoring MC technology seems to be an efficient and safe therapeutic tool for retinal disorders, overcoming the existing translational barrier of non-viral vectors complexed with plasmids due to their poor transfection efficiency.

DST20 niosomes presented appropriate spherical morphology and size for gene therapy purposes, 123 nm, with low PDI and positive zeta potential pointing out not only a good homogeneity and stability of the suspensions, but also an easy interaction with the negatively charged phosphate groups of the DNA material to form nioplexes, respectively<sup>29-31</sup>. It is worth mentioning that differences in the reported size of niosomes between dynamic light scattering and TEM techniques could be explained by the sample processing and treatment performed for both analyses<sup>32</sup>. As expected, complexation of DST20 niosomes with the corresponding DNA almost doubled its original diameter and zeta potential values diminished due to the partial neutralization of the positive amine groups of niosomes by the DNA phosphate groups.

The features observed regarding size, zeta potential and transfection efficiency when complexing niosomes to the three genetic materials, are in accordance with previous studies which confirm that the DNA size bound to niosomes does not affect such physicochemical properties of nioplexes<sup>33</sup> but have different transfection efficiencies *in vitro*<sup>34</sup>. The explanation for the differences observed in transfection efficiencies might reside in two main factors. On the one hand, the magnitude of the increment in the particle-size of nioplexes with respect to the niosomes seems to rule out the possibility that the second phase seen in the ITC titration curves might be due to the binding of more niosomes onto DNA-coated nioplexes. Thus, niosome-DNA binding events occurring at higher ratios than 2/1 would probably involve the reorganization of the previously bound genetic material, which would lead to a reduction in the number of DNA molecules bound per niosome and to the preferential occupation of the most favourable binding sites on the niosome surface. This could also affect the ability of the nioplexes to interact with the cell surface and, consequently, their transfection capacity. On the other hand, this study was developed with a constant DNA quantity of 1.25 µg per condition but it has to be taken into account that DNA length, and therefore weight and molarity, differs

### *Experimental section: Chapter 3*

between the three genetic materials under study, which consequently affects the number of DNA molecules bound to each niosome. This fact can be observed in the ITC assay where different calorimetry curves were obtained depending on the genetic material complexed to the DST20 formulation. Hence, niosomes would be incorporating more MC molecules than plasmids ones, which means a higher rate of expression cassettes per niosome, increasing the probability of efficient gene delivery into the cell and finally a higher transgene expression<sup>25, 34</sup>.

The differences found in GFP expression upon the storage of niosomes could be explained not by a single cause but by several cumulative reasons. In fact, effective gene delivery is affected by size range and zeta potential but many other relevant parameters such as a correct vector morphology and DNA binding affinity may impact on this effectiveness<sup>35</sup>. In this regard, TEM images showed a loss of the spherical shape of niosomes and even the formation of some aggregates after 30 days of storage, which in turn would difficult interactions with the DNA material. Actually, gel retardation and ITC assays confirm this reduction of DNA complexation capacity of niosomes over time. In agarose gels, the lower signal of bands corresponding to DNA protection and release after storage denoted a reduction of these capacities. Accordingly, ITC data would be indicative that the molecular features of the DST20-based nioplexes formed at 2.0 ratio (equivalent to DOTMA/DNA ratio 2/1) could depend on the previous history of the niosomes, explaining the differences mentioned before, such as the physicochemical features, the morphology of niosomes and their ability to protect and release the DNA. Even though DST20 niosomes stored for 30 days at 4°C vectoring MC remained exhibiting a higher gene delivery capacity compared with plasmid nioplexes, additional efforts are required in order to achieve more stable formulations by either performing better characterization methods or by introducing modifications into formulations themselves. Regarding cell viability, the slightly lower values obtained with DST20/MC (2.3kb) nioplexes compared to both DST20/ pGFP(3.5kb) and DST20 pEGFP (5.5kb) at day 0, could be explained by the higher transfection efficiencies obtained with this formulation, since the transfection process itself can cause cellular toxicity. Anyway, all DST20 nioplexes vectoring the three different genetic materials exhibited excellent cell viability values around 90% at day 0, significantly higher than those obtained with positive control Lipofectamine™ 2000 (around 60%), indicating that they were well tolerated by cells. In embryonal rat retinal primary cell cultures, DST20 nioplexes showed clear transgene expression with high cell viability in all conditions, predominantly in glial cells probably due to their high phagocytic capacity. Since IV and SR routes are considered the most clinically viable options to deliver efficiently the genetic material to the back of the eye<sup>36</sup>, nioplexes were injected at

### *Experimental section: Chapter 3*

these levels *in vivo*. In both cases, we did not observe any sign of toxicity or inflammation of the eye fundus upon administrations (data not shown). IV administration of DST20 nioplexes showed GFP expression in the GCL, in accordance with previous works employing non-viral vectors<sup>17, 18</sup>. Effective gene transfer at this level could be clinically relevant for treatment of devastating inherited retinal disorders such as glaucoma, which is considered the first cause of blindness worldwide<sup>37</sup>. After injection of those nioplexes at SR level, transgene expression diffused to the inner nuclear layer (INL) and, importantly, was localized close to the injection site in the retinal pigment epithelium (RPE). For therapeutic clinical practice, gene delivery reaching the outer layers of the retina is deeply desirable since many inherited retinal disorders with no curative treatment to date, such as retinitis pigmentosa, Stagardt's disease or Leber's congenital amaurosis, are associated with more than 200 mutations of genes expressed at the photoreceptors and RPE level<sup>4</sup>. Qualitative analysis after both IV and SR injections showed a higher transgene expression the smaller the DNA was, pointing out that DST20 non-viral vector combined with MC-DNA offers a potential tool for retinal degenerative and inherited diseases. This qualitative analysis was further confirmed by the quantitative analysis (Supplementary Figure S4). In addition, it has been reported that MC technology offers not only a higher but also a sustained gene expression over time, offering key benefits for clinical translation<sup>25, 34</sup>. Despite GFP expression was also observed employing Lipofectamine™ 2000, it has been shown that such formulation is not suitable for *in vivo* experiments due to its high toxicity mainly accused into photoreceptor cells even at low concentrations<sup>38</sup>. In fact, our *in vitro* experiments clearly showed the toxicity of Lipofectamine™ 2000 in retinal cells. Finally, it is noteworthy the high transfection efficiency achieved with DST20/MC nioplexes at the low 2/1 ratio since it allows a higher gene content at small volumes of injection for clinical applications, where the volume to be injected represents an important handicap, and reduces cellular toxicity associated to cationic lipids<sup>39</sup>. Furthermore, the lack of unmethylated CpG content in MC-DNA technology provides additional reduced immunogenic responses, reinforcing DST20/MC complexes as a potential efficient and safe tool for translational retinal gene therapy applications.

**Acknowledgements:** Authors wish to thank the intellectual and technical assistance from the ICTS "NANBIOSIS", more specifically by the Drug Formulation Unit (U10) of the CIBER in Bioengineering, Biomaterials and Nanomedicine (CIBER-BBN) at the University of the Basque Country (UPV/EHU). Technical and human support provided by SGIker (UPV/EHU) and European funding (ERDF and ESF) is

### *Experimental section: Chapter 3*

gratefully acknowledged, as well as to Dr. José Manuel Andreu (CIB-CSIC) for supplying the access to PEAQ-ITC equipment.

### **References**

1. Francis, P. J. Genetics of inherited retinal disease. *Journal of the Royal Society of Medicine*; 2006; **99**, 189-191
2. Lars G Fritzsche, et al. A large genome-wide association study of age-related macular degeneration highlights contributions of rare and common variants. *Nature Genetics*; 2016; **48**, 134-143
3. McClements, M. E. & MacLaren, R. E. Gene therapy for retinal disease. *Translational research : the journal of laboratory and clinical medicine*; 2013; **161**, 241-254
4. Lipinski, D. M., Thake, M. & MacLaren, R. E. Clinical applications of retinal gene therapy. *Progress in retinal and eye research*; 2013; **32**, 22-47
5. Ramamoorth M, N. A. Non viral vectors in gene therapy- an overview. *J Clin Diag Res*; 2015; 1
6. Mingozi, F. & High, K. A. Therapeutic in vivo gene transfer for genetic disease using AAV: progress and challenges. *Nature Reviews Genetics*; 2011; **12**, 341-355
7. Provost, N., et al. Biodistribution of rAAV Vectors Following Intraocular Administration: Evidence for the Presence and Persistence of Vector DNA in the Optic Nerve and in the Brain. *Molecular Therapy*; 2005; **11**, 275-283
8. Mingozi, F. & High, K. A. Immune responses to AAV vectors: overcoming barriers to successful gene therapy. *Blood*; 2013; **122**, 23
9. Keles, E., Song, Y., Du, D., Dong, W. & Lin, Y. Recent progress in nanomaterials for gene delivery applications. *Biomaterials science*; 2016; **4**, 1291-139
10. Rajera, R., Nagpal, K., Singh, S. K. & Mishra, D. N. Niosomes: A Controlled and Novel Drug Delivery System. *Biological and Pharmaceutical Bulletin*; 2011; **34**, 945-953
11. Choi, W., et al. Low toxicity of cationic lipid-based emulsion for gene transfer. *Biomaterials*; 2004; **25**, 5893-5903
12. Karmali PP, C. A. Cationic liposomes as non-viral carriers of gene medicines: resolved issues, open questions, and future promises. *Medicinal Research Reviews*; 2007; **27(5)**, 696-722
13. Dabkowska, A. P., et al. Effect of helper lipids on the interaction of DNA with cationic lipid monolayers studied by specular neutron reflection. *Biomacromolecules*; 2012; **13**, 2391
14. Edilberto Ojeda, Gustavo Puras, Mireia Agirre, Jon Zarate, Santiago Grijalvo. The role of helper lipids in the intracellular disposition and transfection

*Experimental section: Chapter 3*

- efficiency of niosome formulations for gene delivery to retinal pigment epithelial cells. *International journal of pharmaceutics* ; 2016;
15. Taymouri S, V. J. Effect of different types of surfactants on the physical properties and stability of carvedilol nano-niosomes. *Advanced Biomedical Research*; 2016; **5**,
16. G Puras, et al. Protamine/DNA/Niosome Ternary Nonviral Vectors for Gene Delivery to the Retina: The Role of Protamine. *Molecular pharmaceutics*; 2015; **12**, 3658-3671
17. Mashal M, Attia N, Puras G, Martínez-Navarrete G, Fernández E, Pedraz JL. Retinal gene delivery enhancement by lycopene incorporation into cationic niosomes based on DOTMA and polysorbate 60. *Journal of Controlled Release*; 2017; **254**, 55-64
18. Ojeda E, Puras G, Agirre M, Zarate J, Grijalvo S, Eritja R, DiGiacomo L, Caracciolo G, Pedraz JL. The role of helper lipids in the intracellular disposition and transfection efficiency of niosome formulations for gene delivery to retinal pigment epithelial cells. *International Journal of Pharmaceutics*; 2016; **503(1-2)**, 115-26
19. Puras, G., et al. A novel cationic niosome formulation for gene delivery to the retina. *Journal of controlled release : official journal of the Controlled Release Society*; 2014; **174**, 27-36
20. Cinnamon L Hardee, Lirio Milenka Arevalo-Soliz, Benjamin D Hornstein & Lynn Zechiedrich. Advances in Non-Viral DNA Vectors for Gene Therapy. *Genes* ; 2017; **8**, 65
21. Gracey Maniar, L. E., et al. Minicircle DNA vectors achieve sustained expression reflected by active chromatin and transcriptional level. *Molecular therapy : the journal of the American Society of Gene Therapy*; 2013; **21**, 131-138
22. Ahmad-Nejad, P., et al. Bacterial CpG-DNA and lipopolysaccharides activate Toll-like receptors at distinct cellular compartments. *European Journal of Immunology*; 2002; **32**, 1958-1968
23. Tidd, N., Michelsen, J., Hilbert, B. & Quinn, J. C. Minicircle Mediated Gene Delivery to Canine and Equine Mesenchymal Stem Cells. *International Journal of Molecular Sciences*; 2017; **18**, 819
24. Gaspar, V., et al. Minicircle DNA vectors for gene therapy: advances and applications. *Expert Opinion on Biological Therapy*; 2015; **15**, 353-379
25. Fernandes, A. R. & Chari, D. M. Part I: Minicircle vector technology limits DNA size restrictions on ex vivo gene delivery using nanoparticle vectors: Overcoming a translational barrier in neural stem cell therapy. *Journal of controlled release : official journal of the Controlled Release Society*; 2016; **238**, 289-299
26. Liu, N., et al. PIM1-minicircle as a therapeutic treatment for myocardial infarction. *PLoS One*; 2017; **12**, e0173963

*Experimental section: Chapter 3*

27. Villate-Beitia, I., et al. Non-viral vectors based on magnetoplexes, lipoplexes and polyplexes for VEGF gene delivery into central nervous system cells. *International Journal of Pharmaceutics*; 2017; **521**, 130-140
28. Wissing, S. A., Kayser, O. & Müller, R. H. Solid lipid nanoparticles for parenteral drug delivery. *Advanced Drug Delivery Reviews*; 2004; **56**, 1257-1272
29. Gratton, S. E., et al. The effect of particle design on cellular internalization pathways. *Proc.Natl.Acad.Sci.U.S.A.*; 2008; **105**, 11613-11618
30. Jacobs, C., Kayser, O. & Müller, R. H. Nanosuspensions as a new approach for the formulation for the poorly soluble drug tarazepide. *International Journal of Pharmaceutics*; 2000; **196**, 161-164
31. Hosseinkhani, H. & Tabata, Y. Self Assembly of DNA Nanoparticles with Polycations for the Delivery of Genetic Materials into Cells. *Journal of Nanoscience and Nanotechnology*; 2006; **6**, 2320-2328
32. Ojeda, E., et al. Niosomes based on synthetic cationic lipids for gene delivery: the influence of polar head-groups on the transfection efficiency in HEK-293, ARPE-19 and MSC-D1 cells. *Org.Biomol.Chem.*; 2015; **13**, 1068-1081
33. Patrick Kreiss, et al. Plasmid DNA size does not affect the physicochemical properties of lipoplexes but modulates gene transfer efficiency. *Nucleic Acids Research*; 1999; **27**, 3792-3798
34. Klausner, E. A., et al. Corneal gene delivery: chitosan oligomer as a carrier of CpG rich, CpG free or S/MAR plasmid DNA. *J.Gene Med.*; 2012; **14**, 100-108
35. Rezvani Amin, Z., Rahimizadeh, M., Eshghi, H., Dehshahri, A. & Ramezani, M. The effect of cationic charge density change on transfection efficiency of polyethylenimine. *Iran.J.Basic Med.Sci.*; 2013; **16**, **2**, 150-156
36. Conley, S. M. & Naash, M. I. Nanoparticles for retinal gene therapy. *Prog.Retin.Eye Res.*; 2010; **29**, 376-397
37. Almasieh, M., Wilson, A. M., Morquette, B., Cueva Vargas, J. L. & Di Polo, A. The molecular basis of retinal ganglion cell death in glaucoma. *Prog.Retin.Eye Res.*; 2012; **31**, 152-181
38. Kachi, S., et al. Nonviral ocular gene transfer. *Gene Ther.*; 2005; **12**, 843-851
39. Shao, X., et al. Independent effect of polymeric nanoparticle zeta potential/surface charge, on their cytotoxicity and affinity to cells. *Cell Proliferation*; 2015; **48**, 465-474

## ***Chapter 4***

### **Hyaluronic acid hydrogels loaded with cationic niosomes for efficient non-viral gene delivery**

*Published in RSC Advances (2018)*

*Villate-Beitia I, et al. Hyaluronic acid hydrogel scaffolds loaded with cationic niosomes for efficient non-viral gene delivery. RSC Advances 2018,8, 31934-31942. doi: 10.1039/C8RA05125A.*

Bektore ez-biral idealik ez aurkitzeak beste estrategia batzuen garapena ekarri du, adibidez, gene-garraio sistemak eta hiru dimentsioko matrize-teknologiak uztartzea. Konbinaketa horien abantailen artean, sistemen egonkortasuna hobetzea eta toxikotasuna jaistea dira aipagarrienak. Lan honetan, konbinazio berri bat aztertu genuen niosoma eta azido hialuronikozko (HA) hidrogelesen artean, biak ala biak ere oso sakonki ikertuak beren biobateragarritasuna eta molekula ezberdinak jasotzeko gaitasuna direla eta. Hiru niosoma formulazio ezberdinaz aztertu genituen (**1**, **2** eta **3** niosomak), lípido kationiko, lípido laguntzaile eta tensioaktivo ez-ioniko ezberdinez osatuak. Niosoma eta dagozkien nioplexoen karakterizazio osoa egin zen partikulen tamainaren, zeta potentzialaren, polidispersio indizearen eta sagu-zelula mesenkimalak (mMSC) 2D kultiboetan transfektatzeko gaitasunaren arabera. Jarraian, **1** niosoma hautatua izan zen HA hidrogelekin konbinatzeko, erakutsitako transfekzio-maila kontuan hartuta, eta formulazioaren kontzentrazioa bikoitzu zen DNA kantitate handiagoak sartu ahal izateko HA hidrogeletan. Nioplexoz betetako HA hidrogelesen karakterizazio biomekanikoa egin zen eta partikulen distribuzioa, askapen zinetika eta hidrogeleko zelulak 3D kultiboan transfektatzeko gaitasuna aztertu ziren. Lortutako emaitzek erakutsi zutenez, HA hidrogeletan ez zegoen nioplexoren arteko agregaziorik, zelulak azalera guztian zehar hedatu ziren eta, gainera, transfekzio-maila altuak lortu ziren 3D zelula kultiboetan zelula-biziraupen maila egokiak mantenduz. Gure ustez, *in vitro* eredu honen bidez ikasitakoa baliagarria izan daiteke *in vivo* aplikazioetarako gene-garraio sistema ez-biral, lokal eta eraginkorrik diseinatzeko.

La falta de vectores no-virales ideales en terapia génica ha motivado la combinación entre sistemas de liberación génica y scaffolds de ingeniería tisular para incrementar la estabilidad y reducir la toxicidad. En este trabajo, evaluamos una nueva combinación entre vectores no-virales basados en niosomas e hidrogeles de ácido hialurónico (HA), ambos ampliamente estudiados debido a su biocompatibilidad y capacidad de incorporar gran variedad de moléculas, incluyendo ácidos nucleicos. Evaluamos tres formulaciones de niosoma diferentes (niosomas **1**, **2** y **3**), que diferían en la composición de lípido catiónico, lípido helper y tensioactivo no-iónico. Los niosomas y nioplexos –obtenidos tras la adición del ADN– fueron caracterizados en términos de tamaño de partícula, índice de polidispersión (PDI), potencial zeta y capacidad de transfectar células mesenquimales de ratón (mMSC) en cultivos 2D. El niosoma **1** fue seleccionado para su incorporación en hidrogeles de HA debido a su mayor eficiencia de transfección, y la formulación fue concentrada para poder incorporar cantidades de ADN más relevantes en los hidrogeles. Los hidrogeles de HA con nioplexos incorporados fueron caracterizados según sus propiedades mecánicas, distribución de partículas, cinética de liberación de nioplexos y capacidad para transfectar células mMSC en cultivo 3D. Los resultados mostraron que los nioplexos no formaban agregados dentro de los hidrogeles de HA, que las células eran capaces de difundir libremente a través de los hidrogeles y que éstas fueron transfectadas con eficacia y manteniendo una excelente viabilidad celular. Por lo tanto, creemos que el conocimiento generado a través de este modelo *in vitro* puede ser utilizado para diseñar sistemas de liberación génica no-viral y local *in vivo* para aplicaciones biomédicas.

*Experimental section: Chapter 4*

## **Hyaluronic acid hydrogels loaded with cationic niosomes for efficient non-viral gene delivery**

Ilia Villate-Beitia<sup>a,b</sup>, Norman F. Truong<sup>c</sup>, Idoia Gallego<sup>a,d</sup>, Jon Zarate<sup>a,b</sup>, Gustavo Puras<sup>a,b</sup>, José Luis Pedraz<sup>a,b\*</sup> and Tatiana Segura<sup>c,e\*</sup>

*a*NanoBioCel group, School of Pharmacy, University of the Basque Country (UPV/EHU), 01006 Vitoria-Gasteiz, Spain; *b*Biomedical Research Networking Center in Bioengineering, Biomaterials and Nanomedicine (CIBER-BBN), Vitoria-Gasteiz, Spain; *c*Department of Chemical and Biomolecular Engineering, University of California, Los Angeles, CA 90095, USA; *d*Ikerbasque, Basque Foundation for Science, 48013 Bilbao, Spain; *e*Department of Biomedical Engineering, Duke University, Durham, NC 27708, USA.

**Abstract:** The lack of ideal non-viral gene carriers has motivated the combination of delivery systems and tissue-engineered scaffolds, which may offer relevant advantages such as enhanced stability and reduced toxicity. In this work, we evaluated a new combination between niosome non-viral vectors and hyaluronic acid (HA) hydrogel scaffolds, both widely studied due to their biocompatibility as well as their ability to incorporate a wide variety of molecules. We evaluated three different niosome formulations (niosomes **1**, **2** and **3**) varying in composition of cationic lipid, helper lipid and non-ionic tensioactives. Niosomes and nioplexes obtained upon the addition of plasmid DNA were characterized in terms of size, polydispersity, zeta potential and ability to transfect mouse bone marrow cloned mesenchymal stem cells (mMSCs) in 2D culture. Niosome **1** was selected for encapsulation in HA hydrogels due to its higher transfection efficiency and the formulation was concentrated in order to be able to incorporate higher amounts of DNA within HA hydrogels. Nioplex-loaded HA hydrogels were characterized in terms of biomechanical properties, particle distribution, nioplex release kinetics and ability to transfect encapsulated mMSCs in 3D culture. Our results showed that nioplex-loaded HA hydrogel scaffolds presented little or no particle aggregation, allowed for extensive cell spreading and were able to efficiently transfect encapsulated mMSCs with high cellular viability. We believe that the knowledge gained through this *in vitro* model can be utilized to design novel and effective platforms for *in vivo* local and non-viral gene delivery applications.

**Keywords:** non-viral; gene delivery; biomaterials; niosomes; nioplexes.

## *Experimental section: Chapter 4*

### **Introduction**

The biomedical applicability of gene therapy in tissue engineering is still limited by the lack of suitable local gene delivery platforms. The effective delivery of nucleic acids locally would enhance the applicability of gene therapy in many therapeutic fields, such as tissue regeneration and cancer<sup>1, 2</sup>. In this regard, the condensation of genetic material into different carriers (viral or non-viral) enhances the transfection efficiency. For applications in which transient gene expression is desired, such as tissue regeneration, non-viral vectors offer an attractive choice<sup>3</sup>. Additionally, non-viral vectors are characterized by low immunogenicity, high nucleic acid packing capacity, ease of fabrication, high reproducibility and acceptable costs, compared to their viral counterparts<sup>4</sup>. The majority of nanosized non-viral vectors are based on cationic polymers, lipids or peptides. Among the wide variety of non-viral vectors, niosomes have gained interest in recent years due to their high biocompatibility and biodegradability, as well as because of the promising gene transfer results obtained *in vivo*<sup>5, 6</sup>. Niosomes are synthetic, non-ionic surfactant vesicles with a closed bilayer structure<sup>7</sup>. They are based on three principal components: (i) cationic lipids, which are responsible for the electrostatic interaction with the negatively charged DNA molecules<sup>8</sup>, (ii) helper lipids, to improve the physicochemical properties of the suspension<sup>9</sup> and (iii) non-ionic surfactants, which enhance the stability of the formulation and prevent particle aggregation<sup>10</sup>. Complexes formed by niosomes and DNA (known as nioplexes) are usually in the range of 100 – 200 nm and positively charged, which make them suitable for gene delivery applications<sup>11</sup>.

Complementing gene transfer with matrix design for targeted, local DNA delivery has also gained interest in recent years. Hyaluronic acid (HA), an anionic glycosaminoglycan, is one of the primary components of the natural extracellular matrix (ECM) and it is increasingly gaining popularity as a biomaterial in the field of tissue engineering<sup>12</sup>. HA hydrogel scaffolds have been widely studied for their biocompatibility as well as their ability to incorporate a wide variety of molecules, including nucleic acids<sup>13</sup>. Non-viral DNA nanoparticles based on cationic polymers such as poly(ethylene imine) (PEI) have been successfully encapsulated into fibrin<sup>14, 15</sup>, enzymatically degradable PEG hydrogels<sup>16</sup> and PEG-hyaluronic acid<sup>17</sup> hydrogels. In addition, cationic nioplexes have also been successfully encapsulated in polysaccharide-based hydrogels made of  $\kappa$ -carrageenan and of a mixture of methylcellulose and  $\kappa$ -carrageenan<sup>18</sup>. However, despite the fast development of niosome formulations in the field of gene delivery, their applicability for encapsulation in HA hydrogel scaffolds has not yet been studied.

*Experimental section: Chapter 4*

Therefore, the main objective of the present work was to develop an effective platform to deliver DNA locally using niosomes as non-viral vectors from HA hydrogel scaffolds. To our knowledge, this is the first example of niosome-based DNA nanoparticle delivery from HA hydrogels for non-viral gene expression. We explored three different niosome formulations varying in composition of cationic lipid, helper lipid and non-ionic tensioactives (Fig. 1) in complex with a reporter plasmid encoding for *Gaussia luciferase* (*pGluc*) to obtain the nioplexes. The selection of the components, their concentrations and the cationic lipid/DNA mass ratios (w/w) were based on previous studies developed in our laboratory. Niosomes and corresponding nioplexes were characterized in terms of size, PDI, zeta potential and ability to transfect mouse bone marrow cloned mesenchymal stem cells (mMSCs) in 2D culture. HA hydrogels containing nioplexes were characterized in terms of biomechanical properties, particle distribution and nioplex release kinetics. Additionally, the biological activity of released nioplexes upon hydrogel degradation was also evaluated. mMSCs were efficiently transfected in nioplex encapsulated HA hydrogels and presented excellent cellular viability. These results demonstrate the potential for nioplex loaded HA hydrogels for sustained gene delivery.

*Experimental section: Chapter 4*

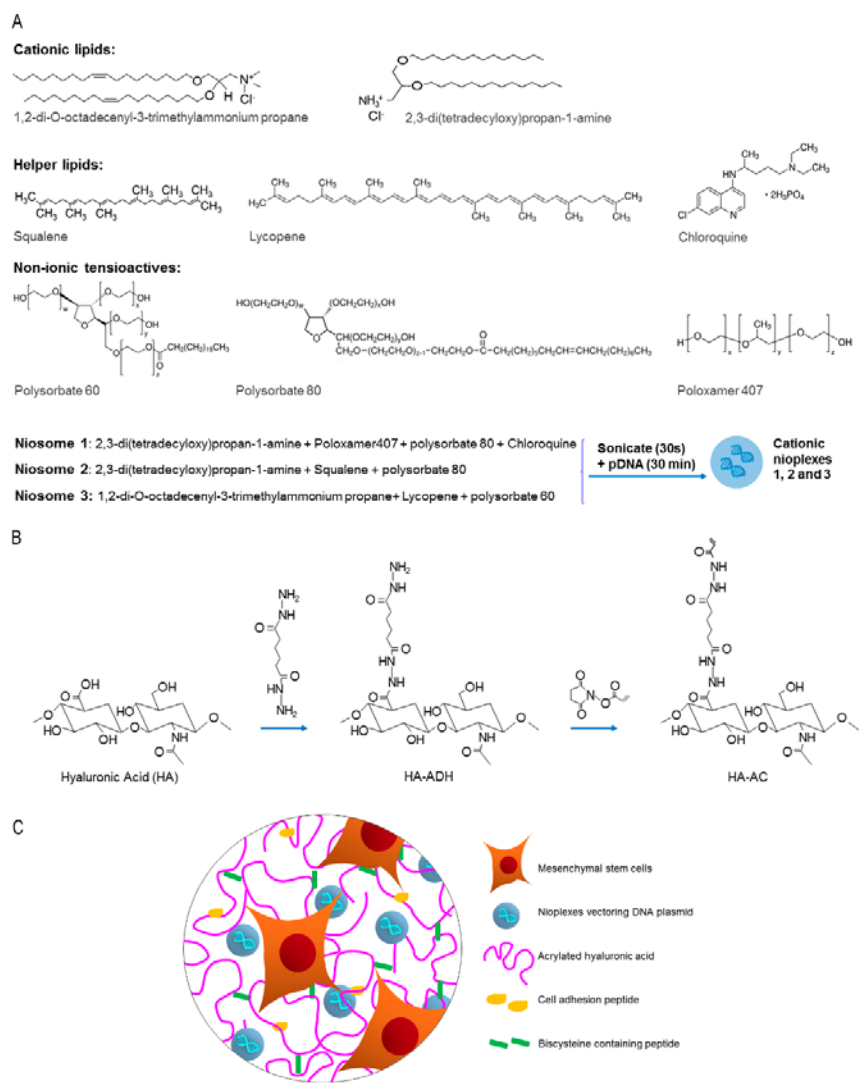


**Figure 1.** General scheme of cationic niosomes and hydrogel scaffolds used in this work. A. Cationic lipid, helper lipid and non-ionic tensioactives components used to elaborate niosome formulations. B. Modification of HA to obtain HA hydrogels. C. Representative scheme of a HA hydrogel with entrapped nioplexes.

## **Experimental section**

### **Formation of niosomes and nioplexes**

Formulations based on niosomes **1**, **2** and **3** (Fig. 1) were prepared by the oil-in-water emulsion technique as previously described<sup>11</sup>. The organic phase of niosome **1** contained 5 mg of cationic lipid 2,3-di(tetradecyloxy)propan-1-amine and 12.5 mg of Poloxamer 407 (Sigma-Aldrich, USA) and 12.5 mg of polysorbate 80 (Sigma-Aldrich, USA) as non-ionic tensioactives, all dissolved in 1 ml of dichloromethane (DCM) (Panreac, USA). The water phase of niosome **1** contained 2.5 mg of helper lipid chloroquine diphosphate salt (Sigma-Aldrich, USA) dissolved in 5 ml of distilled water. In niosome **2**, the organic phase contained 5 mg of cationic lipid 2,3-di(tetradecyloxy)propan-1-amine and 20 µl of helper lipid squalene (Sigma-Aldrich, USA), dissolved in 1 ml of DCM; the aqueous phase contained 25 mg of polysorbate 80 dissolved in 5 ml of distilled water. The organic phase of niosome **3** contained 5 mg of cationic lipid DOTMA (Avanti Polar Lipids, Inc., Alabama, USA), 1.1 mg of helper lipid lycopene (Sigma-Aldrich, USA) and 26 mg of non-ionic tensioactives polysorbate 60 (Sigma-Aldrich, USA), dissolved in 1 ml of DCM, while the water phase consisted of 5 ml of distilled water. The organic phase and the water phase were emulsified by sonication (Branson Sonifier 250, Danbury) for 30 sec at 50 W. The organic solvent was removed from the emulsion by evaporation under magnetic agitation for 3 h at room temperature, obtaining niosome solutions **1**, **2** and **3** at a concentration of 1 mg of cationic lipid/ml. Niosomes were concentrated using Absorbent Gel (Spectrum Labs, USA) and Slide-A-Lyzer MINI Dialysis Units of 10,000 MWCO (Thermo Scientific, USA). Briefly, 500 µl of niosome formulation were introduced in the dialysis units and those were kept in the Absorbent Gel overnight at 4°C. Next, the final volume after dialysis was measured.

The nioplexes were formed by mixing an appropriate volume of a stock solution of a gaussia luciferase expression vector (pGluc) (New England BioLabs, Ipswich, MA) with different volumes of niosomes **1**, **2** and **3** to obtain, respectively, the following cationic lipid/DNA (w/w) mass ratios: 2/1, 15/1 and 18/1. Niosomes and DNA were incubated for 30 min at room temperature to enhance electrostatic interactions and allow the formation of nioplexes. The pGluc plasmid was expanded using an endotoxin-free Giga Prep kit from Qiagen following the manufacturer's instructions.

### **Size, polydispersity index, zeta potential and morphology of niosomes and nioplexes**

The intensity mean diameter (Z-average) and the zeta potential of niosomes and nioplexes were determined by dynamic light scattering and by laser Doppler

## *Experimental section: Chapter 4*

velocimetry, respectively, using a Zetasizer Nano ZS (Malvern Instrument, UK). Briefly, 50 µl of the formulations were resuspended into 950 µl of 0.1 mM NaCl solution. All measurements were carried out in triplicate. Particle hydrodynamic diameter was obtained by cumulative analysis. The Smoluchowski approximation was used to support the calculation of the zeta potential from the electrophoretic mobility. The morphology of niosomes was determined by transmission electron microscopy (TEM) as previously described<sup>5</sup>.

### **Cell culture and 2D transfection**

Mouse bone marrow cloned mesenchymal stem cells (mMSCs, D1, CRL12424) were purchased from ATCC (Manassas, VA) and cultured in Dulbecco's modified Eagle medium (DMEM, Invitrogen) supplemented with 10% bovine growth serum (BGS, Hyclone, Logan, UT) and 1% penicillin/streptomycin (Invitrogen, Grand Island, NY) at 37 °C and 5% CO<sub>2</sub>. The cells were split using trypsin following standard protocols.

For transfection in 2D cell culture, cells were seeded in 48 well plates at a density of 25,000 cells per ml in a total volume of 250 µl per well, and incubated overnight to achieve 70% of confluence at the time of transfection with nioplexes. Nioplexes were suspended in OptiMEM (Gibco, San Diego, CA, USA) transfection medium. Then, growth medium was removed from the plate and cells were exposed for 4 h to nioplexes at 37 °C and 5% CO<sub>2</sub>. After the incubation, nioplexes were removed and fresh growth medium was added to the cells. Lipofectamine 2000™ (Fisher Scientific, USA) at cationic lipid/DNA mass ratio of 2/1 was used as a positive control of the transfection process. Non-treated cells were used as a negative control. Transfection efficiency was measured 48 h after exposure to nioplexes using the Gaussia Luciferase Assay Kit (New England BioLabs, Ipswich, MA) following manufacturer's protocol. Briefly, a 20 µl sample was mixed with a 50 µl 1x substrate solution, pipetted for 2-3 sec, and read for luminescence with a 5 sec integration. Background was determined with media that did not contain any DNA, and values were expressed as relative light units (RLU).

### **HA-acrylate synthesis and formation of HA hydrogels loaded with nioplexes**

Acrylated hyaluronic acid (HA-AC) was prepared using a two-step synthesis as previously described<sup>19</sup>. HA hydrogels were formed by Michael-type addition of biscysteine-containing Ac-GCRDGPQGIWGQDRCG-NH<sub>2</sub> peptides (MMP) (Genescrypt, Piscataway, NJ) onto HA-AC functionalized with cell adhesion Ac-GCGWGRGDSPG-NH<sub>2</sub> peptides (RGD) (Genescrypt). A lyophilized aliquot of RGD

## *Experimental section: Chapter 4*

peptides (0.1 mg) was dissolved in 15  $\mu$ l of 0.3 M HEPES buffer (pH = 8.7), mixed with HA-AC, and allowed to react for 20 min at room temperature. The HA-RGD solution was kept in ice until used. A lyophilized aliquot of the cross-linker (0.91 mg) was then diluted in 18.2  $\mu$ l of 0.3M HEPES buffer (pH = 8.2) immediately before mixing with nioplexes, HA-RGD (final concentration of 500  $\mu$ M RGD), and the cell solution (250,000 cells per 100 $\mu$ l of final gel volume). Three different volumes of nioplexes were loaded into the hydrogels, obtaining final DNA concentrations of 0.055  $\mu$ g/ $\mu$ l, 0.12  $\mu$ g/ $\mu$ l and 0.2  $\mu$ g/ $\mu$ l in hydrogels **2**, **3** and **4**, respectively. Hydrogel **1** did not contain nioplexes and was used as a control. Hydrogel **3** did not contain HEPES buffer since the whole volume was replaced by nioplexes. Hydrogel **4** did not contain HEPES and neither cell growth medium since both volumes were replaced by nioplexes.

For rheology and particle distribution assays, gels were formed in the absence of cells. Gelation was achieved by placing a 40  $\mu$ l drop of the precursor solution between Sigmacoted glass slides for 30 min at 37 °C. The final gel was placed inside 48-well plates for culture. Thorough mixing was used to ensure the nioplexes were uniformly distributed throughout the hydrogel. The gel was then allowed to swell in phosphate-buffered saline (PBS) for 2 hours.

YOYO-1 (Invitrogen, USA), a nucleic acid dye, was used to stain the gels to visualize the distribution of the nioplexes inside the HA hydrogels. The images were taken using the fluorescent (Observer Z1 Zeiss) microscope with 10x magnification.

### **Characterization of HA hydrogel mechanical properties**

The storage and loss moduli were measured with a plate-to-plate rheometer (Physica MCR, Anton Paar, Ashland, VA) using an 8 mm plate under a constant strain of 0.01 and frequency ranging from 0.1 to 10 rad/s. Hydrogels were made as detailed above and cut to 8.0 mm in diameter to fit the plate. A humid hood was used to prevent the hydrogel from drying, and the temperature was maintained at 37 °C throughout the measurement.

### **Radiolabeling DNA**

Plasmid DNA was radiolabeled with dCTP (100  $\mu$ Ci, MP Biomedicals, Santa Ana, CA) using a Nick translation kit (Roche, Indianapolis, IN) as per the manufacturer's protocol. Briefly, an equimolar mixture of dATP, dGTP, dTTP, and  $^{32}$ P-dCTP was prepared and added to the DNA (1  $\mu$ g) solution. Once the enzyme solution was added to the mixture, the final solution (200  $\mu$ l) was gently mixed by pipetting and incubated for 2 h at 15 °C. The reaction was stopped by addition of 10  $\mu$ l of 0.2 M

## *Experimental section: Chapter 4*

ethylenediaminetetraacetic acid (EDTA, pH = 8.0) and heating to 65 °C for 10 min. The DNA was purified using the DNA concentrator kit (Zymo Research, Irvine, CA) following the manufacturer's instructions. The radiolabeled ("hot") DNA concentration was 0.04 µg/µl. This "hot" DNA was then mixed with non-radiolabelled DNA to a concentration of 0.25% "hot" DNA.

### **Nioplex release kinetics and activity**

To determine the extent of release of the encapsulated nioplexes and their activity post encapsulation, gels were formed as described above with 1% radiolabeled DNA. The gels were swelled in PBS for 2 h and the swelling solution was collected. The gels were then placed in 200 µl of release solution, either PBS only or 1 U/mL Collagenase I in PBS. At the indicated time points, 200 µl of the solution was removed, and replaced with fresh release solution. DNA concentrations of collected release solutions and from remaining hydrogels were measured using a scintillation counter. The readout was analyzed using a standard curve.

To determine the activity of the encapsulated nioplexes, a HA gel was prepared and swelled as indicated above using the pGluc plasmid. After swelling in PBS, the gel was degraded through incubation with 100 µl of 0.25% trypsin at 37 °C for 10 min. The collected nioplexes from the degraded hydrogel sample were then used for a bolus transfection (0.625 µg of DNA/well for a 48 well-plate) and compared to freshly made nioplexes. The cell media was collected after 48 h, and transgene expression was measured using the Gaussia Luciferase Assay Kit (New England BioLabs, Ipswich, MA) as described.

### **Gene transfer, cell viability and cell spreading in 3D culture**

Control hydrogel **1** without nioplexes and nioplex-loaded hydrogels **2** and **3** with mMSCs were made as described above, and transfection efficiency was measured at 48 h. Secreted Gluc levels in the media were quantified using a BioLux Gaussia Luciferase Assay Kit (New England BioLabs, Ipswich, MA) as described.

Cell viability in hydrogels **1-3** was studied using a LIVE/DEAD kit (Molecular Probes, Eugene, OR). Briefly, 2 µl of ethidium homodimer-1 and 0.5 µl of calcein AM from the kit were diluted with 1 ml of DMEM. Each gel was stained with 150 µl of this staining solution for 30 min at 37 °C in the dark. Cell viability from hydrogels **2** and **3** was normalized to the cell viability from control hydrogel **1** which contained no nioplexes. To better analyze cell spreading, separate gels were fixed for 30 min at room temperature using 4% paraformaldehyde, rinsed with PBS, treated with 0.1%

## *Experimental section: Chapter 4*

Triton-X for 10 min, and stained for 90 min in the dark with 4',6-diamidino-2-phenylindole (DAPI) for cell nuclei (500x dilution from 5 mg/ml stock) and rhodamine-phalloidin for actin filaments (5 µl per 200 µl final stain solution) in 1% bovine serum albumin solution. The samples were then washed with 0.05% Tween-20. For both cell viability and cell spreading, a Nikon confocal microscope was used to visualize samples. To better visualize the distribution throughout the hydrogel, z-stacks 1213 µm thick were taken for each image, deconvoluted to minimize background, and presented either as maximum intensity projections or as an aerial view of a 3D render of the z-stack.

### **Statistical analysis**

To analyze the differences, a multiple comparison Kruskal-Wallis test followed by a Mann-Whitney U test was performed. Normal distribution was determined using a Shapiro-Wilks test and homogeneity of variance by the Levene test. Data were expressed as mean ± SD, unless stated otherwise. A *p* value <0.05 was considered statistically significant. The analysis was performed using the IBM SPSS Statistics 22.lnk statistical package.

## **Results and discussion**

Since the emergence of non-viral gene delivery from hydrogel scaffolds, emphasis has been placed on optimizing non-viral vectors for combining gene transfer with matrix design and enhancing transfection efficiency. Yet while high concentrations of non-viral DNA complexes in hydrogels have been demonstrated to improve local gene delivery<sup>20</sup>, the physical incorporation of DNA complexes into hydrogels is challenging due to some limitations such as aggregation and inactivation of the complexes inside hydrogel scaffolds<sup>21</sup>. Among the wide variety of non-viral vectors, poly(ethylene imine) (PEI) has been successfully encapsulated in HA hydrogels and effective local transgene expression and ability to induce angiogenesis *in vivo* have been reported<sup>3</sup>. Although PEI derivatives present high gene carrying capacity and ability to achieve high transfection efficiencies, their biomedical application is often restricted due to immunogenicity and cytotoxicity issues<sup>22</sup>. In this regard, niosomes offer several advantages, since they have high compatibility with biological systems and low toxicity because of their non-ionic nature and are biodegradable and non-immunogenic<sup>23</sup>.

The three different niosome formulations used in this work differed in the composition of cationic lipid, helper lipid and non-ionic tensioactives (Fig. 1). These niosome

#### *Experimental section: Chapter 4*

components have previously demonstrated suitability for gene delivery applications. For instance, niosome formulations containing the non-ionic surfactant polysorbate 80 combined with the helper lipid squalene have shown effective gene delivery<sup>5</sup>. In addition, it has been recently shown that the helper lipid lycopene, combined with cationic lipid DOTMA and polysorbate 60, enhances retinal transfection<sup>24</sup> and Poloxamer 407 has been widely used in drug delivery applications<sup>25</sup>. The use of chloroquine has also been reported to enhance gene delivery both *in vitro* and *in vivo*<sup>26</sup>. Therefore, the selection of the components, and their concentrations used to prepare the niosome formulations, as well as the cationic lipid/DNA mass ratios (w/w) to form the corresponding nioplexes were based on available data and previous studies developed in our laboratory.

The physicochemical analysis of formulations used in this work revealed that the mean particle sizes of niosomes **1**, **2** and **3** were  $118.1 \pm 1.8$  nm,  $136.4 \pm 0.9$  nm and  $105.7 \pm 2.3$  nm, respectively (Fig. 2A). Niosomes **1** and **2** were relatively monodisperse ( $\text{PDI} < 0.2$ ) while niosome **3** formed more polydisperse nanoparticle preparations ( $\text{PDI} = 0.4$ ). All formulations formed highly positively charged nanoparticles with zeta potential values of  $+35.9 \pm 2.2$  mV,  $+48.5 \pm 0.6$  mV and  $+32.9 \pm 1.7$  mV, for niosomes **1**, **2** and **3**, respectively (Fig. 2B), necessary to bind to the negatively charged DNA molecules by electrostatic interactions<sup>27, 28</sup>. In addition, positive zeta potential values enhance cellular uptake<sup>29</sup>. Compared to non-treated cells, all formulations presented ability to transfet but nioplexes based on niosome **1** showed significantly higher transgene expression than nioplexes based on niosomes **2** and **3** (Fig. 2C). Although transfection levels of niosomes were lower than the positive control Lipofectamine 2000<sup>TM</sup>, the latest is not considered suitable for *in vivo* gene delivery due to its high cytotoxicity even at low concentrations<sup>30</sup>. Therefore, we selected the nioplexes based on niosome **1** at 2/1 cationic lipid/DNA mass ratio (w/w) formulation to study its applicability for non-viral gene delivery in HA hydrogels.

*Experimental section: Chapter 4*

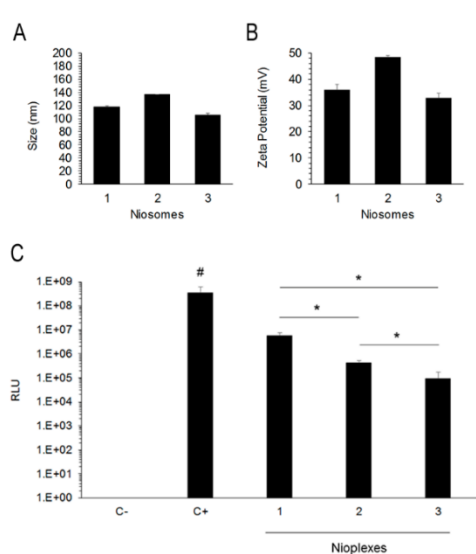


**Figure 2.** Screening of niosome formulations. **A.** Size. **B.** Zeta Potential. **C.** Transfection efficiency 48 h post-exposure of mMSCs to nioplexes based on niosomes **1**, **2** and **3** at cationic lipid/DNA mass ratios (w/w) 2/1, 15/1 and 18/1, respectively. Positive (Lipofectamine 2000™ at a cationic lipid/DNA mass ratio of 2/1) and negative (no DNA) controls are shown for reference. \* $p < 0.05$  for transfection efficiency between niosome formulations, # $p < 0.05$  for transfection efficiency of all niosome formulations relative to the positive control.

The use of nioplexes at low mass ratios presents several advantages, including the possibility of incrementing the dose of DNA as well as decreasing cellular toxicity<sup>31</sup>. Additionally, in order to be able to incorporate higher, more relevant amounts of DNA within HA hydrogels, the formulation based on niosome **1** was concentrated from 1 mg/ml to 2 mg/ml. The TEM images of the concentrated formulation showed that concentration process did not affect morphology and, as expected, more particles were visible in the concentrated sample compared to the non-concentrated one (Fig. 3A-B). Size and PDI values were also maintained similar in the concentrated formulation. In contrast, zeta potential values declined from  $+35.9 \pm 2.2$  mV to  $+25.77 \pm 1.1$  mV, but since values remained above  $+20$  mV, the concentrated formulation should not present an increased propensity to form aggregates along the time<sup>32</sup>. Additionally, the transfection ability of both concentrated and non-concentrated formulations was evaluated at cationic lipid/DNA mass ratio 2/1 and no statistically significant differences ( $p > 0.05$ ) were found between the transfection efficiencies of both formulations (Fig. 3C), indicating that the concentrating process does not affect to the transfection capacity. In view of these results, we decided to use the concentrated formulation at the low cationic lipid/DNA mass ratio 2/1 for encapsulation in HA hydrogels.

*Experimental section: Chapter 4*

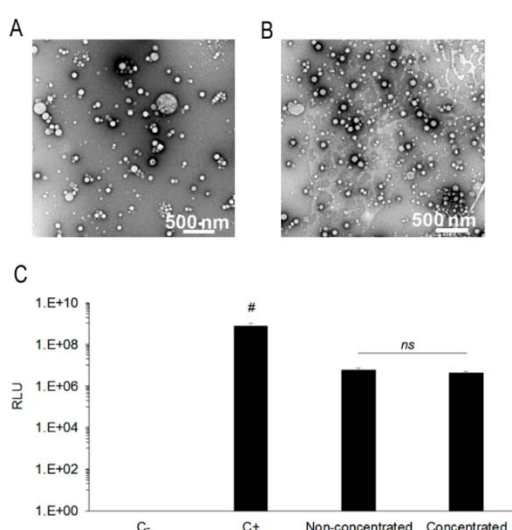


**Figure 3.** Characterization of concentrated niosome formulations. **A-B.** TEM images of non-concentrated (**A**) and concentrated (**B**) formulations based on niosome **1** at 10,000x magnification. Scale bars: 500.0 nm. **C.** Transfection efficiency 48 h post-exposure of mMSCs to nioplexes based on concentrated and non-concentrated niosome **1** at 2/1 cationic lipid/DNA mass ratio (w/w). \* $p < 0.05$  for transfection efficiency between niosome formulations, # $p < 0.05$  for transfection efficiency of all niosome formulations relative to the positive control.

In order to achieve therapeutically relevant levels of DNA<sup>33</sup>, we evaluated three different amounts of nioplexes based on concentrated niosome **1** at 2/1 cationic lipid/DNA mass ratio, obtaining final DNA concentrations of 0.055 µg/µl, 0.12 µg/µl and 0.2 µg/µl in hydrogels **2**, **3** and **4**, respectively. Different DNA concentrations of hydrogels could cause differences in the mechanical properties, which are important factors determining cell proliferation, spreading and transgene expression in hydrogel scaffolds. High hydrogel stiffness (over 800 Pa) has been related to reduced cell spreading and transgene expression, while soft hydrogels (200 – 260 Pa) resulted in enhanced transgene expression<sup>21</sup>. Therefore, we evaluated the mechanical properties of hydrogels as a function of DNA concentration in order to determine their grade of stiffness. Rheological characterization showed high variability in the mechanical properties of hydrogels ranging from an average modulus of ~380 Pa to ~1215 Pa over a frequency range of 0.1-10 rad/s at a constant strain of 0.01 (Fig. 4A-B). Hydrogel **3** presented the highest stiffness among the hydrogels tested, while hydrogel **4**, with the highest DNA concentration, showed to be the softest. Such high values were not expected in hydrogel **3**, however, that condition was not discarded and further studies were carried out in order to determine its transfection capacity despite its high stiffness. The evaluation of the distribution of the nioplexes inside the hydrogel scaffold showed that nioplexes were present uniformly throughout the hydrogels and, in hydrogels **3** and **4**, those were

*Experimental section: Chapter 4*

observed mostly as unaggregated particles (Fig. 4C-E). However, hydrogel **4** did not contain any cell growth medium because it was completely replaced by DNA in order to obtain higher amounts of genetic material. Therefore, it was not a possible candidate for 3D cell culture nor for *in vitro* transfection assays and only hydrogels **2** and **3** were evaluated for gene delivery into encapsulated mMSCs. Yet, the high DNA concentration and absence of particle aggregation in hydrogel **4** suggested that it could be an attractive option for *in vivo* gene delivery. Taken together, these results demonstrate that nioplexes can be successfully encapsulated into HA hydrogels without significant particle aggregation, although high variability in mechanical properties was observed.

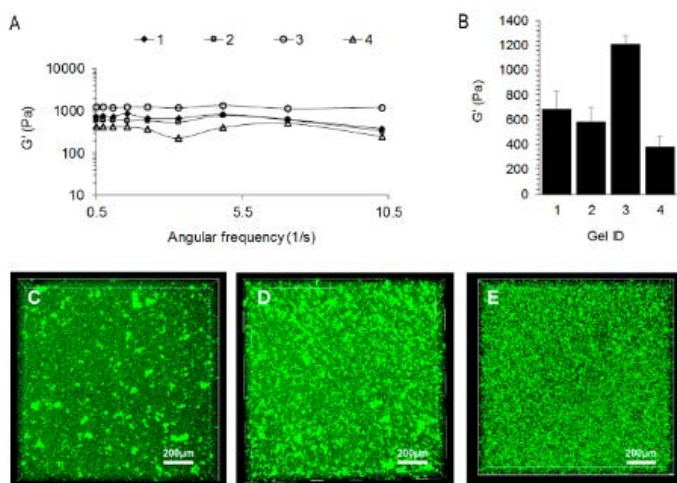


**Figure 4.** Characterization of HA hydrogels loaded with nioplexes. The mechanical properties of the hydrogels were determined using plate-to-plate rheometry over a frequency range of 0.1-10 rad/s at a constant strain of 0.01 (**A**). Average storage modulus (**B**). **C-E.** Particle distribution in hydrogels. **Gel ID:** **1**, control hydrogel without nioplexes; **2**, 0.055  $\mu$ g DNA/ $\mu$ l; **3**, 0.12  $\mu$ g DNA/ $\mu$ l and **4**, 0.2  $\mu$ g DNA/ $\mu$ l. Scale bars: 200  $\mu$ m.

In order to validate that nioplexes maintained the ability to transfect cells after encapsulation in HA hydrogels, we synthesized nioplex-loaded hydrogels, degraded them with trypsin and performed a transfection with the released nioplexes (Fig. 5). Not unexpectedly, nioplexes released from hydrogels degraded with trypsin were still able to efficiently transfect mMSCs in 2D culture, albeit to a somewhat lesser extent than fresh nioplexes (Fig. 5B). When exposing cells to fresh nioplexes + hydrogel + trypsin (Fig. 5C), transfection was similar to that obtained with nioplexes released

*Experimental section: Chapter 4*

from degraded hydrogels (Fig. 5B). When exposing cells to fresh nioplexes + trypsin (Fig. 5D), the difference in transfection was less evident. Cells exposed to naked DNA + hydrogel + trypsin (Fig. 5E) and cells exposed to hydrogels without nioplexes + trypsin (Fig. 5F) did not show luminescence signal. Statistical differences were found between all conditions ( $p < 0.05$ ) except for between conditions "B" and "C" ( $p > 0.05$ ). These results showed that the transfection capacity of the nioplexes was negatively affected by the presence of interfering hydrogel materials and trypsin in the 2D cell culture media, but not by the encapsulation process since there were no statistically significant differences in transfection values between released nioplexes from degraded hydrogels and fresh nioplexes supplemented with degraded hydrogel materials (Fig. 5B-C).

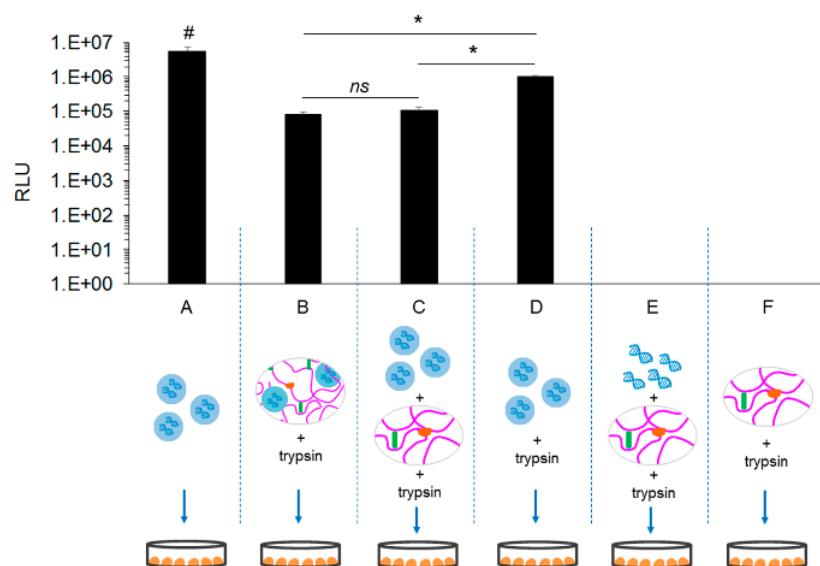


**Figure 5.** Biological activity of nioplexes based on concentrated niosome 1 at 2/1 cationic lipid/DNA mass ratio (w/w). **A.** Fresh nioplexes. **B.** Nioplexes released from degraded HA hydrogels with trypsin. **C.** Fresh nioplexes supplemented with degraded hydrogels with trypsin. **D.** Fresh nioplexes supplemented with trypsin. **E.** Naked DNA supplemented with degraded hydrogels trypsin. **F.** Hydrogels without nioplexes degraded with trypsin. \* $p < 0.05$  for transfection efficiency between different conditions, # $p < 0.05$  for transfection efficiency of all conditions relative to condition "A"

*Experimental section: Chapter 4*

Finally, gene delivery mediated by entrapped nioplexes was evaluated in hydrogels **1** (no nioplexes), **2** (0.055 µg DNA/ µl hydrogel) and **3** (0.12 µg DNA/ µl hydrogel). Two main mechanisms are postulated to contribute to the gene transfer process from hydrogel scaffolds: DNA/nanoparticle release kinetics and rate of cellular infiltration<sup>34</sup>. Nioplexes released after hydrogel degradation could transfect surrounding cells, while infiltrating cells would encounter entrapped nioplexes and become transfected leading to transgene expression inside the hydrogel area<sup>35, 36</sup>. As expected, in the present work the release kinetics of nioplexes were faster in the presence of Collagenase I (Col I), with almost 100% of nioplexes being released by day 7 in presence of Col I, compared to ~80% release by day 7 in PBS alone (Fig. 6A). This progressive release of nioplexes potentially allows for sustained transgene expression, which is essential for therapeutic applicability. Regarding cellular infiltration, for cells cultured in three dimensions, the migration rate of cells through the hydrogel has previously been related to successful non-viral gene transfer<sup>34</sup>. Therefore, we would expect that softer hydrogel scaffolds that allowed for extensive cell spreading would result in enhanced gene transfer. Interestingly, in the present work all hydrogels allowed for extensive cell spreading (Fig. 6C) and, despite its high stiffness, the 3D transfection efficiency was significantly ( $p < 0.05$ ) higher in hydrogel **3** compared to its softer counterparts (Fig. 6B, bars). Therefore, these results suggest that increasing amounts of DNA can be used to overcome limitations of stiffer hydrogels. Moreover, cell viability was excellent in all conditions (Fig. 6B, dots), which indicated that the presence of nioplexes in the HA hydrogels was well tolerated by the cells.

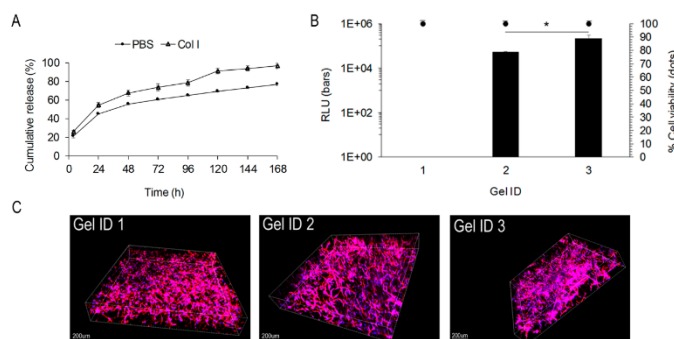


**Figure 6.** **A.** Nioplex release kinetics from HA hydrogels in PBS and in PBS supplemented with Collagenase I (1 U/ml). **B.** Transfection efficiency and cell viability of nioplex-loaded hydrogels **1-3** at 48 h. **C.** Representative images of cell spreading in hydrogels **1**, **2** and **3**. Blue = cell nuclei (DAPI) and red = F-actin (rhodamine-phalloidin). Scale bars: 200 µm. \* $p < 0.05$  for transfection efficiency.

## *Experimental section: Chapter 4*

### **Conclusions**

We successfully developed a process to load concentrated nioplexes into HA hydrogels without aggregation. To our knowledge, this is the first time that niosome formulations composed of 2,3-di(tetradecyloxy)propan-1-amine, Poloxamer 407, polysorbate 80 and chloroquine diphosphate salt are incorporated to HA hydrogels for non-viral gene delivery. In general, HA hydrogel scaffolds loaded with nioplexes presented suitable mechanical properties, little or no particle aggregation, allowed for extensive cell spreading and were able to efficiently transfect encapsulated mMSCs in 3D cultures. We believe that the knowledge gained through this *in vitro* model can be utilized to design novel and effective platforms for *in vivo* local and non-viral gene delivery applications.

### **Conflicts of interest**

There are no conflicts to declare.

### **Acknowledgements**

This project was supported by the Basque Country Government (Department of Education, University and Research, predoctoral grant PRE\_2016\_2\_0302 and Consolidated Groups, IT907-16) and by the Ikerbasque Foundation for Science from the Basque Country. Authors wish to thank the intellectual and technical assistance from the ICTS “NANBIOSIS”, more specifically by the Drug Formulation Unit (U10) of the CIBER in Bioengineering, Biomaterials and Nanomedicine (CIBER-BBN) at the University of the Basque Country (UPV/EHU). The authors thank for technical and human support provided by SGIker of UPV/EHU and European funding (ERDF and ESF). We thank the National Institutes of Health for funding R01HL110592 (TS). I.V.B. thanks the Basque Country Government for the granted fellowship.

### **References**

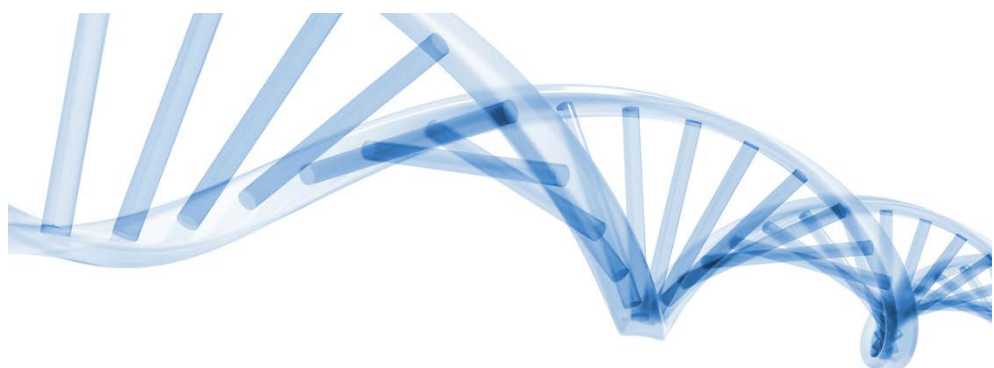
- 1 L. De Laporte and L.D. Shea, *Adv. Drug Deliv. Rev.*, 2007, **59**, 292-307.
- 2 M.D. Krebs, O. Jeon and E. Alsberg, *J. Am. Chem. Soc.*, 2009, **131**, 9204-9206.
- 3 Y. Lei, S. Huang, P. Sharif-Kashani, Y. Chen, P. Kavehpour and T. Segura, *Biomaterials*, 2010, **31**, 9106-9116.
- 4 L. Jin, X. Zeng, M. Liu, Y. Deng and N. He, *Theranostics*, 2014, **4**, 240–255.

*Experimental section: Chapter 4*

- 5 G. Puras, M. Mashal, J. Zárate, M. Agirre, E. Ojeda, S. Grijalvo, R. Eritja, A. Diaz-Tahoces, G. Martínez-Navarrete, M. Avilés- Trigueros, E. Fernández and J.L. Pedraz, *J. Control. Release*, 2014, **174**, 27-36.
- 6 E. Ojeda, G. Puras, M. Agirre, J. Zárate, S. Grijalvo, R. Eritja, G. Martínez- Navarrete, C. Soto-Sánchez, A. Diaz-Tahoces, M. Avilés-Trigueros, E. Fernández and J.L. Pedraz, *Biomaterials*, 2016, **77**, 267-279.
- 7 N. Grimaldi, F. Andrade, N. Segovia, L. Ferrer-Tasies, S. Sala, J. Veciana and N. Ventosa, *Chem. Soc. Rev.* 2016, **45**, 6520-6545.
- 8 P.P. Karmali and A. Chaudhuri, *Med. Res. Rev.*, 2007, **27**, 696-722.
- 9 A.P. Dabkowska, D.J. Barlow, R.A. Campbell, A.V. Hughes, P.J. Quinn and M.J. Lawrence, *Biomacromolecules*, 2012, **13**, 2391-2401.
- 10 F. Liu, J. Yang, L. Huang and D. Liu, *Pharm. Res.*, 1996, **13**, 1642-1646.
- 11 E. Ojeda, M. Agirre, I. Villate-Beitia, M. Mashal, G. Puras, J. Zárate and J.L. Pedraz, *Methods Mol. Biol.* 2016, **1445**, 63-75.
- 12 J.R. Fraser, T.C. Laurent and U.B. Laurent, *J. Int. Med.*, 1997, **242**, 27-33.
- 13 J.B. Leach, K.A. Bivens, C.W. Patrick and C.E. Schmidt, *Biotechnol. Bioeng.* 2003, **82**, 578-589.
- 14 P. Lei, R.M. Padmashali and S.T. Andreadis, *Biomaterials*, 2009, **30**, 3790- 3799.
- 15 J.M. Saul, M.P. Linnes, B.D. Ratner, C.M. Giachelli and S.H. Pun, *Biomaterials*, 2007, **28**, 4705-4716.
- 16 Y.G. Lei and T. Segura, *Biomaterials*, 2009, **30**, 254-265.
- 17 J.A. Wieland, T.L. Houchin-Ray and L.D. Shea, *J. Control. Release*, 2007, **120**, 233-241.
- 18 S. Grijalvo, A. Alagia, G. Puras, J. Zárate, J. Mayr, J.L. Pedraz, R. Eritja and D. Díaz Díaz, *J. Mat. Chem. B*, 2017, **5**, 7756-7767.
- 19 N.F. Truong and T. Segura, *ACS Biomater. Sci. Eng.*, 2018, **4**, 981-987.
- 20 N. Bhattacharai, J. Gunnand M. Zhang, *Adv. Drug Deliv. Rev.*, 2010, **62**, 83-99.
- 21 T. Tokatlian, C. Camb and T. Segura, *Biomaterials*, 2014, **35**, 825-835.
- 22 S. Taranejoo, R. Chandrasekaran, W. Cheng and K. Hourigan, *Carbohydr. Polym.*, 2016, **153**, 160-168.
- 23 S. Moghassemi and A. Hadjizadeh, *J. Control. Release*, 2014, **185**, 22-36.
- 24 M. Mashal, N. Attia, G. Puras, G. Martínez-Navarrete, E. Fernández and J.L. Pedraz, *J. Control. Release*, 2017, **254**, 55-64.
- 25 D. Monti, S. Burgalassi, M.S. Rossato, B. Albertini, N. Passerini, L. Rodriguez and P. Chetoni, *Int. J. Pharm.* 2010, **400**, 32-36.
- 26 C. Yang, T. Hu, H. Cao, L. Zhang, P. Zhou, G. He, X. Song, A. Tong, G. Guo, F. Yang, X. Zhang, Z. Qian, X. Qi, L. Zhou and Y. Zheng, *Mol. Pharm.*, 2015, **12**, 2167-2179.
- 27 H. Hosseinkhani and T. Tabata, *J. Nanosci. Nanotechnol.*, 2006, **6**, 2320– 2328.
- 28 O. Paecharoenchau, N. Niyomtham, T. Ngawhirunpat, T. Rojanarate, B.E. Yingyongnarongkul and P. Opanasopit, *J. Drug Target.*, 2012, **20**, 783–792.

*Experimental section: Chapter 4*

- 29 L. Li, H. Song, K. Luo, B. He, Y. Nie, Y. Yang, Y. Wu and Z. Gu, *Int. J. Pharm.*, 2011, **408**, 183-1890.
- 30 S. Kachi, Y. Oshima, N. Esumi, M. Kachi, B. Rogers, D.J. Zack and P.A. Campochiaro, *Gene Ther.*, 2005, **12**, 843–851.
- 31 E. Ojeda, G. Puras, M. Agirre, J. Zárate, S. Grijalvo, R. Pons, R. Eritja, G. Martínez-Navarrete, C. Soto-Sánchez, E. Fernández and J.L. Pedraz, *Org. Biomol. Chem.*, 2015, **13**, 1068-1081.
- 32 G. Caracciolo and H. Amenitsch, *Eur. Biophys. J.*, 2012, **41**, 815–829.
- 33 P. Moshayedi, L.R. Nih, I.L. Llorente, A.R. Berg, J. Cinkornpumin, W.E. Lowry, T Segura and S.T. Carmichael, *Biomaterials*, 2016, **105**, 145-155.
- 34 J.A. Shepard, A. Huang, A. Shikanov and L.D. Shea, *J. Control. Release*, 2010, **146**, 128–135.
- 35 Y. Lei, S. Gojgini, J. Lam and T. Segura, *Biomaterials*, 2011, **32**, 39–47.
- 36 S. Gojgini, T. Tokatlian and T. Segura, *Mol. Pharm.*, 2011, **8**, 1582-1591.



***Discussion***

***Eztabaida***

***Discusión***



## *Discussion*

Gene therapy can be broadly defined as the introduction of genetic material into target cells in order to modify and control protein expression for therapeutic or experimental purposes<sup>1</sup>. The culmination of the Human Genome Project along with recent advances on molecular biology have provided a better understanding of cellular and pathogenic processes, and several genes have been identified as targets for therapeutic approaches. However, even if gene therapy holds great promise for conceiving new treatments for several diseases, nucleic acid based strategies demand effective and safe carriers, which is the main limitation nowadays. In fact, one of the main reasons why gene therapy clinical trials are still few in number is the lack of suitable and safe approaches to deliver the genetic material to target cells. The success of gene therapy critically depends on suitable transfection vectors, which should be able to: (i) protect nucleic acids against degradation by blood and interstitial nucleases, (ii) promote internalization of the genetic material into target cells and (iii) release the nucleic acids once inside the cell to the correct site<sup>1</sup>. Furthermore, an ideal gene delivery system should be effective, specific, long lasting, safe, easy to use and as inexpensive as possible<sup>2</sup>.

Broadly, gene delivery vectors are mainly classified into two categories: viral vectors and non-viral vectors. According to data updated to June 2014 and presented by The Journal of Gene Medicine<sup>3</sup>, among the over 2,000 clinical trials for gene therapy approved globally, 70% correspond to trials using viral vectors. Moreover, to date only four gene-therapy products have been commercialized, all of them based on viral vectors. In 2003, China approved the first gene therapy product, Gendicine™, based on an adenoviral (Ad) vector and indicated for the treatment of head and neck squamous cell carcinoma<sup>4</sup>. China approved the second gene therapy product, Oncorine™, in 2005, which is also based on an Ad vector and is indicated for the treatment of late stage refractory nasopharyngeal cancer<sup>5</sup>. In Europe, the first approved gene therapy product was Glybera® in 2012, based on an adeno-associated viral (AAV) vector and indicated for the treatment of severe lipoprotein lipase deficiency<sup>6</sup>. In 2015, the gene therapy product IMLYGIC™ was approved in the USA, which is based on a herpes simplex virus (HSV) vector and is indicated for the local treatment of unresectable cutaneous, subcutaneous and nodal lesions in patients with melanoma recurrent after initial surgery<sup>7</sup>. However, according to data updated in 2017<sup>8</sup>, this tendency is inverted when focusing on studies involving delivery strategies for gene editing. Unlike traditional gene therapy methods mainly based in gene addition, in investigations involving gene-editing therapies non-viral vector-based studies are clearly predominant (70%) over viral vector-based studies. Among non-viral vectors used for gene editing, electroporation is the main approach

## *Discussion*

(39%), followed by methods based on lipids (17%) and polymers (8%)<sup>8</sup>. Therefore, it seems that the use of non-viral vector-based delivery systems are gaining importance over viral delivery systems in new gene therapy strategies based on gene edition or correction.

In fact, viruses are powerful tools to deliver genetic material into target cells, but they also present many impediments such as low carrying capacity, expensive and complex production and, most importantly, safety issues, since they usually induce immunogenic responses and they can induce oncogenesis when randomly integrated in the host genome. In this regard, nanotechnology-based non-viral vectors have emerged as promising alternatives due to their potential to overcome many of the limitations of viral vectors. Non-viral vectors present lower immunogenicity, higher nucleic acid packing capacity and ease of fabrication compared to their viral counterparts<sup>9</sup>. Additionally, non-viral formulations can be produced on a large scale with high reproducibility and acceptable costs, and they are relatively stable to storage<sup>1</sup>. Therefore, continuous advances in the fields of material science and nano-engineering have motivated the synthesis, characterization, and functionalization of biocompatible nanomaterials for gene delivery purposes<sup>10</sup>. In addition, the diversity of available nanosized material allows the design of multifunctional vectors specifically tailored for different applications<sup>11</sup>. To date, a wide variety of nanosized non-viral gene delivery vectors have been developed, including cationic lipids<sup>12-14</sup>, polymers<sup>15,16</sup> and magnetic nanoparticles<sup>17</sup>. These molecules can be nanoengineered to transport therapeutic genes into specific organs or cell types and to pass over several extracellular and intracellular barriers. Among the wide plethora of non-viral vectors, recently emerged niosomes are biocompatible, synthetic, non-ionic surfactant vesicles with a closed bilayer structure<sup>18,19</sup>. They are based on three principal components: (i) cationic lipids, which are responsible for the electrostatic interaction with the negatively charged DNA molecules, forming nioplexes<sup>20</sup>, (ii) helper lipids, to improve the physicochemical properties of the suspension<sup>21</sup> and (iii) non-ionic surfactants, which enhance the stability of the formulation and prevent particle aggregation<sup>22</sup>. The global chemical properties of these components influence on the physicochemical characteristics of niosomes, such as size, surface charge and morphology, which in turn determine their ability to enter the cells, follow a particular endocytic pathway, deliver the DNA cargo into the nucleus and, therefore, their transfection efficiency<sup>21,22</sup>. Recently, the potential of niosomes for gene therapy purposes has been demonstrated since it has been reported their capacity to transfet *in vivo* brain and retinal cells in rats<sup>23-26</sup>.

## *Discussion*

Not only the carrier is important, but also the vectored genetic material. Until recently, most efforts have focused on improving nucleic acid delivery strategies either by modifying non-viral vectors or by employing physical methods such as electroporation. Nevertheless, the enhancement of transfection efficiency can also be achieved by modifying the composition and conformation of the genetic material in order to improve its bioavailability, biocompatibility, durability and safety<sup>27</sup>. In this regard, recently a number of groups have produced minicircle DNA by removing the bacterial backbone from plasmid DNA in order to enhance the transfection efficiency<sup>28</sup>. Prokaryotic sequences present in plasmid DNA, such as CpG dinucleotide motifs, origins of replication, and antibiotic selectable markers are necessary to maintain and amplify these plasmids in bacterial hosts, but they decrease their biocompatibility and safety. In fact, several clinical studies have shown that unmethylated CpG motifs induce inflammatory responses<sup>29,30</sup> and necrosis- or apoptosis-mediated cell death in target cells, which in turn results in short-lived and compromised transgene expression<sup>31,32</sup>. Additionally, the sequences of plasmid DNA can also become inaccessible to transcription factors when bacterial sequences associated with histone indicators are close to the gene of interest. These indicators –which are rapidly recognized inside the cells-, induce the packing of the sequences into a dense heterochromatin structure, resulting in poor transgene expression or silencing of the gene of interest<sup>33</sup>. Therefore, minimized expression units that only contain the gene of interest and regulatory sequences such as minicircle (MC) DNA vectors emerge as an attractive alternative to conventional plasmid DNA vectors. Several *in vitro* and *in vivo* studies demonstrated a significant improvement of transfection efficiency with sustained and high transgene expression levels<sup>28</sup> as well as enhanced immunocompatibility and safety profiles. Furthermore, mini DNA vectors have also the potential to overcome many intracellular barriers, presenting higher bioavailability than their larger parent plasmid counterparts<sup>34</sup>.

In addition to the optimization of the carrier and the genetic material, a new trend in non-viral gene therapy is to explore novel complementary synergies between delivery systems and tissue-engineered scaffolds in order to improve the transfection efficiency. In fact, these combined approaches may offer relevant advantages such as enhanced stability and reduced toxicity. Moreover, complementing gene transfer with matrix design would allow an effective, targeted and local DNA delivery, which would enhance the applicability of gene therapy in many therapeutic fields, such as tissue regeneration and cancer<sup>35,36</sup>.

## *Discussion*

Therefore, this doctoral thesis focuses on the development of effective non-viral gene delivery platforms and, for that purpose, the scope of the project includes the following aspects: (i) preparation, characterization and comparative evaluation of the transfection efficiency of three different non-viral vectors based on cationic lipids, polymers and magnetic nanoparticles to deliver a therapeutic plasmid coding for the vascular endothelial growth factor (VEGF) to central nervous system (CNS) cells; (ii) preparation, characterization and evaluation of the transfection process and efficiency of three niosome formulations that only differed on the non-ionic tensioactives component, in order to determine its role in the gene transfer process; (iii) preparation and characterization of niosome formulation and comparative evaluation of the transfection efficiency and cell viability of nioplexes bound to two different genetic materials, a plasmid DNA and a minicircle (MC) DNA; and (iv) exploration of complementary synergies for non-viral gene therapy between niosome formulations and hyaluronic acid (HA) hydrogel scaffolds. In the following sections, each of those studies will be discussed in detail.

**1. The influence of the components of the non-viral vector in the transfection efficiency of a therapeutic plasmid encoding for the vascular endothelial growth factor in cells of the central nervous system.**

Nucleic acid based therapies hold great promise but demand effective and safe carriers. Moreover, efficient transfection of CNS is still a challenge, which retards the development of therapeutic gene delivery strategies for the wide variety of neurodegenerative disorders. In recent years, biocompatible nanomaterials have emerged as potential candidates for that purpose. In fact, different nanosized non-viral vectors have been recently reported to efficiently transfect CNS cells *in vitro* and *in vivo*, such as chitosans<sup>37,38</sup>, cationic lipids<sup>39</sup> and magnetic nanoparticles<sup>17</sup>. Besides, VEGF may be a potential therapeutic gene candidate for CNS disorders<sup>40</sup>, due to the strong relationship between vascular alterations in brain and neurodegenerative diseases<sup>41</sup> and its specific roles in brain angiogenesis and neuronal survival<sup>42,43</sup>.

Based on these considerations, we present a nanoformulation based approach for VEGF gene delivery into CNS cells. For that purpose, three different nanoformulations –ultrapure oligochitosan (UOC), Lipofectamine cationic lipid and NeuroMag magnetic nanoparticles– were complexed to the phVEGFI65aIRESGFP plasmid, which codifies for the human VEGF165a protein and for the green

## *Discussion*

fluorescent protein (GFP). Nanoformulations and resulting nanoplexes – nanoformulations complexed to DNA– were physicochemically characterized in terms of size, superficial charge, polydispersity index (PDI), morphology and capacity to condense, release and protect DNA. *In vitro* transfection studies were carried out in C6 glial cells and in primary neuronal culture cells as CNS cell models, and in HEK293 cells, as a general transfection model. Transfection efficiencies were evaluated in terms of percentage of GFP expressing cells, mean fluorescent intensity (MFI) and VEGF protein expression. Cell viability upon exposition to nanoplexes was also evaluated. Bioactivity of the VEGF protein secreted by transfected primary neuronal culture cells was assessed by a proliferation assay in human umbilical vein endothelial cells (HUVEC).

All nanoformulations and corresponding nanoplexes –magnetoplexes, lipoplexes and polyplexes- presented particle sizes in the nanoscale range (Fig. 1.1.a, bars), which is related to higher cellular uptake values<sup>44</sup>, and exhibited positive surface charge values (Fig. 1.1.a, lines), which is necessary to bind to the negatively charged DNA molecules by electrostatic interactions<sup>45</sup>. Once complexed to DNA, surface charge switched to negative values in all cases. However, magnetoplexes and lipoplexes surface charge values changed from around +20 mV to around -20 mV, whereas polyplexes presented zeta potential values near the zero. It has been described that particles with surface charge values between -20mV and +20 mV form aggregates along the time<sup>46</sup>. Therefore, to avoid aggregation, particularly in the case of polyplexes, all formulations employed in this work were used freshly prepared. PDI values were almost in all cases below 0.5, which is considered acceptable for comparative purposes of nanoparticles sizes measured by cumulative analysis<sup>47</sup>. The exception was cationic lipids, where high PDI values could be attributed to the irregular morphology of these particles (Fig. 1.1.c). In order to further analyze the ability of nanoparticles to bind, release and protect DNA, an agarose gel electrophoresis assay was performed (Fig.1.1.d). Nanoparticles protected DNA from enzymatic degradation, but most of the plasmid was retained in the well, suggesting strong binding to DNA. However, all formulations showed a delicate balance between DNA binding and releasing abilities, necessary for efficient transfection mediated by non-viral vectors<sup>48</sup>.

## Discussion

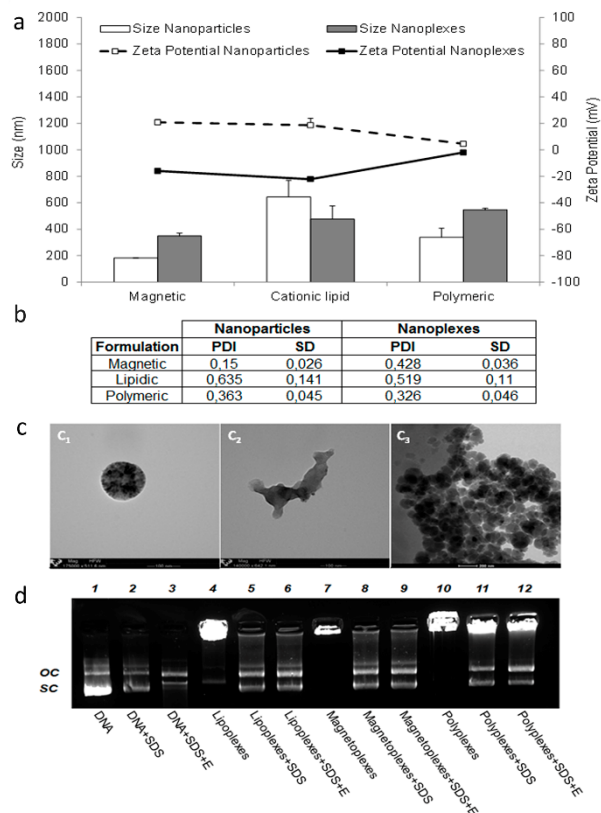
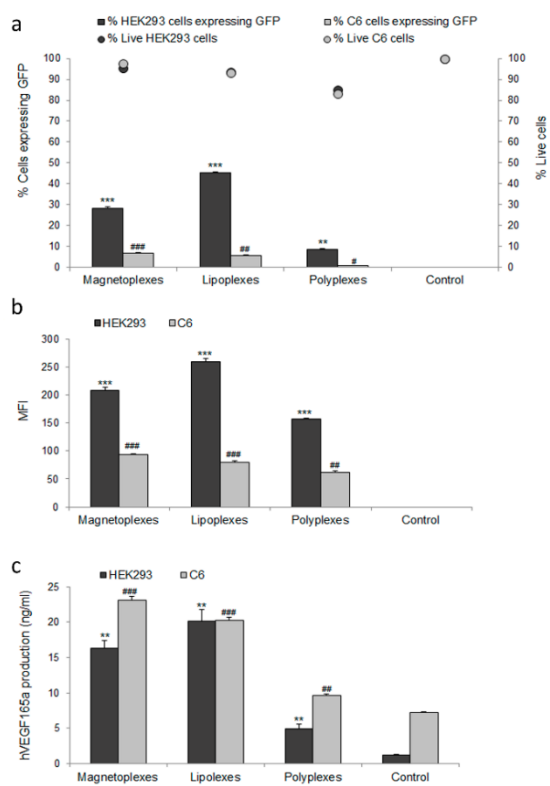


**Figure 1.1.** Physicochemical characterization of nanoparticles and nanoplexes. (a) Size (white and grey bars, which correspond to nanoparticles and nanoplexes, respectively) and zeta potential values (dotted and continuous lines, which correspond to nanoparticles and nanoplexes, respectively). Each value represents the mean  $\pm$  SD, n=3. (b) PDI values. Each value represents the mean  $\pm$  SD, n=3. (c) TEM images of cationic lipid (c<sub>1</sub>) and magnetic (c<sub>2</sub>) nanoparticles and Cryo-TEM images of polymeric (c<sub>3</sub>) nanoparticles. Original magnification 140,000x for cationic lipid nanoparticles, 175,000x for magnetic nanoparticles and 25,000x for polymeric nanoparticles. (d) Binding, protection, and SDS-induced release of DNA from nanoparticles visualized by agarose electrophoresis. Lanes 1–3 correspond to free DNA; lanes 4–6, lipoplexes; lanes 7–9, magnetoplexes; lanes 10–12, polyplexes. Free DNA and nanoplexes were treated with SDS (lanes 2, 5, 8 and 11) and DNase I + SDS (lanes 3, 6, 9, and 12). OC: open circular form, SC: supercoiled form.

## *Discussion*

Once nanoplexes were physicochemically characterized, *in vitro* studies were carried out in three cell lines: HEK293 –a general transfection model-, C6 cells –a CNS transfection model- and primary neuronal culture cells –the most relevant cellular model of CNS-. Before performing assays in primary neuronal culture cells, we analyzed cell viability and transfection efficiency of the nanoplexes in HEK293 and in C6 cells, due to the challenge that represents primary neuronal culture cells transfection with non-viral vectors. Nanoplexes were well tolerated by both cell types, since cell viability was above 90% with magnetoplexes and lipoplexes and above 80% with polyplexes (Fig. 1.2.a, dots). The analysis of transfection efficiency was studied through three different parameters: percentage of GFP expressing cells (Fig. 2a, bars), MFI of those transfected cells (Fig. 1.2b) and the amount of VEGF (ng/ml) secreted by transfected cells (Fig. 1.2.c). The phVEGF165aIRESGFP plasmid codifies for both proteins, VEGF –which is extracellular and, therefore, secreted to the extracellular medium by transfected cells- and GFP –which is intracellular and remains in the cytoplasm of transfected cells-. Therefore, parameters related to GFP were analyzed by flow citometry, while the concentration of VEGF present in cellular supernatants was measured by ELISA. Regarding percentages of GFP expressing cells and MFI values, transfection efficiencies with all nanoplexes were higher in HEK293 cells compared to C6 cells. However, regarding expression of VEGF (ng/ml), comparable values were obtained in HEK293 and C6 cells 48 h after transfection with nanoplexes. Indeed, when transfecting with magnetoplexes, the amounts of secreted VEGF were higher in the supernatant of C6 cells compared to HEK293 cells. It has been reported that non-viral vector mediated transfection processes are cell-dependent, meaning that the transfection efficiency of the same non-viral vector can diverge depending on the transfected cell type<sup>49</sup>. Our results are consistent with this idea, since we found that in HEK293 cells highest transfection was achieved with lipoplexes, while in C6 cells magnetoplexes were more efficient. Polyplexes are in the third position in both cell lines, probably due to their surface charge values near zero, which may affect cellular uptake.

## Discussion



transfection with nanoplexes (HEK293 cells, dark grey bars; C6 cells, light grey bars). Control cells were not treated with nanoplexes. Each value represents the mean  $\pm$ SD, n=3. Statistical significance: \*p<0.05, \*\*p<0.01, \*\*\*p<0.001 compared to control HEK293 cells; #p<0.05, ##p<0.01, ###p<0.001 compared to control C6 cells.

Interestingly, a clear correlation was observed in both cell lines between the three parameters used to analyze transfection efficiencies. At higher percentages of GFP expressing cells, higher levels of secreted VEGF were detected (Fig. 1.3.a and Fig. 1.4.a). Also, at higher MFI values, higher levels of secreted VEGF were observed (Fig. 1.3.b and Fig. 1.4.b). However, when comparing the angles of the slope in those graphs, differences were detected between cell lines, since the gradients were more pronounced in C6 than in HEK293 cells in both correlations –in Figs. 1.3.a and 1.4.a,  $\alpha=22.65^\circ$  in HEK293 vs.  $\alpha=65.42^\circ$  in C6; in Figs. 1.3.b and 1.4.b,  $\alpha=8.42^\circ$  in HEK293 and  $\alpha=23.67^\circ$  in C6 . These data support the fact that although GFP expression and MFI values were lower in C6, VEGF expression levels were comparable in both cell

**Figure 1.2.** Cell viability and transfection efficiencies in HEK293 and C6 cells. (a) Cell viability (HEK293 cells, dark grey dots; C6 cells, light grey dots) 48h after transfection with magnetoplexes, lipoplexes and polyplexes. Control cells were not treated with nanoplexes. Percentages of GFP expressing cells (HEK293 cells, dark grey bars; C6 cells, light grey bars) 48 h after transfection with nanoplexes. Control cells were not treated with nanoplexes. Each value represents the mean  $\pm$ SD, n=3. (b) Mean Fluorescent Intensity (MFI) values 48h post-transfection with nanoplexes (HEK293 cells, dark grey bars; C6 cells, light grey bars). Each value represents the mean  $\pm$ SD, n=3. (c) VEGF production (ng/ml) values 48h post-

## Discussion

lines transfected with nanoplexes. This effect could in part be explained by the higher basal expression of VEGF protein in C6 cells (Fig. 1.2.c, control bars). Therefore, even at lower transfection efficiencies, transfected C6 cells could be able to secret as much VEGF protein as the more efficiently transfected HEK293 cells. Still, the big differences observed suggest that other factors may also be involved, specifically those related to the Internal Ribosome Entry Site (IRES) sequence of the plasmid. IRES sequences are translational enhancers that allow the co-expression of two genes of interest under the same promoter and with a constant ratio of the proteins<sup>50,51</sup>. However, it has been described that cellular IRES often exhibit low efficiencies in transiently transfected cells, which has been attributed to the cell and tissue specificity of the cellular IRES activities<sup>52,53</sup>. In those cases, the expression of the gene downstream of the IRES element is usually lower, while the expression of the gene upstream the IRES sequence is not affected<sup>54</sup>. In our scenario, the VEGF gene is located upstream the IRES element in the phVEGF165aIRESGFP plasmid, and the GFP gene is located downstream that sequence. Therefore, we hypothesized that the IRES sequence of the phVEGF165aIRESGFP plasmid may be working less efficiently in neural cells such as the C6 cell line, and that consequently, the expression of the GFP gene could be affected in those cells, while the VEGF gene is normally expressed.

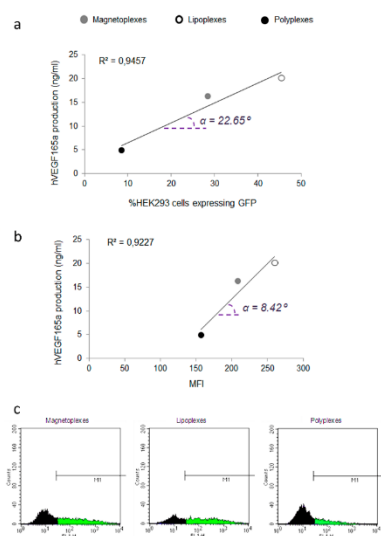


**Figure 1.3.** Correlations between the transfection efficiency parameters in HEK293 cells. (a) Correlation between VEGF production (ng/ml) and percentage of GFP expressing live cells in HEK293 cells 48h post-transfection with magnetoplexes (grey dot), lipoplexes (white dot) and polyplexes (black dot). Each value represents the mean  $\pm$  SD, n=3.  $\alpha$  represents the angle of the slope. (b) Correlation between VEGF production (ng/ml) and MFI values in HEK293 cells 48h post-transfection with nanoplexes. Each value represents the mean  $\pm$  SD, n=3.  $\alpha$  represents the angle of the slope. (c) GFP histograms of HEK293 cells 48h post-transfection with nanoplexes. M1 represents the threshold for GFP positive signal.

## Discussion

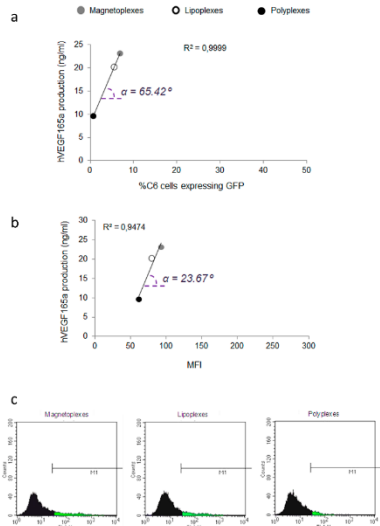


**Figure 1.4.** Correlations between the transfection efficiency parameters in C6 cells. (a) Correlation between VEGF production (ng/ml) and percentage of GFP expressing live cells in C6 cells 48h post-transfection with magnetoplexes (grey dot), lipoplexes (white dot) and polyplexes (black dot). Each value represents the mean  $\pm$ SD, n=3.  $\alpha$  represents the angle of the slope. (b) Correlation between VEGF production (ng/ml) and MFI values in C6 cells 48h post-transfection with nanoplexes. Each value represents the mean  $\pm$ SD, n=3.  $\alpha$  represents the angle of the slope. (c) GFP histograms of C6 cells 48h post-transfection with nanoplexes. M1 represents the threshold for GFP positive signal.

Once the capacity of nanoplexes to transfect HEK293 and C6 cells was analyzed, we performed transfection assays in primary neuronal culture cells, which represent a more challenging scenario for non-viral gene delivery. Cell viabilities (Fig. 1.5.a.) were excellent in this case –near 100% with all nanoplexes-, but transfection efficiencies (Fig. 1.5.a-b) were lower than in the previous cell lines, due to the difficulty of transfecting neuronal cells. GFP expression was only detectable by immunocitochemistry assay –Fig. 1.5.b shows a few scattered fluorescent cells-. This supports the hypothesis of the tissue specificity of the IRES element in the phVEGF165aIRESGFP plasmid. Regarding VEGF expression, we found that these cells presented a high basal production of VEGF, probably due to the glial cells present in the primary culture, which secret angiogenic<sup>55</sup> and neurotrophic<sup>56</sup> factors to support the CNS cells. However, after transfection with nanoplexes, levels of secreted VEGF increased respect to the control in all cases, although statistically significant differences were only found in magnetoplexes transfected cells (Fig. 1.5.c). Next, we analyzed the bioactivity of transfected cells secreted VEGF in HUVEC cells, since these cells are known to respond with increased proliferation to the effect of VEGF<sup>57,58</sup>. Compared to the proliferation control group –HUVEC cells not treated with VEGF-, HUVEC cells exposed to VEGF secreted by primary neuronal culture cells transfected with nanoplexes presented a statistically significant increase in proliferation, which validates that VEGF induced HUVEC cell

## Discussion

proliferation. Furthermore, the increase of proliferation in HUVEC cells was proportional to the increase of VEGF production in primary neuronal culture cells, magnetoplexes obtaining the highest levels of VEGF expression in primary neuronal culture cells and their supernatants achieving the highest levels of proliferation in HUVEC cells, followed in both cases by polyplexes and, finally, lipoplexes. It is remarkable that magnetoplexes transfected CNS cell models more efficiently than their counterparts and that, unexpectedly, polyplexes were more efficient than lipoplexes in primary neuronal culture cells.

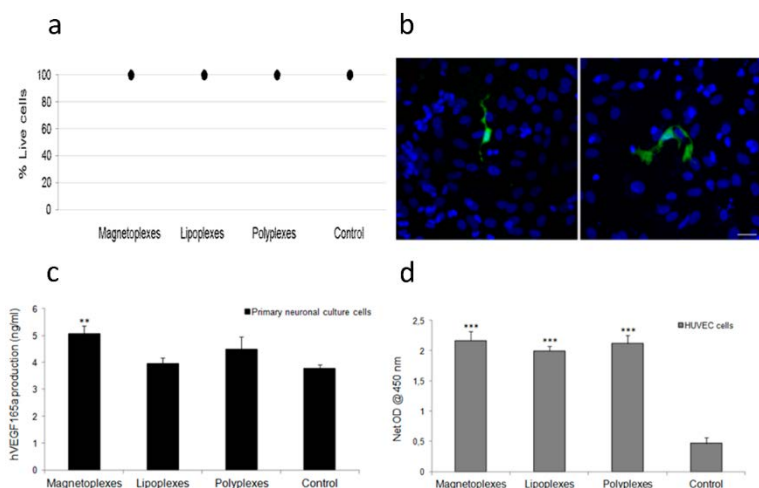


**Figure 1.5.** Primary neuronal culture cells viability, efficiencies of transfection with nanoplexes in those cells and bioactivity of VEGF protein secreted by the transfected cells. (a) Cell viability in primary neuronal culture cells 48h post-transfection with nanoplexes. Each value represents the mean  $\pm$  SD, n=3. (b) Immunocitochemistry images of transfected primary neuronal culture cells. Green, Anti-GFP. Blue, Hoechst. Scale: 25  $\mu$ m. (c) VEGF production (ng/ml) by primary neuronal culture cells 48h after transfection with nanoplexes. Control cells were not treated with nanoplexes. Each value represents the mean  $\pm$  SD, n=3. (d) HUVEC cell proliferation in response to VEGF secreted by primary neuronal culture cells transfected with nanoplexes. Control HUVEC cells were not treated with VEGF. Each value represents the mean  $\pm$  SD, n=6. Statistical significance: \* $p$ <0.05, \*\* $p$ <0.01, \*\*\* $p$ <0.001 compared to control HUVEC cells.

## *Discussion*

Considering these results, non-viral vectors and, in particular, magnetoplexes might constitute a promising approach to deliver the VEGF gene into CNS cells in a safe and controlled way, which is consistent with previous reports<sup>17</sup>. Strong relationships described between vascular alterations and neurodegeneration<sup>40</sup>, along with reported beneficial effects of VEGF protein in animal models of neurodegenerative diseases such as AD<sup>59</sup> and Parkinson's Disease<sup>67</sup>, suggest that VEGF may be a potential therapeutic candidate for CNS disorders. Besides, compared to drug delivery, VEGF gene delivery would demand fewer doses and would allow long-lasting effects. To date, administration of non-viral vectors to SNC is still a challenge for the scientific community, principally due to the invasive nature of the currently available approaches to target the brain, including craniotomy. A recent study has shown that intranasally administered plasmid DNA nanoparticles circumvented the BBB to target the CNS and have successfully transfected rat brain<sup>60</sup>. Therefore, the intranasal route, a safer and non-invasive alternative, merits special attention for non-viral gene delivery into the CNS.

### **2. The role of the non-ionic tensioactive component of niosome formulations in the transfection process and efficiency in rat retina**

Several monogenic retinal disorders are well characterized, with identified mutations that most often affect specific genes in retinal pigment epithelium (RPE) cells<sup>61</sup>. RPE cells perform pivotal functions required for the maintenance of the neural retina, such as protecting the photoreceptor cells and secreting growth factors<sup>62</sup>. In many retinal diseases, including Leber's congenital amaurosis (LCA), retinitis pigmentosa (RP) and age-related macular degeneration (AMD) blindness occurs due to RPE degeneration, which results in photoreceptor loss or dysfunction<sup>61</sup>. Therefore, RPE cells constitute the main target of most ocular gene therapy strategies, and the success of retinal gene transfer strategies depends on the ability to achieve persistent and high levels of transgene expression in RPE cells, ideally from a single administration.

Non-viral gene delivery offers reasonable hope to transfer specific therapeutic genes into the eye. Niosomes have been effectively used for gene delivery to retinal cells both *in vitro* and *in vivo*, and the effect of cationic lipids and helper lipids has been well studied in transfection processes mediated by those formulations<sup>26,63</sup>. To date, niosome formulations containing the cationic lipid DOTMA<sup>18</sup> or the non-ionic surfactant polysorbate 80 combined with the helper lipid squalene<sup>26</sup> have shown

## Discussion

effective gene delivery to the retina. However, the use of other non-ionic surfactants with different chemical properties such as polysorbate 20 and polysorbate 85 for retinal gene transfer has not been explored. Therefore, in this work we elaborated and characterized, in terms of physicochemical properties and transfection efficiency into retinal cells, three niosome formulations that only differed in their non-ionic tensioactives. These niosomes named DST20, DST80 and DST85 were based on the cationic lipid DOTMA, combined with squalene as helper lipid and polysorbates 20, 80 or 85 as non-ionic surfactants.

Non-ionic tensioactives in niosome formulations act as emulsifiers creating a steric barrier that avoids aggregation<sup>22</sup>. Polysorbates 20 and 85 share the same chemical root structure as polysorbate 80, but the three molecules differ in their hydrophyilic parts and number of hydroxyl groups, therefore presenting different (HLB) values (Figure 2.1.). The HLB parameter determines the oil (HLB < 9) or water (HLB > 11) solubility of the non-ionic surfactants<sup>64</sup>. Among the three non-ionic surfactants tested, polysorbate 20 is the most hydrophilic, due to the presence of 2 hydroxyl groups and a lauric acid, with a HLB value of 16.7. Polysorbate 80 is next with HLB = 15 and polysorbate 85 is the less hydrophilic of the three non-ionic surfactants, due to the presence of three oleic acids in its chemical structure, with a HLB value of 11.

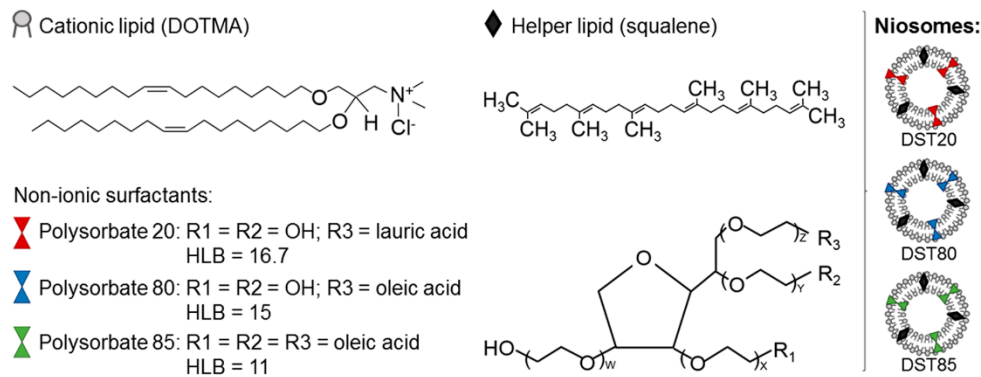


**Figure 2.1.** General scheme of niosomes and chemical structures of niosome components.

### *Discussion*

The physicochemical parameters of formulations are key factors that determine transfection efficiency. DST20, DST80 and DST85 niosomes revealed mean particle sizes between 100 nm and 225 nm (Fig. 2.2.A, bars), suitable for gene delivery purposes<sup>65</sup>. Little oscillations in particle sizes upon the addition of plasmid DNA at cationic lipid/DNA ratios 2/1, 5/1 and 10/1 were probably due to the balance between the larger space demanded by the lipid and the higher DNA condensation when increasing mass ratios<sup>26</sup>. In all conditions, formulations showed narrow size distributions as indicated by the low PDI values (Fig. 2.2.B). The surface charge of the formulations has an impact on their stability, and zeta potential values under -30 mV and over +30 mV avoid particle aggregation<sup>46</sup>. In addition, positive zeta potential values promote electrostatic interactions with negatively charged DNA to form nioplexes<sup>45</sup>. The three niosome formulations presented suitable zeta potential values over +40 mV (Fig. 2.2.A, dots). As expected, at low cationic lipid/DNA mass ratios surface charge values of nioplexes clearly declined, demonstrating that the amine groups of the niosomes electrostatically interacted with the phosphate groups of the DNA resulting in partial neutralization of surface charges<sup>66</sup>. In order to determine the morphology of our formulations, niosomes were examined under a TEM microscope at different magnifications, corroborating that all formulations presented a clear spherical shape (Fig. 2.2.C-E). The ability of nioplexes to protect and release plasmid DNA at different cationic lipid/DNA mass ratios was evaluated by a gel retardation assay. We found that all formulations were able to protect plasmid DNA even at the lowest cationic lipid/DNA mass ratio 2/1 (Fig. 2.2.F). The exception were DST80 nioplexes, which showed higher ability to protect DNA at higher cationic lipid/DNA mass ratios. However, since our purpose was to develop efficient niosome formulations for retinal gene delivery *in vivo*, in all formulations we selected the lowest cationic lipid/DNA mass ratio for posterior transfection assays, which allows increasing the amount of DNA to administer *in vivo* and reduces cellular toxicity associated to cationic lipids<sup>67</sup>.

## Discussion

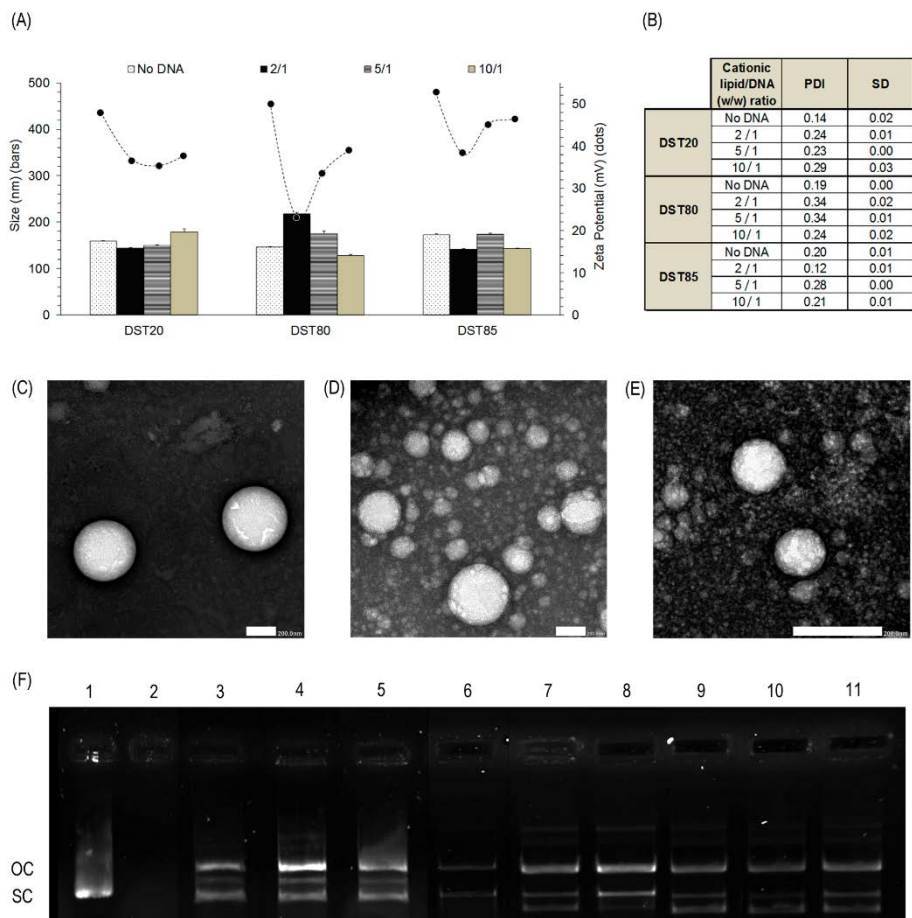


**Figure 2.2.** Physicochemical characterization of DST20, DST80 and DST85 niosomes and their corresponding nioplexes at cationic lipid/DNA (w/w) ratios 2/1, 5/1 and 10/1. **(A)**. Size values are represented with bars and zeta potential values with dots. Each value represents the mean  $\pm$  SD, n=3. **(B)**. PDI values. Each value represents the mean  $\pm$  SD, n=3. **(C-E)**. TEM images of niosomes. Scale bars: 200.0 nm. **(C)** DST20 niosomes at 20,000x magnification, **(D)** DST80 niosomes at 20,000x magnification and **(E)** DST85 niosomes at 40,000x magnification. **(F)**. Agarose gel electrophoresis assay for analyzing the ability of DST20, DST80 and DST85 nioplexes at different cationic lipid/DNA (w/w) ratios to protect the pCMS-EGFP plasmid. DNase I enzyme and SDS were added in lanes 2-11. Lanes 1-2 correspond to naked DNA. Lanes 3, 4 and 5 correspond to DST20 nioplexes at cationic lipid/DNA mass ratios 2/1, 5/1 and 10/1, respectively. Lanes 6, 7 and 8 correspond to DST80 nioplexes at cationic lipid/DNA mass ratios 2/1, 5/1 and 10/1, respectively. Lanes 9, 10 and 11 correspond to DST85 nioplexes at cationic lipid/DNA mass ratios 2/1, 5/1 and 10/1, respectively. OC and SC are indicated on the left.

## *Discussion*

cationic lipid/DNA mass ratios 2/1, 5/1 and 10/1, respectively. Lanes 9, 10 and 11 correspond to DST85 nioplexes at cationic lipid/DNA mass ratios 2/1, 5/1 and 10/1, respectively. OC: open circular form, SC: supercoiled form.

---

Once the formulations were fully characterized, we performed *in vitro* transfection studies at cationic lipid/DNA mass ratio 2/1 in the well-known transfection model HEK-293 cell line and with the retinal model ARPE-19 cell line in accordance to the aim of our study. In both cell lines, nioplexes showed excellent cell viabilities above 95% in HEK-293 and above 85% in ARPE-19, demonstrating that they were well tolerated by both types of cells. This was further confirmed by the healthy appearance of HEK-293 and ARPE-19 under the microscope 48 h after transfection (Fig. 2.3.A<sub>2</sub> and 3B<sub>2</sub>). In contrast, transfection positive control Lipofectamine 2000™ showed lower cell viability values than nioplexes in both cells, around 90% in HEK-293 cells and around 55% in ARPE-19 cells, which in accordance with previous reports<sup>26</sup>, indicates that in retinal cells nioplexes are much better tolerated. In fact, Lipofectamine 2000™ is not considered suitable for retinal gene delivery due to its high toxicity to photoreceptor cells even at low concentrations<sup>68</sup>. Regarding transfection efficiency, we found that DST85 niosomes were the most efficient transfecting HEK-293 cells (Fig. 2.3.A<sub>1</sub>), while DST20 nioplexes showed the highest transfection values in ARPE-19 cells (Fig. 2.3.B<sub>1</sub>). It is generally accepted that non-ionic surfactants with low HLB values and high liposolubility enhance the cellular uptake of the formulations<sup>69,70</sup>. This is consistent with results in HEK-293 cells, since polysorbate 85 presents the lowest HLB value among the three non-ionic surfactants tested. Interestingly, in ARPE-19 cells, polysorbate 20 containing niosomes seemed to be the most efficient for gene transfer. As previously mentioned, polysorbate 20 has the highest HLB value and therefore, the lowest lipophilicity. All together suggests that other cell-dependent mechanisms such as the cell internalization mechanisms and endocytic pathways could explain the higher efficiency of DST20 nioplexes to transfect retinal cells.

## Discussion

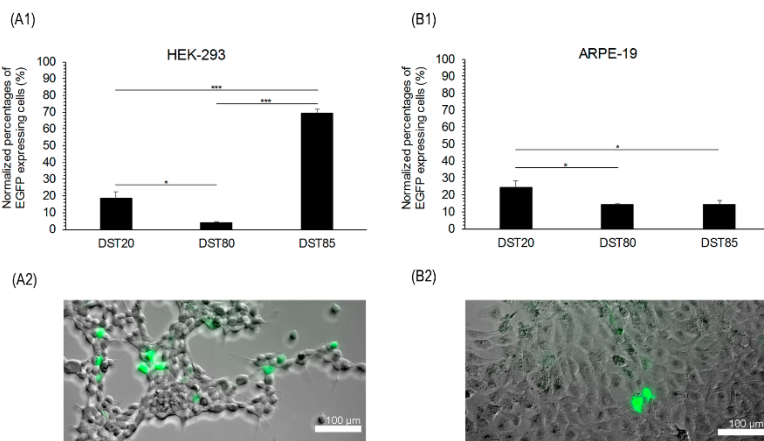


**Figure 2.3.** Transfection efficiency and cell viability assay in HEK-293 and ARPE-19 cells 48 h post-addition of DST20, DST80 and DST85 nioplexes vectoring the pCMS-EGFP plasmid at cationic lipid/DNA mass ratio 2/1. **(A<sub>1</sub>)**. Normalized percentages of EGFP expressing HEK-293 cells evaluated by flow cytometry. Each value represents the mean  $\pm$  SD, n = 3. Statistical significance: \*  $p < 0.05$ , \*\* $p < 0.01$ , \*\*\* $p < 0.001$ . **(A<sub>2</sub>)**. Representative fluorescence microscope image of EGFP expression in HEK-293 cells transfected with DST85 nioplexes captured at 20x magnification. Scale bar: 100  $\mu$ m. **(B<sub>1</sub>)**. Normalized percentages of EGFP expressing ARPE-19 cells evaluated by flow cytometry. Each value represents the mean  $\pm$  SD, n = 3. Statistical significance: \*  $p < 0.05$ , \*\* $p < 0.01$ , \*\*\* $p < 0.001$ . **(B<sub>2</sub>)**. Representative fluorescence microscope image of EGFP expression in ARPE-19 cells transfected with DST20 nioplexes captured at 20x magnification. Scale bar: 100  $\mu$ m.

In this regard, in order to further understand the transfection process with DST20, DST80 and DST85 nioplexes in ARPE-19 cells, we analyzed the cell entry mechanisms and intracellular trafficking pathways followed by the formulations. Non-viral vectors usually enter the cells via endocytosis, being CME and CvME the most common and well-studied endocytic pathways<sup>71</sup>. The CvME route has been generally considered a non-acidic and non-digestive endocytic pathway<sup>72</sup>, while the CME pathway is believed to integrate the endocytosed vesicles into late endosomes, which then deliver their cargos to lysosomes<sup>73</sup>. However, controversial data exist in this regard, since it has also been described that caveosomes can join the classical endocytic pathway, eventually fusing with lysosomes<sup>74,75</sup>. In addition, the acid pH in lysosomes is believed to cause the dissociation of the DNA from the non-viral vector<sup>76</sup> which, according to some authors, facilitates the cytosolic release of nanoparticles and enhances the nuclear entry of DNA<sup>77</sup>. Nevertheless, other studies

## Discussion

reported that in absence of endosomal escape mechanisms, the acid environment and the enzymatic activity of lysosomes causes the degradation of nioplexes, impeding the access of DNA molecules into the nucleus<sup>78</sup>. In our study, we found that when nioplexes entered predominantly through CME, which was the case of DST85 nioplexes, they also co-localized with late endosome lysosomal compartments which apparently resulted in a lower transfection efficiency (Figure 2.4.). In contrast, when nioplexes entered through CvME, as in the case of DST20 nioplexes, they seemed to avoid late endosomes and transfection efficiency increased. Therefore, our results are in accordance with the lysosomal degradation hypothesis upon CME-mediated cell entry, which in turn would explain the higher transfection efficiency of DST20 nioplexes in ARPE-19 cells. DST80 nioplexes showed very low co-localization values in ARPE-19 cells with both CME and CvME pathways, which might be explained by the presence of other cellular internalization pathways. In fact, a recent study reported that niosomes based on polysorbate 80, squalene and 1-(2-dimethylaminoethyl)-3-[2,3-di(tetradecyloxy) propyl] urea showed higher tendency to enter the cells through macropinocytosis than through CME or CvME<sup>13</sup>.

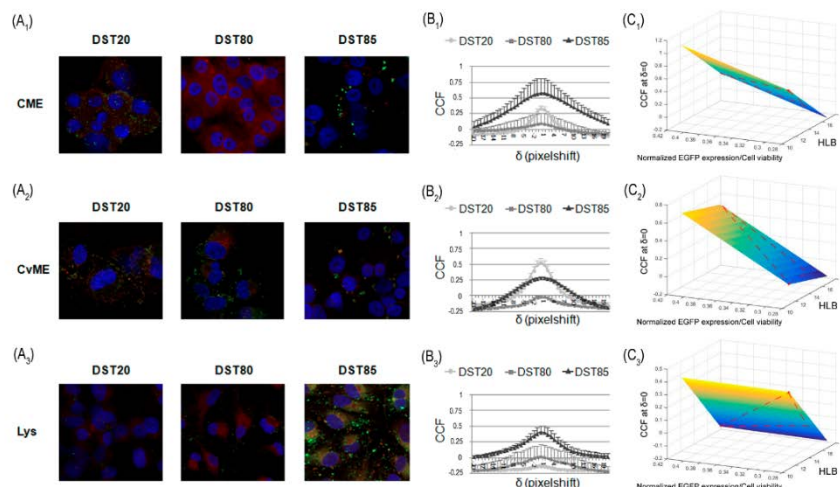


**Figure 2.4.** Endocytic and intracellular trafficking pathways detection assay of DST20, DST80 and DST85 nioplexes in ARPE-19 cells. **(A<sub>1-3</sub>)** Confocal microscopy merged images showing ARPE-19 cells co-incubated with nioplexes containing the FITC-labeled pCMS-EGFP plasmid (green) and with the endocytic vesicle marker (red): AlexaFluor546-Transferrin for CME, AlexaFluor555-Cholera toxin B for CvME and Lysotracker (Lys) for late endosomal compartment. **(B<sub>1-3</sub>)** Co-localization values of red and green signals determined by cross-

## *Discussion*

correlation analysis in each case. Data are represented as mean  $\pm$  SEM, n=3. (**C<sub>1-3</sub>**). 3D plots relating HLB values and the corresponding transfection efficiency and co-localization with intracellular pathways CME (**C<sub>1</sub>**), CvME (**C<sub>2</sub>**) and late endosomes (**C<sub>3</sub>**).

---

Based on these results, we selected the formulation DST20 for retinal gene delivery. Before moving on to *in vivo* assays, we performed a preliminary *in vitro* transfection assay in a primary culture of rat retinal cells with DST20 nioplexes, and we observed effective transgene expression (Figure 2.5.). Encouraged by those findings, we carried out an *in vivo* study to assess whether the DST20 nioplexes were able to transfet the rat retinas after SR (Fig. 2.6.B-C) and IV injections (Fig. 2.6.D-E). In most cases, efficient transfection of ganglion cells of the retina can be achieved by IV injections, whereas transfecting cells in the outer retina, such as photoreceptor and the RPE, requires the more invasive SR injection<sup>68,79</sup>. In accordance, our results show that IV administration of DST20 nioplexes was successful to transfet predominantly ganglion cells of the retina (Figure 2.6.D), while with SR administration efficient transgene expression was observed in the inner layers of the retina, with clear diffusion to the outer layers including RPE cells (Figure 2.6.B). Considering that many blinding diseases are associated to mutations in specific genes of the RPE, achieving transfection at this level is highly desirable for therapeutic purposes. Unfortunately, SR injection is one of the most invasive methods and implies significant risk of complications such as inflammation, damage to the lens and retinal detachment<sup>80</sup>. Although many efforts are conducted to increasing RPE transgene expression after IV injection, at present the SR administration remains more efficient for RPE cells transfection. Additionally, research is also being directed towards ocular topical instillation of drugs. In fact, efficient topical drug delivery to the RPE layer of the retina with microfluidizer produced small liposomes has been recently reported<sup>81</sup>. This method does not imply any risks of retinal damage and it would be the ideal administration method for non-viral vectors carrying nucleic acids. However, in the field of gene therapy more research is still needed to improve the efficiency of gene delivery through this approach and become clinically relevant for retinal diseases.

## Discussion

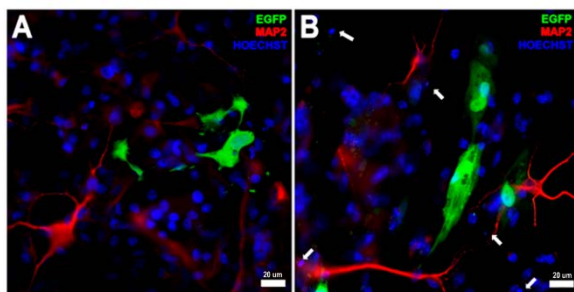


**Figure 2.5.** EGFP expression in embryonal rat retinal primary cells analyzed by fluorescence immunocytochemistry 96 h post-addition of DST20 nioplexes at cationic lipid/DNA mass ratio 2/1. **(A).** EGFP expression in cells exposed to DST20 nioplexes. **(B).** EGFP expression in cells exposed to Lipofectamine 2000™. Red: MAP2 neuronal dendrite marker; Blue: Hoechst 33342 (cell nuclei); Green: EGFP. Scale bar: 20  $\mu$ m.

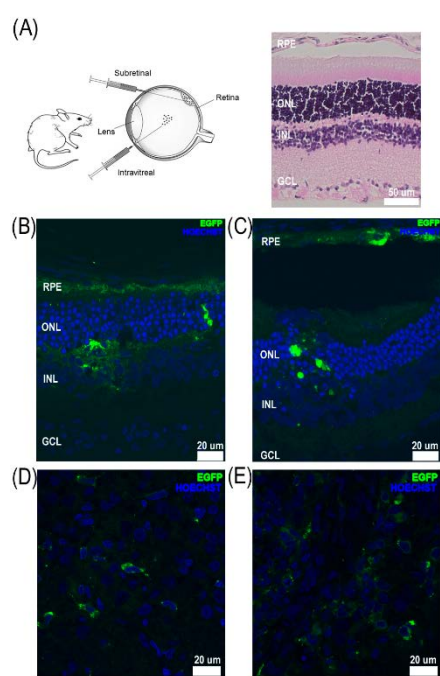


**Figure 2.6.** *In vivo* expression of EGFP after subretinal and intravitreal injection of DST20 nioplexes at cationic lipid/DNA mass ratio 2/1. **(A).** Confocal fluorescence micrographs of retinal cross sections showing EGFP signal after subretinal administration of DST20 nioplexes. **(B).** Confocal fluorescence micrographs of retinal cross sections showing EGFP signal after subretinal administration of the positive control Lipofectamine 2000™. **(C).** Fluorescence immunohistochemistry showing EGFP positive signal located in the ganglion cell layer after intravitreal administration of DST20 nioplexes. **(D).** Fluorescence immunohistochemistry showing EGFP positive signal located in the ganglion cell layer after intravitreal administration of the positive control Lipofectamine 2000™. Blue: Hoechst 33342 (cell nuclei); Green: EGFP. Scale bars: 20  $\mu$ m. RPE (retinal pigment epithelium), ONL (outer nuclear layer), INL (inner nuclear layer), GCL (ganglion cell layer).

## *Discussion*

In summary, we elaborated and characterized three niosome formulations that only differed in the non-ionic tensioactives. We found that the novel DST20 niosome formulation, based on polysorbate 20 combined with cationic lipid DOTMA and helper lipid squalene, efficiently transfected rat retina both *in vitro* and *in vivo* at the low cationic lipid/DNA mass ratio 2/1. Targeted cells strongly depended on the administration route. SR injection transfected the inner layers of the retina and showed clear diffusion to outer layers including the RPE, while IV injection transfected predominantly the ganglion cell layer. With the advancement of DNA compaction technology and vector engineering strategies, efficient transfection through less invasive administration routes and prolonged transgene expression may be achievable goals.

### **3. The influence of the genetic material in niosome formulations in their transfection efficiency in rat retina**

In addition to improving the delivery formulation as discussed in the previous section, we were now interested in the optimization of the DNA payload itself. Various elements of plasmid DNA vectors have been studied and optimized so far in order to increase or prolong transgene expression, including the promoter sequence, enhancer sequences, polyadenylation signals and the removal of CpG motifs to decrease inflammatory responses<sup>82-86</sup>. Nevertheless, plasmid DNA vectors also contain a bacterial backbone, which consists of prokaryotic replication origin sequences and antibiotic resistance genes. This bacterial backbone allows for the propagation of plasmid DNA in bacterial hosts, but it has recently been related to decreased transgene expression and lower biocompatibility and safety profile of the gene delivery complex. Therefore, minimized expression units that only contain the gene of interest and regulatory sequences such as minicircle (MC) DNA vectors emerge as an attractive alternative to conventional, larger plasmid DNA vectors. MCs are small circular DNA vectors with no antibiotic resistant genes or bacterial backbone sequences, which make them superior to regular plasmids. MC-DNA has a reduced size compared with conventional plasmid DNA with the same expression cassette and the content of unmethylated CpG dinucleotides is considerably reduced (Fig. 3.1.). Thus, their use results in sustained transgene expression because of a lower activation of nuclear transgene silencing mechanisms, and reduced immunogenic responses *in vivo*<sup>87-92</sup>. Due to its minimal size and lack of bacterial backbone sequences, minicircle DNA presents a promising alternative to plasmid DNA for non-viral gene delivery in terms of biosafety and improved gene transfer. Several studies have shown that minicircle DNA vectors provide enhanced

## Discussion

transgene expression in a variety of organ systems *in vivo* including the liver<sup>93-95</sup>, heart<sup>96,97</sup> and skeletal muscle<sup>97</sup>, but minicircles have not yet been assessed for retinal gene delivery in complex with niosome formulations.

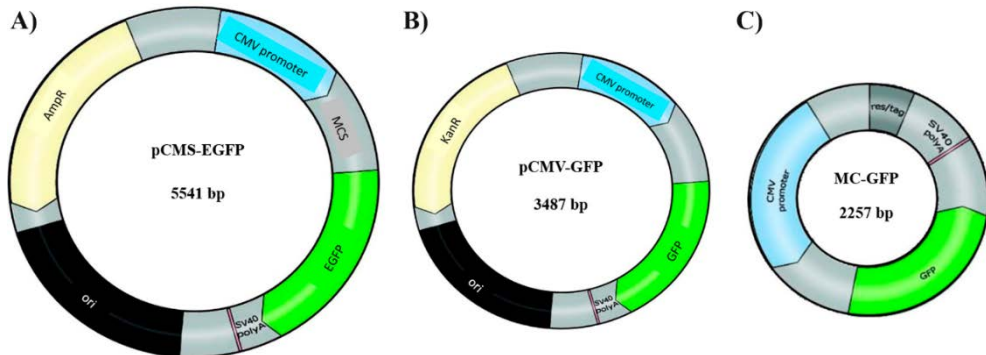


**Figure 3.1.: DNA material composition.**

(A) pEGFP 5.5 kb, (B) pGFP 3.5 kb, (C) MC-GFP 2.3 kb. MC: minicircle; GFP: green fluorescent protein; EGFP: enhanced green fluorescent protein; pCMS: plasmid containing Cytomegalovirus promoter, Multiple cloning site and SV40 promoter; pCMV: cytomegalovirus promoter plasmid; bp: base pairs.

Therefore, our goal was to provide as far as we were concerned, the first evidence that niosome based non-viral vectors combined with the MC technology is an effective technique for future clinical applications in the retinal gene therapy field. We employed DST20 formulation comprised of cationic lipid 1,2-di-O-octadecenyl-3-trimethylammonium propane (DOTMA), the helper lipid Squalene and the non-ionic surfactant polysorbate Tween 20<sup>24-26</sup>. The resulting niosomes were combined with three different DNA materials consisting on MC-GFP of 2257 bp, pGFP of 3487 bp and pEGFP of 5541 bp, to form the corresponding nioplexes. Niosomes and nioplexes were characterized in terms of particle size, polydispersity index (PDI), zeta potential, morphology and stability. The capacity of niosomes to protect and release these DNA materials as well as the binding interactions between cationic niosomes and DNAs at molecular level was also analyzed. *In vitro* experiments were performed to evaluate both the efficiency and cell viability of transfection over time and at different temperatures with the three DNA materials complexed to DST20 niosomes in human ARPE-19 retinal pigment epithelium cells. Additionally, the transfection capacity of these nioplexes was assessed by *ex vivo* experiments in

## *Discussion*

embryonary rat retinal primary cells and by *in vivo* administration of nioplexes to rat eyes via intravitreal (IV) and subretinal (SR) injections.

DST20 niosomes presented appropriate spherical morphology and size for gene therapy purposes, 123 nm, with low PDI and positive zeta potential pointing out not only a good homogeneity and stability of the suspensions, but also an easy interaction with the negatively charged phosphate groups of the DNA material to form nioplexes, respectively<sup>45,98,99</sup>. It is worth mentioning that differences in the reported size of niosomes between dynamic light scattering and TEM techniques could be explained by the sample processing and treatment performed for both analyses<sup>13</sup>. As expected, complexation of DST20 niosomes with the corresponding DNA almost doubled its original diameter and zeta potential values diminished due to the partial neutralization of the positive amine groups of niosomes by the DNA phosphate groups (Figure 3.2.A-B).

The features observed regarding size, zeta potential and transfection efficiency when complexing niosomes to the three genetic materials, are in accordance with previous studies which confirm that the DNA size bound to niosomes does not affect such physicochemical properties of nioplexes<sup>100</sup> but have different transfection efficiencies *in vitro*<sup>101</sup>. The explanation for the differences observed in transfection efficiencies might reside in two main factors. On the one hand, the magnitude of the increment in the particle-size of nioplexes with respect to the niosomes seems to rule out the possibility that the second phase seen in the ITC titration curves might be due to the binding of more niosomes onto DNA-coated nioplexes. Thus, niosome-DNA binding events occurring at higher ratios than 2/1 would probably involve the reorganization of the previously bound genetic material, which would lead to a reduction in the number of DNA molecules bound per niosome and to the preferential occupation of the most favourable binding sites on the niosome surface. This could also affect the ability of the nioplexes to interact with the cell surface and, consequently, their transfection capacity. On the other hand, this study was developed with a constant DNA quantity of 1.25 µg per condition but it has to be taken into account that DNA length, and therefore weight and molarity, differs between the three genetic materials under study, which consequently affects the number of DNA molecules bound to each niosome. This fact can be observed in the ITC assay where different calorimetry curves were obtained depending on the genetic material complexed to the DST20 formulation (Figure 3.2.D). Hence, niosomes would be incorporating more MC molecules than plasmids ones, which

## Discussion

means a higher rate of expression cassettes per niosome, increasing the probability of efficient gene delivery into the cell and finally a higher transgene expression<sup>92,101</sup>.

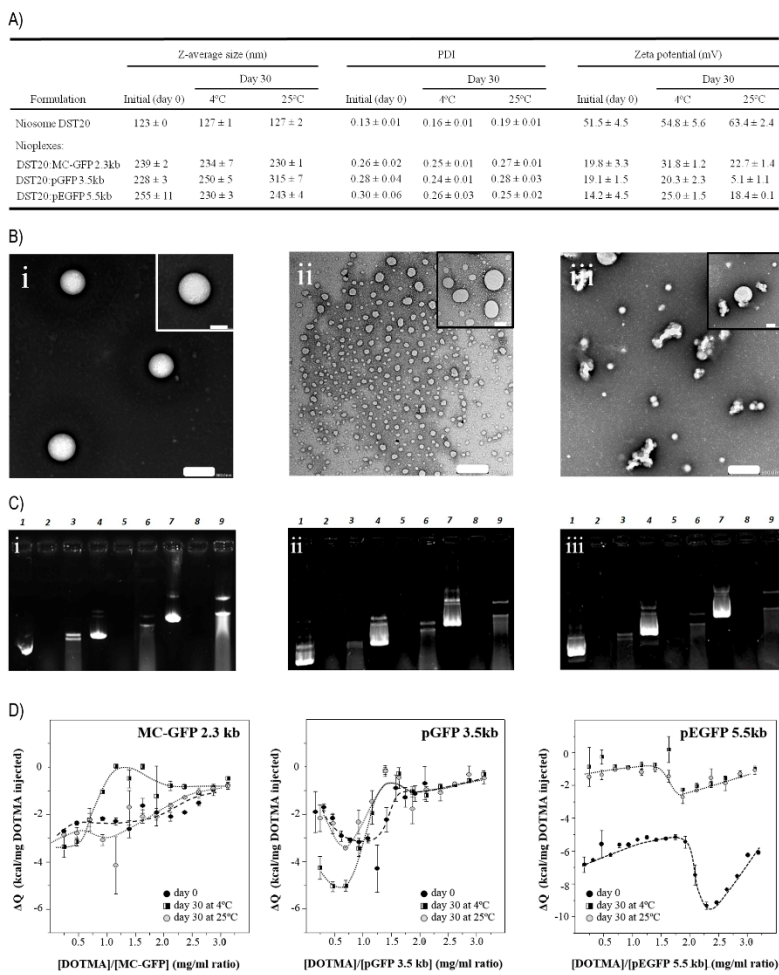


**Figure 3.2.: Physicochemical characterization and stability measurements of niosomes and nioplexes.** (A) Physicochemical characterization of DST20 niosomes at day 0 and at day 30 of storage at 4°C and 25°C, and corresponding nioplexes. Each value represents the mean ± SD from three measurements. (B) TEM images of DST20 niosomes at day 0 (i), at day 30 of storage at 4°C (ii) and 25°C (iii). Scale bars: 500 nm (outer images) and 200 nm (inner images). (C) Gel retardation assay to analyze the capacity of DST20 niosomes to protect and

## *Discussion*

release the DNA material at day 0 (i), at day 30 of storage at 4°C (ii) and 25°C (iii). DNase I enzyme and SDS were added in lanes 3, 6 and 9 to evaluate both protection and release in MC-GFP, pGFP 3.5 kb and pEGFP 5.5 kb niosomes, respectively. As controls, lanes 1, 4 and 7 correspond to control naked MC-GFP, pGFP 3.5 kb and pEGFP 5.5 kb, respectively, and lanes 2, 5 and 8 to those naked DNAs after adding DNase I enzyme, respectively. (D) ITC study of DNA titration with DST20 niosomes. Corresponding variation of heat evolved per mg of DOTMA injected vs. the ratio of DOTMA/DNA concentrations expressed in mg/ml. Symbols represent the experimental data whereas the discontinuous line illustrate the tendency of the ITC profiles.

---

The differences found in GFP expression upon the storage of niosomes (Fig. 3.3.) could be explained not by a single cause but by several cumulative reasons. In fact, effective gene delivery is affected by size range and zeta potential but many other relevant parameters such as a correct vector morphology and DNA binding affinity may have an impact on this effectiveness<sup>102</sup>. In this regard, TEM images showed a loss of the spherical shape of niosomes and even the formation of some aggregates after 30 days of storage, which in turn would difficult interactions with the DNA material. Actually, gel retardation and ITC assays confirm this reduction of DNA complexation capacity of niosomes over time. In agarose gels, the lower signal of bands corresponding to DNA protection and release after storage denoted a reduction of these capacities (Fig. 3.2.C). Accordingly, ITC data would be indicative that the molecular features of the DST20-based niosomes formed at 2.0 ratio (equivalent to DOTMA/DNA ratio 2/1) could depend on the previous history of the niosomes, explaining the differences mentioned before, such as the physicochemical features, the morphology of niosomes and their ability to protect and release the DNA. Even though DST20 niosomes stored for 30 days at 4°C vectoring MC remained exhibiting a higher gene delivery capacity compared with plasmid niosomes (Fig. 3.3.), additional efforts are required in order to achieve more stable formulations by either performing better characterization methods or by introducing modifications into formulations themselves.

## Discussion

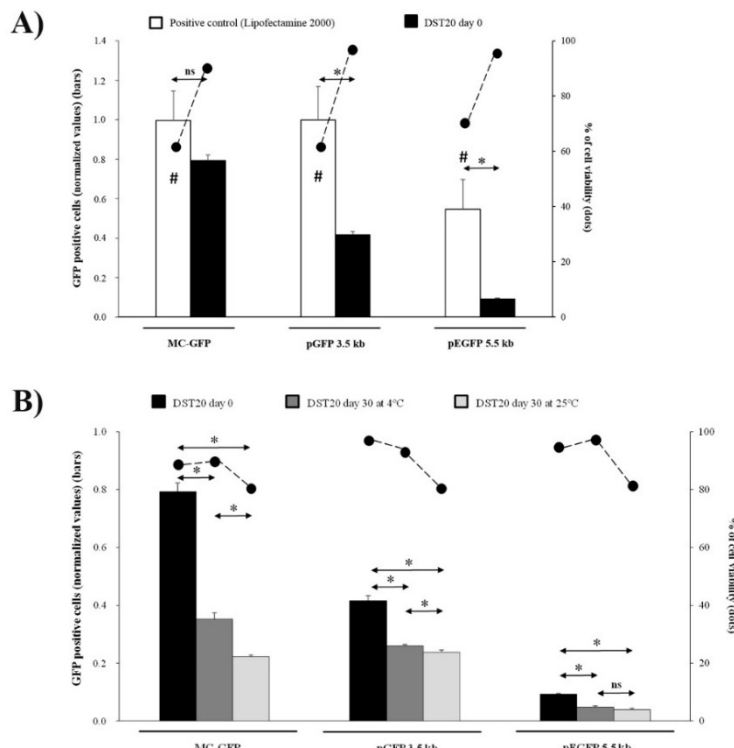


**Figure 3.3.: Transfection efficiency of nioplexes and cell viability in ARPE-19 cell line.** Flow cytometry evaluation of GFP positive live cells (bars) and viability (dots) after transfection employing (A) DST20 niosomes at day 0 and (B) after 30 days of storage at 4°C and 25°C, bound to either MC-GFP, pGFP 3.5 kb or pEGFP 5.5 kb. Data are presented as mean  $\pm$  SD,  $n = 3$ . \* $P < 0.05$  for transfection efficiency groups, # $P < 0.05$  for cell viability relative to its respective Lipofectamine™ 2000; ns means no statistically significant differences.

Since IV and SR routes are considered the most clinically viable options to deliver efficiently the genetic material to the back of the eye<sup>103</sup>, nioplexes were injected at these levels *in vivo*. IV administration of DST20 nioplexes showed GFP expression in the GCL, in accordance with previous works employing non-viral vectors<sup>24,25</sup>. Effective gene transfer at this level could be clinically relevant for treatment of devastating inherited retinal disorders such as glaucoma, which is considered the first cause of blindness worldwide<sup>104</sup>. After injection of those nioplexes at SR level, transgene expression diffused to the inner nuclear layer (INL) and, importantly, was localized close to the injection site in the retinal pigment epithelium (RPE). For therapeutic clinical practice, gene delivery reaching the outer layers of the retina is

## Discussion

deeply desirable since many inherited retinal disorders with no curative treatment to date, such as retinitis pigmentosa, Stagardt's disease or Leber's congenital amaurosis, are associated with more than 200 mutations of genes expressed at the photoreceptors and RPE level 4. Qualitative analysis after both IV (Fig. 3.5.) and SR (Fig. 3.6.) injections showed a higher transgene expression the smaller the DNA was, pointing out that DST20 non-viral vector combined with MC-DNA offers a potential tool for retinal degenerative and inherited diseases. In addition, it has been reported that MC technology offers not only a higher but also a sustained gene expression over time, offering key benefits for clinical translation<sup>92,101</sup>. Despite GFP expression was also observed employing Lipofectamine™ 2000, it has been shown that such formulation is not suitable for *in vivo* experiments due to its high toxicity mainly accused into photoreceptor cells even at low concentrations<sup>68</sup>. In fact, our *in vitro* experiments clearly showed the toxicity of Lipofectamine™ 2000 in retinal cells (Fig. 3.3., Fig. 3.4.). Finally, it is noteworthy the high transfection efficiency achieved with DST20:MC nioplexes at the low 2/1 ratio since it allows a higher gene content at small volumes of injection for clinical applications, where the volume to be injected represents an important handicap, and reduces cellular toxicity associated to cationic lipids<sup>67</sup>. Furthermore, the lack of unmethylated CpG content in MC-DNA technology provides additional reduced immunogenic responses, reinforcing DST20:MC complexes as a potential efficient and safe tool for translational retinal gene therapy applications.

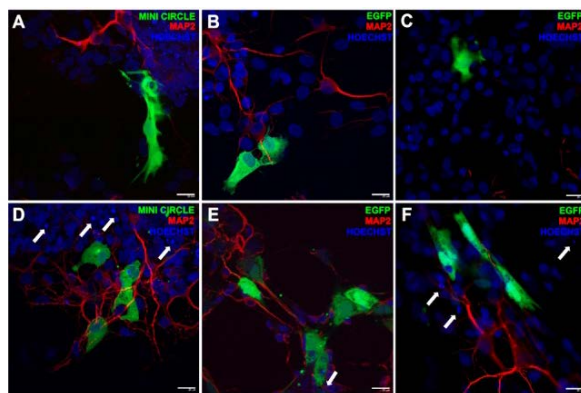


**Figure 3.4.: GFP expression in embryonic rat retinal primary cells.** Fluorescence immunocytochemistry showing GFP positive signal located mainly in glial cells after transfection with DST20 nioplexes, carrying either (A) MC-GFP, (B) pGFP 3.5 kb or (C) pEGFP 5.5 kb. (D-F) images of their counterpart positive controls exposed to Lipofectamine™

## Discussion

2000. Cell nuclei were counterstained with Hoechst 33342 (pseudocolored blue) and neuronal dendrites with MAP2 (red color). White arrows indicate apoptotic nuclei. Scale bars: 20  $\mu$ m.

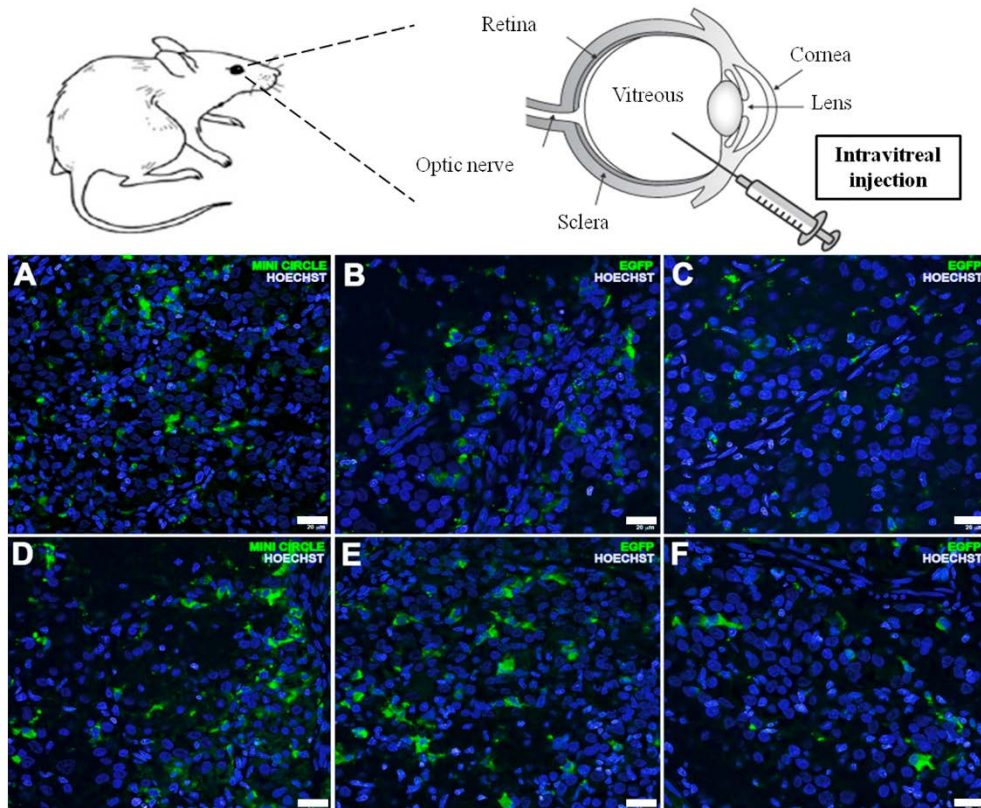


**Figure 3.5.: *In vivo* expression of GFP after intravitreal injection of nioplexes.** Confocal fluorescence micrographs of retinal cross sections showing GFP signal after intravitreal administration of DST20 nioplexes carrying either (A) MC-GFP, (B) pGFP 3.5 kb or (C) pEGFP 5.5 kb. (D-F) images of their counterpart positive controls. RPE (retinal pigment epithelium), OS (outer segments), ONL (outer nuclear layer), INL (inner nuclear layer), GCL (ganglion cell layer). Cell nuclei were counterstained with Hoechst 33342 (pseudocolored blue). Scale bars: 20  $\mu$ m.

## Discussion

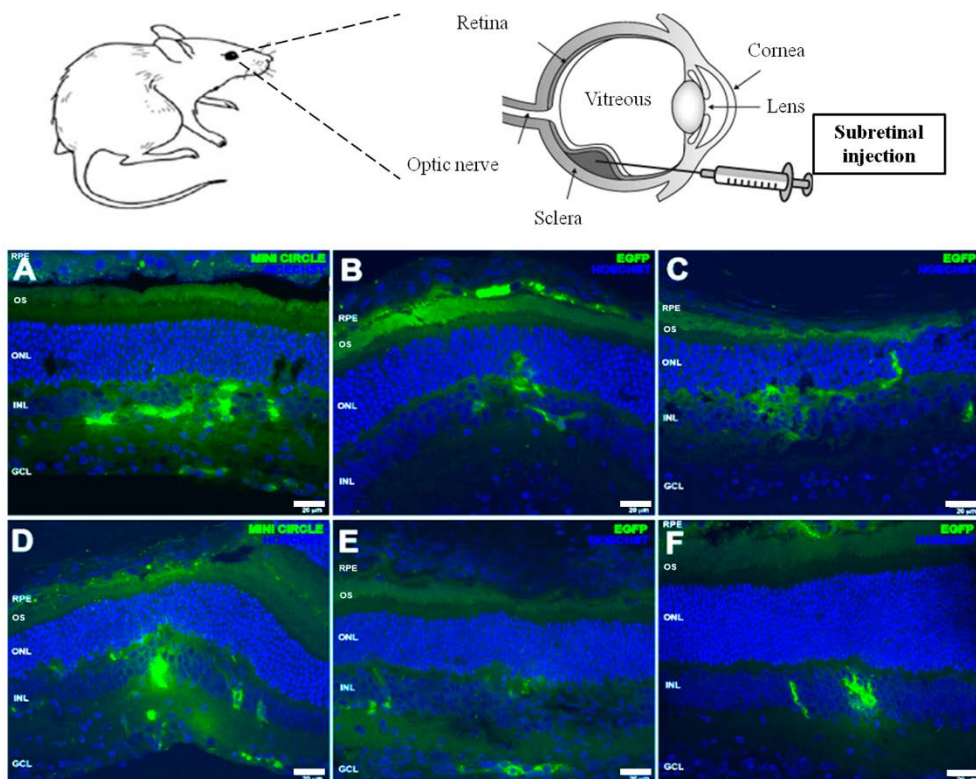


**Figure 3.6.: *In vivo* expression of GFP after subretinal injection of nioplexes.** Confocal fluorescence micrographs of retinal cross sections showing GFP signal after subretinal administration of DST20 nioplexes carrying either (A) MC-GFP, (B) pGFP 3.5 kb or (C) pEGFP 5.5 kb. (D-F) images of their counterpart positive controls. RPE (retinal pigment epithelium), OS (outer segments), ONL (outer nuclear layer), INL (inner nuclear layer), GCL (ganglion cell layer). Cell nuclei were counterstained with Hoechst 33342 (pseudocolored blue). Scale bars: 20  $\mu$ m.

Therefore, the main findings of this study are the following: (1) DST20 niosomes is a non-viral vector able to protect genetic material and release it with controlled kinetics; (2) the capacity of niosomes to protect and interact with DNA material is affected over time and temperature of storage; (3) DST20 niosomes complexed with different genetic material, varying in terms of size and composition, present similar size and zeta potential but have different transfection efficiencies *in vitro*, meanwhile

## *Discussion*

cell viability is not affected; (4) DST20 nioplexes containing MC-DNA present higher transfection efficiency than those containing plasmids in *in vitro* assays, even after DST20 storage for 30 days; and (5) DST20 nioplexes are able to transfer the genetic material not only in *ex vivo* primary retinal cell cultures but also after *in vivo* injection in rat retinas regardless the via of administration, being those carrying MC-DNA the ones that present the higher rate of GFP signal. Therefore, DST20 niosomes vectoring MC technology seems to be an efficient and safe therapeutic tool for retinal disorders, overcoming the existing translational barrier of non-viral vectors complexed with plasmids due to their poor transfection efficiency.

### **4. Tridimesional aspects of non-viral gene delivery systems: exploring complementary synergies between niosomes and hyaluronic acid hydrogel scaffolds**

In addition to the optimization of the carrier and the genetic material, a new trend in non-viral gene therapy is to explore novel complementary synergies between delivery systems and tissue-engineered scaffolds in order to improve the transfection efficiency. In fact, these combined approaches may offer relevant advantages such as enhanced stability and reduced toxicity. Moreover, complementing gene transfer with matrix design would allow an effective, targeted and local DNA delivery, which would enhance the applicability of gene therapy in many therapeutic fields, such as tissue regeneration and cancer<sup>35,36</sup>. Hyaluronic acid (HA), an anionic glycosaminoglycan, is one of the primary components of the natural extracellular matrix (ECM) and it is increasingly gaining popularity as a biomaterial in the field of tissue engineering<sup>105</sup>. HA hydrogels have been widely studied for their biocompatibility as well as their ability to incorporate a wide variety of molecules, including nucleic acids<sup>106</sup>.

Therefore, the main objective of the present work was to develop an effective platform to deliver DNA locally using niosomes as non-viral vectors from HA hydrogel scaffolds. To our knowledge, this is the first example of niosome-based DNA nanoparticle delivery from HA hydrogels for non-viral gene expression. We explored three different niosome formulations (niosomes **1**, **2** and **3**) varying in composition of cationic lipid, helper lipid and non-ionic tensioactives (Fig. 4.1.) in complex with a reporter plasmid encoding for *Gaussia luciferase* (pGluc) to obtain the nioplexes. The selection of the components, their concentrations and the cationic lipid/DNA mass ratios (w/w) were based on previous studies developed in our laboratory. Niosomes and corresponding nioplexes were characterized in terms of size, PDI,

## Discussion

zeta potential and ability to transfect mouse bone marrow cloned mesenchymal stem cells (mMSCs) in 2D culture. HA hydrogels containing nioplexes were characterized in terms of biomechanical properties, particle distribution and nioplex release kinetics. Additionally, the biological activity of released nioplexes upon hydrogel degradation was also evaluated. mMSCs were efficiently transfected in nioplex encapsulated HA hydrogels and presented excellent cellular viability. These results demonstrate the potential for nioplex loaded HA hydrogels for sustained gene delivery.

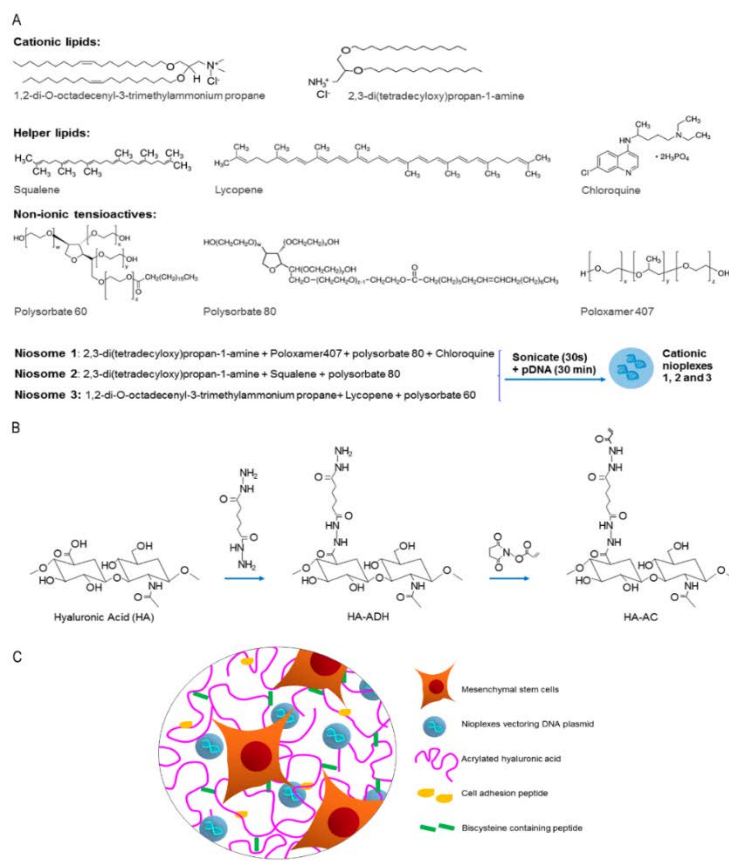


**Figure 4.1.** General scheme of cationic niosomes and hydrogel scaffolds used in this work.  
**A.** Cationic lipid, helper lipid and non-ionic tensioactives components used to elaborate

## *Discussion*

niosome formulations. **B.** Modification of HA to obtain HA hydrogels. **C.** Representative scheme of a HA hydrogel with entrapped nioplexes.

---

Yet while high concentrations of non-viral DNA complexes in hydrogels have been demonstrated to improve local gene delivery<sup>107</sup>, the physical incorporation of DNA complexes into hydrogels is challenging due to some limitations such as aggregation and inactivation of the complexes inside hydrogel scaffolds<sup>108</sup>. Among the wide variety of non-viral vectors, poly(ethylene imine) (PEI) has been successfully encapsulated in HA hydrogels and effective local transgene expression and ability to induce angiogenesis *in vivo* have been reported<sup>109</sup>. Although PEI derivatives present high gene carrying capacity and ability to achieve high transfection efficiencies, their biomedical application is often restricted due to immunogenicity and cytotoxicity issues<sup>110</sup>. In this regard, niosomes offer several advantages, since they have high compatibility with biological systems and low toxicity because of their non-ionic nature and are biodegradable and non-immunogenic<sup>64</sup>. In this work, *in vitro* transfection efficiencies obtained with nioplex encapsulated HA hydrogels 48 hours after exposure were comparable to those reported with PEI/DNA encapsulated HA hydrogels<sup>111</sup>. Therefore, reasonable hope suggests that nioplex encapsulated HA hydrogels could also be able to transfet cells *in vivo* and further studies in this direction would be of remarkable interest in order to explore this possibility.

The three different niosome formulations differed in the composition of cationic lipid, helper lipid and non-ionic tensioactives (Fig. 4.1.). The niosome components used in this work have previously demonstrated suitability for gene delivery applications. For instance, niosome formulations containing the non-ionic surfactant polysorbate 80 combined with the helper lipid squalene have shown effective gene delivery<sup>26</sup>. In addition, it has been recently shown that the helper lipid lycopene, combined with cationic lipid DOTMA and polysorbate 60, enhances retinal transfection<sup>24</sup> and Poloxamer 407 has been widely used in drug delivery applications<sup>112</sup>. The use of chloroquine has also been reported to enhance gene delivery both *in vitro* and *in vivo*<sup>113</sup>. Therefore, the selection of the components, and their concentrations used to prepare the niosome formulations, as well as the cationic lipid/DNA mass ratios (w/w) to form the corresponding nioplexes were based on available data and previous studies developed in our laboratory.

Niosomes and nioplexes were fully characterized in terms of size, PDI and zeta potential, as well as transfection efficiency in a 2D culture of mMSCs (Fig. 4.2.). The

## Discussion

three niosome formulations presented positive zeta potential values (Fig. 4.2.B), necessary to bind to the negatively charged DNA molecules by electrostatic interactions<sup>45,66</sup>. In addition, positive zeta potential values enhance cellular uptake<sup>44</sup>. Compared to non-treated cells, all formulations showed ability to transfect, with nioplexes based on niosome **1** resulting in the highest transfection efficiency (Fig. 4.2.C). Therefore, we selected the nioplexes based on niosome **1** at 2/1 cationic lipid/DNA mass ratio (w/w) formulation to study its applicability for non-viral gene delivery in HA hydrogels.

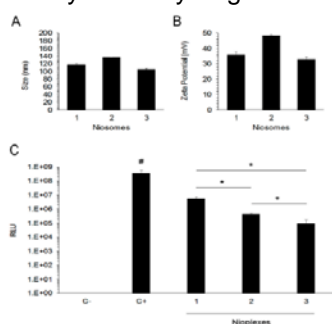


**Figure 4.2.** Screening of niosome formulations. **A.** Size. **B.** Zeta Potential. **C.** Transfection efficiency 48 h post-exposure of mMSCs to nioplexes based on niosomes **1**, **2** and **3** at cationic lipid/DNA mass ratios (w/w) 2/1, 15/1 and 18/1, respectively. Positive (Lipofectamine 2000™ at a cationic lipid/DNA mass ratio of 2/1) and negative (no DNA) controls are shown for reference.

The use of nioplexes at low mass ratios presents several advantages, including the possibility of incrementing the dose of DNA as well as decreasing cellular toxicity<sup>13</sup>. Additionally, in order to be able to incorporate higher, more relevant amounts of DNA within HA hydrogels, the formulation based on niosome **1** was first concentrated from 1 mg/ml to 2 mg/ml. The TEM images of the concentrated formulation showed that concentration did not affect morphology and, as expected, more particles were visible in the concentrated sample (Fig. 4.3.A-B). Size and PDI values were also maintained similar in the concentrated formulation. Although the zeta potential values clearly declined in the concentrated niosome, values remained above +20 mV, meaning that the stability of the formulation should not be affected. In fact, particles with surface charge values between -20 mV and +20 mV present more propensity to form aggregates along the time<sup>46</sup>. Additionally, the transfection ability of both concentrated and non-concentrated formulations was evaluated at cationic lipid/DNA mass ratio 2/1 and no statistically significant differences were found between the transfection efficiencies of both formulations (Fig. 4.3.C), indicating that the concentrating process does not affect the transfection capacity. In view of these

## Discussion

results, we decided to use the concentrated formulation at the low cationic lipid/DNA mass ratio 2/1 for encapsulation in HA hydrogels.

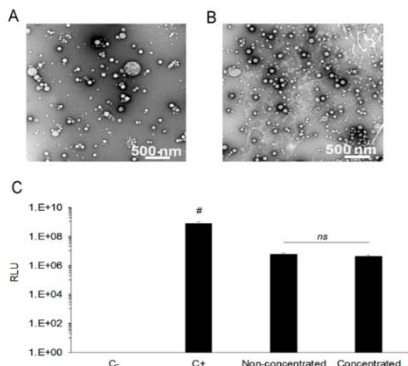


**Figure 4.3.** Characterization of concentrated niosome formulations. **A-B.** TEM images of non-concentrated (**A**) and concentrated (**B**) formulations based on niosome **1** at 10,000x magnification. Scale bars: 200.0 nm. **C.** Transfection efficiency 48 h post-exposure of mMSCs to nioplexes based on concentrated and non-concentrated niosome **1** at 2/1 cationic lipid/DNA mass ratio (w/w).

In order to achieve therapeutically relevant levels of DNA<sup>114</sup>, we evaluated three different amounts of concentrated nioplexes, obtaining final DNA concentrations of 0.055 µg/µl, 0.12 µg/µl and 0.2 µg/µl in hydrogels **2**, **3** and **4**, respectively. Different DNA concentrations of hydrogels could cause differences in the mechanical properties, which are important factors determining cell proliferation, spreading and transgene expression in hydrogel scaffolds. High hydrogel stiffness (over 800 Pa) has been related to reduced cell spreading and transgene expression, while soft hydrogels (200 – 260 Pa) resulted in enhanced transgene expression<sup>108</sup>. Therefore, we evaluated the mechanical properties of hydrogels as a function of DNA concentration in order to determine their grade of stiffness. Rheological characterization showed high variability in the mechanical properties of hydrogels (Fig. 4.4.A-B). Hydrogel **3** presented the highest stiffness among the hydrogels tested, while hydrogel **4**, with the highest DNA concentration, showed to be the softest. Such high values were not expected in hydrogel **3**, however, that condition was not discarded and further studies were carried out in order to determine its transfection capacity despite its high stiffness. The evaluation of the distribution of the nioplexes inside the hydrogel scaffold showed larger DNA clusters in hydrogel **2**, which could be attributed to the presence of higher amounts of cell growth medium containing peptides and proteins that could interact with the nioplexes resulting in particle aggregation. Hydrogels **3** and **4**, despite their higher DNA concentrations, presented a homogeneous distribution of nioplexes with no aggregates (Fig. 4.4.C-E). However, since hydrogel **4** did not contain any cell growth medium, it was not a possible candidate for 3D cell culture nor for transfection assays and only hydrogels **2** and **3** were evaluated for *in vitro* gene delivery to mMSCs. Yet, the high DNA

## Discussion

concentration and absence of particle aggregation in hydrogel **4** suggested that it could be an attractive option for *in vivo* gene delivery. Taken together, these results demonstrate that nioplexes can be successfully encapsulated into HA hydrogels without significant particle aggregation, although high variability in mechanical properties was observed.

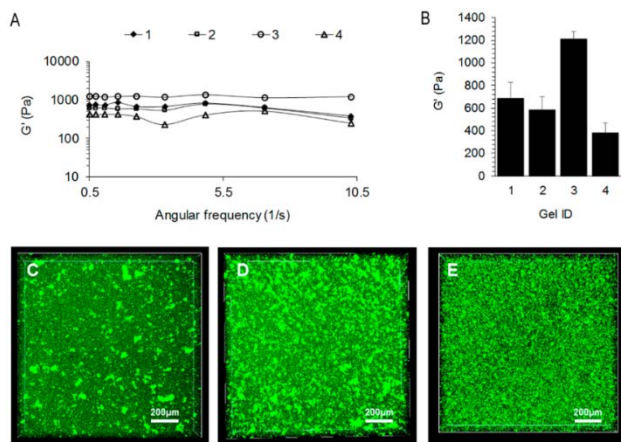


**Figure 4.4.** Characterization of HA hydrogels loaded with nioplexes. The mechanical properties of the hydrogels were determined using plate-to-plate rheometry over a frequency range of 0.1-10 rad/s at a constant strain of 0.01 (**A**). Average storage modulus (**B**). **C-E.** Particle distribution in hydrogels. **Gel ID:** **1**, control hydrogel without nioplexes; **2**, 0.055 µg DNA/µl; **3**, 0.12 µg DNA/µl and **4**, 0.2 µg DNA/µl. Scale bars: 200 µm.

In order to validate that nioplexes maintained the ability to transfect cells after encapsulation in HA hydrogels, we synthesized nioplex-loaded hydrogels, degraded them with trypsin and performed a transfection with the released nioplexes (Fig. 4.5.). Results showed that the transfection capacity of the nioplexes was negatively affected by the presence of interfering hydrogel materials and trypsin in the 2D cell culture media, but not by the encapsulation process since there were no statistically significant differences in transfection values between released nioplexes from degraded hydrogels and fresh nioplexes supplemented with degraded hydrogel materials (Fig. 4.5.B-C). In addition to the hydrogel components, the negative effect of trypsin in the transfection efficiency of non-viral vectors has been widely described<sup>109</sup>.

## Discussion

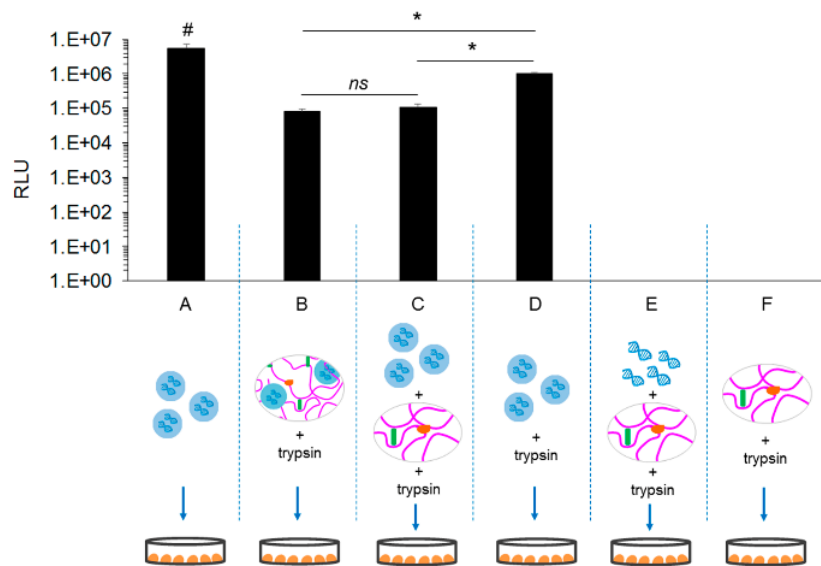


**Figure 4.5.** Biological activity of nioplexes based on concentrated niosome 1 at 2/1 cationic lipid/DNA mass ratio (w/w). **A.** Fresh nioplexes. **B.** Nioplexes released from degraded HA hydrogels with trypsin. **C.** Fresh nioplexes supplemented with degraded hydrogels with trypsin. **D.** Fresh nioplexes supplemented with trypsin. **E.** Naked DNA supplemented with degraded hydrogels trypsin. **F.** Hydrogels without nioplexes degraded with trypsin. \* $p < 0.05$  for transfection efficiency between different conditions, # $p < 0.05$  for transfection efficiency of all conditions relative to condition “A”.

Two main mechanisms are postulated to contribute to the gene transfer process from hydrogel scaffolds: DNA/nanoparticle release kinetics and rate of cellular infiltration<sup>115</sup>. Nioplexes released after hydrogel degradation could transfect surrounding cells, while infiltrating cells would encounter entrapped nioplexes and become transfected leading to transgene expression inside the hydrogel area<sup>116,117</sup>. In this regard, for cells cultured in three dimensions, the migration rate of cells through the hydrogel has previously been related to successful non-viral gene transfer<sup>115</sup>. Therefore, we would expect that softer hydrogel scaffolds that allowed for extensive cell spreading would result in enhanced gene transfer. In the present work, nioplexes were released from the gels within 7 days in the presence of Col I and the process was slightly slower in the absence of enzymatic degradation (Fig. 4.6.A). This progressive release of nioplexes potentially allows for sustained transgene expression, which is essential for therapeutic applicability.. Regarding cell spreading and transfection efficiency in 3D culture, interestingly, all hydrogels

## Discussion

including hydrogel **3** allowed for extensive cell spreading (Fig. 4.6.C-E) and, despite its high stiffness, the highest transfection values were obtained in hydrogel **3** (Fig. 6B, bars). Therefore, these results suggest that increasing amounts of DNA can be used to overcome limitations of stiffer hydrogels. Moreover, cell viability was excellent in all conditions (Fig. 4.6.B, dots), which indicated that the presence of nioplexes in the HA hydrogels was well tolerated by the cells.

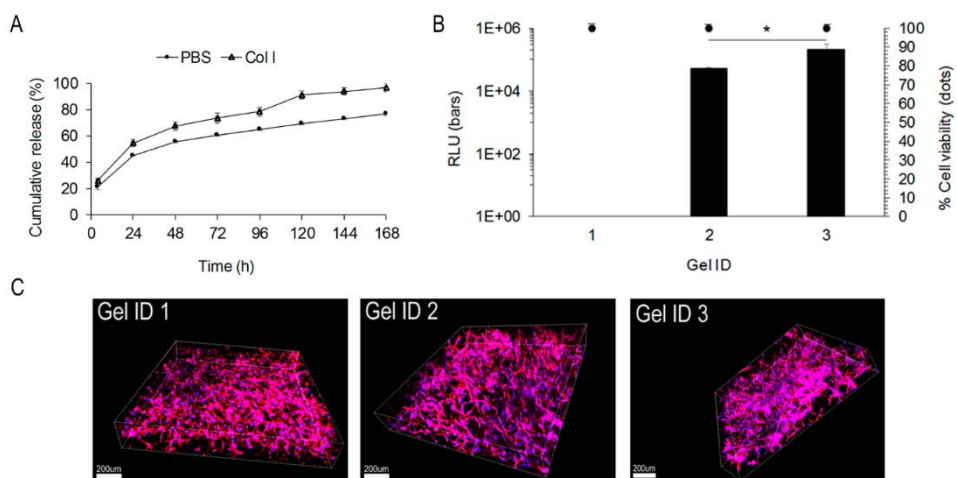


**Figure 4.6.** **A.** Nioplex release kinetics from HA hydrogels in PBS and in PBS supplemented with Collagenase I (1 U/ml). **B.** Transfection efficiency and cell viability of nioplex-loaded hydrogels **1-3** at 48 h. **C.** Representative images of cell spreading in hydrogels **1**, **2** and **3**. Blue = cell nuclei (DAPI) and red = F-actin (rhodamine-phalloidin). Scale bars: 200  $\mu$ m. \* $p < 0.05$  for transfection efficiency.

To sum up, we successfully developed a process to load concentrated nioplexes into HA hydrogels without aggregation. To our knowledge, this is the first time that niosome formulations composed of 2,3-di(tetradecyloxy)propan-1-amine, Poloxamer 407, polysorbate 80 and chloroquine diphosphate salt are incorporated to HA hydrogels for non-viral gene delivery. In general, HA hydrogel scaffolds loaded with nioplexes presented suitable mechanical properties, little or no particle aggregation, allowed for extensive cell spreading and were able to efficiently transfect encapsulated mMSCs in 3D cultures. We believe that the knowledge gained through this *in vitro* model can be utilized to design novel and effective platforms for *in vivo* local and non-viral gene delivery applications.

### *Discussion*

As a whole, this doctoral thesis describes and explores key factors that determine the transfection efficiency of non-viral vectors and that need to be taken into account when developing efficient non-viral gene delivery systems. Those key aspects include the composition and physicochemical properties of non-viral vectors, the composition and conformation of the genetic material and the combination of delivery systems with other technologies such as matrix design. We believe that the concept of a unique universal non-viral vector is nowadays obsolete, and that future non-viral gene delivery platforms will be based on multifunctional vectors specifically tailored for different applications. Although non-viral vectors are still far from clinical practice, reasonable hope suggests that next generation delivery systems for gene addition and, most importantly, gene editing strategies may be based non-viral vector systems, which, ideally, would be suitable for administration via non-invasive routes.

***References are listed in pages 316 to 325.***

## *Eztabaida*

Gene-terapiaren helburua da material genetiko arrotza zeluletan txertatzea horien proteina-espresioa aldatzeko edota kontrolatzeko, eta aplikazio terapeutikoak zein esperimentalak izan ditzake<sup>1</sup>. Giza Genomaren Proiektuak eta azken urteetan biologia molekularren arloan egindako aurrerapenek prozesu zelularrak eta patologikoak hobeto ulertzea ahalbidetu dute. Aldi berean, aurrerapauso horiek gene-terapiarako jomuga izan litezkeen hainbat gene identifikatzen lagundu dute gaixotasun genetiko ezberdinei dagokienean. Halere, nahiz eta gene-terapiak potentzial handia erakutsi duen batez ere gaixotasun monogenikoen tratamendurako, bektore seguru eta eraginkorragaratzera ezinbesteko baldintza da gene-transferentzian oinarritutako estrategia terapeutikoak erabilera klinikora iristeko. Izan ere, gene-terapiaren arrakasta bektoren eraginkortasunaren menpe dago erabat. Gaur egun uste da honako hauek direla bektoreek bete beharreko baldintza nagusiak gene-garraioa modu efizienteean eman dadin: (i) material genetikoa nukleasen erasotik babesteko gai izan behar dira, (ii) azido nukleikoak zelulan barneratzeko gai izan behar dira eta (iii) material genetikoa zelula barruko konpartimentu egokian askatzeko gaitasuna izan behar dute. Gainera, gene-garraio sistema idealak espezifikoak, iraunkorrapak, seguruak, erabilerrazak eta ahalik eta ahalik eta kosturik baxuenekoak izan behar dira<sup>2</sup>.

Orohar, gene-garraiorako bektoreak bi multzotan sailkatzen dira: bektore biralak eta ez-biralak. *The Journal of Gene Medicine* aldizkariak 2014an argitaratutako datuen arabera, mundu-mailan gene-terapiako 2000 entsegu kliniko inguru daude abian eta, horietatik, %70ek bektore biralak erabiltzen dituzte geneak garraiatzeko<sup>3</sup>. Gainera, gaur egun soilik lau gene-terapia produktu iritsi dira merkatura eta laurak bektore biraletan oinarrituta daude. Lehen gene-terapia produktu medizinala Gendicine™ izan zen eta Txinan onartu zen 2003 urtean. Bektore gisa adenobirus (Ad) eraldatu bat darama eta lepoko zein buruko kartzinomen tratamendurako balio du<sup>4</sup>. Bigarren gene-terapia produktua ere, Oncorine™ izenekoa, Txinan onartu zen 2005ean eta Ad eraldatu batean oinarritutako bektore birala darama. Beste sendagairik onartzen ez duen minbizi nasofaringeoaren tratamenduan gomendatuta dago<sup>5</sup>. Europa-mailan, lehen gene-terapia produktua 2012. urtean merkaturatu zen, Glybera® izenez. Medikamentu horrek birus adenoasoziatua (AAV) darama gene-garraitzale gisa eta lipoproteina lipasa entzimaren defizitaren tratamenduan erabiltzen da<sup>6</sup>. Azkenik, 2015ean IMLYGIC™ gene-terapia produktua merkaturatu zen Estatu Batuetan, herpes simplex (HSV) birusean oinarrituta eta melanoma errepikakorra duten pazienteei zuzenduta<sup>7</sup>. Dena dela, 2017an eguneratutako datuen arabera, gene-terapia konbentzionalean bektore biralak nagusi diren arren, gene-edizio estrategia berrietan bektore ez-biralak gailendu dira. Izan ere, gene-edizio ikerketen

## *Eztabaida*

%70ek metodo ez-biralak erabiltzen ditu, elektroporazioa lehen estrategia izanik (%39) eta atzetik lipofekzioan (%17) eta polimeroetan (%8) oinarritutako metodoak egonik<sup>8</sup>. Beraz, ematen du bektore ez-biraletan oinarritutako gene-garraio sistemek birusei lekua hartu dietela gene-edizio eta genoma-zuzentze estrategia berriean.

Izan ere, birusak garraio-sistema sendoak diren arren, desabantaila ugari dituzte, besteak beste, karga-gaitasun txikia, ekoizpen konplexua eta garestia edota immune-erantzunei eta mutagenesiari lotutako segurtasun arazoak. Zentzu horretan, nanoteknologian oinarritzen diren bektore ez-biralak etorkizun oparoko alternatiba gisa jaio dira birusek dituzten mugak gainditzeko gai direlako. Birusak ez bezala, bektore ez-biralak gai dira tamaina handiko material genetikoa garraiatzeko, ekoizpen erraza eta kostu baxukoa dute, erabilerrazak dira, ez dute segurtasun arazorik ematen eta ez dute erantzun immunerik pizten<sup>9</sup>. Gainera, formulazio ez-biralak eskala handian ekoiztu daitezke eta biltegiratzean beren propietateak egonkor mantentzen dira epe luzez<sup>1</sup>. Beraz, abantaila horiek guztiak eta nanoingeniaritzan zein materialen zientzian egindako aurrerapenek gene-garraiorako mota guztietaiko bektore ez-biral biobateragarrien sintesia, karakterizazioa eta funtzionalizazioa bultzatu dituzte<sup>11</sup>. Gaur egun, nano-eskalako bektore ez-biralak material ezberdinez osatuta egon daitezke, eta batez ere lipido kationikoz<sup>12-14</sup>, polimeroz<sup>15, 16</sup> edota partikula magnetikoz<sup>17</sup> osatutakoak erabiltzen dira. Molekula horiek era ezberdinatan egokitu daitezke gene terapeutikoak ehun edo zelula espezifikoetara garraiatzeko eta zelulaz kanpoko zein barneko hesiak gainditu ahal izateko. Bektore ez-biralen aukera zabalaren artean, niosoma izenekoak lipido kationikoz eta tentsoaktibo ez-ionikoz osatutako besikula sintetiko eta biobateragarriak dira<sup>18, 19</sup>. Hiru osagai nagusi dituzte: (i) lipido kationikoa, karga positiboa du eta beraz karga negatibodun DNA molekulekin elkarrekintza elektrostatikoak ahalbidetzen ditu<sup>20</sup>, (ii) lipido laguntzailea, formulazioaren ezaugarri fisiko-kimikoak hobetzen laguntzen duena<sup>21</sup> eta (iii) tentsoaktibo ez-ionikoa, formulazioaren egonkortasuna bermatzeko eta partikulen agregazioa ekiditeko<sup>22</sup>. Osagai horien ezaugarriek niosoma formulazioaren propietate fisiko-kimikoak – tamaina, karga, polidispersioa, morfologia, etab.- baldintzatuko dituzte eta, aldi berean, horiek niosomek zeluletan sartzeko, material genetikoa nukleoraino helarazteko eta transfekzio prozesua eraginkortasunez bideratzeko duten gaitasuna baldintzatuko dute<sup>21, 22</sup>. Duela gutxiko ikerketek erakutsi dute niosomak gai direla arratoien erretinako zein garuneko zelulak *in vivo* transfektatzeko<sup>23-26</sup>.

Bektoreaz gain, horrek garraiatzen duen material genetikoaren ezaugarriak ere oso garantzitsuak dira transfekzio-prozesuan. Oraintsu arte, gene-terapiaren

## Eztabaida

eraginkortasuna handitzeko estrategia ia guztiak bektoreen egokitzapenetan edota elekpororazioa bezalako prozesu fisikoaren erabilera oinarritzen ziren. Hala ere, transfekzio-efizientziaren hobekunza material genetikoaren konposizioan eta konformazioan aldaketak eginez ere lortu daiteke, adibidez, bere bioerabilgarritasuna, biobateragarritasuna, iraunkortasuna eta segurtasuna areagotuz<sup>27</sup>. Zentzu horretan, azken aldean ikerketa-talde batzuk *minicircle* (MC) teknologia garatu dute, hau da, DNA plasmidoei bakteria-sekuentziak ezabatu dizkiete eta soilik gene terapeutikoa eta sekuentzia erregulatzaila mantendu dituzte<sup>28</sup>. Plasmidoetako sekuentzia prokariotikoak, besteak beste CpG motiboak, erreplikazio jatorria eta antibiotikoekiko erresistentzia, beharrezkoak dira plasmidoak bakterioetan hedatzeko, baina material genetikoaren bioerabilgarritasuna eta segurtasuna gutxitzen dituzte. Iza ere, hainbat ikerketa klinikoren arabera, CpG sekuentzia ez-metilatuek hantura erantzuna pizten dute<sup>29</sup>, <sup>30</sup> eta baita nekrosi- edo apoptosis-bidezko zelula heriotza ere, transgene-expresioa modu esanguratsuan murriztuz<sup>31</sup>, <sup>32</sup>. Gainera, kasu batzuetan zeluletan transkripzio-faktoreek ez dute modurik izaten plasmidoen sekuentziatarri iristeko, adibidez, histona-markatzaileekin lotutako bakterio-sekuentziak transgenetik gertu kokatuta daudenean. Markatzaile horiek berehala ezagutzen ditu ostatu-zelulak eta plasmido-sekuentziak heterokromatina konpaktu bilakatzea eragiten du, transgenearren expresioa oztopatuz eta, askotan, erabat isilaraziz<sup>33</sup>. Beraz, expresio-unitate minimizatuak, *minicircle*-ak kasu, plasmidoen ordez erabili daitezke horien mugak gainditu eta transfekzio eraginkorragoak lortze aldera. *In vitro* zein *in vivo* ikerketa ugarik erakutsi dute *minicircle* teknologia erabilita transfekzio-efizientzia igo egiten dela, expresio iraunkorrik lortzen direla eta segurtasun zein immuno-bateragarritasun profil hobeak lortzen direla<sup>28</sup>. Horrez gain, *miniDNA* bektoreek erraztasun handiagoa dute zelulaz kanpoko zein barneko hesiak gainditu eta zelulen nukleoraino iristeko, plasmidoena baino bioerabilgarritasun handiagoa lortuz<sup>34</sup>.

Azkenik, bektoreak eta material genetikoa azterzeaz eta hobetzeaz gain, gene-garraio sistema ez-biral eraginkorrik lortzeko, horiek beste teknologia batzuekin uztartzea da gaur egungo joera nagusietako bat. Adibidez, gene-garraio sistemak eta ehun-ingeniaritza konbinatu daitezke sinergia berriak lortzeko. Iza ere, konbinaketa horiek ekar ditzaketen abantailen artean, garraio-sistemek egonkortasun handiagoa eta toxikotasun baxuagoa dira aipagarrienak. Gainera, bektore ez-birralak, esaterako, hiru dimensioko matrize edo hidrogeletan txertatuta, epe luzeko gene-garraio lokalizatua lortu daiteke eta, horrek, gene-terapiaren

## *Eztabaida*

aplikazio klinikoa erraztuko luke hainbat gaixotasunetan, besteak beste, minbizian edota ehunen birsorkuntzan<sup>35, 36</sup>.

Aurreko guztia kontutan hartuta, doktoretza-tesi honen helburua gene-garraiorko sistema ez-biral eraginkorren garapenean sakontzea izan da, horretarako ondorengo aspektu nagusien inguruko ikerketan oinarritura: (i) material ezberdinez –lipido kationikoz, polimeroz eta nanopartikula magnetikoz- osatutako hiru bektore ez-biralen arteko konparaketa ezaugarri fisiko-kimikoei eta endotelio baskularraren hazkunza faktorearen genea daraman plasmidoa nerbio sistema zentraleko zeluletara garraiatzeko gaitasunari dagokienez; (ii) niosomen tentsoaktibo ez-ionikoak transfekzio-prozesuan eta eraginkortasunean duen garrantziaren azterketa, (iii) material genetikoaren ezaugarriek niosomek bideratutako transfekzio-efizientzian duten garrantziaren azterketa hiru DNA molekula ezberdinaren konparaketaren bitartez eta (iv) niosomen eta azido hialuronikoz osatutako hidrogelen arteko konbinaketaren ikerketa transfekzio lokalizatua eta eraginkorra lortze aldera. Ondorengo ataletan, doktoretza-tesian ikertutako aspektu horiek guztien eztabaida sakona egingo da.

- 1. Bektore ez-biralen osagaien eragina endotelio baskularraren hazkunza-faktorearen genea daraman plasmidoa nerbio sistema zentraleko zeluletara garraiatzeko eta horien transfekzioa burutzeko gaitasunean.**

Azido nukleikoen erabilera oinarritzen diren terapietan itxaropen handia pitzu dute, baina bektore eraginkor eta seguruen beharra dute. Gainera, nerbio sistema zentraleko (NSZ) zelulak transfektatzea erronka handia da oraindik eta hori oztopo da neuroendekapenezko gaitzei aurre egiteko gene terapeutikoen garraioan oinarritzen diren estrategien garapenarentzat. Azken urteetan, nanomaterial biobateragarriek bide berriak zabaldu dituzte erronka horri aurre egiteko. Izen ere, zenbait ikerketaren arabera, nanopartikulaz osatutako bektore ez-biralak gai dira NSZko zelulak transfektatzeko, besteak beste, kitosanoz osatutako partikulak<sup>37, 38</sup>, lipido kationikoak<sup>39</sup> edota nanopartikula magnetikoa<sup>17</sup>. Bestalde, endotelio baskularraren hazkunza-faktorea (VEGF) hautagai egokia izan daiteke gene terapeutiko gisa NSZri eragiten dioten gaitzei aurre egiteko<sup>40</sup>, garuneko asaldura baskularren eta neuroendekapenezko gaitzen artean dagoen lotura estuagatik<sup>41</sup> eta baita proteina horrek garuneko angiogenesian zein neuronen biziraupenean jokatzen dituen rol espezifikoengatik ere<sup>42, 43</sup>.

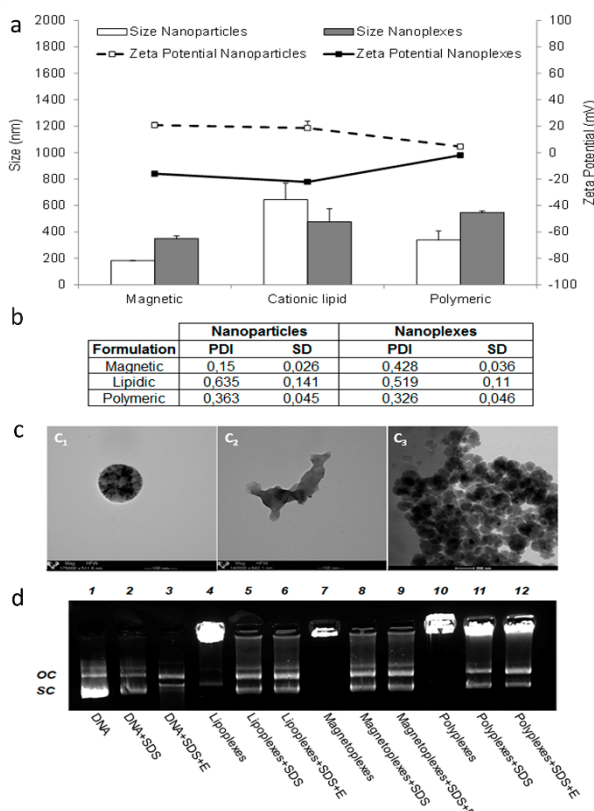
## Eztabaida

Aurrekoa kontuan hartuta, nanoformulazioetan oinarritutako estrategia terapeutiko bat proposatu dugu ikerketa honetan, VEGF genea NSZko zeluletara garraiatu eta horiek transfektatzeko asmoz. Horretarako, hiru nanoformulazio ezberdin erabili ditugu, hiru material ezberdinez osatuta daudenak: oligokitosano ultrapuruz (UOC) osatutako bektore polimerikoa, Lipofectamine 2000™ bektore lipidikoa eta *Neuromag* partikula magnetikoak. Formulazio horiei phVEGF165aIRESGFP plasmidoa gehitu zitzaien, giza VEGF165a proteinaren eta GFP proteina berde fluoreszentearen sekuentziak daramatzana. Nanoformulazioak eta DNA molekulak elkartuta nanoplexoak osatu genituen, alegia, poliplexoak, lipoplexoak eta magnetoplexoak, hurrenez hurren. Nanoformulazioak eta dagozkien nanoplexoak fisiko-kimikoki karakterizatu genituen tamainari, zeta potentzialari, polidispersio indizeari (PDI), morfologiari eta DNA eusteko, babesteko eta askatzeko duten gaitasunari dagokionez. *In vitro* transfekzio entseguak egin genituen C6 gliazeluletan eta neurona kultibo primarioetan NSZko zelula-eredu gisa, eta HEK-293 zeluletan transfekzio-eredu orokor gisa. Transfekzio-efizientzien ebaluazioa GFP proteinaren expresioa, bataz besteko fluoreszentzia intentsitatea (MFI) eta VEGF proteinaren produzioa neurtuta egin zen. Zelulen biziraupena ere aztertu zen nanoplexoien eraginpean egon ostean. VEGF proteinaren bioaktibitatea neurtzeko proteina horren efektuarekiko sentiberak diren HUVEC edo zilborresteko giza endotelio-zelulak erabili ziren.

Nanoformulazio eta nanoplexo –magnetoplexo, lipoplexo eta poliplexo- guztiekin nanometro-eskalako tamaina zuten (1.1.a irudia, barrak), eta hori egokia da formulazioek zelulan sartzeko duten gaitasuna hobetzeko<sup>44</sup>. Gainera, nanoformulazioek gainazaleko karga positiboak zituzten denek (1.1.a irudia, lerroak), ezinbesteko ezaugarria karga negatibodun DNA molekulekin elkarrekintza elektrostatikoak eratzeko<sup>45</sup>. Espero bezala, behin DNA molekulekin lotuta, nanoplexoien zeta potentzialak balio negatiboak hartu zituen kasu guztieta. Magnetoplexoien eta lipoplexoien zeta potentzialak -20 mV ingurukoak izan ziren neurketetan, poliplexoenak berriz zerotik gertu agertu ziren. Literaturaren arabera, -20 mV baino gutxiagoko eta +20 mV baino gehiagoko zeta potentziala duten partikulek joera txikiagoa dute agregatuak sortzeko, aldiz, bi balio horien arteko zeta potentzial balioak dituzten partikulek joera handiagoa izango lukete euren artean agregazioa sortzeko<sup>46</sup>. Beraz, batez ere poliplexoen kasuan, agregazioa ekiditeko, formulazioak prestatu berritan erabili ziren lan honetan. PDI balioak 0,5 baino baxuagoak izan ziren kasu guztieta, orokorrean onargarritzat jotzen den balioa aldi berean eta metatze-analisiengatik neurtutako partikulen arteko konparaketak egiteko<sup>47</sup>. Salbuespena lipido kationikoen PDI balioak izan ziren oso altuak zirelako,

## Eztabaidea

eta horretarako arrazoia nanoformulazio horien tamaina irregularra izan daiteke (1.1.c irudia). Nanopartikulek DNA molekulak eusteko, babesteko eta askatzeko zuten gaitasuna aztertzeko, elektroforesia egin genuen agarosa geletan (1.1.d irudia). Emaitzan arabera, nanoformulazioak gai izan ziren DNA molekulak degradaziotik babesteko eta gogor eutsi zioten DNArri, geleko putzuetan itsatsita geratu baitzen hau. Hala ere, DNA askatzeko gaitasuna ere erakutsi zuten nanoformulazioek, eta euste- eta askatze-gaitasunaren arteko erlazio orekatua ezinbestekoa da transfezkzia eraginkortasunez bideratu ahal izateko<sup>48</sup>.



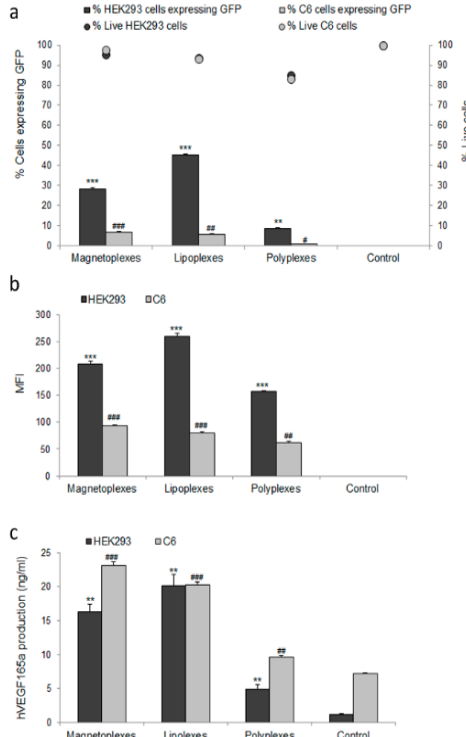
**1.1. Irudia.** Nanopartikulen eta nanoplexoien karakterizazio fisiko-kimikoa. (a) Tamaina (barra txuriak eta grisak, nanopartikulei eta nanoplexoiei dagozkienak hurrenez hurren) eta zeta potentziala (ierro puntukatuak eta jarraiak, nanopartikulei eta nanoplexoiei dagozkienak hurrenez hurren). Balio bakoitzak bataz besteko  $\pm$ SD adierazten du, n = 3. (b) PDI balioak. Balio bakoitzak bataz besteko  $\pm$ SD adierazten du, n = 3. (c) TEM bidezko nanopartikula magnetikoen (c1) eta lipido kationikoen (c2) irudiak eta cryo-TEM bidezko UOC nanopartikula

## Eztabaida

polimerikoen (c3) irudiak. Jatorrizko magnifikazioa: x140.000 lipido kationikoen kasuan, x175.000 nanopartikula magnetikoen kasuan eta x25.000 UOC nanopartikula polimerikoen kasuan. (d) Nanopartikulek duten gaitasuna DNA molekulak eusteko, babesteko eta askatzeko agarosa geleko elektroforesan. 1-3 zutabeak: bektorerik gabeko DNA askea; 4-6 zutabeak: lipoplexoak; 7-9 zutabeak: magnetoplexoak; 10-12 zutabeak: poliplexoak. DNA askea eta nanoplexoei SDS (2, 5, 8 eta 11 zutabeetan) eta DNase I + SDS (3, 6, 9 eta 12 zutabeetan) gehitu zitzaien. OC: DNAren forma zirkular irekia. SC: DNAren forma super-kiribildua.

---

Nanoplexoak fisiko-kimikoki karakterizatu ostean, *in vitro* entseguak egin genituen hiru zelula-lerrotan: HEK-293 –transfekzio-eredu orokorra-, C6 glia-zelulak –NSZko transfekzio eredu- eta neurona kultibo primarioetan –NSZko zelula-eredu aipagarriena-. Lehenik eta behin, nanoformulazioen transfekzio-efizientzia eta horiek zelulen biziraupenean duten eragina HEK-293 eta C6 zeluletan aztertu genituen. Nanoplexoen onarpema biziraupen aldetik egokia izan zen bi zelula-lerroetan, zelulen %80 inguruk biziraun baitzuen nanoplexoen eraginpean egon ondoren (1.2.a irudia, puntuak). Transfekzio-efizientziaren analisia egiteko hiru parametro hartu genituen kontuan: GFP proteinaren espresioa izan zuen zelulen ehunekoa 1.2.a irudia, barrak), zelula transfektatueten MFI balioak (1.2.b irudia) eta zelula transfektatuek ekoiztutako VEGF proteinaren kontzentrazioa ng/ml-tan (1.2.c irudia). Erabilitako plasmidoak bi proteinen gene-sekuentzia dauka, VEGF –zelulaz kanpoko proteina eta, beraz, zelulaz kanpoko mediora jariatzten dena- eta GFP –zelulaz barnekoa eta, beraz, zitoplasman geratzen dena-. Hori dela eta, GFP proteinarekin lotutako parametroak fluxu-zitometriaren bidez neurtu ziren eta VEGF proteinari dagozkionak, berriz, ELISA teknikaren bitartez. GFP proteinaren espresioa zuten zelula-ehunekoari eta MFI balioei dagokienez, transfekzio-efizientziak altuagoak izan ziren HEK-293 zeluletan C6 zeluletan baino nanoplexo guztiekin. Aldiz, VEGF proteinaren ekoizpena antzekoa izan zen bi zelula-lerroetan eta, magnetoplexoen kasuan, balio hori altuagoa izan zen C6 zeluletan HEK-293 zeluletan baino. Literaturaren arabera, bektore ez-biralen bidezko transfekzio-efizientziak zelula-motaren araberakoak dira eta, beraz, horiek zelula-mota batetik bestera ezberdinak izan daitezke<sup>49</sup>. Gure emaitzak bat datozi ideia horrekin, zeren eta HEK-293 zelula-lerroan transfekzio-maila altuena lipoplexoekin lortu genuen eta C6 zeluletan, aldiz, magnetoplexoekin. Poliplexoak izan ziren transfekzio-maila baxuenak lortu zituztenak bi zelula-lerroetan, ziurrenik euren zeta potentzial balioa (zerotik gertuko) dela eta, horrek zeluletan barneratzeko gaitasuna kaltetu dezakeelako.



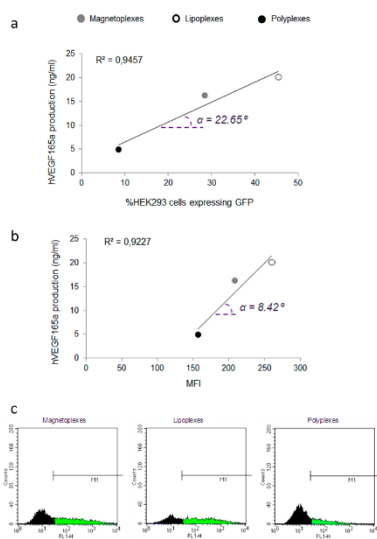
eraginpean egon. Balio bakoitzak bataz besteko  $\pm$ SD adierazten du, n = 3. Esangura estatistiko maila: \*p < 0,05, \*\*p < 0,01, \*\*\*p < 0,001 HEK-293 zelula-kontrolekiko; #p < 0,05, ##p < 0,01, ###p < 0,001 C6 zelula-kontrolekiko.

**1.2. Irudia.** Zelulen biziraupena eta nanoplexoen transfekzio-efizientzia HEK-293 eta C6 zelula-lerroetan. (a) Zelulen biziraupena (HEK-293 zelulak, puntu gris ilunak eta C6 zelulak, puntu gris argiak) eta transfekzio-efizientzia (HEK-293 zelulak, barra gris ilunak eta C6 zelulak, barra gris argiak) nanoplexoekin transfekzioa egin eta 48 ordura. Zelula-kontrolak ez ziren nanoplexoen eraginpean egon. Balio bakoitzak bataz besteko  $\pm$ SD adierazten du, n = 3. (b) MFI balioak (HEK-293 zelulak, barra gris ilunak eta C6 zelulak, barra gris argiak) nanoplexoekin transfekzioa egin eta 48 ordura. Zelula-kontrolak ez ziren nanoplexoen eraginpean egon. Balio bakoitzak bataz besteko  $\pm$ SD adierazten du, n = 3. (c) VEGF ekoizpena (ng/ml-tan) (HEK-293 zelulak, barra gris ilunak eta C6 zelulak, barra gris argiak) nanoplexoekin transfekzioa egin eta 48 ordura. Zelula-kontrolak ez ziren nanoplexoen

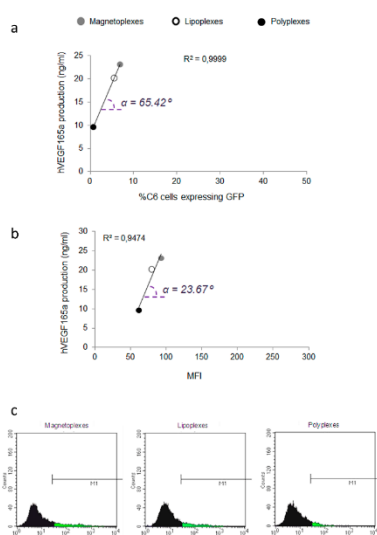
Aipagarria da korrelazio argia zegoela bi zelula-lerroetan transfekzio-efizientzia neurtzeko erabilitako hiru parametroen artean. GFP proteinaren expresioa zuten zelula-ehunekoa zenbat eta altuagoa izan, orduan eta VEGF ekoizpen altuagoa antzeman genuen (1.3.a eta 1.4.a irudiak). Era berean, zenbat eta MFI balio altuagoak izan, orduan eta VEGF ekoizpen altuagoa antzeman genuen (1.3.b eta 1.4.b irudiak). Hala ere, malda-angeluak konparatuta, ezberdintasunak topatu genituen bi zelula-lerroen artean. Izan ere, malda nabarmenagoa zen C6 zeluletan HEK-293 zeluletan baino bi korrelazioei dagokienez –1.3.a eta 1.4.a irudietan,  $\alpha = 22,65^\circ$  HEK-293 zeluletan eta  $\alpha = 65,42^\circ$  C6 zeluletan; 1.3.b eta 1.4.b irudietan,  $\alpha = 8,42^\circ$  HEK-293 zeluletan eta  $\alpha = 23,67^\circ$  C6 zeluletan-. Emaitza horiek bat datozen lehenago aipatutakoarekin, alegia, nahiz eta GFP expresioan eta MFI balioetan

### *Eztabaida*

ezberdintasunak dauden nanoplexoekin tansfektatutako bi zelula-lerroen artean, VEGFren ekoizpena antzekoa dela bi kasuetan. Fenomeno horren arrazoietako bat izan daiteke C6 zelulek modu basalean HEK-293 zelulek baino VEGF gehiago ekoizten dutela berez (1.2.c irudia, kontrol-barrak). Beraz, nahiz eta transfekzio-maila baxuagoa izan, VEGF ekoizpena HEK-293 zelulen mailara iritsi daiteke. Hala ere, beste faktoreren batek ere parte hartu behar du fenomeno hori guztiz azaldu ahal izateko. Zentzu horretan, uste dugu plasmidoaren IRES (*Internal Ribosome Entry Site*) sekuentziak, VEGF eta GFP geneak bereizten dituenak, eragina izan dezakeela. IRES sekuentziak translazioa abiarazten duten faktoreak dira eta bi generen aldi bereko espresio bereitzua ahalbidetzen dute, alegia, kasu honetan, VEGF eta GFP geneak promotore beraren gidaritzapean egongo lirateke baina bi proteina ezberdin sortzen dituzte proportzio berean IRES sekuentziari esker<sup>50, 51</sup>. Halere, jakina da IRES sekuentziak ez direla beti gai bi proteinen arteko proportzioa konstante mantentzeko eta, askotan, efizientzia baxua dutela behin-behinean transfektatutako zeluletan ehun- edota zelula-motaren arabera<sup>52, 53</sup>. Kasu horietan, IRESaren ondoren datorren genearen espresioa kaltetzen da, IRESaren aurretik doan genearen espresioan aldaketarik egon gabe<sup>54</sup>. Gure kasuan, VEGF genea IRES sekuentziaren aurretik doa eta GFP genea, berriz, atzetik. Beraz, uste dugu IRESa dela eta, GFP proteinaren espresioa kaltetuta egon daitekeela NSZko zeluletan, alegia, C6 zeluletan. Horrek azalduko luke VEGF ekoizpenean ia diferentziarik egon ez arren GFPren espresioa baxuagoa izatea C6 zeluletan HEK-293 zelulekin alderatuta.



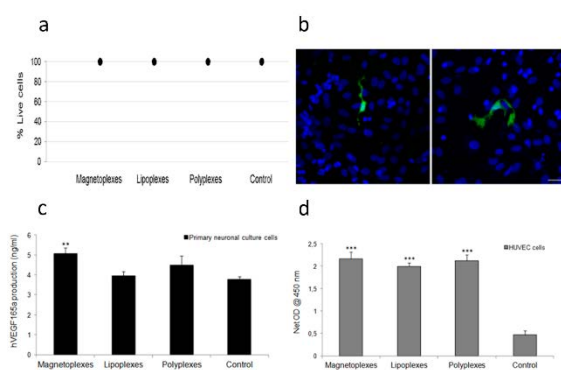
**1.3. Irudia.** Transfekzio-efizientzia neuritzeko erabilitako parametroen arteko korrelazioa HEK-293 zeluletan. (a) VEGF ekoizpenaren (ng/ml) eta GFP espresatzen dute zelula-ehunekoaren arteko korrelazioa magnetoplexoekin (puntu grisa), lipoplexoekin (puntu zuria) eta poliplexoekin (puntu beltza) transfekzioa egin eta 48 ordura. Balio bakoitzak bataz besteko  $\pm SD$  adierazten du, n = 3.  $\alpha$  sinboloak maldaren angelua adierazten du. (b) VEGF ekoizpenaren (ng/ml) eta MFI balioen arteko korrelazioa nanoplexoekin transfekzioa egin eta 48 ordura. Balio bakoitzak bataz besteko  $\pm SD$  adierazten du, n = 3.  $\alpha$  sinboloak maldaren angelua adierazten du. (c) GFP espresioaren araberako histogramak HEK-293 zeluletan nanoplexoekin transfekzioa egin eta 48 ordura. M1 da GFP seinale positiboaren atalasea.



**1.4. Irudia.** Transfekzio-efizientzia neuritzeko erabilitako parametroen arteko korrelazioa C6 zeluletan. (a) VEGF ekoizpenaren (ng/ml) eta GFP espresatzen dute zelula-ehunekoaren arteko korrelazioa magnetoplexoekin (puntu grisa), lipoplexoekin (puntu zuria) eta poliplexoekin (puntu beltza) transfekzioa egin eta 48 ordura. Balio bakoitzak bataz besteko  $\pm SD$  adierazten du, n = 3.  $\alpha$  sinboloak maldaren angelua adierazten du. (b) VEGF ekoizpenaren (ng/ml) eta MFI balioen arteko korrelazioa nanoplexoekin transfekzioa egin eta 48 ordura. Balio bakoitzak bataz besteko  $\pm SD$  adierazten du, n = 3.  $\alpha$  sinboloak maldaren angelua adierazten du. (c) GFP espresioaren araberako histogramak C6 zeluletan nanoplexoekin transfekzioa egin eta 48 ordura. M1 da GFP seinale positiboaren atalasea.

## Eztabaida

Behin nanoplexoek HEK-239 eta C6 lerro zelularrak transfektatzeko zuten gaitasuna aztertuta, gene-transferentzia entseguak egin genituen neurona kultibo primarioetan, horiek NSZko eredu gisa esanguratsuagoak direlako. Zelula-biziraupena (1.5.a irudia) bikaina izan zen kasu guztieta –%100 inguru nanoplexo guztiekin-, baina transfekcio-efizientziak (1.5.a-b irudia) aurreko zelula-lerroetan baino baxuagoak izan ziren, neurona-zelulak baitira transfektatzen zailenetakoak. GFP proteinaren expresioa kasu honetan immunozitokimika bidez aztertu zen (1.5.b irudian fluoreszentzia berdedun zelula bakan batzuk ikus daitezke). Horrek berriro ere erabilitako plasmidoaren IRES sekuentziaren ehun-espezifikotasunaren hipotesia babesten du. VEGF proteinaren expresioari dagokionez, emaitzen arabera neurona kultibo primarioetako zelulek modu basalean VEGF endogeno kantitate handiak ekoizten dituzte eta, ziurrenik glia-zelulak dira horren erantzule, jakina baita faktore angiogenikoak<sup>55</sup> eta neurotrofikoak<sup>56</sup> askatzea dela euren funtzio nagusietako bat NSZko beste zelulei babesa emateko. Modu guztieta, nanoplexoekin transfektatutako zelulen VEGF ekoizpena zelula-kontrolena baino altuagoa izan zen kasu guztieta, baina differentzia estatistikoki esanguratsua kontrolekiko soilik magnetplexoekin lortu zen (1.5.c irudia). Jarraian, zelula transfektatuek ekoitzutako VEGF proteinaren aktibitate biologikoa ikertu genuen HUVEC zelula-lerroan, proteina horren efektuari bikoizketa azkarraz erantzuten diona<sup>57, 58</sup>. Kontrolarekin konparatuta –VEGFren eraginpean jarri gabeko zelulak-nanoplexoekin transfektatutako zelulek askatutako VEGF proteinaren eraginpean egondako zelulek bikoizte-tasa altuagoa erakutsi zuten. Horrek baieztagatzen du VEGF gai dela zelula-lerro horretan bikoizketa abiarazteko eta, gainera, bikoiztasaren igoera VEGF kontzentrazioarekiko proporcionala izan zen. Aipagarria da, beraz, magnetoplexoak izan zirela eraginkorrenak NSZko zelulak transfektatzen, atzetik poliplexoak eta, azkenik, lipoplexoak zituztela.



**1.5. Irudia.** Zelula-biziraupena, transfekcio-efizientzia eta VEGF proteinaren aktibitate biologikoa neurona kultibo primarioetan nanoplexoekin eraginpean egon eta 48 ordura. (a) Zelula-biziraupena. Balio bakoitzak bataz besteko  $\pm$ SD adierazten du, n = 3. (b) Transfektatutako neurona kultibo primarioen immunohistokimika irudiak.

## *Eztabaida*

Berdez, anti-GFP. Urdienz, Hoescht. Eskala-barra: 25 µm. (c) VEGF ekoizpena (ng/ml-tan) nanoplexoekin transfektatutako neurona kultibo primarioetan. Kontrol-zelulak ez ziren nanoplexoen eraginpean egon. Balio bakoitzak bataz besteko ±SD adierazten du, n = 3. (d) HUVEC zelula-lerroaren bikoizketa-erantzuna VEGF proteinaren eraginpean egon ondoren. Kontrol-zelulak ez ziren VEGF proteinaren eraginpean egon. Balio bakoitzak bataz besteko ±SD adierazten du, n = 6. Esangura estatistiko maila: \* $p < 0,05$ , \*\* $p < 0,01$ , \*\*\* $p < 0,001$  HUVEC zelula-kontrolekiko.

Emaitzak horiek kontuan hartuta, esan genezake bektore ez-biralak eta, batez ere, nanopartikula magnetikoak, VEGF genea NSZko zeluletara modu seguru eta eraginkorrean garraiatzeko aukera egokia izan daitezkeela, beste ikerketa batzuek bat datozen emaitzak izanik<sup>17</sup>. Alterazio baskularren eta neuroendekapen prozesuen arteko erlazioa<sup>40</sup> aintzat hartuta eta baita VEGF proteina Alzheimer gaixotasun ereduko<sup>59</sup> zein Parkinson gaixotasun ereduko<sup>57</sup> animalietan izan dituen efektu onuragarriak ere, uste dugu VEGF gene terapeutikoa hautagai ona izan daitekeela NSZko gaitzei aurre egiteko. Bestalde, farmako-garraioarekin konparatuta, VEGF gene-garraioari esker dosiak gutxitzea eta denboran iraunkorrik diren efektu terapeutikoak lortzea posible izango litzateke. Gaur egun, bektore ez-biralak NSZra helaraztea erronka handia da oraindik ere eta, askotan, eman-bide inbaditzaileak erabili behar izaten dira, adibidez, garuneko ebakuntza. Hala ere, aurrerapauso handiak ari dira egiten zentzu horretan eta duela gutxiko ikerketa batek erakutsi du posible dela bektore ez-biralak garunera sudur-barneko eman-bide ez-inbaditzailea erabilita iristea<sup>60</sup>. Beraz, komenigarria litzateke arreta berezia jartzea sudur-barneko eman-bidearen ikerketan, alternatiba seguru eta ez-inbaditzailea baita NSZko zeluletara alegatzeko.

## **2. Niosoma formulazioetako tentsoaktibo ez-ionikoaren rola arratoi-erretinako zelulen transfekzio-prozesuan eta eraginkortasunean**

Erretinako gaitz monogeniko asko ondo karakterizatuta daude eta horien erantzule diren geneak eta inplikatutako mutazioak ondo ezagutzen dira. Kasu gehienetan, mutazioek erretinako epitelio pigmentarioko (RPE) zelulei eragiten diete<sup>61</sup> eta zelulamota horren funtzio nagusia erretina neurala mantentzea izaten da, adibidez, foto-errezeptore gisa jarduten duten zelulak babestuz eta hazkuntza-faktoreak askatuz<sup>62</sup>. Erretinako gaixotasun askotan, besteak beste Leberren amaurosi kongenitoa (LCA), erretinitis pigmentosoa (RP) edota adinari lotutako endekapen makularra (AMD), RPEko zelulen endekapenak itsu geratzea eragin dezake. Iza ere, RPEko zelulen degenerazioak foto-errezeptoreen galera edota disfuntzioa eragiten ditu<sup>61</sup>. Beraz,

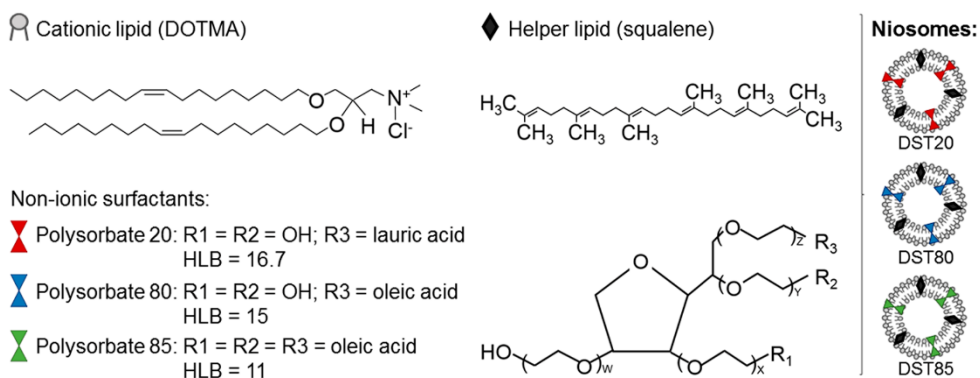
## *Eztabaida*

RPEko zelulak jomuga dira erretinako gaitz genetikoei aurre egiteko gene-terapia bidezko estrategia gehienetan. Erretinako gene-transferentziaren arrakasta transgene-espresio altu eta iraunkorrik lortzearen menpe dago kasu gehienetan.

Bektore ez-biralen bidezko gene-garraioak aukera aparta eskaintzen du gene terapeutikoak modu seguru eta eraginkorrean erretinara bideratzeko. Niosoma izeneko bektore ez-birala arrakasta handiz erabili dira zentzu horretan *in vitro* zein *in vivo* entseguetan. Formulazio horiek hiru osagai nagusi dituzte eta horietako biren -lipido kationikoaren eta lipido laguntzailearen- eragina transfekzio prozesuan eta eraginkortasunean ondo aztertuta daude<sup>26, 63</sup>. Bestalde, DOTMA lipido kationikoaz<sup>18</sup> edota Tween 80 tentsoaktibo ez-ionikoaz eta eskualeno lipido laguntzaileaz<sup>26</sup> osatutako niosoma formulazioen eraginkortasuna frogatuta dago erretinako zelulen transfekzioan. Hala eta guztiz ere, beste tentsoaktibo ez-ioniko batzuen erabilera, esaterako Tween 20 edo Tween 80, ez da oraindik ikertu gene-transferentzia prozesuetan. Beraz, lan honetan hiru niosoma formulazio prestatu eta aztertu genituen, soilik tentsoaktibo ez-ionikoan ezberdinak zirenak. Hiru niosoma formulazioen osagaiak ondokoak izan ziren: DOTMA lipido kationikoa, eskualenoa lipido laguntzaile gisa eta Tween 20, 80 edo 85 tentsoaktibo ez-ionikoetako bat. Horrela, DST20, DST80 eta DST85 izeneko niosoma formulazioak osatu genituen. Horiek fisiko-kimikoki karakterizatu ostean, transfekzio- eta zelula-barneko trafiko-entseguak egin genituen *in vitro* eta, jarraian, arratoi-erretinako zelulak transfektatu genituen *in vivo*.

Niosoma formulazioetan, tentsoaktibo ez-ionikoen emulsionatzale gisa jarduten dute, hesi esteriko bat sortuz partikulen agregazioa ekiditeko<sup>22</sup>. Lan honetan erabilitako hiru tentsoaktiboek oinarritzko egitura kimiko bera dute, baina beren atal hidrofilikoak eta daukaten hidrozilo-talde kopurua ezberdinak dira (2.1. irudia). Ezberdintasun kimiko horiek direla eta, Tween 20, 80 eta 85 tentsoaktiboek hidrofilo-lipofilo balantze (HLB) balio desberdinak dituzte. HLB balioak molekularen olio- (HLB < 9) edo ur-disolbagarritasuna (HLB > 11) adierazten du<sup>64</sup>, eta lan honetan erabilitako tentsoaktiboen artean, Tween 20 da hidrofilikoena azido laurikoaren eta 2 hidroxilo-talderen eraginez (HLB = 16,7). Aldiz, Tween 85 lipofilikoena da (HLB = 11), bere egitura kimikoak dituen hiru azido oleikoak direla eta.

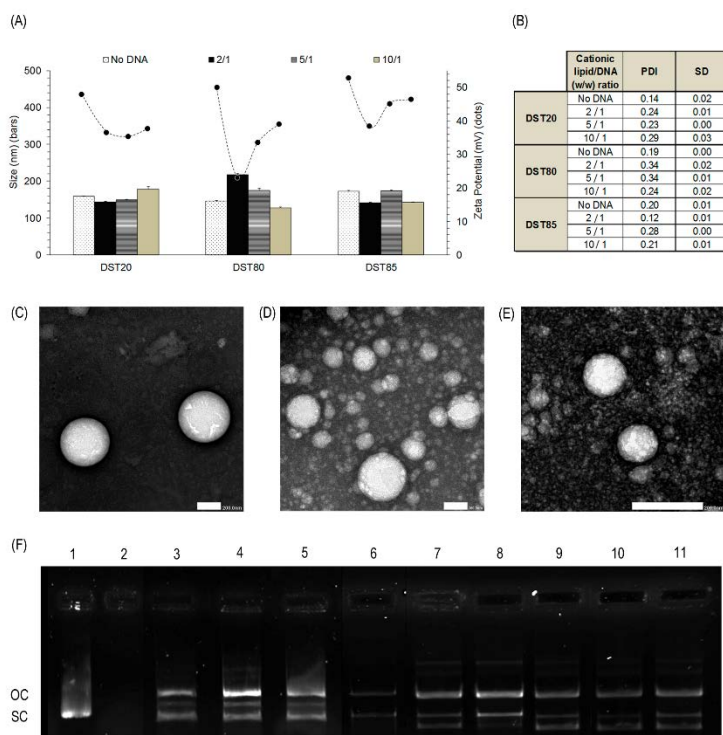
## Eztabaida



### 2.1. Irudia. Niosomen eskema orokorra eta niosomen osagaien egitura kimikoak.

Formulazioen parametro fisiko-kimikoek transfekzio-efizientzia baldintzatu dezakete. DST20, DST80 eta DST85 partikulek 100 eta 225 nm arteko tamainak zituzten (2.2.A irudia, barrak) eta horiek egokiak dira gene-garraioan erabiltzeko<sup>65</sup>. Partikulen tamainan oszilazio txikiak topatu genituen nioplexoak lortzeko niosmei DNA molekulak 2/1, 5/1 eta 10/1 lipido kationikoa/DNA masa ratioetan gehitu ondoren. Aldaera horiek DNA molekulek hartzen duten espazioaren eta ratio altuetan gertatzen den DNAren kondentsazio handiagoaren balantzearen araberakoak izaten dira<sup>26</sup>. Egoera guztietan, PDI balioek erakusten dutenez, formulazioen tamainen distribuzioa estua izan zen, beraz, partikulek tamaina homogeneoak zituztela ondorioztatu dezakegu (2.2.B irudia). Formulazioen gainazaleko kargari dagokionez, horrek formulazioaren egonkortasuna baldintzatzen du eta -30 mV eta +30 mV arteko zeta potentzial balioek partikulen agregazioa eragiten dutela uste da<sup>46</sup> eta, beraz, hobe da balio horiek baino negatiboagoak edo positiboagoak diren partikulak sortzea. Gainera, zeta potentzial balio positiboak zelulan barneratzeko gaitasun handiagoarein erlazionatuta daude, mintz plasmatikoak karga negatiboa duenez, elkarrekintza elektrostatikoak sortzen direlako karga positibodun nanopartikulekin<sup>45</sup>. Lan honetako hiru niosoma formulazioek zeta potentzial balio egokiak agertu zituzten, +40 mV-etik gorakoak (2.2.A irudia, puntuak). Espero bezala, DNA molekulak gehitzean, gainazaleko kargen balioak jaitsi egin ziren, niosomen amina taldeek DNAren fosfato taldeekin elkarrekintzak osatu zituztelako eta, beraz, kargak partzialki neutralizatu zirelako<sup>66</sup>. Gure partikulen morfologia aztertzeko, TEM bidezko mikroskopio irudiak atera genituen eta denek itxura esferikoa zutela baieztago genuen (2.2.C-E irudiak). Formulazioek DNA babesteko eta askatzeko zuten gaitasuna aztertzeko

elektroforesi-entseguak egin genituen agarosa geletan. Gure emaitzen arabera, formulazio guztiak gai izan ziren DNA molekulak babesteko, baita lipido kationikoa/DNA masa ratio baxuenetan ere. Beharbada, DST80 nioplexoak izan ziren salbuespina, ratio baxuetan DNA babesteko gaitasun baxuagoa erakutsi zuten eta. Modu guztieta, kontuan hartuta ratio baxuak erabiltzeak gene-terapien abantaila handiak dakartzala, aipagarriena DNA dosi handiagoak erabili ahal izatea lipido gutxirekin –oso egokia *in vivo* entseguetarako-, ondorengo entseguetarako 2/1 ratio baxua aukeratu genuen formulazio guztieta.



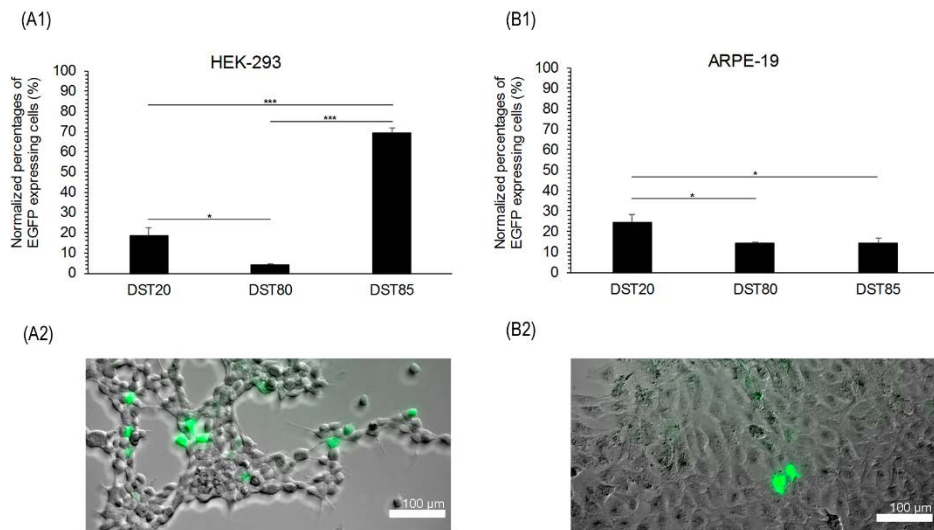
**2.2. Irudia.** DST20, DST80 eta DST85 niosoma eta nioplexoen karakterizazio fisiko-kimikoa, ondoko lipido kationikoa/DNA masa ratioak erabilita: 2/1, 5/1 eta 10/1. (A). Tamaina balioak barren bidez adierazita daude eta zeta potentzialak, puntuen bidez. Balio bakoitzak bataz besteko  $\pm$ SD adierazten du,  $n = 3$ . (B) PDI balioak. Balio bakoitzak bataz besteko  $\pm$ SD adierazten du,  $n = 3$ . (C-E) Niosomen TEM irudiak. Eskala-barrak: 200,0 nm. (C) DST20 niosomak x20.000 magnifikazioan, (D) DST80 niosomak x20.000 magnifikazioan eta (E) DST85 niosomak x40.000 magnifikazioan. (F) Elektroforesi-entsegu agarosa geletan, DST20, DST80 eta DST85 formulazioek DNA babesteko eta askatzeko duten gaitasuna

### *Eztabaida*

aztertzeko lipido kationikoa/DNA masa ratio ezberdinan. DNase I entzima gehitu zen 2-11 zutabeetan. 1-2 zutabeetan DNA askea dago. 3, 4 eta 5 zutabeetan DST20 nioplexoak ageri dira 2/1, 5/1 eta 10/1 ratioetan, hurrenez hurren. 6, 7 eta 8 zutabeetan DST20 nioplexoak ageri dira 2/1, 5/1 eta 10/1 ratioetan, hurrenez hurren. 9, 10 eta 11 zutabeetan DST20 nioplexoak ageri dira 2/1, 5/1 eta 10/1 ratioetan, hurrenez hurren. OC: DNArren forma zirkular irekia. SC: DNArren forma super-kiribildua.

---

Behin formulazioak erabat karakterizatu ostean, *in vitro* transfekzio-entseguak egin genituen lipido kationikoa/DNA 2/1 masa ratioa erabilita bi zelula-lerrotan: HEK-293, transfekzio-eredu orokor gisa, eta ARPE-19, erretinako zelula-eredu gisa. Zelulen biziraupen-maila bikaina izan zen nioplexoen eraginpean egon ondoren, %95eko biziraupenetik gora HEK-293 zelula-lerroan eta %85etik gora ARPE-19 zelula-lerroan. Beraz, formulazioak biobateragarriak direla esan dezakegu zelula-lerro horietan. Gainera, zelulak mikroskopio bidez aztertuta ikusi genuen itxura osasuntsua zutela bi zelula-lerroek 2.3.A<sub>1</sub> eta 2.3.B<sub>1</sub> irudietan antzeman daitekeen moduan. Aldiz, Lipofectamine 2000™ kontrol positiboa erabilita, zelulen biziraupena asko kaltetu zen, batez ere ARPE-19 zelula ereduau, %55eraino jaitsi baitzen. Datu horiek bat datoaz beste ikerketa batzuen emaitzekin, izan ere, Lipofectamine 2000™ konposatura ez da egokia erretinako gene-garraiorako bertako zelulentzat oso toxikoa delako baita kontzentrazio baxuetan ere<sup>68</sup>. Transkezio-efizientziari dagokionez, HEK-293 zelula-lerroan DST85 nioplexoak erabilita lortu genituen emaitza onenak (2.3.A<sub>1</sub> irudia). Aldiz, ARPE-19 zelula-lerroan, DST20 nioplexoak izan ziren transfekzio-maila altuena lortu zutenak (2.3.B<sub>1</sub> irudia). Orokorean, uste da HLB balio baxuak dituzten eta, beraz, liposolubilitate handiagoa dute tentsoaktibo ez-ionikoen zelulan barneratzea errazten dutela<sup>69, 70</sup>. Ideia hori bat dator HEK-293 zeluletan ikusi dugunarekin, Tween 85 baita HLB balio baxuena duen tentsoaktibo lan honetan ikertutakoenean artean. Harrigarria bada ere, ARPE-19 zelula-lerroan tentsoaktibo hidrofilikoena duen niosoma formulazioa izan da transfekzioan eraginkorrena, alegia, DST20 formulazioa. Horrek guztiak iradokitzen du zelulamotaren araberako beste mekanismo batzuk ere abian direla, esate baterako, zeluletan barneratzeko bide endozitikoak, eta horiek ere paper garrantzitsua joka dezaketela formulazioen transfekzio-efizientzia baldintzatzeko orduan.

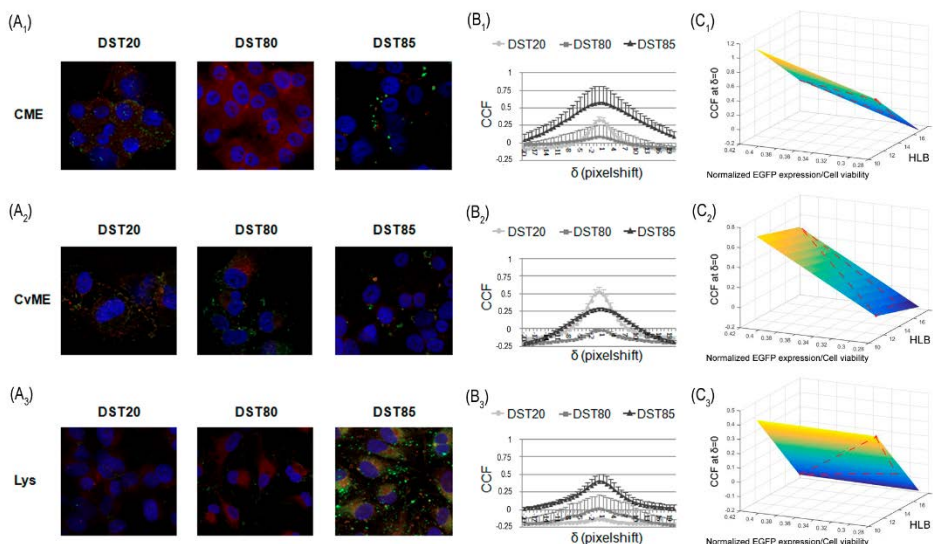


**2.3. Irudia.** Transfekzio-efizientzia DST20, DST80 eta DST85 nioplexoekin transfektatutako HEK-293 eta ARPE-19 zelula-lerroetan, 2/1 lipido kationikoa/DNA masa ratioa eta pcMS-EGFP plasmidoa erabilita. (A<sub>1</sub>) Transfekzio-efizientzia HEK-293 zelula-lerroan. (A<sub>2</sub>) EGFP expresioa DST85 nioplexoekin transfektatutako HEK-293 zeluletan erakusten duen fluoreszentzia-mikroskopio bidezko irudia, x20 magnifikazioan. (B<sub>1</sub>) Transfekzio-efizientzia ARPE-19 zelula-lerroan. (B<sub>2</sub>) EGFP expresioa DST20 nioplexoekin transfektatutako ARPE-19 zeluletan erakusten duen fluoreszentzia-mikroskopio bidezko irudia, x20 magnifikazioan. Balio bakoitzak bataz besteko  $\pm$ SD adierazten du, n = 3. Esanahi estatistiko maila: \*p < 0,05, \*\*p < 0,01, \*\*\*p < 0,001. Eskala-barrak: 100 nm.

Nioplexoen bidezko transfekzio prozesua hobeto ulertze aldera, zelulan barneratzeko mekanismoak eta formulazio bakoitzak jarraitutako bide endozitikoak aztertu genituen. Bektore ez-birala normalean endozitosi bidez sartzen dira zeluletan eta katrina bidezko endozitosia (CME) eta kabeola bidezkoa (CvME) izaten dira ohikoenak<sup>71</sup>. CvME bide orohar ez-azidiko eta ez-degradatziale gisa ulertzen da<sup>72</sup> eta CME bidea, berriz, lisosomekin fusionatzen dela uste da<sup>73</sup>. Halere, eztabaida handia dago oraindik ere zentzu horretan eta, zenbait ikertzaileren arabera, kabeolak ere lisosomekin fusionatzen dira<sup>74, 75</sup>. Gainera, lisosometako pH azidoaren inguruan ere zalantzak daude. Ikertziale batzuen ustez, pH azidoa transfekziorako onuragarria da lisosometako pH azidoa, DNA bektore ez-biralek askatzea eragiten duelako eta, horrela, libre geratzen delako nukleoraino iristeko<sup>76</sup>.

## Eztabaida

77. Aldiz, beste batzuen esanetan, lisosometako pH azidoak transfekzioa oztopatzen du, bektore ez-biralen zein horiek garraiatzen duten DNAren degradazioa eragiten duelako<sup>78</sup>. Gure ikerketaren arabera, nioplexoak CME bide endozitikoaren bitartez barneratzen baziren ARPE-19 zeluletan, lisosomekin besteek baino gehiago ko-lokalizatzen zuten eta transfekzio-maila baxuagoak lortzen zitzutzen. Hori izan zen DST85 nioplexoen kasua (2.4. irudia). Aldiz, nioplexoek CvME bide erabiltzen zutenean, gutxiago ko-lokalizatzen zuten lisosomekin eta transfekzio-maila altuagoak lortzen zitzutzen. Beraz, gure emaitzak bat datozi lisosometan DNA molekulen degradazioa gertatzen dela dioten hipotesiekin, eta horrek azalduko luke DST20 nioplexoek nahiz eta HLB balio altuko tentsoaktibo ez-ionikoa izan, beste nioplexoek baino transfekzio-maila altuagoak lortzea ARPE-19 zeluletan. DST80 nioplexoei dagokienez, oso ko-lokalizazio baxua erakutsi zuten CME zein CvME bide endozitikoekin, beharbada beste sarbide batzuk erabili zutelako. Izan ere, duela gutxiko ikerketa baten arabera, Tween 80, 1-(2-dimetilaminoetil)-3-[2,3-di(tetradeziloxi) propil] urea eta eskualnoz osatutako nioplexoak makropinozitosi bidez barneratzen dira zeluletan<sup>13</sup>.



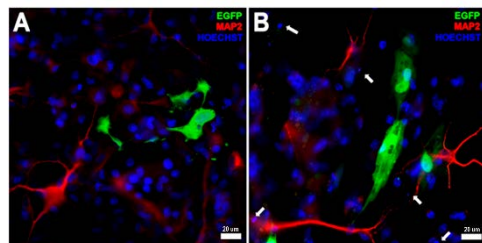
**2.4. Irudia.** Bide endozitikoak eta zelula-barneko trafikoa aztertzeko entsegua DST20, DST80 eta DST85 nioplexoekin ARPE-19 zeluletan. (A1-3) mikroskopio konfokal irudiak, ARPE-19 zelulak eta FITC markatzalea daraman pCMS-EGFP plasmidoa (berdez) garraiatzen duten nioplexoak ikusgai. Gorri: CME (AlexaFluor546-Transferrina), CvME (AlexaFluor555-Kolera toxina) edo lisosoma (Lysotracker). (B1-3) Kolore gorri eta berdearen arteko ko-lokalizazio balioak, zeharkako korrelazio bidez aztertuta. Balio bakoitzak bataz besteko  $\pm$ SD adierazten

### *Eztabaida*

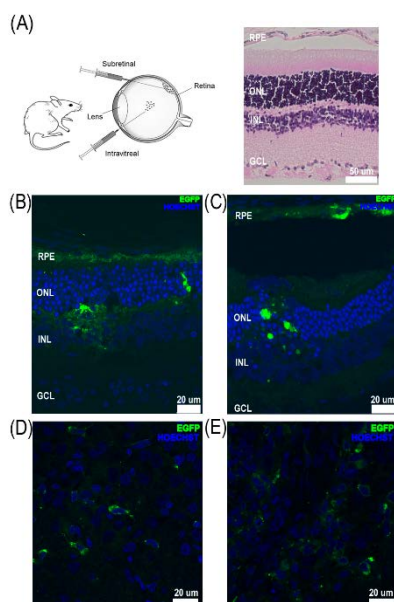
du, n = 3. (C1-3) 3D grafikoak, HLB balioen, transfekzio-efizientziaren eta bide endozitiko bakoitzaren arteko erlazia aztertzeko.

---

Aurreko guztia kontuan hartuta, DST20 formulazioa hautatu genuen erretinarako gene-garraioa bideratzeko. *In vivo* entseguak egin baino lehen, erretinako kultibo primarioetan egin genituen gene-transferentzia saioak DST20 nioplexoekin eta GFP espresio-maila egokiak antzeman genituen (2.5. irudia). Emaitzak horiek indartuta, *in vivo* entseguak egin genituen arratoi-erretinan, DST20 formulazioa erretinako zelulak transfektatzeko gai ote zen jakiteko bitreo-barneko (IV) (2.6.D-E irudia) eta erretina-azpiko (SR) (2.6.B-C irudia) injekzioen ondoren. Normalean, IV injekzioen bitartez erretinako ganglio-geruzako zelulak transfekatzea lortu daiteke eta SR injekzioen bidez, berriz, erretinaren geruza sakonagoetara iristea posible izan daiteke<sup>68, 79</sup>. Kontzeptu horrekin bat datozen gure emaitzak ere. Izan ere, IV injekzioaren bidez batez ere ganglio-geruzako zelulak transfektatu genituen DST20 nioplexoekin (2.6.D irudia) eta SR injekzioaren bitartez RPE geruzako zeluletaraino iristea lortu genuen DST20 nioplexoekin (2.6.B irudia). Kontuan hartuta itsu geratzea eragiten duten erretinako gaitz gehienak RPE geruzako zeluletan gertatzen diren mutazioek eragiten dituztela, geruza horretan transfekzioa lortzea oso garrantzitsua da aplikazio terapeutikoetarako. Tamalez, SR injekzioak oso inbaditzailak dira eta arrisku larriak ditu, adibidez, inflamazioa, lentea kaltetzea edota erretina-askatza<sup>80</sup>. Nahiz eta saiakera ugari egin diren RPE geruzara iristeko IV injekzioen bidez, ez da oraindik lortu eta SR injekzioek eraginkorrenak izaten jarraitzen dute RPE geruza transfektatzeko. Bestalde, ikerketa-lerro berriak eman-bide okular topiko eraginkorrik lortzen zuzenduta daude. Izan ere, eman-bide ez-inbaditzaila litzateke eta erabilera klinikora iristeko oso egokia. Duela gutxi, farmakoak garraiatzen dituzten mikrofluidika bidez eratutako liposomak begian topikoki aplikatuta RPE geruzara iristea lortu da<sup>81</sup>, baina geneekin ez da oraindik antzekorik lortu. Beraz, oso interesgarria litzateke bide hori aztertzea gene-terapia ez-biralaren bidez gene terapeutikoak RPE geruzaraino bideratzeko eta, zentzu horretan, lan honetan garatutako DST20 niosoma formulazioa egokia izan daiteke ikerketa-lerro hori bultzatzeko.



**2.5. Irudia.** EGFP espresioa arratoiaren erretinako zelulen kultibo primarioetan. (A) EGFP espresioa DST20 nioplexoekin transfekzioa egin eta 96 ordura. (B) EGFP espresioa Lipofectamine 2000™ kontrol positiboarekin transfekzioa egin eta 96 ordura. Gorri: MAP2 neuronen dendrita markatzailea. Urdinez: Hoescht (zelulen nukleoak). Berdez: EGFP. Eskala-barra: 20  $\mu$ m.



**2.6. Irudia.** (A) Arratoi-erretinaren egitura osoa eta *in vivo* bitreo-barneko (IV) eta erretina-azpiko (SR) injekzioen eskema orokorra. SR injekzioaren bidez lortutako EGFP espresioa DST20 nioplexoekin (B) eta Lipofectamine 2000™ kontrol positiboarekin (C). IV injekzioaren bidez lortutako EGFP espresioa DST20 nioplexoekin (D) eta Lipofectamine 2000™ kontrol positiboarekin. Urdinez: Hoescht (zelulen nukleoak). Berdez: EGFP. Eskalabarrik: 20  $\mu$ m. RPE (erretinako epitelio pigmentarioa), ONL (kanpoko nukleo geruza), INL (barneko nukleo geruza), GCL (ganglio-zelulen geruza).

Laburbilduz, soilik tentsoaktibo ez-ionikoan ezberdintzen ziren hiru niosoma formulazio garatu eta karakterizatu ditugu. Gure emaitzen arabera, DST20 formulazioa –Tween 20, DOTMA eta eskualenoz osatua- izan da eraginkorrena arratoi-erretinako zeluletan gene-transferentzia bideratzeko, lipido kationiokoa/DNA masa ratio baxua (2/1) erabilita. *In vivo*, iritsitako zelula-geruzak eman-bidearen araberakoak izan dira. SR injekzioen bidez RPE geruzako zeluletaraino iristea lortu

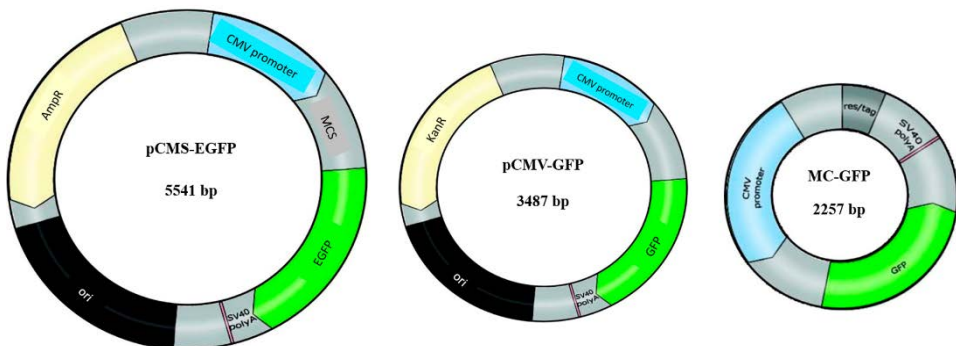
## *Eztabaida*

dugu, aldiz, IV injekzioen bidez ganglio-zelulen geruza transfektatu dugu. Bektore-ingeniaritzan zein eman-bide ez-inbaditzileen ikerketan aurrera egin ahala, posible izan daiteke begian topikoki emandako formulazioak RPE geruzaraino iristea eta bertako zelulak gene terapeutikoekin transfekatztea.

### **3. Material genetikoaren eragina niosomen bidezko erretinako gene-transferentziaren eraginkortasunean**

Aurreko ataletan egin bezala formulazioaren ezaugarriak hobetzeaz gain, gene-transferentzia eraginkortasunez gauzatzeko ezinbestekoa da material genetikoaren propietateak ere ondo ezagutzea eta beharrezko aldaketak egitea. Orain arte, DNA plasmidoetan hainbat egokitzapen egin dira transfekzio-efizientzia hobetze aldera, besteak beste, promotore-sekuentzia hobetuz, sekuentzia indartzaileak gehituz, poliadensilazio seinaleekin jokatuz edota CpG motiboak kenduz hantura-erantzunak ekiditeko<sup>82-86</sup>. Halere, DNA plasmidoek oinarri bakterianoa dute, alegia, erreplikazio-jatorriaren sekuentzia eta antibiotikoen erresistentziarako geneak. Oinarri prokariotiko hori ezinbestekoa da plasmidoak laborategian bikoiztu eta mantendu ahal izateko, baina transgene-expresioa gutxitu dezake eta, gainera, gene-garraio sistemaren bioerabilgarritasuna eta segurtasun profila kaltetzen dituzte. Beraz, expresio-unitate minimoak, bakarrik intereseko transgenea eta beharrezko sekuentzia erregulatzalez osatuak, adibidez, minicircle (MC) egiturak, plasmido konbentzionalen ordezko alternatiba erakargarriak dira. MC egiturak DNA molekula zirkular itxiak dira eta ez daukate ez antibiotikoekiko erresistentziarako generik eta ezta sekuentzia bakterianorik ere. MC egiturek plasmido tradicionalek baino tamaina txikiagoa dute nahiz eta expresio-kasete bera mantendu (3.1. irudia). Egitura berri horien ezaugarriak direla eta, MC material genetikoak ez du erantzun immunerik ez eta transgenea isilarazteko mekanismorik pizten zelula-ostatuetan. Beraz, transgenearren expresio-maila altuagoak eta denboran iraunkorragoak lortu daitezke *in vivo* teknologia berri horri esker<sup>87-92</sup>. Beraz, tamaina txikiari eta sekuentzia bakterianorik ez izateari esker, MC egiturak plasmidoak baino egokiagoak izan daitezke gene-terapia ez-biralean biosegurtasunari eta eraginkortasunari dagokionez. Ikerketa askok erakutsi dute MC DNA molekulek transgene-expresioa hobetzen dutela hainbat organotan *in vivo*, gibela<sup>93-95</sup>, bihotza<sup>96, 97</sup> eta muskulu eskeletikoa<sup>97</sup> barne. Halabaina, MC teknologiaren eraginkortasuna ez da oraindik ikertu erretinako zelulen transfekzioan eta niosoma formulazioak bektore ez-biral gisa erabilita.

## Eztabaida



**3.1. Irudia.** DNA material genetikoaren ezaugarriak. (A) pEGFP 5,5 kb, (B) pGFP 3,5 kb, (C) MC-GFP 2,3 kb. MC: minicircle; GFP: proteina berde fluoreszentea; EGFP: proteina berde fluoreszente indartua; pCMS: plasmidoa, zitomegalobirusaren promotorea, klonazio eremu anitza eta SV40 promotorea dituena; pCMV: zitomegalobirusaren promotorea daraman plasmidoa; bp: base-pareak.

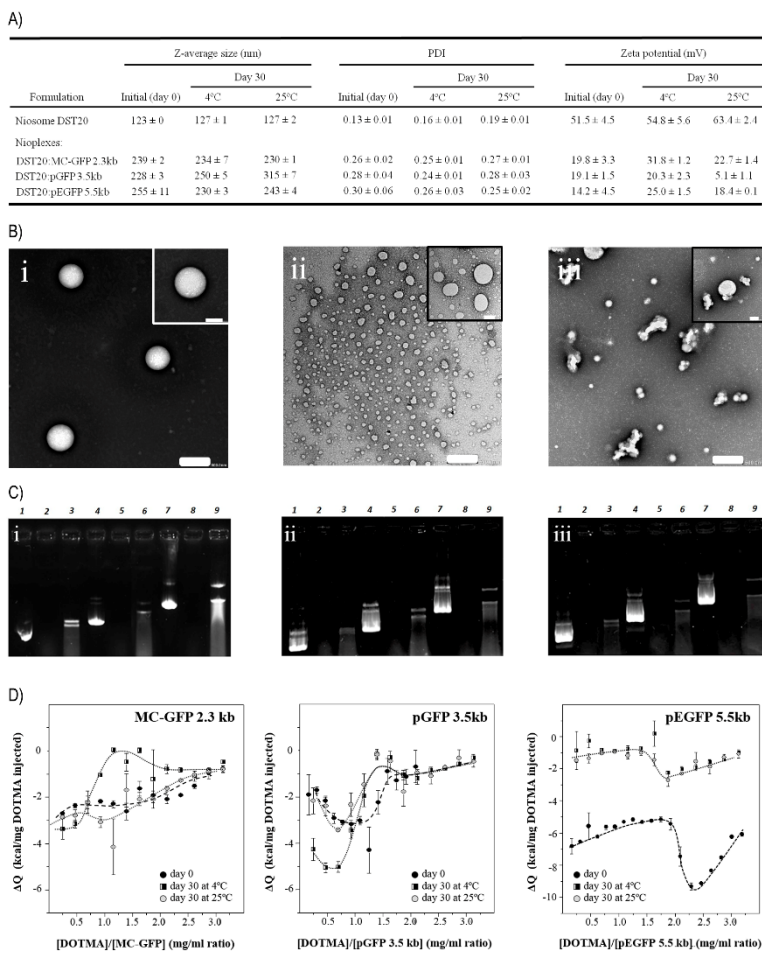
Beraz, aurreko kontuan hartuta, lan honen helburua da MC teknologia niosoma formulazioekin konbinatuz, gene-garraio sistema berri horren erretinako zelulen transfekziorako eraginkortasunaren inguruko lehen ebidentziak ematea. Horretarako, MC teknologia plasmido koblentzionalekin konparatu dugu eta aurreko lanean garatutako DST20 niosoma formulazioa –Tween 20, DOTMA eta eskualenoz osatua- erabili dugu gene-transferentzia bideratzeko, erretinako zelulak transfektatzeko egokiena zela erakutsi genuen eta. Beraz, nioplexoak eratzeko, DST20 niosomak ondorengo hiru material genetikoetako batekin elkartu genituen: MC-GFP (2257 bp), pGFP (3487 bp) edo pEGFP (5541 bp). Niosomak eta nioplexoak fisiko-kimikoki karakterizatu genituen tamaina, zeta potentziala, polidispersio indizea, morfologia eta egonkortasunaren arabera. Gainera, DST20 niosomek material genetiko ezberdinak degradaziotik babesteko eta askatzeko zuten gaitasuna ere ikertu genuen, baita niosoma eta DNA molekulen arteko elkarrekintza molekularren nondik norakoak ere. *In vitro* esperimentuen bidez, formulazioen transfekzio-efizientzia eta horien eraginpean egon ondoren zelulek agertutako biziraupen-maila ikertu genituen. Horretarako, erretinako epitelio pigmentarioko ARPE-19 zelulak erabili genituen eta formulazio ezberdinak aztertu genituen: DST20 niosomak material genetiko ezberdinei lotuta, prestatu berrian, 4°C-tan hilabetez biltegiratu ostean eta 25°C-tan hilabetez biltegiratu ostean. Horrela, material genetikoaren eragina azterzeaz gain, formulazioen egonkortasuna ere aztertu eta konparatu genuen. Azkenik, erretinako zelulen kultibo primarioan eta

## *Eztabaida*

*in vivo* arratoi-erretinan transfekzio-entseguak bideratu genituen, hiru material genetikoen artean eraginkorrena zein zen erabaki ahal izateko.

DST20 niosomek morfologia esferikoa eta gene-garriarako tamaina egokia erakutsi zuten, 123 nm-ko diametroko partikulak. Gainera, PDI balio baxuek tamainen distribuzio homogeneoa adierazi zuten eta zeta potentzialaren balio positiboak egokiak ziren karga negatibodun DNA molekuletako fosfato taldeekin elkarrekintza elektrostatikoen bidez lotzeko<sup>45, 98, 99</sup>. Aipatzeko da TEM bidez lortutako irudietan ikusten diren partikula-tamainen eta DLS teknikaren bidez neurtutako partikula-tamainen arteko ezberdintasuna laginen prozesaketa ezberdinagatik dela<sup>13</sup>. Espero bezala, niosoma formulazioei DNA molekulak gehitzean, partikulen diametroa ia bikoiztu egin zen eta zeta potentziala, berriz, jaitsi, niosomen amina taldeak DNA molekulen fosfato taldeekin partzialki neutralizatu zirelako (3.2.A-B irudia).

DST20 niosomak hiru material genetiko ezberdinekin elkartu ostean lortutako nioplexoen tamaina, zeta potentziala eta transfekzio-efizientziari dagozkion datuak bat datozen beste ikerketa batzuekin, non material genetiko ezberdinek ez dituzten ia formulazioen parametro fisiko-kimikoetan eraginik<sup>100</sup> baina bai transfekzio-efizientzian *in vitro*<sup>101</sup>. Gene-transferentziaren eraginkortasunean antzemandako desberdintasunak azaltzeo bi arrazoi nagusi egon daitezke. Batetik, partikulen tamainan DNA gehitzean ikusten den igoerak alde batera uzten du ITC kurbei begiratuta litekeena zen nioplexoen arteko agregazioa. Beraz, lipido kationikoa/DNA ratioaren arabera, molekulen antolaera aldatu daiteke eta DNA molekulak niosoma formulazioaren gainazaleko leku mesedegarrienetan lotuko dira, ratioak igotzeak niosoma bakoitzeko DNA molekula gutxiago lotzea ekarriko lukeelarik. Horrek niosomek zelulen gainazalarekin interakzioak osatzeko gaitasuna baldintzatuko luke eta, beraz, baita horien transfekzio-gaitasuna ere. Bestetik, ikerketa honetan DNA kantitate konstanteak erabili ziren ~1,25 µg kondizio bakoitzeko- baina kontuan hartzekoa da DNA molekulen tamainak eta, beraz, baita horien masa eta molaritatea ere, ezberdina izango dela material genetiko mota bakoitzarentzat. Horrek niosoma bakoitzari lotutako DNA molekula-kopurua baldintzatuko du, eta ITC entseguan erraz antzeman daiteke daiteke fenomeno hor, DNA mota bakoitzarentzat formulazioen kalorimetria-kurbak ezberdinak baitira (3.2.D irudia). Beraz, ematen du niosoma formulazioek MC molekula gehiago jaso zituztela plasmido molekulak baino eta, horrek, MC daramaten formulazioen transfekzio-probabilitatea jaso egiten du<sup>92, 101</sup>.



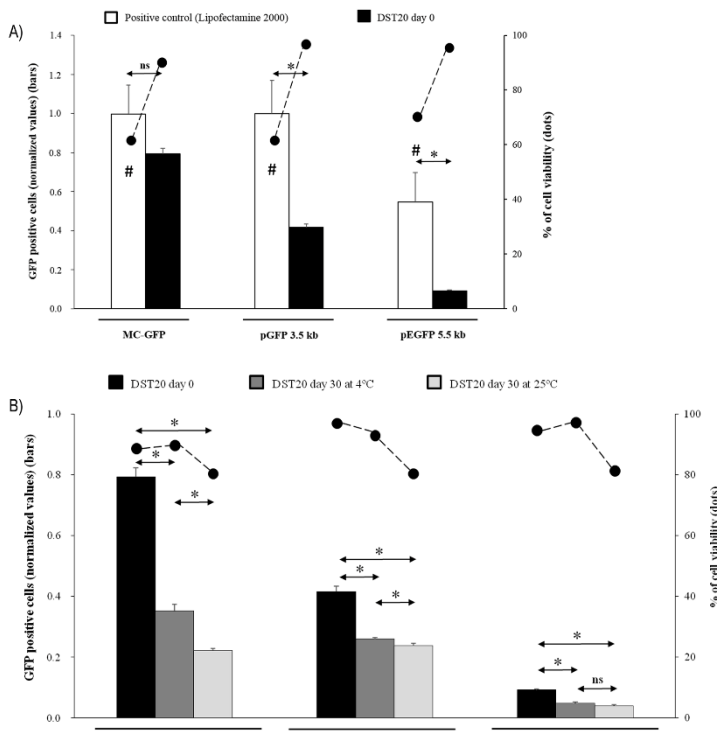
**3.2. Irudia.** Niosoma eta nioplexoen karakterizazio fisiko-kimikoa eta egonortasun neurketa. (A) DST20 nioplexoen karakterizazio fisiko-kimikoa prestatu berrian (0 eguna) eta hilabetera (30 eguna) 4°C-tan edo 25°C-tan biltegiratu ondoren. Balio bakoitzak bataz besteko  $\pm$ SD adierazten du,  $n = 3$ . (B) DST20 niosomen TEM irudiak (i) 0 egunean, (ii) 30 egunean 4°C-tan biltegiratuta eta (iii) 30 egunean 25°C-tan biltegiratuta. Eskala-barrak: 500 nm (irudi nagusiak) eta 200 nm (txertatutako irudiak). (C) Elektroforesi-entsegu agarosa geletan DST20 niosomek material genetiko ezberdinak babesteko eta askatzeko zuten gaitasuna ikertzeko, (i) 0 egunean, (ii) 30 egunean 4°C-tan biltegiratuta eta (iii) 30 egunean 25°C-tan biltegiratuta. DNase I entzima eta SDS gehitu ziren 3, 6 eta 9 zutabeetan MC-GFP, pGFP eta pEGFP material genetikoen babes eta askapena ikertzeko, hurrenez hurren. Kontrol gisa, 1,

### *Eztabaida*

4 eta 5 zutabeetan MC-GFP, pGFP eta pEGFP material genetiko biluziak ipini ziren hurrenez hurren eta 2, 5 eta 8 zutabeetan horiek berak + DNase I entzima. (D) ITC entsegua DNA molekulen eta DST20 niosomen arteko elkarrekintza ikertzeko. Bero-bariazioaren eboluzioa gehitutako DOTMA kantitatearen (mg) eta DOTMA/DNA kontzentrazioen (mg/ml) araberakoa izan zen. Grafiketako ikurrek datu esperimentalak adierazten dituzte eta ikurrak lotzen dituzten lerroek, berriz, ITC perfilaren joera adierazten dute.

---

Formulazioak biltegiratu aurretik eta ondoren transgene-espresioan ikusitako ezberdintasunak (3.3. irudia) azaltzeko faktore-metaketak hartu behar dira kontuan. Izan ere, gene-garraioa aspektu askok baldintzatzen dute, partikulen tamaina, gainazaleko karga, morfologia eta DNArekin lotzeko gaitasuna barne<sup>102</sup>. Zentzu horretan, TEM irudietan itxura esferikoaren galera eta baita agregazioen sorrera ere antzeman daitezke 30 egunez biltegiratuta egon ostean eta, horrek, DNA molekulekin elkarrekintzak modu egokian sortzea oztopatu dezake. Halaber, elektroforesi eta ITC entseguetan garbi ikus daiteke niosomek DNA molekulei eusteko gaitasuna jaitsi egiten dela denboran zehar. Agarosa-geletan, DNA banden seinale ahulagoak formulazioaren babes eskasagoa adierazten dute (3.2.C irudia). Era berean, ITC entseguetako datuek adierazten dute DST20 nioplexoen ezaugarriak niosomen araberakoak direla eta, horiek 30 egunez biltegiratu badira, propietate fisiko-kimikoak kaltetuta egongo direla. Nahiz eta MC material genetikoa daramaten DST20 nioplexoen transfekzio-maila 30 egunera plasmidoak daramatzaten DST20 nioplexoek 0 egunean lortzen dutena baino altuagoa izan (3.3. irudia), ikerketa-esfortzu handiagoak zuzendu behar dira formulazio egonkorragoak lortze aldera.

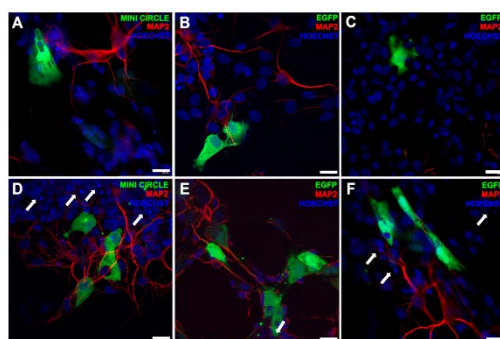


**3.3. Irudia.** Nioplexoen transfekzio-efizientzia eta zelulen biziraupena ARPE-19 zelularerroan. Fluxu zitometria bidez neurututako EGFP positiboak diren zelula biziak (barrak) eta zelula-populazioaren biziraupena (puntuak) transfekzioaren ondoren, (A) DST20 niosomak prestatu berritan erabilita (0 eguna) eta (B) 30 egunez 4°C-tan edo 25°C-tan biltegiratuta egon ondoren, eta MC-GFP, pGFP edo pEGFP material genetikoak garraiatzen dituztela. Balio bakoitzak bataz besteko  $\pm$ SD adierazten du, n = 3. \* $p$  < 0,05 transfekzio-efizientziari dagokionez eta # $p$  < 0,05 zelula-biziraupenari dagokionez, Lipofectamine 2000™ kontrol positiboarekin alderatuta, ns siglek ez dagoela differentzia estatistikorik adierazten dute.

Gaur egun, bitreo-barneko (IV) eta erretina-azpiko (SR) injekzioak dira klinikian erabilgarriak diren eman-bide bakarrak, nahiz eta oso inbaditzaleak izan<sup>103</sup>. Beraz, eman-bide horien bitartez injektatu ziren material genetiko ezberdindun DST20 nioplexoak *in vivo* arratoi-erretinetan. Aurreko ikerketetan bezala, IV injekzioen bidez erretinako ganglio-zelula geruzara iristea lortu zen<sup>24, 25</sup>. Maila honetako gene-transferentzia eraginkorra erabilgarria izan daiteke glaukoma bezalako gaixotasunetan<sup>104</sup>. Bestalde, SR injekzioen bidez RPE geruzaraino iristea lortu zen. Erabilera terapeutikorako, geruza hori transfekatzeara da desiragarriena, bertako

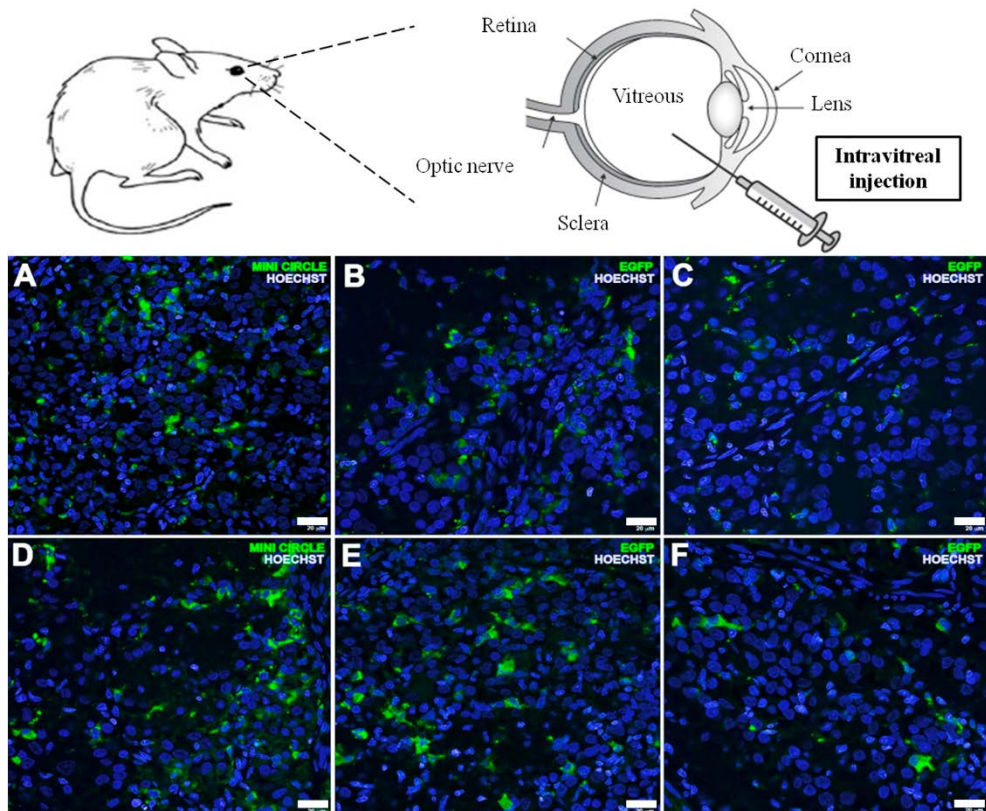
## Eztabaida

zeluletan gertatzen diren mutazioek eragiten baitituzte erretinako gaitz hereditario gehienak, eta horien erantzule diren 200 mutazio baino gehiago ezagutzen dira gaur egun. Immunohistokimika irudien analisi kualitatiboaren bidez antzeman genuen transgene handiagoa MC zeramaten DST20 nioplexoekin transfektatutako erretinetan, bai IV (3.5. irudia) zein SR (3.6. irudia) injekzioen ostean. Beraz, DST20 bektore ez-biralaren eta MC DNA molekulen arteko konbinaketa egokia izan liteke erretinako gaitzei aurre egiteko gene-terapia estrategietan erabiltzeko. Gainera, literaturaren arabera, MC teknologiak ez du bakarrik gene-transferentzia hobetzen, baizik eta denboran irauten duen transgene-espresioa ahalbidetzen du, klinikan aplikagarria izateko faktore gakoa dena<sup>92, 101</sup>. Nahiz eta GFP expresioa Lipofectamine 2000™ kontrol positiboa erabilita ere antzeman genuen, formulazio hori ez da egokia *in vivo* entseguetarako erretinan, bertako zeluletan toxikotasun handia eragiten duelako baita kontzentrazio baxuetan ere<sup>68</sup>. Izen ere, gure *in vitro* entseguek ARPE-19 zeluletan garbi erakutsi zuten Lipofectamine 2000™ bektorearen toxikotasun handia (3.3. eta 3.4. irudiak). Azkenik, aipatzeko da DST20/MC nioplexoak 2/1 lipido kationikoa/DNA masa ratioan erabiltzeak abantaila garrantzitsuak dituela, besteak beste, DNA dosia handitu ahal izatea efektu terapeutiko nabarmenagoa lortzeko eta niosoma kantitate txikiagoak erabiltzea lipido kationikoei lotutako toxikotasun arazoak ekiditeko<sup>67</sup>. Gainera, MC molekulek ez dutenez ez CpG motiborik ez beste oinarri prokariotikorik, euren bioerabilgarritasuna eta segurtasun profila plasmido konbentzionalena baino egokagoak dira.



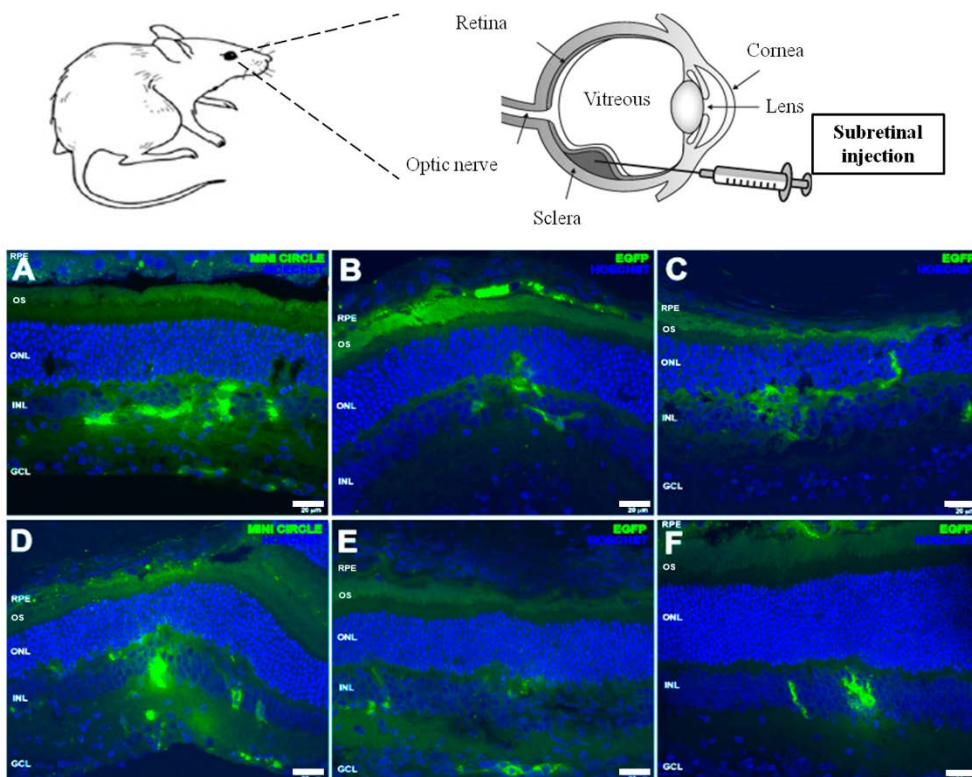
**3.4. Irudia.** GFP expresioa erretinako zelulen kultibo primarioan. Fluoreszentzia immuno-histokimika irudiak, non GFP seinalea batez ere glia-zeluletan antzeman daitekeen, DST20 nioplexoak erabilita ondoko material genetikoetako bati lotuta: (A) MC-GFP, (B) pGFP eta (C) pEGFP. (D-F) bakoitzari dagokion kontrol positiboa Lipofectamine 2000™ bektore gisa erabilita. Zelula-nukleoak Hoescht 33342 markatzailearekin tindatu ziren (urdinez) eta neuronen dendritak MAP2 markatzailearekin (gorriz). Gezi zuriek nukleo apoptotikoak adierazten dituzte. Eskala-barrak: 20 µm.

## Eztabaida



**3.5. Irudia.** *In vivo* GFP espresioa IV injekzioaren ondoren. Erretinako mikroskopio fluoreszente irudiak, GFP seinalea erakusten dutenak transfekzioa egiteko DST20 nioplexoak ondorengo material genetikoetako bati lotuta erabilita: (A) MC-GFP, (B) pGFP eta (C) pEGFP. (D-F) bakoitzari dagokion kontrol positiboa Lipofectamine 2000™ bekture gisa erabilita. RPE (erretinako epitelio pigmentarioa), OS (kanpo-segmentuak), ONL (kanpoko nukleo geruza), INL (barneko nukleo geruza), GCL (ganglio-zelulen geruza). Zelula-nukleoak Hoescht 33342 markatzailearekin tindatu ziren (urdinez). Eskala-barrak: 20  $\mu$ m.

## Eztabaida



**3.6. Irudia.** *In vivo* GFP espresioa SR injekzioaren ondoren. Erretinako mikroskopio fluoreszente irudiak, GFP seinalea erakusten dutenak transfekzioa egiteko DST20 niosomek ondorengo material genetikoetako bati lotuta erabilita: (A) MC-GFP, (B) pGFP eta (C) pEGFP. (D-F) bakoitzari dagokion kontrol positiboa Lipofectamine 2000™ bektore gisa erabilita. RPE (erretinako epitelio pigmentarioa), OS (kanpo-segmentuak), ONL (kanpoko nukleo geruza), INL (barneko nukleo geruza), GCL (ganglio-zelulen geruza). Zelula-nukleoak Hoescht 33342 markatzailearekin tindatu ziren (urdinez). Eskala-barrak: 20  $\mu$ m.

Laburbilduz, lan honetako aurkikuntza nagusiak ondorengoa dira: (1) DST20 niosomak material genetikoa babesteko eta era kontrolatuan askatzeko gai diren bektore ez-biralak dira; (2) niosomek material genetikoa babesteko eta horrekin elkarrekintzak osatzeko gaitasuna kaltetu egiten dira biltegiratze denboraren eta temperaturaren arabera; (3) material genetiko ezberdinei lotutako niosoma

## *Eztabaida*

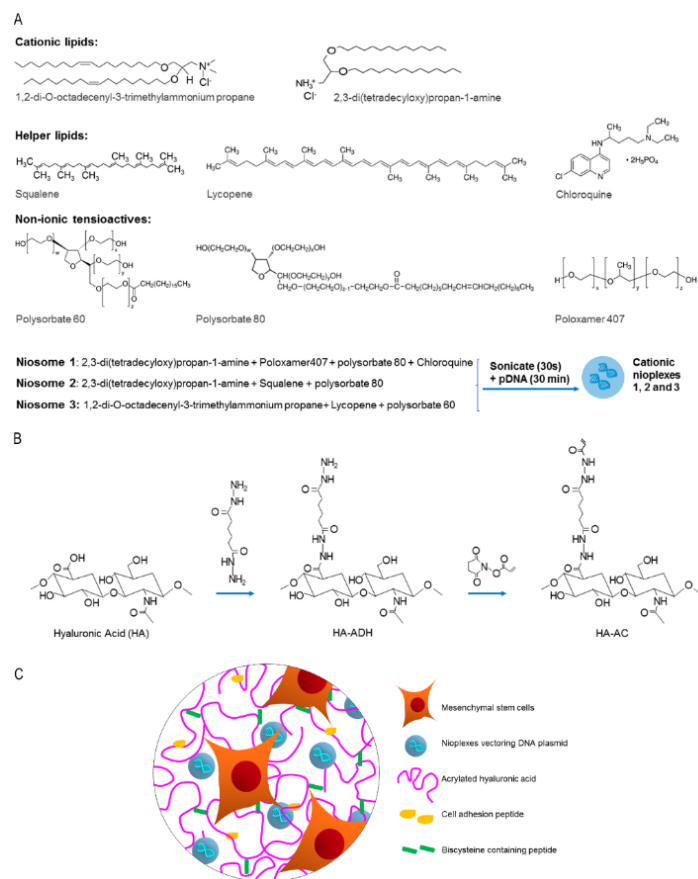
formulazioen parametro fisiko-kimikoak antzekoak dira, baina *in vitro* transfekzio-gaitasun ezberdinak dituzte nahiz eta denek zelula-biziraupen maila egokiak erakutsi; (4) MC daramaten DST20 nioplexoek plasmidoak daramatzatenek baino transfekzio-efizientzia altuagoa dute *in vitro*, baita 30 egunez biltegiratuta egon ondoren ere; eta (5) DST20 nioplexoak gai dira erretinako zelulen kultibo primarioak transfektatzeko eta baita *in vivo* ere erretinako zelulak transfektatzeko IV eta SR injekzioen bidez, eta kasu honetan ere MC daramaten DST20 nioplexoak dira transfekzio-gaitasun handiena erakutsi dutenak. Beraz, DST20/MC nioplexoak sistema ez-biral egokia izan daitezke gene terapeutikoak modu seguru eta eraginkorrean erretinara garraiatzeko eta bertako zeluletan gene terapeutikoen espresio iraunkorra lortzeko.

### **4. Gene-garraio sistema ez-biralen aspektu tridimentzialak: niosomen eta azido hialuronikozko hidrogelen arteko sinergia bateragarrien bila**

Bektorea eta garraiatutako material genetikoa hobetzeaz gain, gene-terapia ez-biralean gaur egungo joera da beste teknologia batzuekin konbinaketa berriak bilatzea transfekzio-efizientzia hobetze aldera. Izan ere, estrategia konbinatu horiek abantaila handiak izan ditzakete, aipagarrienak egonkortasun hobia eta toxikotasun baxuagoa lortzea direlarik. Gainera, gene-transferentzia matrizeen diseinuarekin uztartuta, DNA garraio lokala, eraginkorra eta ehun zehatzetara zuzendua posible litzateke eta, horrek, gene-terapiaren aplikazio klinikoa erraztuko luke, besteak beste, minbiziaren tratamenduan edota ehunen birsortzean<sup>35, 36</sup>. Azido hialuronikoa (HA) glikosamino anionikoa da eta zelulaz kanpoko matrizearen osagai natural nagusietako bat da. Azken aldian, bere erabilerak biomaterial gisa arreta erakarri du ehun-ingeniaritzan, biobateragarria delako eta molekula ezberdinak barneratzeko gai delako, azido nukleikoak barne<sup>105, 106</sup>.

Hori dela eta, lan honen helburua da DNA-garraioa modu lokalean egin ahal izateko niosoma eta HA hidrogelen arteko konbinaketaren bidez, plataforma ez-biral seguru eta eraginkorra garatzeko lehen urratsak ematea. Guk dakigula, lehen aldia da niosoma eta HA hidrogelen teknologiak uztartzen direna gene-garraio ez-biralen baitan. Hiru niosoma formulazio ezberdin prestatu eta aztertu genituen (**1, 2 eta 3** niosomak), lipido kationiko, lipido laguntzaile eta tentsoaktibo ez-ioniko ezberdinez osatutakoak (4.1. irudia). Nioplexoak eratzeko, niosoma horiei luziferasa genearen sekuentzia daraman DNA plasmidoa (pGluc) gehitu genien. Niosomen osagaien, lipido kationikoen kontzentrazioaren eta lipido kationikoa/DNA masa ratioen aukeraketa aurretik egindako ikerketetan oinarrituta egin genuen. Niosomak eta

nioplexoak fisiko-kimikoki zein biologikoki karakterizatu genituen tamaina, PDI, zeta potentziala eta sagu-hezurmuietik klonatutako ama-zelula mesenkimalak (mMSC) 2D kultiboetan transfektatzeko gaitasunari dagokionez. Jarraian, nioplexodun HA hidrogeletatik ere aztertu genuen. Azkenin, mMSC zelulak hiru-dimentsiotan hazi genituen nioplexodun HA hidrogeletan eta nioplexoen askapen-zinetika HA hidrogeletatik ere aztertu genuen. Azkenin, mMSC zelulak hiru-dimentsiotan hazi genituen nioplexodun HA hidrogeletan eta nioplexoen transfekzio-efizientzia ebaluatu genuen 3D kultibo horietako zeluletan.



**4.1. Irudia.** Niosoma kationikoen eta hidrogeleten eskema orokorra. A. Niosoma formulazioak prestatzeko erabilitako lipido kationiko, lipido laguntzaile eta tentsoaktibo ez-ionikoen egitura kimikoak. B. HA molekuletan eginiko moldaketa kimikoak HA hidrogelak osatzeko. C. Nioplexodun HA hidrogeleten eskema orokorra.

## Eztabaida

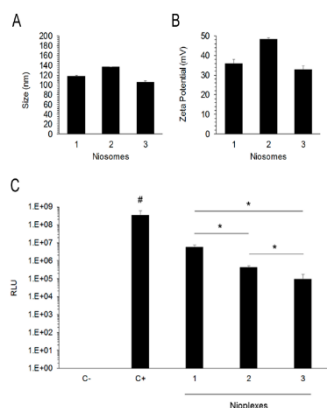
Nahiz eta DNA kontzentrazio altuek gene-garraio lokala hobetzen duten hidrogeletan<sup>107</sup>, DNA kantitate handiak hidrogeletan txertatzea erronka handia da, azido nukleikoen agregazioa edota inaktibazioa ekidin behar dira eta<sup>108</sup>. Bektore ez-biralen aukera zabalaren artean, poli(etileno imina) edo PEI polimeroz osatutako partikulak, DNA molekulei lotuta poliplexoak osatuz, arrakasta handiz txertatu dira hidrogeletan eta transgene-espresio maila altuak lortzea zein *in vivo* angiogenesia abiaraztea posible izan dira<sup>109</sup>. Hala eta guztiz ere, nahiz eta PEI molekulen eratorriak oso eraginkorrik diren gene-garraiorako, toxikoak dira eta erantzun immunea pizten dute eta, beraz, ez dira egokiak erabilera klinikorako<sup>110</sup>. Zentzu horretan, niosomak alternatiba aparta izan daitezke sistema biologikoekin duten bateragarritasuna dela eta. Gainera, niosomak biodegradagarriak dira, toxikotasun oso baxua dute eta ez dute erantzun immunerik sortzen<sup>64</sup>. Lan honetan, nioplexodun HA hidrogeletan lortutako transfekzio-eficientziak *in vitro* beste lan batzuetan PEI poliplexodun HA hidrogeletan lortutako antzekoak dira<sup>111</sup>. Beraz, espero izatekoa litzateke *in vivo* entseguetan ere nioplexodun HA hidrogelak gene-transferentzia eraginkorra bideratzeko gai izatea eta interesgarria litzateke ikerketa-lerro horretan sakontzea etorkizunera begira.

Lan honetan erabilitako hiru niosoma formulazioek osagai ezberdinak zituzten (4.1. irudia), denak aurretik ikertuak beste gene-garraio ez-biral aplikazio batzuetarako. Esate baterako, Tween 80 daramaten formulazioak eskualeno lipido laguntzailearekin batera, gene-transferentziarako egokiak direla erakutsi da<sup>26</sup>. Bestalde, lycopene lipido laguntzailea DOTMA lipido kationikoarekin eta Tween 60 tentsoaktibo ez-ionikoarekin konbinatuta, formulazio horiek gai izan ziren erretinako zelulak transfektatzeko aurreko ikerketetan<sup>24</sup> eta Poloxamer 407 ere oso erabilia izan da gene-garraiorako bektore ez-biralen prestaketan<sup>112</sup>. Gainera, klorokinaren erabilerak formulazioen gene-transferentzia gaitasuna indartzen duela uste da, bai *in vitro* eta baita *in vivo* ere<sup>113</sup>. Beraz, niosomak prestatzeko erabilitako osagaiak, kontzentrazioak eta lipido kationikoa/DNA masa ratioak aurreko ikerketetako emaitzetan oinarrituta aukeratu genituen.

Hasteko, niosomak eta nioplexoak fisiko-kimikoki zein biologikoki karakterizatu genituen tamaina, PDI, zeta potentziala eta mMSC zelulan 2D kultiboetan transfektatzeko gaitasuna kontuan hartuta (4.2. irudia). Hiru formulazioek zeta potentzial positiboak zituzten (4.2.B irudia), ezinbestekoa karga negatibodun DNA molekulekin elkarrekintza elektrostatikoen bidez lotzeko<sup>45, 66</sup>. Gainera, partikulen gainazaleko karga positiboek zeluletan barneratzea errazten dute<sup>44</sup>. Formulazioen eraginpean jarri gabeko kontrol-zelulekin konparatuta, formulazio guztiak erakutsi

## Eztabaida

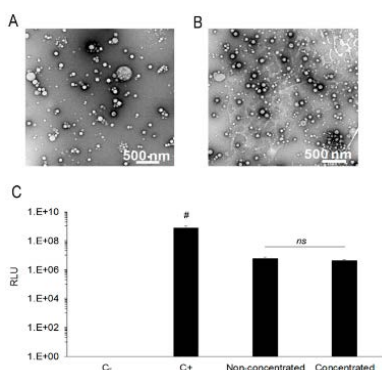
zuten zelulak transfektatzeko gaitasuna, baina **1** nioplexoak izan ziren transfekzio-efizientzia handiena erakutsi zutenak, Lipofectamine 2000™ kontrol positiboaren atzetik (4.2.C irudia). Lipofectamine 2000™ kontrol positibo gisa erabiltzen da, baina ez da egokia *in vivo* entsegutarako eta ezta aplikazio klinikorako ere toxikotasun handia eragiten duelako. Beraz, HA hidrogelekin konbinatzeko **1** nioplexoak aukeratu genituen entsegu horien ondoren.



**4.2. Irudia.** Niosoma formulazioen karakterizazioa. A. Tamaina (nm). B. Zeta potentziala (mV). C. Transfekzio-efizientzia mMSC zelulen 2D kultiboan, nioplexoen eraginpean ipini eta 48 ordura neurtuta. 1, 2 eta 3 nioplexoen lipido kationikoa/DNA masa ratioak 2/1, 15/1 eta 18/1 izan ziren, hurrenez hurren. Kontrol negatiboa (C-) tratamendurik gabeko zelulek osatzen dute eta kontrol positiboa (C+), berriz, Lipofectamine 2000™ bektorearekin transfektatutako zelulek osatzen dute. RLU: *Relative Light Units*, alegia, luziferasa transgenearren expresio-mailaren adierazle diren seinale lumuniko unitateak.

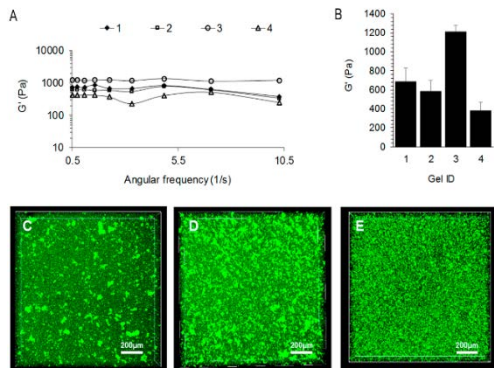
Nioplexoak masa ratio baxuetan erabiltzeak abantailen artean, garrantzitsuenak DNA kantitate handiagoak erabili ahal izatea formulazio-bolumen txikiagoak erabilita eta lipido kationikoei lotutako toxikotasuna gutxitzea dira<sup>13</sup>. Horrez gain, DNA kantitate are handiagoak txertatu ahal izateko HA hidrogelek onartzen dituzten niosoma bolumen baxuetan, **1** niosoma formulazioaren kontzentrazioa bikoiztu genuen (1 mg/ml-tik 2 mg/ml-ra). Kontzentratutako niosoma formulazioa TEM bidez aztertu genuen eta irudietan ikus daiteke partikulen morfologia ez zela aldatu kontzentrazio-prozesuan zehar eta, espero bezala, partikula gehiago ikusten dira formulazio kontzentratuaren irudietan ez-kontzentratuarekin alderatuta (4.3.A-B irudiak). Bestalde, partikulen tamaina eta PDI balioak ere antzera mantendu ziren. Zeta potentzial balioek behera egin bazuten ere, +20 mV-en gainetik mantendu ziren, balio egokia beraz partikulen agregazioa ekiditeko<sup>46</sup>. Gainera, ez genuen ezberdinotasunik aurkitu niosoma kontzentratuen eta ez-kontzentratuen transfekzio-efizientzian (4.3.C irudia), beraz, gene-transferentzia gaitasuna ere ez zen kaltetu kontzentrazio-prozesuan zehar. Emaitza horiek kontuan hartuta, formulazio kontzentratua 2/1 masa ratioan aukeratu genuen HA hidrogelekin konbinatzeko.

## Eztabaida



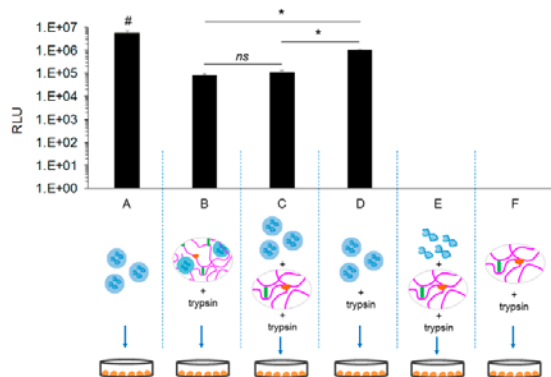
**4.3. Irudia.** Niosoma kontzentratuen karakterizazioa. A-B. Niosoma ez-kontzentratuen (A) eta kontzentratuen (B) TEM irudiak  $\times 10.000$  magnifikazioan. Eskala-barra: 200 nm. C. Transfekzio-efizientzia mMSC zelulen 2D kultiboetan formulazioen eraginpean egon eta 48 ordura.

Terapeutikoki egokiak izan daitezkeen DNA kantitateak lortze aldera<sup>114</sup>, HA hidrogeletan hiru nioplexo kantitate ezberdin txertatu genituen hiru hidrogeletan, honako amaierako DNA kontzentrazioak lortuz **2**, **3** eta **4** hidrogeletan, hurrenez hurren: 0,055 µg/ml, 0,12 µg/ml eta 0,2 µg/ml. Kontrol gisa, nioplexorik gabeko eta, beraz, DNArik gabeko hidrogelak erabili ziren (**1** hidrogela). Material genetiko kontzentrazio ezberdinek hidrogelen ezaugarri biomekanikoetan eragin dezakete, eta horiek zelulen hidrogel barneko hedapena eta gene-transferentzia baldintzatzen dituzten faktore garrantzitsua dira. Hidrogel zurrunak (800 Pa baino gehiagokoak) zelulen hapea baxuarekin erlazionatuta daude eta hidrogel bigunak (200 eta 260 Pa artean), berriz, transgene-expresio indartuarekin daude erlazionatuta<sup>108</sup>. Beraz, **1**, **2**, **3** eta **4** hidrogelen propietate mekanikoak aztertu genituen beren zurruntasun-maila ezagutzeko. Erreologia bidezko karakterizazioaren arabera, hidrogelek oso zurruntasun-maila ezberdinak erakutsi zituzten, **3** hidrogela zurrunena izanik eta **4** hidrogela bigunena (4.4.A-B irudia). Nioplexoen distribuzioa hidrogelen barruan nahiko homogeneoa izan zen eta **3** eta **4** hidrogeletan, partikulek ez zuten batere agregaziorik sortu. Zelula-hazkuntzarako mediorik ez zuen **4** hidrogela ezin zen 3D kultiboak egiteko erabili, baina *in vivo* entsegutarako hautagai egokia izan daiteke bere propietate biomekanikoei esker. Transfekzio-entseguan 3D kultiboetan, beraz, **2** eta **3** hidrogeletan egin ziren, **1** hidrogela kontrol negatibo gisa erabilita. Orohar, emaitza horiek erakusten dute nioplexoak, baita DNA kantitate handiak garraituta ere, agregaziorik sortu gabe eta ezaugarri mekaniko egokiak mantenduz txertatu daitezkeela HA hidrogeletan.



**4.4 Irudia.** Nioplexodun HA hidrogelen karakterizazioa. A. Hidrogelen propietate mekanikoak erreologia bidez neurtu ziren 0,1 eta 10 rad/s-ko frekuentzian eta 0,01-eko tentsio konstantea aplikatuta. B. Batez besteko zurruntasuna. C-E. Partikulen distribuzioa hidrogeletan. Gel ID: 1 nioplexorik gabeko hidrogel kontrola; 2: 0,055 µg/ml DNA; 3: 0,12 µg/ml DNA eta 4: 0,2 µg/ml DNA.

Behin hidrogeletik askatuta nioplexoek transfekzio-gaitasuna mantentzen zutela ziurtatzeko, nioplexo-aktibitate entsegu bat egin genuen (4.5. irudia). Nioplexoak hidrogeletan txertatu ondoren, horiek tripsinaren bidez degradatu genituen eta nioplexodun produktu horrekin transfekzioa egin genuen mMSC zelulen 2D kultiboetan. Emaitzen arabera, nioplexoak gai izan ziren transfekzioa bideratzeko hidrogeletatik askatuak izan ondoren, baina prestatu berrian baino efizientzia baxuagoa erakutsi zuten. Hala ere, aipatzekoa da transfekzioa egiteko, nioplexoez gain hidrogel degradatua eta tripsina ere bazituen nahasketarik erabili genituela eta, ziurrenik, produktu horiek izan ziren transfekzio-prozesua oztopatu zutenak<sup>109</sup>.

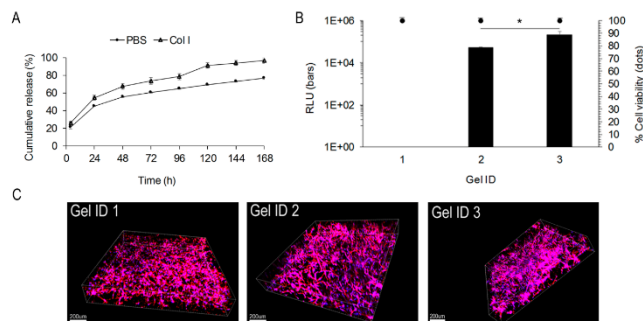


lotu gabea) + tripsinarekin degradatutako HA hidrogelak. F. Nioplexorik gabeko hidrogelak tripsinarekin degradatuta.

**4.5 Irudia.** Nioplexoak aktibitate biologikoa HA hidrogeletatik askatu eta gero. A. nioplexo prestatu berriak. B. Tripsinarekin degradatutako HA hidrogeletatik askatutako nioplexoak. C. Nioplexo prestatu berriak + tripsinarekin degradatutako hidrogelak. D. Nioplexo prestatu berriak + tripsina. E. DNA askea (niosomei

## Eztabaida

Bi mekanismo nagusik baldintzatzen dute gene-transferentzia hidrogeletan: DNA/nanopartikula konplexuen askapen-zinetikak eta zelula-infiltrazio tasak<sup>115</sup>. Hidrogelaren degradazioaren ondorioz askatutako nioplexoek inguruko zelulak transfektatuko lituzkete eta, era berean, hidrogelean zehar infiltratu eta hedatzen diren zelulek nioplexoekin topo egingo lukete eta barneratu egingo lituzkete, transfekzioa gauzatuz<sup>116, 117</sup>. Zentzu horretan, 3D kultiboetako gene-transferentzia baxuagoa da hidrogeleko zelulak ez badira gai azalera guztian zehar hedatzeko eta, beraz, hidrogel zurrunegiak ez dira komenigarriak<sup>115</sup>. Lan honetan, nioplexoek 7 egun behar dituzte hidrogeletik ia erabat askatzeko kolagenasa I entzimaren presentzian, eta zertxobait motelago askatzen dira entzima hori ez badago (4.6.A irudia). Nioplexoen askatze progresibo hori komenigarria aplikazio terapeutikoetarako, transgene-espresio iraunkorra ahalbidetzen duelako. Hidrogeletako 3D transfekzio-entseguei eta zelula-hedapenari dagokionez, esan dezakegu zelulak hidrogel guztietan hedatzeko gai izan zirela, baita **3** hidrogelean ere bere zurruntasuna kontuan hartuta harrigarria bada ere (4.6.C-E irudia). Gainera, transfekzio-maila altuagoa izan zen **3** hidrogelean –DNA kantitate handiagoa ere bazuen- **2** hidrogelean baino (4.6.B irudia, barrak) eta horrek adierazten du, beharbada, DNA kantitate handiek hidrogelen zurruntasuna nolabait konpentsatzen dutela. Horrez gain, kasu guztietan eta nioplexorik gabeko **1** hidrogelekin alderatuta, zelulen biziraupena bikaina izan zen, nioplexoen presentziak hidrogeletako 3D kultiboetako zelulak kaltetzen ez dituela erakutsiz (6.B irudia, puntuak).



**4.6. Irudia.** (A) Nioplexoen askapen-zinetika HA hidrogeletatik kolagenasa I entzimarekin (1 U/ml) eta entzimari gabe. (B) Transfekzio-efizientzi eta, zelulen biziraupena nioplexodun HA hidrogeletako 3D zelula kultiboetan. (C-E) Zelula-hedapenaren adierazgarri diren mikroskopio konfokal bidezko irudiak **1**, **2** eta **3** hidrogeletan. Urdinez: DAPI (zelula-nukleoak) eta gorriz: F-aktina (zelula-zitoplasma). Eskala-barra: 200  $\mu$ m.

## *Eztabaida*

Laburbilduz, kontzentratutako nioplexoak agregaziorik sortu gabe HA hidrogeletan txertatzeko prozesua garatu dugu lan honetan. Guk dakigula lehen aldia da 2,3-di(tetradeziloxil)propan-1-amina, Poloxamer 407, Tween 80 eta klorokinaz osatutako niosoma formulazioen eta HA hidrogelen arteko konbinaketa egiten dela gene-garraio ez-biralaren baitan. Orohar, nioplexodun HA hidrogelek propietate mekaniko egokiak erakutsi zituzten, partikulek ez zuten agregaziorik sortu hidrogelen barruan eta zelulak modu egokian hedatu ziren hidrogeletan, gene-transferentzia arrakastatsua lortuz mMSC zelulen 3D kultiboetan. Gure ustez, *in vitro* eredu honetan ikasitako baliagarria izan daiteke niosoma eta HA hidrogelen teknologiak uztartuz gene-garraio sistema ez-biral seguru eta eraginkorak garatzeko *in vivo* aplikazioetarako.

Dena batuz, doktoretza-tesi honek bektore ez-biralen transfekzio-gaitasunean eragiten duten eta gene-garraio sistema eraginkorren diseinuan kontuan hartu beharreko faktore gakoak aztertu ditu. Aspektu horiek honakoak biltzen dituzte: bektore ez-biralen konposizioa eta ezaugarri fisiko-kimikoak, garaiatutako material genetikoaren konposizioa eta egitura eta garrio-sistemen eta hiru-dimentsioko matrizeen teknologiak uztartzea. Gure ustez, bektore ez-biral unibertsal eta bakarraren kontzeptua atzean utzi beharra dago eta etorkizuneko gene-garraio ez-birala aplikazio bakoitzera egokitutako bektoreen diseinuan oinarritu beharra dago. Nahiz eta bektore ez-biralak ez diren oraindik erabilera klinikora iritsi, egin diren aurrerapenek itxaropena pizten dute eta lortutako ebidentziek iradokitzen dute etorkizun hurbilean material genetikoa bektore ez-biralen eta eman-bide ez-inbaditzaleetan barrena burutuko dela.

***Erreferentzia-zerrenda 316 -325 orrietan dago.***



## *Discusión*

En términos generales, la terapia génica se define como la introducción de material genético en células diana con el fin de modificar o controlar su expresión génica, pudiendo tener objetivos terapéuticos o experimentales<sup>1</sup>. La culminación del Proyecto del Genoma Humano, junto con los avances recientes en el campo de la biología molecular, han facilitado comprender procesos patológicos y celulares que, a su vez, ha permitido identificar genes diana para distintas estrategias terapéuticas. De todos modos, a pesar de que la terapia génica posee gran potencial para el tratamiento de distintas enfermedades, las estrategias basadas en el uso de ácidos nucleicos exigen el uso de vectores capaces de vehiculizar el ADN a las células diana de forma segura y efectiva, lo cual hoy en día sigue siendo uno de los mayores retos de las terapias basadas en transferencia genética. De hecho, la falta de vectores eficaces es la principal razón que limita el número de ensayos clínicos basados en terapia génica. El éxito de la transferencia génica depende en gran medida de la idoneidad del vector utilizado y éstos deberían ser capaces de: (i) proteger los ácidos nucleicos frente a la degradación enzimática, (ii) promover la internalización celular del material genético y (iii) liberar los ácidos nucleicos en el correcto compartimento intracelular<sup>1</sup>. Además, un vector ideal debe ser eficaz, seguro, específico, duradero, fácil de manejar y tener el mínimo coste posible<sup>2</sup>.

En general, los vectores se clasifican en dos grandes grupos: los virales y los no-virales. Según datos publicados por *The Journal of Gene Medicine* en 2014<sup>3</sup>, existen alrededor de 2.000 ensayos clínicos basados en terapia génica aprobados a nivel mundial y, de ellos, el 70% usan vectores virales. Además, hoy en día sólo cuatro medicamentos basados en la terapia génica han sido comercializados y todos ellos se basan en el uso de vectores virales. En 2003, China aprobó por primera vez un medicamento de terapia génica, Gendicine™, basado en un vector adenoviral (Ad) e indicado para el tratamiento del carcinoma de células escamosas de cabeza y cuello<sup>4</sup>. En segundo medicamento de terapia génica también fue aprobado en China, en el año 2005, y fue denominado Oncorine™. Este segundo producto contiene un vector basado en un virus adenoasociado (AAV) y está indicado en el tratamiento de cáncer nasofaríngeo de estadio avanzado y refractario<sup>5</sup>. En Europa, el primer producto comercializado basado en terapia génica fue Glybera® y se aprobó en 2012. Este medicamento contiene también un vector viral AAV y está indicado para combatir el déficit severo de la lipoproteína lipasa<sup>6</sup>. En 2015, fue Estados Unidos quien aprobó su primer medicamento de terapia génica, denominado IMLYGIC™ y que contiene como vector viral el virus del herpes simplex (HSV). Está indicado para tratar lesiones cutáneas, subcutáneas y nodales en pacientes con melanoma recurrente tras cirugía inicial<sup>7</sup>. Sin embargo, según datos

## *Discusión*

actualizados en el año 2017, en las nuevas estrategias de edición genómica existe una tendencia cada vez mayor en el uso de sistemas no-virales. Al contrario que los métodos convencionales de terapia génica basados en la adición de un gen funcional, las nuevas estrategias basadas en la edición o corrección de la secuencia del genoma prefieren el uso de sistemas no-virales frente a los virales, siendo el 70% de los estudios realizados en este sentido de carácter no-viral<sup>8</sup>. Entre las estrategias no-virales, la principal consiste en el uso del método físico de la electroporación (39%), seguido por los vectores no-virales lipídicos (17%) y los poliméricos (8%)<sup>8</sup>. Por lo tanto, parece que el uso de vectores no-virales está ganando terreno a los vectores virales para el transporte de material genético en las recién surgidas estrategias de edición genética.

De hecho, a pesar de que los virus son herramientas altamente eficaces para el transporte génico, presentan también muchos inconvenientes como una baja capacidad de carga, producción compleja y costosa y problemas de seguridad relacionados con la respuesta inmune y la mutagénesis insercional. En este sentido, los vectores no-virales basados en nanotecnología, a pesar de su menor eficiencia de transfección, ofrecen innumerables ventajas incluyendo una baja inmunogenicidad, alta capacidad de carga y facilidad de fabricación a un coste asequible<sup>9</sup>. Además, las formulaciones no-virales pueden ser producidas a gran escala con alta reproductibilidad y son relativamente estables durante el almacenamiento<sup>1</sup>. Por lo tanto, los avances constantes en el campo de los biomateriales y la nano-ingeniería han motivado la síntesis, caracterización y funcionalización de nanomateriales biocompatibles para transportar material genético<sup>10</sup>. Asimismo, la gran variedad de nanomateriales disponibles ha permitido el diseño de vectores multifuncionales específicamente adaptados para distintas aplicaciones<sup>11</sup>. Hasta la fecha, se han desarrollado vectores no-virales compuestos de distintos materiales, siendo los más comunes los que se basan en lípidos catiónicos<sup>12-14</sup>, polímeros<sup>15-16</sup> y nanopartículas magnéticas<sup>17</sup>. Estas moléculas se pueden modificar a través de la nanoingeniería para que distribuyan el material genético en órganos y células diana de forma específica o para que puedan atravesar distintas barreras tanto extra- como intracelulares. Entre la amplia gama de vectores no-virales disponibles, los denominados niosomas constituyen uno de los ejemplos más recientes y se trata de vesículas de surfactante no-iónico sintéticas y biocompatibles que forman una bicapa lipídica cerrada<sup>18, 19</sup>. Se basan en tres componentes principales: (i) el lípido catiónico –responsable de la interacción electrostática con las moléculas de ADN de carga negativa-, el lípido *helper* –para mejorar las características de la suspensión- y (iii) el tensioactivo no-

## *Discusión*

iónico –capaz de aumentar la estabilidad de la formulación y evitar la formación de agregados<sup>22</sup>. Las propiedades físico-químicas globales de estos componentes tienen gran influencia sobre las características de los niosomas como, por ejemplo, el tamaño de las partículas, la carga superficial o la morfología. A su vez, esas propiedades determinarán la habilidad de los niosomas para penetrar en las células, seguir una ruta endocítica en particular, liberar la carga de ADN en el núcleo y, por tanto, su eficiencia de transfección<sup>22-23</sup>. Es importante recalcar, además, que estudios recientes han demostrado que los vectores no-virales basados en niosomas son capaces de transfectar células de retina y sistema nervioso central (SNC) tanto *in vitro* como *in vivo* en ratas<sup>23-26</sup>.

En cualquier caso, no sólo el vector utilizado es importante a la hora de determinar la eficiencia de transfección, sino que las propiedades del material genético transportado también influyen en el proceso. Hasta hace poco, la mayoría de estrategias destinadas a incrementar la eficiencia de transfección en terapia génica no-viral se han centrado en mejorar la vehiculización del material genético, ya sea mediante la introducción de modificaciones en el vector o a través del uso de métodos físicos como la electroporación. Sin embargo, la potenciación de la transferencia génica se puede conseguir mediante la optimización del material genético en cuanto a su composición y conformación, ya que esto permite tanto mejorar la biodisponibilidad y biocompatibilidad del ADN como obtener una mayor duración de la expresión génica<sup>27</sup>. En este sentido, varios grupos de investigación han desarrollado recientemente la denominada tecnología *minicircle* (minicírculo en inglés, abreviado MC), que consiste en la delección de las secuencias bacterianas de los plásmidos convencionales, manteniendo únicamente el gen de interés y las secuencias reguladoras<sup>28</sup>. Las secuencias procariotas de los plásmidos convencionales incluyen motivos CpG, orígenes de replicación y genes de resistencia a antibióticos. A pesar de que esas secuencias son necesarias para poder propagar y mantener los plásmidos en huéspedes bacterianos en el laboratorio, obstaculizan su aplicabilidad clínica, ya que pueden inducir respuestas inflamatorias y muerte celular por apoptosis o necrosis. Ello, además de suponer un problema de seguridad, reduce la expresión del transgen de manera notoria<sup>31, 32</sup>. Además, las secuencias de ADN de los plásmidos convencionales pueden resultar en muchas ocasiones inaccesibles a la maquinaria de transcripción de la célula diana, sobre todo si las secuencias bacterianas asociadas a los indicadores de histonas se encuentran adyacentes al gen de interés. Estos indicadores –que son rápidamente reconocidos por la célula diana- producen el empaquetamiento de las secuencias en una estructura densa de heterocromatina, lo cual resulta en la

## *Discusión*

reducción de la expresión del transgen o en su silenciamiento<sup>33</sup>. Por lo tanto, las unidades de expresión minimizadas como el MC constituyen una alternativa prometedora a los plásmidos convencionales para incrementar la eficacia de la transfección y la duración de la expresión del gen de interés. Varios estudios *in vitro* e *in vivo* han demostrado una mejora significativa en los niveles y duración de la expresión génica mediante el uso de la tecnología MC, así como mejores perfiles de seguridad e inmunocompatibilidad<sup>18</sup>. Por otro lado, las estructuras de ADN “mini” también poseen mayor capacidad para atravesar barrera extra- e intracelulares, aumentando su biodisponibilidad en los tejidos diana<sup>34</sup>.

Además de la optimización del vector y del material genético, una nueva tendencia en terapia génica no-viral es la exploración de sinergias complementarias con otras tecnologías, por ejemplo, con el diseño de matrices tridimensionales o hidrogeles. Estas estrategias combinadas pueden proporcionar ventajas significativas a los sistemas de terapia génica no-viral como, por ejemplo, mayor estabilidad y menor toxicidad. Asimismo, el hecho de complementar la transferencia génica con el diseño de matrices tridimensionales permitiría distribuir el ADN terapéutico de manera local y efectiva, lo cual acercaría estas estrategias a su aplicación clínica en el tratamiento del cáncer o la regeneración tisular<sup>35, 36</sup>.

Tomando en cuenta todo lo anterior, esta tesis doctoral se centra en el desarrollo de sistemas efectivos de liberación génica no-virales y, para ello, lleva a cabo los siguientes estudios: (i) preparación, caracterización y evaluación comparada de la eficiencia de transfección de tres vectores comerciales basados en lípidos catiónicos, polímeros y nanopartículas magnéticas que transportan un plásmido que codifica el factor de crecimiento vascular (VEGF) a las células del SNC; (ii) preparación, caracterización y evaluación del proceso y eficiencia de transfección de tres formulaciones de niosomas que únicamente difieren en el tensioactivo no-iónico para dilucidar el rol que desempeña ese componente en la transfección mediada por niosomas; (iii) preparación y caracterización de niosomas unidos a tres tipos de material genético –MC y plásmidos de distinto tamaño– y evaluación comparada de su eficiencia de transfección; y (iv) exploración de sinergias complementarias para terapia génica no-viral entre niosomas e hidrogeles de ácido hialurónico (HA). En las siguientes secciones, estos estudios se discutirán en detalle.

## *Discusión*

### **1. La influencia de la composición de los vectores no-virales en su eficiencia de transfección con un plásmido terapéutico que codifica el gen de crecimiento del endotelio vascular en células del sistema nervioso central**

Las terapias basadas en ácidos nucleicos son esperanzadoras pero requieren el uso de vectores eficaces y seguros. Además, la transfección de células del SNC constituye todavía un gran reto, lo cual retrasa el desarrollo de estrategias terapéuticas basadas en la liberación génica para enfermedades que afectan al SNC. En los últimos años, los nanomateriales biocompatibles han surgido como candidatos prometedores para desempeñar esa función, y ya se han conseguido los primeros resultados de transfección en el SNC tanto *in vitro* como *in vivo* utilizando quitosanos<sup>37, 38</sup>, lípidos catiónicos<sup>39</sup> o nanopartículas magnéticas<sup>17</sup>. Por otro lado, el gen del VEGF podría ser adecuado como gen terapéutico para el SNC<sup>40</sup> dada la estrecha relación descrita entre las alteraciones vasculares en cerebro y los procesos neurodegenerativos<sup>41</sup> y por sus roles específicos en angiogénesis cerebral y supervivencia neuronal<sup>42, 43</sup>.

Basándonos en esas consideraciones, presentamos un estudio basado en la liberación del gen VEGF en células del SNC a través de distintos vectores no-virales. Para ello, utilizamos tres nanoformulaciones diferentes –oligoquitosano ultrapuro (UOC) en una formulación polimérica, Lipofectamina en la formulación lipídica y NeuroMag en la magnética- y los unimos al plásmido phVEGF165aIRESGFP –que contiene el gen de la proteína VEGF y de la proteína verde fluorescente (GFP)- para obtener los nanoplexos correspondientes. Las nanoformulaciones y los nanoplexos fueron caracterizados en términos de tamaño, carga, índice de polidispersión (PDI), morfología y habilidad para condensar, proteger y liberar el ADN. Se llevaron a cabo estudios de transfección *in vitro* para determinar la eficiencia de transfección en líneas celulares del SNC –C6 y cultivo primario de neuronas- y en la línea celular HEK293 –utilizada como modelo general de transfección-. La eficiencia de transfección fue evaluada atendiendo a tres parámetros: porcentaje de células que expresa GFP, la intensidad de fluorescencia media (MFI) y la expresión de VEGF. También se analizó la viabilidad celular tras la exposición a los nanoplexos. La bioactividad de la proteína VEGF secretada por las células de cultivo primario de neurona transfectadas se evaluó en células endoteliales de la vena umbilical humana (HUVEC), que responden con gran proliferación al efecto del VEGF.

## *Discusión*

Todas las nanoformulaciones y nanoplexes –magnetoplexes, lipoplexes, poliplexos– presentaron partículas del rango nanométrico (Figura 1.1.a, barras), lo cual se ha relacionado con una mayor captación celular<sup>44</sup> y exhibieron potenciales zeta positivos (Figura 1.1.a, líneas), lo cual es necesario para establecer interacciones electroestáticas con las moléculas de ADN de carga negativa<sup>45</sup>. Una vez unidos al ADN, la carga superficial de los nanoplexes descendió notablemente, alcanzando valores de alrededor de – 20 mV en el caso de los magnetoplexes y lipoplexes, y valores cercanos al cero en el caso de los poliplexos. Teniendo en cuenta que se ha descrito que las partículas con valores de potencial zeta situados entre – 20 mV y + 20 mV son más propensos a formar agregados<sup>46</sup>, en este trabajo utilizamos siempre formulaciones recién preparadas para evitar la agregación sobre todo en el caso de los poliplexos. Los valores de PDI fueron inferiores a 0,5 en prácticamente todos los casos, lo cual se considera aceptable para fines comparativos entre tamaños de partículas medidos por análisis cumulativo<sup>47</sup>. La excepción fueron los lipoplexes, donde los valores de PDI elevados fueron atribuidos a su irregular morfología (Fig. 1.1.c). Con el fin de estudiar la capacidad de las nanoformulaciones de condensar, proteger y liberar el ADN, se llevó a cabo un ensayo de electroforesis en gel de agarosa (Figura 1.1.d). Las nanopartículas fueron capaces de proteger el ADN frente a la degradación enzimática y la retención de la mayoría del ADN en el pocillo superior del gel sugiere una fuerte interacción entre las nanopartículas y el material genético. Sin embargo, al añadir el SDS, las nanoformulaciones fueron capaces de liberar el ADN, lo cual indica un equilibrio entre capacidad de condensación y liberación, necesario para llevar a cabo la transfección<sup>48</sup>.

## Discusión

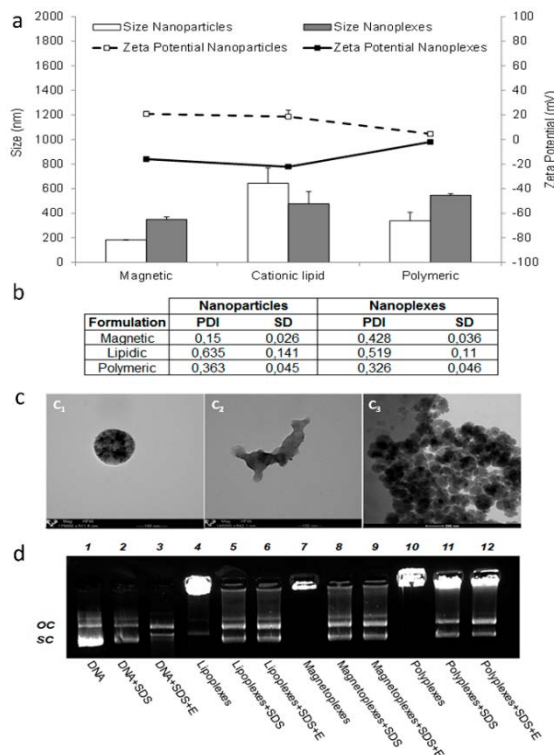


**Figura 1.1.** Caracterización físico-química de nanopartículas y nanoplexes. (a) Tamaño (barras blancas y grises, que corresponden a nanopartículas y nanoplexes, respectivamente) y potencial zeta (líneas discontinuas y continuas, que corresponden a nanopartículas y nanoplexes, respectivamente). Cada valor representa el promedio  $\pm$  SD, n = 3. (b) Valores de PDI. Cada valor representa el promedio  $\pm$  SD, n = 3. (c) Imágenes de TEM de nanopartículas magnéticas (c1) y lípido catiónico (c2), e imágenes de cryo-TEM de las partículas poliméricas (c3). Magnificación original: x140.000 en lípido catiónico, x175.000 en partículas magnéticas y x25.000 en partículas poliméricas. (d) Unión, protección y liberación de ADN visualizado en electroforesis en gel de agarosa. Columnas: 1-3, ADN libre; 4-6, lipoplexos; 7-9, magnetoplexos. Se añadió SDS en las columnas 2, 5, 8 y 11 y se añadió DNase I + SDS en las columnas 3, 6, 9 y 12. OC: forma circular abierta del ADN. SC: forma supercompacta del ADN.

## *Discusión*

Una vez los nanoplexos fueron caracterizados, se llevaron a cabo estudios de transfección *in vitro* en tres líneas celulares: HEK-293 –modelo de transfección general-, C6 –modelo de SNC-, y cultivo primario de neuronas –modelo de SNC más relevante desde el punto de vista terapéutico-. Antes de pasar a los cultivos primarios de neurona, la viabilidad celular y la eficiencia de transfección de los nanoplexos se estudió en HEK293 y C6. Los nanoplexos fueron bien tolerados por ambas líneas celulares, con viabilidades celulares superiores al 90% con los magnetoplexos y lipoplexos y superiores al 80% con los poliplexos (Figura 1.2.a, puntos). El análisis de la eficiencia de transfección se estudió a través de tres parámetros: porcentaje de células que expresan GFP (Fig. 1.2.a, barras), MFI (Fig. 1.2.b) y expresión de VEGF (ng/ml) (Fig. 1.2.c). El plásmido utilizado codifica para VEGF –extracelular- y para GFP –intracelular- y, por lo tanto, la evaluación de la expresión de VEGF se realizó mediante la técnica ELISA, mientras que la de GFP se realizó a través de la citometría de flujo. En cuanto al porcentaje de células que expresan GFP y al MFI, las eficiencias de transfección de todas las formulaciones fueron superiores en HEK193 en comparación con la línea C6. Sin embargo, en cuanto a la producción de VEGF, en ambas líneas celulares se obtuvieron niveles parecidos tras la transfección. Se ha descrito que la eficiencia de transfección con vectores no-virales depende del tipo celular<sup>49</sup>, lo cual coincide con nuestros resultados ya que en HEK293 los lipoplexos fueron los más eficientes, mientras que en C6 lo fueron los magnetoplexos. Los poliplexos no alcanzaron niveles elevados en ningún tipo celular, probablemente debido a su carga superficial cercana al cero, que dificulta la captación celular.

## Discusión

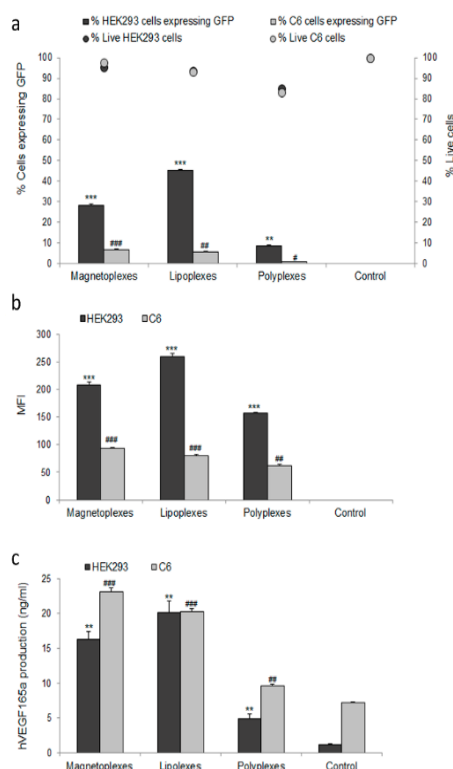


**Figura 1.2.** Viabilidad celular y eficiencia de transfección en células HEK293 y C6 48 h después de la transfección con nanoplexos. (a) Viabilidad celular (HEK293, puntos gris oscuro; C6, puntos gris claro) y porcentajes de células que expresan GFP (HEK293, barras gris oscuro; C6, barras gris claro). Las células control fueron tratadas con ninguna formulación. Cada valor representa el promedio  $\pm$  SD, n = 3. (b) Valores de MFI. (HEK293, barras gris oscuro; C6, barras gris claro). Cada valor representa el promedio  $\pm$  SD, n = 3. (c) Producción de VEGF (ng/ml). (HEK293, barras gris oscuro; C6, barras gris claro). Cada valor representa el promedio  $\pm$  SD, n = 3. Significancia estadística: \*p < 0,05, \*\*p < 0,01, \*\*\*p < 0,001 respecto a las células HEK293 control; #p < 0,05, ##p < 0,01, ###p < 0,001 respecto a células C6 control.

Se observó una clara correlación en ambas líneas celulares entre los tres parámetros utilizados para evaluar la eficiencia de transfección. Cuanto mayor era el porcentaje de células que expresa GFP, mayor era también el valor de MFI (Fig. 1.3.a y 1.4.a). Asimismo, cuanto mayor era el porcentaje de células que expresa GFP, mayor era también la expresión de VEGF (Fig. 1.3.b y 1.4.b). Sin embargo, al comparar los ángulos de la pendiente de las correlaciones, se observó que estas eran más pronunciadas en las células C6 en comparación con HEK293. Es decir, la producción de VEGF alcanzó valores similares en ambos casos, pero la expresión de GFP fue inferior en C6. Estos datos pueden deberse a dos factores. Por un lado, las células C6 expresan un nivel basal de VEGF superior al de las células HEK293, por lo tanto, a pesar de presentar menor grado de transfección, se puede llegar más rápido a niveles elevados de VEGF. Por otro lado, la explicación puede residir en la naturaleza órgano-específica de la secuencia IRES del plásmido empleado. Esta secuencia se encarga de mantener a ambos genes bajo el mismo promotor, de modo que las dos proteínas se expresen a la vez, pero de manera

## Discusión

independiente<sup>50,51</sup>. La secuencia IRES también debe garantizar que las dos proteínas se expresen en la misma proporción, pero eso es algo que no siempre ocurre. De hecho, algunas secuencias IRES funcionan mejor en unos órganos que en otros y es frecuente que no puedan garantizar una expresión equilibrada de ambas proteínas en células del SNC<sup>52,53</sup>. Por lo tanto, teniendo en cuenta los datos obtenidos en este estudio, podemos deducir que la secuencia IRES no ha funcionado correctamente en las células C6 del SNC, viéndose afectada la expresión del gen que se encuentra después del elemento IRES en la secuencia del plásmido<sup>54</sup>. La expresión del VEGF, situada por delante del IRES en la secuencia del plásmido, no se vería afectada y eso explicaría la obtención de valores similares de VEGF en ambas líneas celulares.

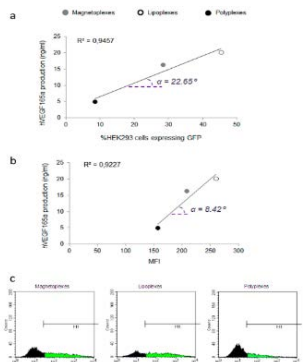


**Figura 1.3.** Correlaciones entre los tres parámetros utilizados para evaluar la eficiencia de transfección en células HEK293. (a) Correlación entre producción de VEGF y porcentaje de células transfectadas. Cada valor representa el promedio  $\pm$  SD, n = 3. (b) Correlación entre producción de VEGF y valores de MFI. Cada valor representa el promedio  $\pm$  SD, n = 3. (c) Histogramas de GFP en células HEK293 48 h después de la transfección. M1 indica el umbral de señal positiva de GFP.

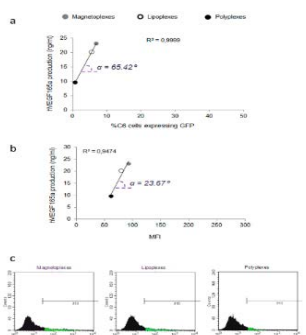


**Figura 1.4.** Correlaciones entre los tres parámetros utilizados para evaluar la eficiencia de transfección en células C6. (a) Correlación entre producción de VEGF y porcentaje de células transfectadas. Cada valor representa el promedio  $\pm$  SD, n = 3. (b) Correlación entre producción de VEGF y valores de MFI. Cada valor representa el promedio  $\pm$  SD, n = 3. (c) Histogramas de GFP en células C6 48 h después de la transfección. M1 indica el umbral de señal positiva de GFP.

Una vez analizada la capacidad de transfección de los nanoplexes en células HEK293 y C6, llevamos a cabo estudios de transfección en células de cultivo primario de neurona, que representan un modelo más relevante desde el punto de

## Discusión

vista terapéutico. Las viabilidades celulares fueron excelentes (Fig. 1.5.a) en todos los casos, pero las eficiencias de transfección resultaron más bajas que en las anteriores líneas celulares, probablemente debido a la gran dificultad que supone la transfección en neuronas. La expresión de GFP se estudió mediante inunohistoquímica (Fig. 1.5.b) y se observaron algunas células dispersas que expresaban señal verde fluorescente. Esta baja señal de GFP refuerza la idea de la especificidad de tejido de la secuencia IRES del plásmido. En cuanto a la expresión de VEGF, observamos que había una producción basal de VEGF elevada en cultivos primarios de neuronas, probablemente atribuible a la presencia de células gliales encargadas de secretar factores angiogénicos y neurotróficos para mantener las células del SNC<sup>55, 56</sup>. A pesar de que los niveles de VEGF se vieron incrementados tras la transfección en todos los casos, sólo se pudieron detectar diferencias estadísticamente significativas respecto al control en el caso de los magnetoplexes (Fig. 1.5.c). A continuación, evaluamos la bioactividad de la proteína VEGF secretada por células transfectadas en células HUVEC, que responden con gran proliferación al efecto de esa proteína<sup>57, 58</sup>. Observamos que, en comparación con células control no tratadas con VEGF, las tratadas con VEGF secretado por células transfeccadas con nanoplexes respondieron con elevada proliferación a su efecto. Además, este incremento en la proliferación fue proporcional a la cantidad de VEGF presente en el sobrenadante celular (Fig. 1.5.c).

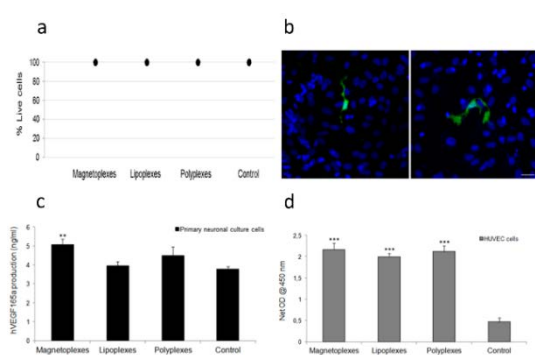


**Figura 1.5.** Viabilidad celular y eficiencia de transfección en células de cultivo primario de neurona y bioactividad de la proteína VEGF secretada por células transfectadas. (a) Viabilidad celular 48 h después de la transfección. Cada valor representa el promedio  $\pm$  SD, n = 3. (b) Imágenes de inmunohistoquímica donde se observa señal de GFP (verde). Azul: Hoescht (núcleos celulares). Escala: 25  $\mu$ m. (c) Producción de VEGF (ng/ml) por células de cultivo primario de neurona 48 h después de la transfección. Las células control no fueron tratadas con nanoplexes. Cada valor representa el promedio  $\pm$  SD, n = 3. (d) Proliferación de células HUVEC en respuesta a la proteína VEGF secretada por células transfectadas. Las células control no fueron tratadas con VEGF. Cada valor representa el promedio  $\pm$  SD, n = 3. Significancia estadística: \*p < 0,05, \*\*p < 0,01, \*\*\*p < 0,001 respecto a las células HUVEC control.

## *Discusión*

Tomando en cuenta los resultados de este trabajo, podemos decir que los vectores no-virales estudiados y, en particular, los magnetoplexos pueden ser adecuados para transportar el gen terapéutico VEGF a células del SNC de forma segura y eficaz, lo cual coincide con trabajos anteriores<sup>17</sup>. La estrecha relación descrita entre alteraciones vasculares en SNC y procesos neurodegenerativos<sup>40</sup>, junto con efectos beneficiosos descritos en modelos animales de Alzheimer y Parkinson tras la administración del factor VEGF<sup>57, 59</sup>, sugieren que el gen de VEGF puede ser un candidato terapéutico apropiado para tratar alteraciones del SNC. Además, en comparación con la liberación de fármacos, la liberación de genes presenta varias ventajas, como la posibilidad de administrar menores dosis y conseguir un efecto terapéutico duradero. La administración de vectores no-virales al SNC *in vivo* supone un gran reto todavía, ya que la mayoría de las veces es necesario recurrir a vías de administración muy invasivas que no tendrían cabida en la aplicación clínica. Sin embargo, se han hecho algunos avances en la búsqueda de vías no-invasivas para vehiculizar genes al SNC, y uno de los más prometedores es el uso de la vía intranasal. Un estudio reciente ha demostrado que se pueden transfectar células del SNC de rata a través de la administración intranasal de vectores no-virales<sup>60</sup>. Por lo tanto, creemos que sería interesante explorar esta vía no-invasiva en el campo de la terapia génica no-viral del SNC.

### **2. El rol del tensioactivo no-iónico de las formulaciones de niosomas en su eficiencia y proceso de transfección en retina de rata**

Existen varias enfermedades retinianas monogénicas bien caracterizadas, con mutaciones identificadas que en la mayoría de los casos afectan a genes específicos en las células del epitelio pigmentario (RPE) de la retina<sup>61</sup>. Las células RPE desempeñan funciones esenciales para el mantenimiento y correcto funcionamiento de retina neural, entre otras, protegen las células fotorreceptoras mediante la secreción de factores de crecimiento<sup>62</sup>. En varias enfermedades retinianas como, por ejemplo, la amaurosis congénita de Leber (LCA), la retinitis pigmentosa (RP) y la degeneración macular relacionada con la edad (AMD), la ceguera ocurre debido a la degeneración de las células RPE, lo cual lleva a pérdida o disfunción de las células fotorreceptoras<sup>61</sup>. Por lo tanto, las células RPE constituyen la principal diana en la mayoría de estrategias de terapia génica en ojo, y el éxito de estas estrategias depende de la capacidad de alcanzar niveles persistentes y elevados de la expresión del transgen, idealmente tras una única administración.

## *Discusión*

Los vectores no-virales poseen gran potencial para transferir genes terapéuticos específicos a células de la retina. Los denominados niosomas ya se han utilizado de manera eficaz para transfectar células retinianas tanto *in vitro* como *in vivo*, y la influencia de dos de sus componentes –el lípido catiónico y el lípido *helper*- ha sido estudiado en profundidad<sup>26, 63</sup>. Sin embargo, aún queda un importante margen de mejora para la transferencia génica en retina mediante el uso de niosomas y, para ello, es necesario investigar el rol que desempeña en la eficiencia de transfección su tercer componente, es decir, el tensioactivo no-iónico. Hasta la fecha, la mayoría de niosomas utilizados para transferir genes al ojo contenían el polisorbato 80 como tensioactivo no-iónico, pero no se han explorado otras opciones como el polisorbato 20 o el 85. Por tanto, en este trabajo elaboramos y caracterizamos, en cuanto a las propiedades físico-químicas y capacidad de transfección en células de la retina- tres formulaciones de niosomas que sólo diferían en el componente del tensioactivo no-iónico. Los niosomas utilizados contenían en su composición el lípido catiónico DOTMA, el lípido *helper* escualeno y uno de los siguientes tensioactivos no-iónicos: polisorbato 20, 80 o 85. Los niosomas se denominaron, según su composición, DST20, DST80 y DST85 (Figura 2.1.).

Los tensioactivos no-iónicos actúan como agentes emulsificadores en los niosomas, creando una barrera estérica que evita la agregación de las partículas<sup>22</sup>. Los tres polisorbatos utilizados comparten la misma estructura química básica, pero difieren en sus partes hidrófilas y en el número de grupos hidroxilo, difiriendo por tanto también en su balance hidrófilo-lipófilo (HLB) (Figura 2.1.). El parámetro HLB determina la liposolubilidad (HLB < 9) o hidrosolubilidad (HLB > 11) de los compuestos<sup>64</sup>. Entre los tres polisorbatos estudiados en este trabajo, el polisorbato 20 es el más hidrófilo, debido a la presencia de dos grupos hidroxilo y un ácido láurico, con un valor de HLB de 16,7. Le sigue en polisorbato 80 (HLB = 15), y el polisorbato 85 es el menos hidrófilo debido a la presencia de tres ácidos oleicos en su estructura química, con un HLB de 11.

## Discusión

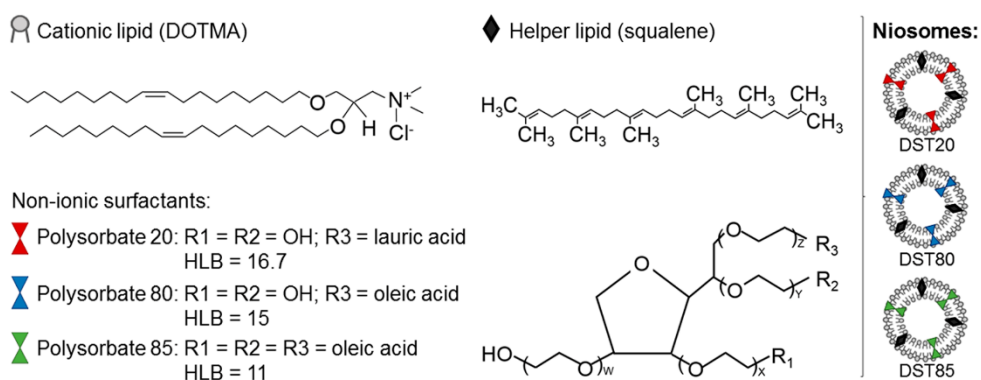


**Figura 2.1.** Esquema general de los niosomas y estructura química de sus componentes.

Los parámetros físico-químicos de las formulaciones son factores clave que determinan la eficiencia de trasfección de los niosomas. Las formulaciones DST20, DST80 y DST85 presentaron un tamaño medio de partículas entre 100 y 225 nm (Fig. 2.2.A, barras), lo cual es apropiado para la liberación génica<sup>65</sup>. Las pequeñas oscilaciones en el tamaño de las partículas tras la adición del plásmido en ratios peso/peso de lípido catiónico/ ADN 2/1, 5/1 y 10/1 se debieron probablemente a un balance entre el mayor espacio requerido por el lípido y la mayor condensación de ADN a mayores ratios<sup>26</sup>. En todas las condiciones, las partículas mostraron distribuciones de tamaño estrechas tal y como indican los bajos valores de PDI (Fig. 2.2.B). La carga superficial de las partículas tiene un impacto en la estabilidad de las formulaciones, y valores de potencial zeta entre – 30 mV y + 30 mV se han relacionado con una mayor propensidad para formar agregados<sup>46</sup>. Por otro lado, las cargas superficiales positivas facilitan la captación celular y permiten la formación de complejos con las moléculas de ADN de carga negativa a través de interacciones electrostáticas<sup>45</sup>. Los tres niosomas presentaron valores de potencial zeta superiores a + 40 mV (Fig. 2.2.A, líneas). Como era de esperar, al añadir el ADN estos valores descendieron, lo cual demuestra la interacción entre los grupos amina del lípido catiónico y los grupos fosfato del ADN, que neutraliza parcialmente la carga superficial<sup>66</sup>. Para determinar la morfología de las partículas, los niosomas se examinaron bajo el microscopio TEM y se pudo observar que todas presentaron forma esférica (Fig. 2.2.C-E). la habilidad de los nioplexes para proteger y liberar el plásmido se analizó mediante electroforesis en gel de agarosa (Fig. 2.2.F). Las bandas de ADN observadas indican que todas las formulaciones fueron capaces de

## Discusión

proteger el ADN frente a la degradación enzimática, incluso al ratio más bajo (2/1). La excepción fue quizá el DST80, que no pudo proteger en su totalidad al ADN frente a la acción de la DNase I. sin embargo, teniendo en cuenta que el objetivo de este trabajo era encontrar formulaciones más eficientes para la transfección en retina *in vivo*, seleccionamos el ratio 2/1 en todas las formulaciones, ya que permite incrementar la dosis de ADN a administrar sin aumentar el volumen total de la formulación. Esto puede incrementar la eficiencia de transfección y, además, reduce notablemente la toxicidad celular asociada a los lípidos catiónicos<sup>67</sup>.

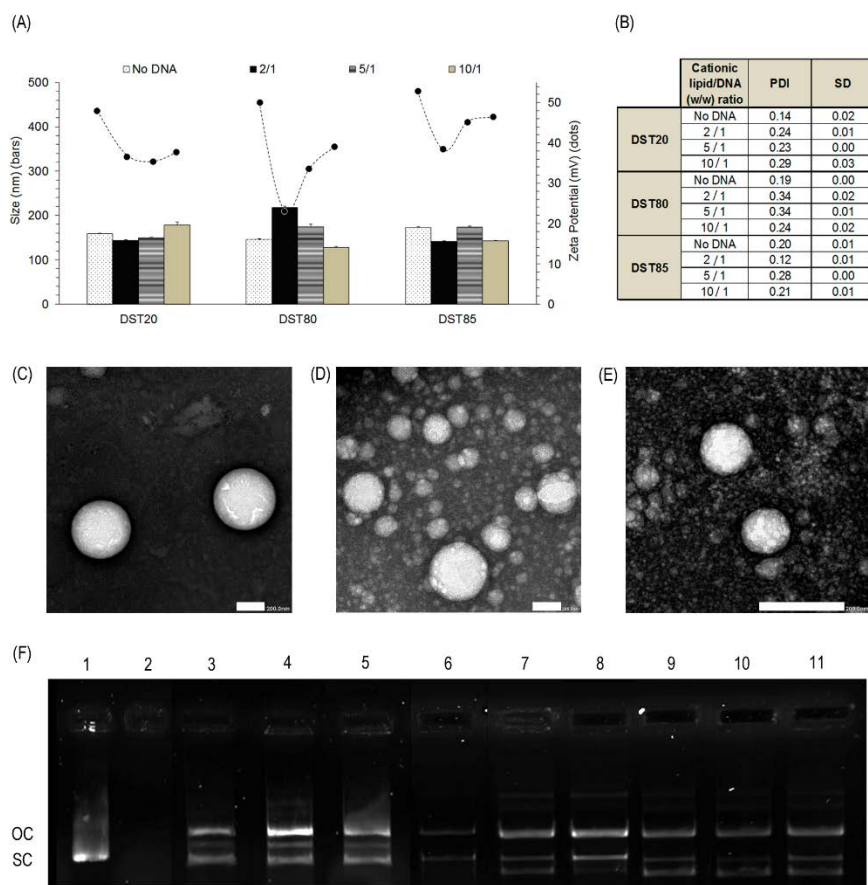


**Figura 2.2.** Caracterización físico-química de los niosomas DST20, DST80, DST85 y sus correspondientes nioplexos utilizando ratios peso/peso de lípido catiónico/ ADN 2/1, 5/1 y 10/1. (A) Los valores de tamaño se representan con barras y el potencial zeta con puntos. Cada valor representa el promedio  $\pm$  SD, n = 3. (B) Valores de PDI. Cada valor representa el

## *Discusión*

promedio ± SD, n = 3. (C-E) Imágenes de TEM de las partículas. Escala: 200 nm. (C) DST20, magnificación x20.000; (D) DST80, magnificación x20.000 y (E) DST85, magnificación x40.000. (F) Electroforesis en gel de agarosa para analizar la habilidad de los nioplexos de proteger y liberar el plásmido pCMS-EGFP. La enzima DNase I y el SDS se añadieron en las columnas 2-11. Columnas: 1-2, ADN desnudo; 3-5, nioplexos DST20, ratios 2/1, 5/1 y 10/1; 6-8, DST80, ratios 2/1, 5/1 y 10/1; 9-11, DST85, ratios 2/1, 5/1 y 10/1. OC: forma circular abierta del ADN. SC: forma supercompacta del ADN.

---

Una vez las formulaciones totalmente caracterizadas, se llevaron a cabo estudios de transfección *in vitro* –utilizando el ratio 2/1 en todos los casos- en las líneas celulares HEK293 –como modelo de transfección general- y ARPE19 –como modelo celular de la retina-. En ambos tipos celulares los nioplexos mostraron viabilidades celulares excelentes, superiores a 95% en HEK293 (Fig. 2.A<sub>1</sub>) y superiores a 85% en ARPE19 (Fig. 2B<sub>1</sub>), lo cual demuestra que fueron bien tolerados por las células. Esto también se corroboró por la sana apariencia de las células transfectadas en ambas líneas, 48 h después de la transfección (Fig. 2.3.A<sub>2</sub> y B<sub>2</sub>). Por el contrario, las células ARPE19 transfectadas con el control positivo Lipofectamine 2000™ exhibieron una baja viabilidad celular de alrededor del 55%, lo cual es consistente con estudios anteriores que afirman que este compuesto produce gran citotoxicidad en células de retina incluso a bajas concentraciones<sup>68</sup>. En cuanto a la eficiencia de transfección, la formulación DST85 fue la más eficaz en las células HEK293 (Fig. 2.A<sub>1</sub>), mientras que en ARPE19 la formulación con mayor eficiencia de trasnfeción fue DST20 (Fig. 2.B<sub>1</sub>). En general, se considera que las formulaciones con valores bajos de HLB y mayor liposolubilidad suelen captarse de manera más fácil por las células<sup>69, 70</sup>. Esto concuerda con los datos obtenidos en HEK293, ya que el polisorbato 85 es el que presenta un HLB más bajo entre los tensioactivos testados. Sin embargo, en ARPE19 ocurre lo contrario, puesto el polisorbato 20 es el más hidrófilo entre los tres, lo cual nos llevó a pensar que otros mecanismos dependientes del tipo celular podría desempeñar un papel importante a la hora de determinar la eficiencia de transfección de los nioplexos, por ejemplo, los mecanismos de internalización celular y las rutas endocíticas.

## Discusión

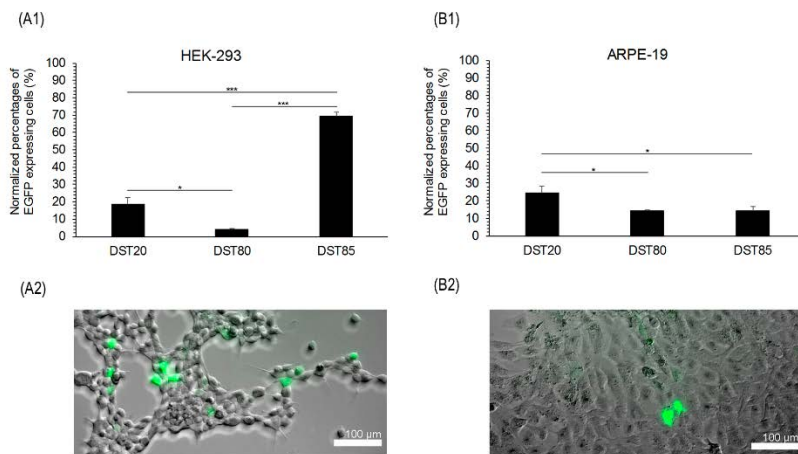


**Figura 2.3.** Eficiencia de transfección en HEK293 y ARPE19, 48 h después de la transfección con los nioplexos DST20, DST80 y DST85. (A1) Eficiencia de transfección en la línea celular HEK293. (A2) Imagen representativa de microscopio de fluorescencia donde se observa señal de EGFP en células HEK293 transfectadas con los nioplexos DST85. Magnificación x20. (B1) Eficiencia de transfección en la línea celular ARPE19. (B2) Imagen representativa de microscopio de fluorescencia donde se observa señal de EGFP en células ARPE19 transfectadas con los nioplexos DST20. Magnificación x20. Escala: 100 nm. Cada valor representa el promedio  $\pm$  SD, n = 3. Significancia estadística: \*p < 0,05, \*\*p < 0,01, \*\*\*p < 0,001.

En ese sentido, con el fin de entender el proceso de transfección con los nioplexos DST20, DST80 y DST85 en células ARPE19, analizamos los mecanismos de internalización celular y las rutas endocíticas que tomaron las formulaciones. Los vectores no-virales suelen internalizarse en las células a través de la endocitosis, siendo la endocitosis mediada por clatrinas o CME y la mediada por caveolas o CvME las más utilizadas<sup>71</sup>. La ruta CvME es considerada no-acídica y no-digestiva, mientras que las vesículas endocíticas formadas en la ruta CME suelen fusionarse con los lisosomas<sup>72, 73</sup>. Sin embargo, existe cierta controversia en este sentido ya que algunos autores afirman que las vesículas de la ruta CvME o caveosomas también se fusionan con los lisosomas en ciertos casos<sup>74, 75</sup>. Además, tampoco está claro si la fusión con el lisosoma favorece o no la transfección. Según algunos investigadores, la fusión con el lisosoma permite que el ADN se libere del vector, facilitando así su llegada al núcleo y, por tanto, favoreciendo la eficiencia de transfección<sup>76, 77</sup>. Por el contrario, otros autores sostienen que la fusión con el lisosoma conlleva la degradación del ADN, impidiendo así que ocurra la

## Discusión

transferencia génica<sup>78</sup>. En nuestro estudio, observamos que los nioplexos que entraban predominantemente por la vía CvME co-localizaban menos con el lisosoma y su eficiencia de transfección era mayor, como es el caso de la formulación DST20 (Figura 2.4.). En cambio, las formulaciones que entraban predominantemente a través de la ruta CME en las células, co-localizaban más con el lisosoma y la eficiencia de transfección era menor, como es el caso de los nioplexos DST85. Por lo tanto, nuestro estudio coincide con la hipótesis de degradación en el lisosoma, ya que parece que las formulaciones que evitan el compartimento lisosomal son las que mayor eficiencia de transfección obtienen. En cuanto a la formulación DST80, no observamos co-localización con ninguna de las dos rutas estudiadas, lo cual indicaría que puede usar otras vías como la macropinocitosis para entrar en las células. De hecho, un estudio reciente de liberación génica en células de la retina concluyó que los vectores no-virales lipídicos que contenían polisorbato 80 entraban predominantemente vía macropinocitosis en las células<sup>13</sup>.

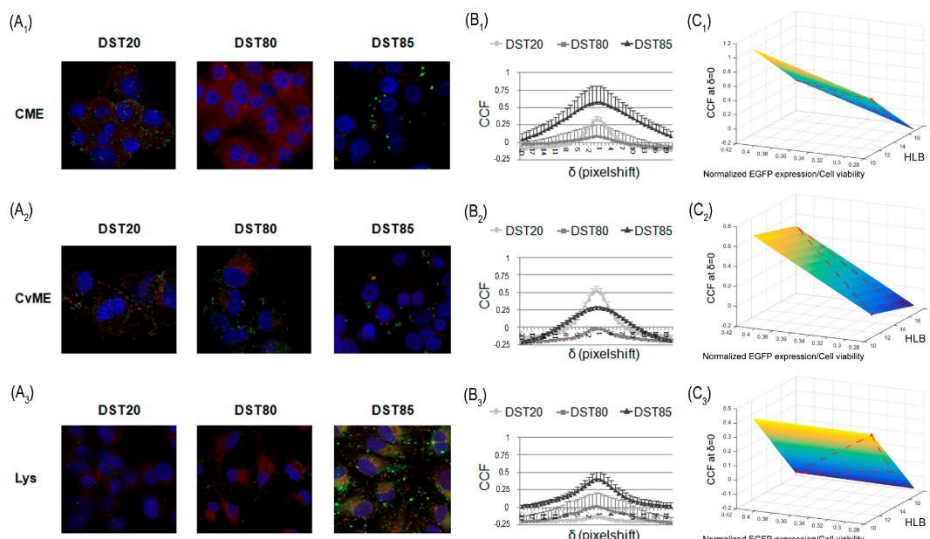


**Figura 2.4.** Rutas endocíticas y de tráfico intracelular de los nioplexos DST20, DST80 y DST85 en células ARPE19. (A1-3) Imágenes de microscopía confocal donde se observa co-localización entre los nioplexos que contienen el plásmido marcado con FITC (verde) y las rutas endocíticas (rojo). AlexaFluor546-Transferrin (CME), AlexaFluor555-CholeraToxin (CvME) y Lysotracker (lisosomas). (B1-3) Valores de co-localización entre la señal verde y roja determinadas por correlación cruzada. Los datos se presentan como promedio  $\pm$  SEM, n

## Discusión

= 3. (C1-3) Representaciones 3D que relacionan el valor de HLB, la eficiencia de transfección y la co-localización con los compartimentos intracelulares.

Basándonos en esos resultados, seleccionamos la formulación DST20 para realizar ensayos de transfección en retina *in vivo*. En primer lugar, llevamos a cabo un ensayo de transfección en cultivo primario de retina para validar la funcionalidad de los nioplexos y observamos una elevada señal de EGFP y células de apariencia sana (Figura 2.5.). Animados por estos resultados, administramos los nioplexos DST20 en retina de rata a través de inyecciones intravítreas (IV) (Figura 2.6.D-E) y subretinianas (SR) (Figura 2.6.B-C). En la mayoría de casos, la inyección IV permite transfectar células de la capa ganglionar de la retina, mientras que con las inyecciones SR, a pesar de ser más invasivas, es posible llegar a la capa de células RPE, las más interesantes desde el punto de vista terapéutico<sup>68, 79</sup>. En concordancia, nuestro estudio demostró que fuimos capaces de transfectar células de la capa ganglionar a través de las inyecciones IV, mientras que con las inyecciones SR conseguimos ver transfección también en la capa RPE. Desafortunadamente, la inyección SR es altamente invasiva y conlleva riesgo de inflamación, daño en las lentes e incluso desprendimiento de la retina<sup>80</sup>. Por lo tanto, no es aplicable en la práctica clínica y sería conveniente explorar nuevas de administración no-invasivas para transfectar células de la retina. En este sentido, se han hecho grandes avances en la liberación de fármacos, ya que recientemente se ha conseguido que un medicamento administrado de manera tópica en el ojo llegara a la parte posterior de la retina<sup>81</sup>. Este tipo de administración no implicaría riesgo alguno para el paciente y sería el ideal también para las formulaciones no-virales de terapia génica.

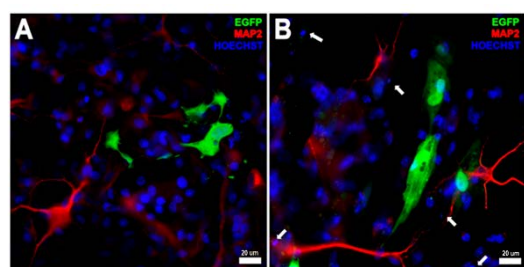


**Figura 2.5.** Expresión de la proteína EGFP en cultivo primario de células embrionarias de retina, analizada a través de inmunocitoquímica 96 h después de la transfección. (A) Expresión de EGFP tras transfectar con nioplexos DST20. (B) Expresión de EGFP tras transfectar con el control positivo Lipofectamine 2000<sup>TM</sup>. Rojo: MAP2 (marcador de dendritas neuronales); azul: HOECHST (núcleos celulares); verde: EGFP. Escala: 20 μm.

## Discusión

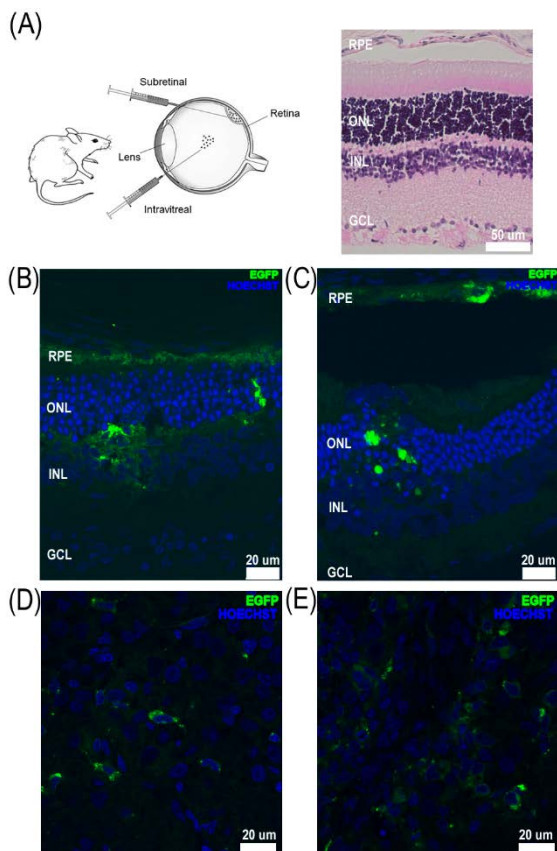


**Figura 2.6.** Expresión de EGFP en retina de rata *in vivo* tras inyecciones IV y SR. (A) Esquema general de las inyecciones IV y SR. (B) Micrografías de microscopía confocal de secciones de retina en la que se observa señal de EGFP tras la administración SR de nioplexes DST20. (C) Micrografías de microscopía confocal de secciones de retina en la que se observa señal de EGFP tras la administración SR de Lipofectamine 2000<sup>TM</sup>. (D) Inmunohistoquímica de fluorescencia en la que se observa señal de EGFP tras la administración IV de nioplexes DST20. (E) Inmunohistoquímica de fluorescencia en la que se observa señal de EGFP tras la administración IV de Lipofectamine 2000<sup>TM</sup>. Azul: Hoescht (núcleos celulares); verde: EGFP. Escala: 20  $\mu$ m. RPE (epitelio pigmentario de la retina), ONL (capas nucleares exteriores de la retina); INL (capas nucleares interiores de la retina); GCL (capa de células ganglionares de la retina).

En conclusión, hemos elaborado y caracterizado tres formulaciones de niosomas que únicamente diferían en su componente de tensioactivo no-iónico. Descubrimos que la formulación DST20, compuesta por DOTMA, escualeno y polisorbato 20, presentó alta eficiencia de transfección en células de la retina tanto *in vitro* como *in vivo*. Las células trasfectadas *in vivo* dependieron claramente de la vía de administración, ya que se llegó a la capa ganglionar a través de las inyecciones IV y a hasta la capa RPE a través de inyecciones SR. Gracias a los avances en ingeniería de vectores y de ADN, esperamos que en un futuro próximo estas formulaciones puedan ser administradas a través de vías no invasivas para la transferencia de genes terapéuticos a nivel de la capa RPE de la retina.

## Discusión

### 3. La influencia del material genético de las formulaciones de niosomas en su eficiencia de transfección en retina de rata

Además de la optimización de la formulación discutida en la sección anterior, la optimización del propio material genético es también necesaria en terapia génica no-viral. Hasta la fecha se han investigado varios elementos de los plásmidos para incrementar o prolongar la expresión génica como, por ejemplo, la secuencia del promotor, los motivos CpG, las señales de poliadenilación o las secuencias potenciadoras<sup>82-86</sup>. Sin embargo, los plásmidos también contienen una base bacteriana que consiste en las secuencias procariotas de origen de replicación y los genes de resistencia a antibióticos. Esas secuencias son esenciales para poder propagar los plásmidos de ADN en huéspedes bacterianos en el laboratorio, pero se han relacionado recientemente con respuestas inflamatorias, baja biocompatibilidad y reducción de la expresión génica. Por lo tanto, unidades mínimas de expresión génica como la estructura MC han surgido como alternativas prometedoras a los plásmidos convencionales. Los MC son secuencias de ADN circulares mínimas que a las que se les han eliminado las secuencias bacterianas y que únicamente contienen el gen de interés y las secuencias reguladoras. Por lo tanto, los MC pueden contener el mismo casete de expresión que sus plásmidos parentales, pero presentan un tamaño menor (Figura 3.1.). Gracias a su mayor biocompatibilidad, su uso permite una expresión génica más elevada y duradera, así como un mejor perfil de seguridad *in vivo*<sup>87-92</sup>. Distintos estudios han demostrado una mejora de la expresión génica utilizando la tecnología MC en diversos órganos, incluyendo el hígado<sup>93-95</sup>, el corazón<sup>96, 97</sup> y el músculo esquelético<sup>97</sup>, pero su aplicación en transferencia génica en retina y mediada por niosomas no ha sido aún estudiada.

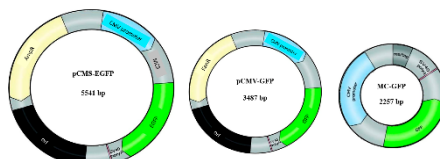


**Figura 3.1.** Composición del material genético. (A) pEGFP 5,5 kb, (B) pGFP 3,3 kb, (C) MC-GFP 2,3 kb. MC: minicircle; GFP: proteína verde fluorescente; EGFP: proteína verde fluorescente potenciada; pCMS: plásmido que contiene el promotor del citomegalovirus, una región de clonaje múltiple y el promotor SV40; pCMV: plásmido con promotor de citomegalovirus; bp: pares de bases.

## *Discusión*

Por lo tanto, el objetivo de este estudio fue proporcionar la primera evidencia de la eficiencia de transfección en retina con la tecnología MC combinada con los niosomas y compararla con la eficiencia de transfección de los plásmidos convencionales. Para ello, empleamos la formulación DST20, ya estudiada en el capítulo anterior, debido a su alta eficiencia de transfección en retina. Para formar los distintos nioplexos, unimos la formulación DST20 a tres tipos de material genético, dos plásmidos de distinto tamaño (pEGFP y pGFP) y un MC. Los niosomas y nioplexos fueron caracterizados en términos de tamaño de partícula, potencial zeta, PDI, morfología, estabilidad y habilidad de interacción con los distintos materiales genéticos. La capacidad de las formulaciones de proteger y liberar el material genético se estudió mediante electroforesis en geles de agarosa. Se llevaron a cabo estudios *in vitro* para evaluar la eficiencia de transfección y la viabilidad celular en la línea celular ARPE19. También se evaluó y comparó la eficiencia de transfección de las distintas formulaciones en cultivo primario de retina y en ensayos *in vivo* tras administraciones IV y SR.

Los niosomas DST20 presentaron morfología esférica y tamaños de partículas en el rango nanométrico, ambos apropiados para la terapia génica. Además, exhibieron valores bajos de PDI que indican gran homogeneidad en el tamaño, y potenciales zeta positivos, necesarios para la interacción electrostática con las moléculas de ADN de carga negativa<sup>45, 98, 99</sup>. Como era de esperar, al añadir el material genético el diámetro original de las partículas se vio incrementado, mientras que el potencial zeta se redujo debido a la parcial neutralización de las cargas por la interacción de los grupos amina del lípido catiónico y los grupos fosfato de las moléculas de ADN (Figura 3.2.A-B).

Los distintos materiales genéticos no alteraron las propiedades físico-químicas de las formulaciones, ya que los tres nioplexos presentaron características similares en cuanto al tamaño, la carga o el PDI, lo cual coincide con otros estudios<sup>100</sup>. Sin embargo, la eficiencia de transfección sí que varía de un material genético a otro, cuya explicación puede deberse a dos factores. Por un lado, la magnitud del incremento del incremento del tamaño de las partículas al añadir el ADN descarta la posibilidad de la agregación entre nioplexos. Por tanto, los eventos de unión entre niosoma y ADN a ratios peso/peso de lípido catiónico/ADN superiores conlleva probablemente la reorganización del material genético previamente unido, lo que resultaría en menos moléculas de ADN unidas por cada partícula de niosoma. Esto también afectaría a la capacidad de los niosomas de interaccionar con la membrana celular, lo cual tendría un impacto en la eficiencia de transfección. Por otro lado,

## Discusión

este estudio se llevó a cabo con una cantidad constante de ADN de 1,25 µg por condición, pero también deben considerarse otros factores como la longitud, el peso y la molaridad de cada tipo de material genético estudiado, ya que esos factores también afectaría a la cantidad de moléculas de ADN unidas a cada partícula de niosoma. Este hecho se observó en el ensayo ITC donde se obtuvieron diferentes curvas calorimétricas con cada nioplexo (Figura 3.2.D). Por tanto, las partículas de niosomas incorporarían mayor cantidad de moléculas MC que de plásmidos, lo que significa una mayor tasa de cassetes de expresión por niosoma, incrementando así la probabilidad de transfección de los niosomas que vectorizan moléculas MC<sup>92, 101</sup>.

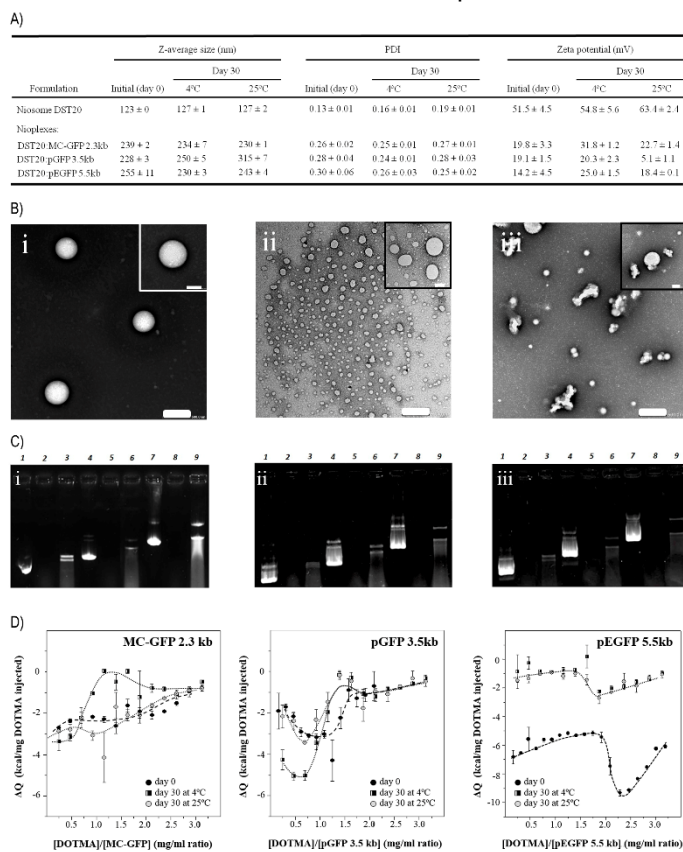


**Figura 3.2.** Caracterización físico-química y estudios de estabilidad de niosomas y nioplexos. (A) caracterización físico-química de niosomas y nioplexos a día 0 y a día 30 tras ser almacenados a 4°C y a 25°C. Cada valor representa el promedio ± SD, n = 3. (B) Imágenes de niosomas DST20 a día 0 (i), día 30 almacenados a 4°C (ii) y día 30 almacenados a 25°C. Escala: 500 nm (imágenes externas) y 200 nm (imágenes internas). (C) Ensayo de

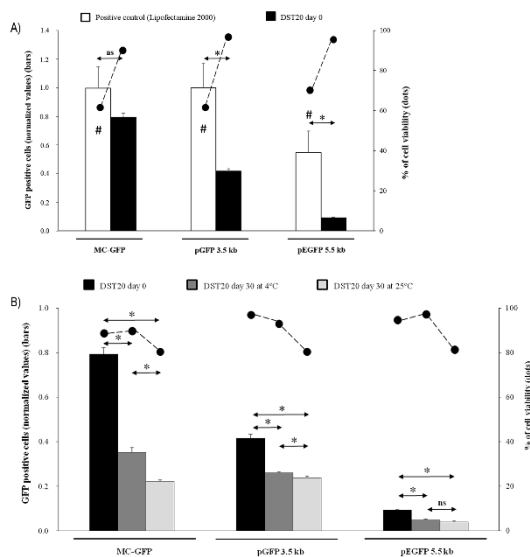
## *Discusión*

electroforesis en gel de agarosa para analizar la capacidad de proteger y liberar el ADN de los niosomas a día 0 (i), día 30 almacenado a 4°C (ii) y día 30 almacenado a 25°C (iii). Se añadió DNase I y SDS en las columnas 3, 6 y para evaluar la protección y liberación de MC-GFP, pGFP y pEGFP, respectivamente. Las columnas 1, 4 y 7 corresponden al control no unido a niosomas de cada material genético. Las columnas 2, 5 8 contienen cada material genético no unido a niosomas a los que se les ha añadido el enzima DNase I. (D) Estudio ITC con niosomas DST20 y los tres tipos de material genético. Variación de calor evoluciona por mg de DOTMA inyectado vs. el ratio de DOTMA/ADN expresado en mg/ml. Los símbolos representan los datos experimentales, mientras que las líneas discontinuas representan la tendencia de los perfiles ITC.

---

Las diferencias observadas en la expresión de GFP tras el almacenamiento durante 30 días a 4°C y a 25°C (Figura 3.3.) pueden explicarse por un cúmulo de factores. De hecho, la eficiencia de transfección de los niosomas puede verse afectada por variaciones en distintos parámetros como el tamaño de las partículas, su potencial zeta, su morfología o su afinidad por el ADN<sup>102</sup>. En este sentido, las imágenes de TEM demostraron una pérdida de la morfología esférica transcurridos 30 días e incluso cierta agregación de partículas (Figura 3.2.C), lo cual dificultaría las interacciones con el ADN. En realidad, esto fue confirmado por los ensayos de ITC y de electroforesis, ya que tanto la capacidad de interacción con las moléculas de ADN como la habilidad de protección frente a la degradación enzimática se vieron afectadas por el transcurso del tiempo. A pesar de que los nioplexos que contenían MC a día 30 presentaron eficiencias de transfección superiores que los nioplexos que contenían plásmido a día 0 (Figura 3.3.), se requieren mayores esfuerzos para desarrollar formulaciones más estables, ya sea mediante la utilización de métodos de caracterización más precisos o mediante la modificación de las formulaciones.

## Discusión



Dado que las vías de administración IV y SR son hoy en día las más viables para liberar genes terapéuticos en retina<sup>103</sup>, los nioplexos unidos a los distintos tipos de material genético fueron inyectados a través de esas vías en rata *in vivo*. En concordancia con estudios anteriores, la inyección IV alcanzó predominantemente células de la capa ganglionar, mientras que a través de las inyecciones SR fue posible observar cierto nivel de transfección en la capa RPE. La transfección a ese nivel es la más relevante clínicamente, ya que la mayoría de enfermedades monogénicas retinianas que cursan con ceguera son causadas por mutaciones específicas de los genes de las células de esa capa<sup>104</sup>. El análisis cualitativo de la expresión de GFP *in vivo* demostró que, tanto en la inyección IV como en la SR, la mayor eficiencia de transfección se consiguió con los nioplexos que vectorizaban el MC (Figuras 3.5. y 3.6.), sugiriendo que esta tecnología podría tener gran potencial para transferir genes terapéuticos en retina. Es importante mencionar también que la ausencia de motivos CpG y secuencias bacterianas en la tecnología MC los hace más biocompatible, lo que facilitaría su uso en aplicaciones clínicas. Por otro lado, también se observó alta eficiencia de transfección con la formulación Lipofectamine 2000™ utilizada como control positivo, pero su aplicación está limitada por su elevada citotoxicidad en células de la retina, incluso a bajas concentraciones. De hecho, en nuestro trabajo también hemos encontrado núcleos apoptóticos en células de cultivo primario de retina al utilizar este compuesto (Figura 3.4.D-F).

## Discusión

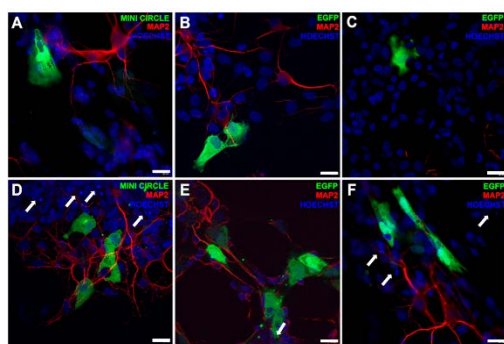


**Figura 3.4.** Expresión de la proteína GFP en células de cultivo primario de retina transfectadas con nioplexos DST20 que vectorizan (A) MC-GFP, (B) pGFP o (C) pEGFP. Las imágenes (D-F) corresponden al control positivo de cada tipo de material genético utilizando Lipofectamine 2000™. Azul: Hoescht (núcleos celulares), rojo: MAP2 (dendritas neuronales) y verde: GFP. Las flechas blancas indican núcleos apoptóticos. Escala: 20  $\mu$ m.

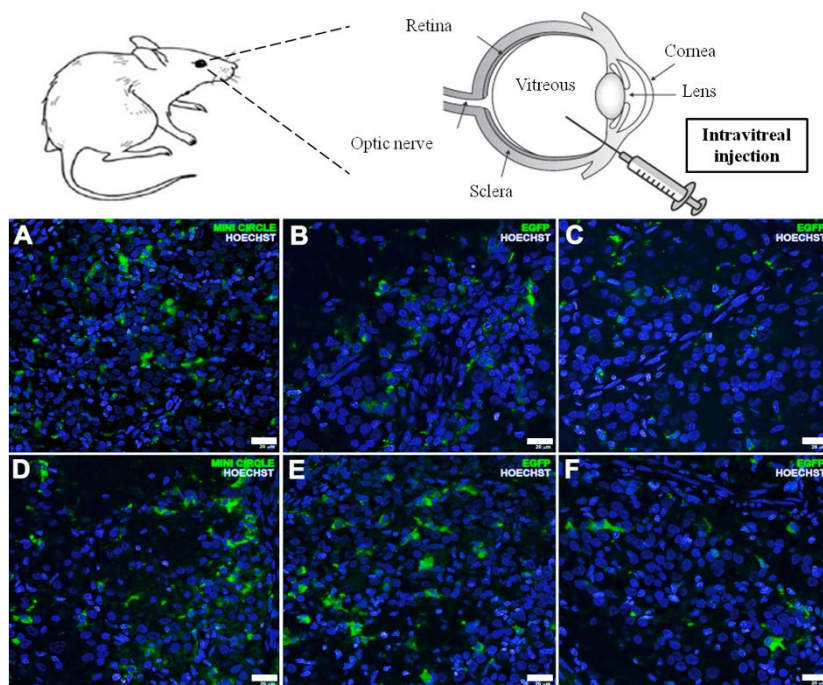


**Figura 3.5.** Expresión de la proteína GFP *in vivo* tras la administración IV de los nioplexos que vectorizan (A) MC-GFP, (B) pGFP o (C) pEGFP. Las imágenes (D-F) corresponden al control positivo de cada tipo de material genético utilizando Lipofectamine 2000™. Azul: Hoescht (núcleos celulares), rojo: MAP2 (dendritas neuronales) y verde: GFP. Las flechas

## Discusión

blancas indican núcleos apoptóticos. Escala: 20 µm. RPE (epitelio pigmentario de la retina); OS (segmentos externos); ONL (capas nucleares exteriores de la retina); INL (capas nucleares interiores de la retina); GCL (capa de células ganglionares de la retina).

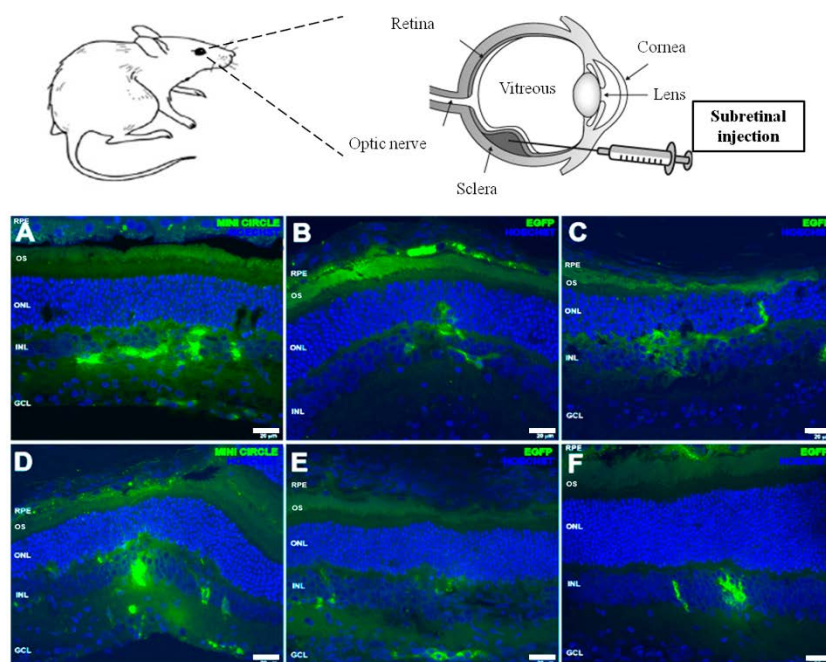


**Figura 3.6.** Expresión de la proteína GFP *in vivo* tras la administración SR de los nioplexos que vectorizan (A) MC-GFP, (B) pGFP o (C) pEGFP. Las imágenes (D-F) corresponden al control positivo de cada tipo de material genético utilizando Lipofectamine 2000<sup>TM</sup>. Azul: Hoescht (núcleos celulares), rojo: MAP2 (dendritas neuronales) y verde: GFP. Las flechas blancas indican núcleos apoptóticos. Escala: 20 µm. RPE (epitelio pigmentario de la retina); OS (segmentos externos); ONL (capas nucleares exteriores de la retina); INL (capas nucleares interiores de la retina); GCL (capa de células ganglionares de la retina).

## *Discusión*

En conclusión, los principales hallazgos de este estudio son los siguientes: (i) los niosomas DST20 son capaces de proteger y liberar de forma adecuada los diferentes tipos de material genético; (ii) la capacidad de los niosomas de proteger, liberar e interaccionar con el ADN se ve afectada con el transcurso del tiempo y la temperatura de almacenaje; (iii) los parámetros físico-químicos de los niosomas DST20 unidos a distintos materiales genéticos no varían, mientras que sí se observan diferencias en su eficiencia de transfección; (iv) los nioplexos DST20 que contienen MC presentan mayor eficiencia de transfección que los que contienen plásmidos, *in vitro*, incluso después de 30 días de almacenaje; (v) los nioplexos son capaces de transferir material genético de forma eficaz tanto *ex vivo* en cultivo primario de retina como *in vivo* tras inyecciones IV y SR, y los que contienen MC presentan mayor eficiencia de transfección en todos los casos. Por lo tanto, consideramos que los niosomas DST20 unidos a MC representan un método eficiente y seguro para vehiculizar genes a la retina, y podría tener cabida en la aplicación clínica para transportar genes terapéuticos en distintas enfermedades retinianas.

### **4. Aspectos tridimensionales de los sistemas no-virales de liberación génica: búsqueda de nuevas sinergias complementarias entre niosomas e hidrogeles de ácido hialurónico**

Además de la optimización del vector no-viral y del material genético discutidos en secciones anteriores, una nueva tendencia hoy en día es buscar nuevas sinergias entre sistemas de liberación génica no-viral e ingeniería tisular para mejorar la eficiencia de transfección. De hecho, estas estrategias combinadas pueden ofrecer varias ventajas, como una mayor estabilidad de los sistemas de liberación y una menor toxicidad. Además, el hecho de complementar la transferencia génica con el diseño de matrices tridimensionales permite llevar a cabo una liberación local y efectiva del ADN, lo que facilitaría su aplicabilidad clínica en el tratamiento de enfermedades como el cáncer o en la regeneración tisular<sup>35, 36</sup>. El ácido hialurónico (HA) es un glicosaminoglicano aniónico y constituye uno de los componentes principales de la matriz extracelular<sup>105</sup>. Su uso y estudio se ha incrementado en los últimos años debido a su biocompatibilidad y su capacidad de incorporar una amplia variedad de moléculas, incluyendo los ácidos nucleicos<sup>106</sup>.

Por lo tanto, el objetivo principal de este trabajo fue desarrollar un sistema de liberación génica eficiente basado en la combinación de niosomas e hidrogeles de ácido hialurónico. Elaboramos tres formulaciones de niosoma diferentes (niosomas

## Discusión

1, 2 y 3), con distinta composición de lípido catiónico, lípido *helper* y tensioactivo no-iónico (Figura 4.1.). Unimos los niosomas al plásmido que codifica el gen de la luciferasa para obtener los correspondientes nioplexes. Los niosomas y nioplexes fueron caracterizados en cuanto al tamaño, potencial zeta, PDI y eficiencia de transfección de células mesenquimales de ratón (mMSC) en cultivos 2D. Los hidrogeles de HA que contenían los nioplexes fueron caracterizados atendiendo a sus propiedades biomecánicas, distribución de partículas y cinética de liberación de los nioplexes. También se evaluó la actividad de los nioplexes una vez liberados de los hidrogeles y su capacidad de transfectar células mMSC encapsuladas en hidrogeles en cultivos 3D.

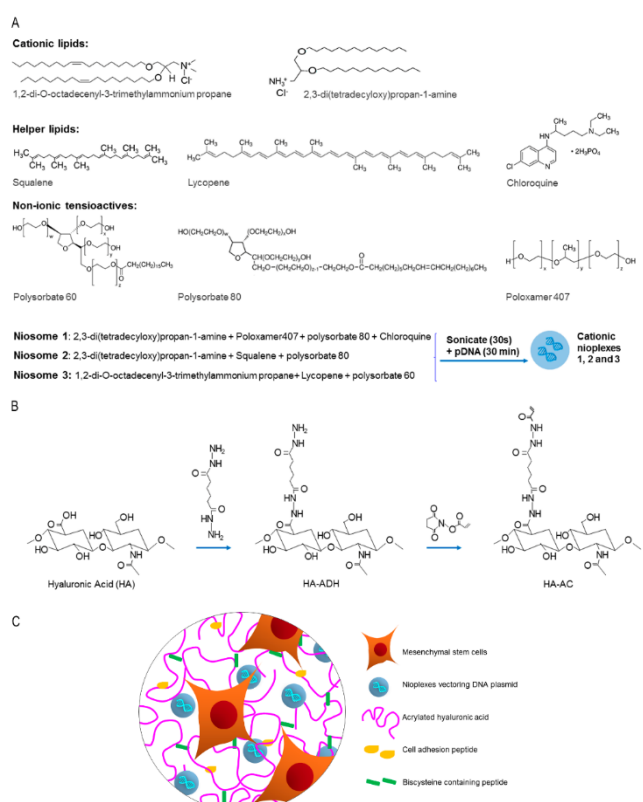


**Figura 4.1.** Esquema general de los niosomas catiónicos e hidrogeles de HA utilizados en este trabajo. (A) Lípidos catiónicos, lípidos *helper* y tensioactivos no-iónicos utilizados en este trabajo. (B) Modificación del HA para obtener hidrogeles de HA. (C) Esquema representativo de hidrogeles de HA con nioplexes y células encapsuladas.

## *Discusión*

A pesar de que altas concentraciones de complejos de ADN/vectores no-virales en hidrogeles han demostrado mayores eficiencias de transfección<sup>107</sup>, la introducción física de grandes cantidades de ADN no es tarea fácil dada su tendencia a formar agregados en los hidrogeles<sup>108</sup>. Entre la gran variedad de vectores no-virales, los formados por derivados del polímero poli(etileno imina) o PEI han demostrado alta eficiencia de transfección en hidrogeles tanto *in vitro* como *in vivo*<sup>109</sup>. Si embargo, su aplicabilidad clínica está limitada por la elevada citotoxicidad de los compuestos derivados del PEI<sup>110</sup>. En este sentido, los niosomas podrían ser una alternativa apropiada dada su alta compatibilidad con sistemas biológicos y su demostrada capacidad de transfección<sup>64</sup>. En este trabajo, además, las eficiencias de transfección obtenidas con los niosomas encapsulados fueron similares a las obtenidas con PEI en trabajos anteriores<sup>111</sup>, lo que indica que los niosomas pueden ser buenos candidatos para sustituir al PEI y evitar los problemas de toxicidad manteniendo la alta capacidad de transfección.

Los tres niosomas utilizados en este trabajo diferían en su composición (Figura 4.1.) y los componentes fueron escogidos en base a los resultados de trabajos anteriores. Por ejemplo, las formulaciones con polisorbato 80 combinado con escualeno han demostrado ser eficaces en otros estudios<sup>26</sup>. También se ha demostrado recientemente que la incorporación de licopeno en formulaciones que contienen DOTMA y polisorbato 60 mejora su eficiencia de transfección<sup>24</sup>, y el Poloxamer 407 es ampliamente utilizado para liberación de fármacos<sup>112</sup>. Por su parte, la cloroquina mejora la eficiencia de transfección *in vitro* e *in vivo*<sup>113</sup>. Por lo tanto, la selección de los componentes, su concentración y los ratios peso/peso de lípido catiónico/ADN utilizados en este trabajo se basó en estudios anteriores.

Los tres niosomas presentaron valores de potencial zeta positivos (Figura 4.2.B), necesario para la interacción con las moléculas de ADN de carga negativa<sup>45, 66</sup>. Además, la carga superficial positiva facilita la captación celular de las partículas<sup>44</sup>. En comparación con las células control no tratadas, todas las formulaciones fueron capaces de transfectar células mMSC en cultivo 2D, pero las basadas en el niosoma 1 fueron las que exhibieron mayor eficiencia de transfección (Figura 4.2.C). A pesar de que la formulación usada como control positivo –Lipofectamine 2000™- fue la más eficaz, su aplicabilidad está limitada debido su citotoxicidad, por lo que escogimos el niosoma 1 para continuar con el estudio.

## Discusión

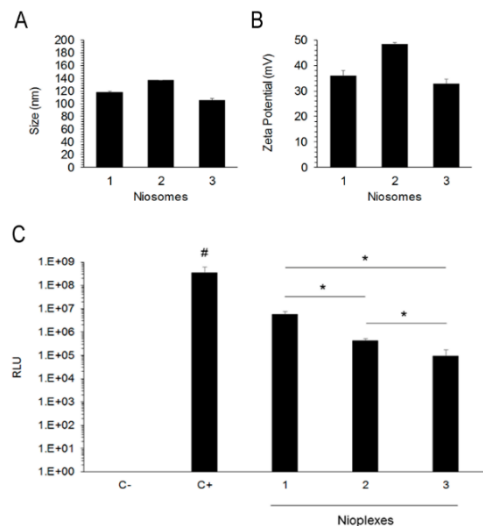


**Figura 4.2.** Caracterización de los niosomas. (A) Tamaño (nm). (B) Potencial zeta. (C) Eficiencia de transfección a las 48 h en células mMSC utilizando niosomas 1, 2 y 3. C+: control positivo, células tratadas con Lipofectamine 2000™. C-: control negativo, células no tratadas. Cada valor representa el promedio  $\pm$  SD, n = 3. RLU: Relative light units (expresión del transgen luciferasa).

El uso de nioplexes a ratios bajos permite incrementar la dosis de ADN y reducir la toxicidad celular asociada a los lípidos catiónicos<sup>13</sup>. Además de usar los niosomas 1 al ratio peso/peso lípido catiónico/ADN 2/1, para conseguir introducir cantidades terapéuticamente más relevantes en los hidrogeles, concentraremos la formulación del niosoma de 1 mg/ml a 2 mg/ml. Las imágenes de TEM de la formulación concentrada muestran que ni el tamaño ni la morfología se vieron afectadas por el proceso de concentración y, como era de esperar, se observa mayor número de partículas en la muestra concentrada (Figura 4.3.B). Asimismo, la capacidad de transfección de células mMSC en cultivo 2D tampoco se vio afectada (Fig. 4.3.C), por lo que se decidió utilizar la formulación concentrada para los estudios en hidrogeles de HA.

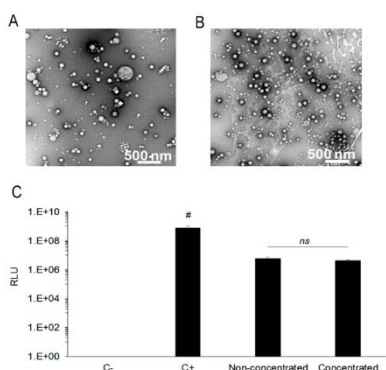


**Figura 4.3.** Caracterización de la formulación concentrada y no concentrada. (A-B) Imágenes de TEM de la formulación no concentrada (A) y concentrada (B). Magnificación: x10.000. Escala: 500 nm. (C) Eficiencia de transfección a las 48 h en células mMSC. Cada valor representa el promedio  $\pm$  SD, n = 3. RLU: Relative light units (expresión del transgen luciferasa).

## Discusión

Para obtener cantidades de ADN terapéuticamente relevantes<sup>114</sup>, evaluamos tres cantidades diferentes de nioplexos en los hidrogeles, obteniendo concentraciones finales de 0,055 µg/ml, 0,12 µg/ml y 0,2 µg/ml de ADN en los hidrogeles **2**, **3** y **4**, respectivamente. El hidrogel **1** no contenía nioplexos y fue utilizado como control negativo. Las distintas concentraciones de ADN en los hidrogeles pueden ocasionar diferencias en sus propiedades mecánicas, las cuales determinan en gran medida la eficiencia de transfección en los hidrogeles. Se ha descrito que los hidrogeles más rígidos (> 800 Pa) impiden la difusión celular, dificultando así que ocurra la transfección, mientras que los hidrogeles más blandos (200 – 260 Pa) facilitarían la difusión celular y, por tanto, la transfección<sup>108</sup>. La evaluación reológica de los hidrogeles reveló gran variabilidad en las propiedades mecánicas de los hidrogeles, siendo el hidrogel **3** el más rígido y el hidrogel **4** el más blando (Figura 4.4.A-B). En cuanto a la distribución de los nioplexos dentro de los hidrogeles, estos mostraron en su mayoría una distribución homogénea y sin agregados (Fig. 4.4.C-E). Aunque no se pudo utilizar para cultivar células en 3D debido a que no contenía medio celular en su composición, el hidrogel **4** presentó características muy favorables para aplicaciones *in vivo*, debido a su alta concentración de ADN, ausencia de excesiva rigidez y distribución homogénea de los nioplexos. Para aplicaciones de transfección celular en cultivos 3D de células mMSC, utilizamos los hidrogeles **2** y **3**. En general, estos resultados demuestran que los nioplexos pueden ser incorporados en hidrogeles de HA manteniendo sus propiedades mecánicas y sin crear agregados.

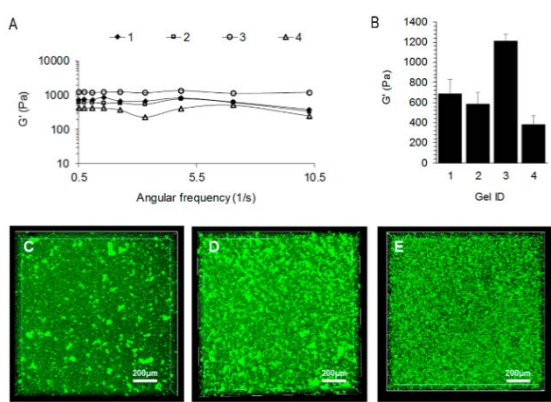


**Figura 4.4.** Caracterización de los hidrogeles de HA con nioplexos. (A) Las propiedades mecánicas de los hidrogeles se evaluaron utilizando reometría en un rango de frecuencia de 0,1-10 rad/s y a una tensión constante de 0,1. (B) Promedio de medidas reológicas. (C-E) Distribución de los nioplexos en los hidrogeles **2**, **3** y **4**. Gel ID: **1**, hidrogel control sin nioplexos; **2**, 0,055 µg/ml ADN; **3**, 0,12 µg/ml ADN; **4**, 0,2 µg/ml ADN. Escala: 200 µm.

## Discusión

Para determinar si los nioplexos mantenían su bioactividad una vez liberados del hidrogel, realizamos una transfección en cultivo 2D con nioplexos liberados de hidrogeles degradados con tripsina. Tal y como se observa en la Figura 4.5., a pesar de que la eficiencia de transfección se vio ligeramente reducida, los nioplexos seguían manteniendo su actividad y su capacidad de transfección. La disminución en la eficiencia era, de todos modos, de esperar, ya que la presencia de tripsina y otros productos procedentes de la degradación de los hidrogeles pueden interferir en el proceso de transfección<sup>109</sup>.

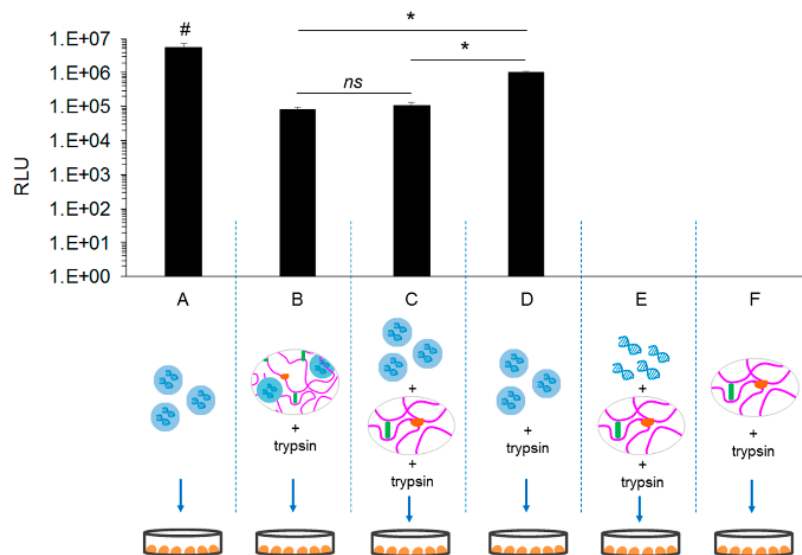


**Figura 4.5.** Actividad biológica de los nioplexos liberados de hidrogeles de HA.

Se postula que existen dos mecanismos principales que determinan la eficiencia de transfección en los hidrogeles: la cinética de liberación de los nioplexos y la tasa de infiltración celular en el hidrogel<sup>115</sup>. Los nioplexos liberados tras la degradación del hidrogel transfectarían las células de su alrededor, mientras que a medida que las células se infiltran en el hidrogel encontrarían nioplexos en su camino, que fagocitarían iniciando el proceso de transfección<sup>116, 117</sup>. En este sentido, se espera que los hidrogeles más blandos permitan una mayor infiltración celular y, por tanto, proporcionen una mayor eficiencia de transfección que los hidrogeles más rígidos<sup>115</sup>. Volviendo a la cinética de liberación, para su aplicación terapéutica interesa que los nioplexos se liberen de forma progresiva y sostenida, de modo que

## Discusión

permitan prolongar el efecto terapéutico. Precisamente, eso es lo que observamos en este trabajo, ya que la totalidad de los nioplexos es liberada del hidrogel en 7 días en presencia de la enzima colagenasa y la cinética de liberación es algo más lenta en ausencia de esa enzima (Figura 4.6.A). Finalmente, estudiamos la capacidad de transfección de los nioplexos incorporados, junto con células mMSC, en hidrogeles de ácido hialurónico. Los resultados demostraron que las células difundieron en todos los hidrogeles y, a pesar de ser el más rígido, la mayor eficiencia de transfección se obtuvo en el hidrogel **3**, que también poseía mayor cantidad de ADN (Figura 4.6.B). Por lo tanto, esto sugiere que las cantidades elevadas de ADN compensan la excesiva rigidez del hidrogel en el proceso de transfección. Además, las viabilidades celulares fueron excelentes en todos los casos, lo cual indica que la presencia de los nioplexos en los hidrogeles no resulta tóxica para las células.

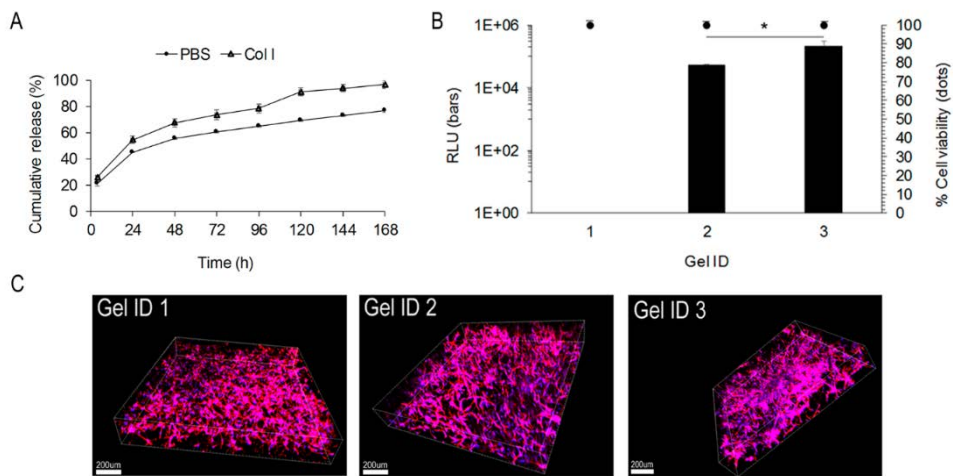


**Figura 4.6.** (A) Cinética de liberación de los nioplexos de los hidrogeles de HA en presencia y ausencia de colagenasa I (Col I). (B) Eficiencia de transfección (barras) y viabilidad celular (puntos) en cultivos 3D en los hidrogeles **1**, **2** y **3**. Cada valor representa el promedio  $\pm$  SD, n = 3. (C-E) Imágenes representativas de difusión celular en los hidrogeles **1**, **2** y **3**. Azul: DAPI (núcleos celulares), rojo: F-actina (citoplasma). Escala: 200  $\mu$ m.

En conclusión, desarrollamos con éxito un método para incorporar formulaciones concentradas de niosomas en hidrogeles de HA. En general, los hidrogeles de HA que contenían nioplexos presentaron propiedades mecánicas adecuadas, una distribución de partículas homogénea y sin agregados, cinéticas de liberación de nioplexos adecuadas, permitieron gran difusión celular y fueron capaces de transfectar células mMSC en cultivos 3D con excelente viabilidad celular. Creemos

### *Discusión*

que el conocimiento adquirido a través de este modelo *in vitro* puede ser utilizado para diseñar sistemas de liberación génica no-viral, local y eficiente para aplicaciones *in vivo*.

Para terminar, esta tesis doctoral, en su totalidad, describe y explora los factores clave que determinan la eficiencia de transfección y que se deben tener en cuenta a la hora de diseñar sistemas no-virales de liberación génica. Estos aspectos clave incluyen la composición y las propiedades físico-químicas de los vectores no-virales, la composición y conformación del material genético y la búsqueda de sinergias complementarias con otras tecnologías como la ingeniería tisular. En nuestra opinión, el concepto del vector no-viral único y universal ha quedado obsoleto, y debemos trabajar en el diseño de partículas multifuncionales específicamente adaptadas para cada aplicación. Gracias a los continuos avances para prolongar e incrementar la expresión de genes terapéuticos en sistemas de liberación génica no-viral, junto con los estudios realizados sobre la administración a través de vías no-invasivas, su aplicación clínica está cada vez más cerca.

## **References / Erreferentziak / Referencias**

1. Pezzoli D, Chiesa R, De Nardo L, Candiani G. We still have a long way to go to effectively deliver genes!. *J Appl Biomater Funct Mater.* 2012;10(2):82-91.
2. Rodríguez-Gascón A, del Pozo-Rodríguez A, Solinis MA. Non-viral delivery systems in gene therapy. In: Dr Francisco Martín, ed. *Gene therapy - tools and potential applications.* InTech; 2013.
3. The journal of gene medicine. Gene therapy clinical trials worldwide. <http://www.wiley.com/legacy/wileychi/genmed/clinical/>. Accessed 01/07, 2015.
4. Li Y, Li B, Li CJ, Li LJ. Key points of basic theories and clinical practice in rAd-p53 ( gendicine ) gene therapy for solid malignant tumors. *Expert Opin Biol Ther.* 2015;15(3):437-454. doi: 10.1517/14712598.2015.990882 [doi].
5. Liang M. Clinical development of oncolytic viruses in china. *Curr Pharm Biotechnol.* 2012;13(9):1852-1857. doi: BSP/CPB/E-Pub/000276-13-1 [pii].
6. Yla-Herttula S. Endgame: Glybera finally recommended for approval as the first gene therapy drug in the european union. *Mol Ther.* 2012;20(10):1831-1832. doi: 10.1038/mt.2012.194 [doi].
7. Pol J, Kroemer G, Galluzzi L. First oncolytic virus approved for melanoma immunotherapy. *Oncoimmunology.* 2015;5(1):e1115641. doi: 10.1080/2162402X.2015.1115641 [doi].
8. Shim G, Kim D, Park GT, Jin H, Suh SK, Oh YK. Therapeutic gene editing: Delivery and regulatory perspectives. *Acta Pharmacol Sin.* 2017;38(6):738-753. doi: 10.1038/aps.2017.2 [doi].
9. Jin L, Zeng X, Liu M, Deng Y, He N. Current progress in gene delivery technology based on chemical methods and nano-carriers. *Theranostics.* 2014;4(3):240-255. doi: 10.7150/thno.6914 [doi].
10. Keles E, Song Y, Du D, Dong WJ, Lin Y. Recent progress in nanomaterials for gene delivery applications. *Biomater Sci.* 2016;4(9):1291-1309. doi: 10.1039/c6bm00441e [doi].
11. Srikanth M, Kessler JA. Nanotechnology-novel therapeutics for CNS disorders. *Nat Rev Neurol.* 2012;8(6):307-318. doi: 10.1038/nrneurol.2012.76 [doi].
12. Yin H, Kanasty RL, Eltoukhy AA, Vegas AJ, Dorkin JR, Anderson DG. Non-viral vectors for gene-based therapy. *Nat Rev Genet.* 2014;15(8):541-555. doi: 10.1038/nrg3763 [doi].
13. Ojeda E, Puras G, Agirre M, et al. Niosomes based on synthetic cationic lipids for gene delivery: The influence of polar head-groups on the transfection efficiency in HEK-293, ARPE-19 and MSC-D1 cells. *Org Biomol Chem.* 2015;13(4):1068-1081. doi: 10.1039/c4ob02087a [doi].

14. Jubeli E, Maginty AB, Khalique NA, et al. Cationic lipids bearing succinic-based, acyclic and macrocyclic hydrophobic domains: Synthetic studies and in vitro gene transfer. *Eur J Med Chem.* 2017;125:225-232. doi: S0223-5234(16)30757-7 [pii].
15. Pack DW, Hoffman AS, Pun S, Stayton PS. Design and development of polymers for gene delivery. *Nat Rev Drug Discov.* 2005;4(7):581-593. doi: nrd1775 [pii].
16. Agirre M, Zarate J, Puras G, Ojeda E, Pedraz JL. Improving transfection efficiency of ultrapure oligochitosan/DNA polyplexes by medium acidification. *Drug Deliv.* 2015;22(1):100-110. doi: 10.3109/10717544.2013.871373 [doi].
17. Soto-Sanchez C, Martinez-Navarrete G, Humphreys L, et al. Enduring high-efficiency in vivo transfection of neurons with non-viral magnetoparticles in the rat visual cortex for optogenetic applications. *Nanomedicine.* 2015;11(4):835-843. doi: 10.1016/j.nano.2015.01.012 [doi].
18. Choi WJ, Kim JK, Choi SH, Park JS, Ahn WS, Kim CK. Low toxicity of cationic lipid-based emulsion for gene transfer. *Biomaterials.* 2004;25(27):5893-5903. doi: 10.1016/j.biomaterials.2004.01.031 [doi].
19. Grimaldi N, Andrade F, Segovia N, et al. Lipid-based nanovesicles for nanomedicine. *Chem Soc Rev.* 2016;45(23):6520-6545. doi: 10.1039/c6cs00409a [doi].
20. Karmali PP, Chaudhuri A. Cationic liposomes as non-viral carriers of gene medicines: Resolved issues, open questions, and future promises. *Med Res Rev.* 2007;27(5):696-722. doi: 10.1002/med.20090 [doi].
21. Dabkowska AP, Barlow DJ, Campbell RA, Hughes AV, Quinn PJ, Lawrence MJ. Effect of helper lipids on the interaction of DNA with cationic lipid monolayers studied by specular neutron reflection. *Biomacromolecules.* 2012;13(8):2391-2401. doi: 10.1021/bm300639n [doi].
22. Liu F, Yang J, Huang L, Liu D. Effect of non-ionic surfactants on the formation of DNA/emulsion complexes and emulsion-mediated gene transfer. *Pharm Res.* 1996;13(11):1642-1646.
23. Puras G, Martinez-Navarrete G, Mashal M, et al. Protamine/DNA/niosome ternary nonviral vectors for gene delivery to the retina: The role of protamine. *Mol Pharm.* 2015;12(10):3658-3671. doi: 10.1021/acs.molpharmaceut.5b00422 [doi].
24. Mashal M, Attia N, Puras G, Martinez-Navarrete G, Fernandez E, Pedraz JL. Retinal gene delivery enhancement by lycopene incorporation into cationic niosomes based on DOTMA and polysorbate 60. *J Control Release.* 2017;254:55-64. doi: S0168-3659(17)30491-1 [pii].
25. Ojeda E, Puras G, Agirre M, et al. The role of helper lipids in the intracellular disposition and transfection efficiency of niosome formulations for gene delivery to

- retinal pigment epithelial cells. *Int J Pharm.* 2016;503(1-2):115-126. doi: 10.1016/j.ijpharm.2016.02.043 [doi].
26. Puras G, Mashal M, Zárate J, et al. A novel cationic niosome formulation for gene delivery to the retina. *J Control Release.* 2014;174:27.
27. Nafissi N, Alqawlaq S, Lee EA, Foldvari M, Spagnuolo PA, Slavcev RA. DNA ministrings: Highly safe and effective gene delivery vectors. *Mol Ther Nucleic Acids.* 2014;3:e165. doi: 10.1038/mtna.2014.16 [doi].
28. Munye MM, Tagalakis AD, Barnes JL, et al. Minicircle DNA provides enhanced and prolonged transgene expression following airway gene transfer. *Sci Rep.* 2016;6:23125. doi: 10.1038/srep23125 [doi].
29. B S, H H, M V, et al. Vaccination with plasmid DNA activates dendritic cells via toll-like receptor 9 (TLR9) but functions in TLR9-deficient mice. *J Immunol.* 2003;171(11):5908.
30. Rodriguez EG. Nonviral DNA vectors for immunization and therapy: Design and methods for their obtention. *J Mol Med (Berl).* 2004;82(8):500-509. doi: 10.1007/s00109-004-0548-x [doi].
31. Mitsui M, Nishikawa M, Zang L, et al. Effect of the content of unmethylated CpG dinucleotides in plasmid DNA on the sustainability of transgene expression. *J Gene Med.* 2009;11(5):435-443. doi: 10.1002/jgm.1317 [doi].
32. Takahashi Y, Nishikawa M, Takakura Y. Development of safe and effective nonviral gene therapy by eliminating CpG motifs from plasmid DNA vector. *Front Biosci (Schol Ed).* 2012;4:133-141. doi: 256 [pii].
33. Riu E, Chen ZY, Xu H, He CY, Kay MA. Histone modifications are associated with the persistence or silencing of vector-mediated transgene expression in vivo. *Mol Ther.* 2007;15(7):1348-1355. doi: S1525-0016(16)32422-4 [pii].
34. HS W, ZJ C, G Z, et al. A novel micro-linear vector for in vitro and in vivo gene delivery and its application for EBV positive tumors. *PLoS One.* 2012;7(10):e47159.
35. De Laporte L, Shea LD. Matrices and scaffolds for DNA delivery in tissue engineering. *Adv Drug Deliv Rev.* 2007;59(4-5):292-307. doi: S0169-409X(07)00029-4 [pii].
36. Krebs MD, Jeon O, Alsberg E. Localized and sustained delivery of silencing RNA from macroscopic biopolymer hydrogels. *J Am Chem Soc.* 2009;131(26):9204-9206. doi: 10.1021/ja9037615 [doi].
37. Puras G, Zarate J, Aceves M, et al. Low molecular weight oligochitosans for non-viral retinal gene therapy. *Eur J Pharm Biopharm.* 2013;83(2):131-140. doi: 10.1016/j.ejpb.2012.09.010 [doi].

38. Puras G, Zarate J, Diaz-Tahoces A, Aviles-Trigueros M, Fernandez E, Pedraz JL. Oligochitosan polyplexes as carriers for retinal gene delivery. *Eur J Pharm Sci.* 2013;48(1-2):323-331. doi: 10.1016/j.ejps.2012.11.009 [doi].
39. Ojeda E, Puras G, Agirre M, et al. The influence of the polar head-group of synthetic cationic lipids on the transfection efficiency mediated by niosomes in rat retina and brain. *Biomaterials.* 2016;77:267-279. doi: 10.1016/j.biomaterials.2015.11.017 [doi].
40. Ruiz de Almodovar C, Lambrechts D, Mazzone M, Carmeliet P. Role and therapeutic potential of VEGF in the nervous system. *Physiol Rev.* 2009;89(2):607-648. doi: 10.1152/physrev.00031.2008 [doi].
41. Fournier NM, Lee B, Banasr M, Elsayed M, Duman RS. Vascular endothelial growth factor regulates adult hippocampal cell proliferation through MEK/ERK- and PI3K/akt-dependent signaling. *Neuropharmacology.* 2012;63(4):642-652. doi: 10.1016/j.neuropharm.2012.04.033 [doi].
42. Herran E, Perez-Gonzalez R, Igartua M, Pedraz JL, Carro E, Hernandez RM. VEGF-releasing biodegradable nanospheres administered by craniotomy: A novel therapeutic approach in the APP/Ps1 mouse model of alzheimer's disease. *J Control Release.* 2013;170(1):111-119. doi: 10.1016/j.jconrel.2013.04.028 [doi].
43. Carmeliet P, Ruiz de Almodovar C. VEGF ligands and receptors: Implications in neurodevelopment and neurodegeneration. *Cell Mol Life Sci.* 2013;70(10):1763-1778. doi: 10.1007/s00018-013-1283-7 [doi].
44. Bivas-Benita M, Romeijn S, Junginger HE, Borchard G. PLGA-PEI nanoparticles for gene delivery to pulmonary epithelium. *Eur J Pharm Biopharm.* 2004;58(1):1-6. doi: 10.1016/j.ejpb.2004.03.008 [doi].
45. Hosseinkhani H, Tabata Y. Self assembly of DNA nanoparticles with polycations for the delivery of genetic materials into cells. *J Nanosci Nanotechnol.* 2006;6(8):2320-2328.
46. Caracciolo G, Amenitsch H. Cationic liposome/DNA complexes: From structure to interactions with cellular membranes. *Eur Biophys J.* 2012;41(10):815-829. doi: 10.1007/s00249-012-0830-8 [doi].
47. Reed BE, Grainger RG, Peters DM, Smith AJ. Retrieving the real refractive index of mono- and polydisperse colloids from reflectance near the critical angle. *Opt Express.* 2016;24(3):1953-1972. doi: 10.1364/OE.24.001953 [doi].
48. Alatorre-Meda M, Taboada P, Hartl F, Wagner T, Freis M, Rodriguez JR. The influence of chitosan valence on the complexation and transfection of DNA: The weaker the DNA-chitosan binding the higher the transfection efficiency. *Colloids Surf B Biointerfaces.* 2011;82(1):54-62. doi: 10.1016/j.colsurfb.2010.08.013 [doi].

49. Ojeda E, Puras G, Agirre M, et al. Niosomes based on synthetic cationic lipids for gene delivery: The influence of polar head-groups on the transfection efficiency in HEK-293, ARPE-19 and MSC-D1 cells. *Org Biomol Chem*. 2015;13(4):1068-1081. doi: 10.1039/c4ob02087a [doi].
50. Fussenegger M, Moser S, Bailey JE. pQuattro vectors allow one-step multigene metabolic engineering and auto-selection of quattrocistronic artificial mammalian operons. *Cytotechnology*. 1998;28(1-3):229-235. doi: 10.1023/A:1008014706196 [doi].
51. Allera-Moreau C, Delluc-Clavieres A, Castano C, et al. Long term expression of bicistronic vector driven by the FGF-1 IRES in mouse muscle. *BMC Biotechnol*. 2007;7:74. doi: 1472-6750-7-74 [pii].
52. Ngoi SM, Chien AC, Lee CG. Exploiting internal ribosome entry sites in gene therapy vector design. *Curr Gene Ther*. 2004;4(1):15-31.
53. Renaud-Gabardos E, Hantelys F, Morfoisse F, Chaufour X, Garmy-Susini B, Prats AC. Internal ribosome entry site-based vectors for combined gene therapy. *World J Exp Med*. 2015;5(1):11-20. doi: 10.5493/wjem.v5.i1.11 [doi].
54. Jopling CL, Willis AE. N-myc translation is initiated via an internal ribosome entry segment that displays enhanced activity in neuronal cells. *Oncogene*. 2001;20(21):2664-2670. doi: 10.1038/sj.onc.1204404 [doi].
55. Egervari K, Potter G, Guzman-Hernandez ML, et al. Astrocytes spatially restrict VEGF signaling by polarized secretion and incorporation of VEGF into the actively assembling extracellular matrix. *Glia*. 2016;64(3):440-456. doi: 10.1002/glia.22939 [doi].
56. Du J, Gao X, Deng L, Chang N, Xiong H, Zheng Y. Transfection of the glial cell line-derived neurotrophic factor gene promotes neuronal differentiation. *Neural Regen Res*. 2014;9(1):33-40. doi: 10.4103/1673-5374.125327 [doi].
57. Herran E, Ruiz-Ortega JA, Aristieta A, et al. In vivo administration of VEGF- and GDNF-releasing biodegradable polymeric microspheres in a severe lesion model of parkinson's disease. *Eur J Pharm Biopharm*. 2013;85(3 Pt B):1183-1190. doi: 10.1016/j.ejpb.2013.03.034 [doi].
58. Bai Y, Leng Y, Yin G, et al. Effects of combinations of BMP-2 with FGF-2 and/or VEGF on HUVECs angiogenesis in vitro and CAM angiogenesis in vivo. *Cell Tissue Res*. 2014;356(1):109-121. doi: 10.1007/s00441-013-1781-9 [doi].
59. Herran E, Perez-Gonzalez R, Igartua M, Pedraz JL, Carro E, Hernandez RM. Enhanced hippocampal neurogenesis in APP/Ps1 mouse model of alzheimer's disease after implantation of VEGF-loaded PLGA nanospheres. *Curr Alzheimer Res*. 2015;12(10):932-940. doi: CAR-EPUB-71312 [pii].

60. BT H, AE A, L P, O S, MJ C, BL W. Intranasal administration of plasmid DNA nanoparticles yields successful transfection and expression of a reporter protein in rat brain. *Gene Ther.* 2014;21(5):514.
61. Koirala A, Conley S, Naash M. A review of therapeutic prospects of non-viral gene therapy in the retinal pigment epithelium. *Biomaterials.* 2013;34(29):7158.
62. Strauss O. The retinal pigment epithelium in visual function. *Physiol Rev.* 2005;85(3):845-881. doi: 85/3/845 [pii].
63. Ojeda E, Agirre M, Villate-Beitia I, et al. Elaboration and physicochemical characterization of niosome-based nioplexes for gene delivery purposes. *Methods Mol Biol.* 2016;1445:63-75. doi: 10.1007/978-1-4939-3718-9\_5 [doi].
64. Moghassemi S, Hadjizadeh A. Nano-niosomes as nanoscale drug delivery systems: An illustrated review. *J Control Release.* 2014;185:22-36. doi: 10.1016/j.jconrel.2014.04.015 [doi].
65. Andar AU, Hood RR, Vreeland WN, Devoe DL, Swaan PW. Microfluidic preparation of liposomes to determine particle size influence on cellular uptake mechanisms. *Pharm Res.* 2014;31(2):401-413. doi: 10.1007/s11095-013-1171-8 [doi].
66. Paecharoenchai O, Niyomtham N, Ngawhirunpat T, Rojanarata T, Yingyongnarongkul BE, Opanasopit P. Cationic niosomes composed of spermine-based cationic lipids mediate high gene transfection efficiency. *J Drug Target.* 2012;20(9):783-792. doi: 10.3109/1061186X.2012.716846 [doi].
67. Shao XR, Wei XQ, Song X, et al. Independent effect of polymeric nanoparticle zeta potential/surface charge, on their cytotoxicity and affinity to cells. *Cell Prolif.* 2015;48(4):465-474. doi: 10.1111/cpr.12192 [doi].
68. Kachi S, Oshima Y, Esumi N, et al. Nonviral ocular gene transfer. *Gene Ther.* 2005;12(10):843-851. doi: 3302475 [pii].
69. Huang YZ, Gao JQ, Chen JL, Liang WQ. Cationic liposomes modified with non-ionic surfactants as effective non-viral carrier for gene transfer. *Colloids Surf B Biointerfaces.* 2006;49(2):158-164. doi: S0927-7765(06)00082-8 [pii].
70. Huang Y, Rao Y, Chen J, Yang VC, Liang W. Polysorbate cationic synthetic vesicle for gene delivery. *J Biomed Mater Res A.* 2011;96(3):513-519. doi: 10.1002/jbm.a.32999 [doi].
71. Rejman J, Oberle V, Zuhorn IS, Hoekstra D. Size-dependent internalization of particles via the pathways of clathrin- and caveolae-mediated endocytosis. *Biochem J.* 2004;377(Pt 1):159-169. doi: 10.1042/BJ20031253 [doi].
72. Nichols B. Caveosomes and endocytosis of lipid rafts. *J Cell Sci.* 2003;116(Pt 23):4707-4714. doi: 10.1242/jcs.00840 [doi].

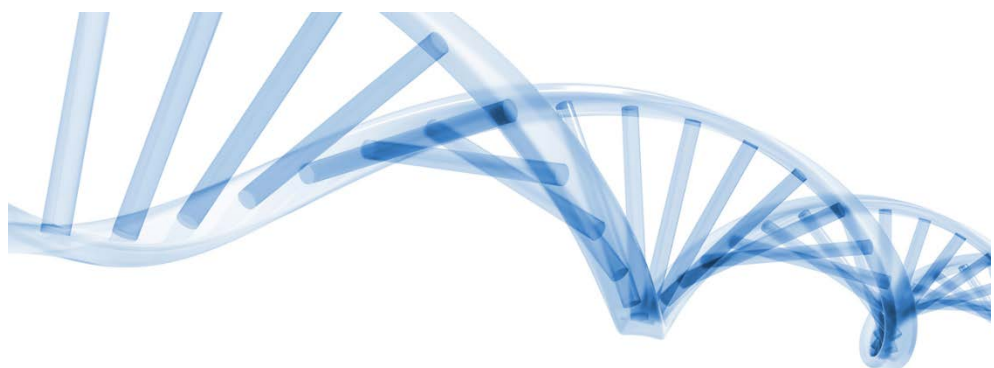
73. Luzio JP, Parkinson MD, Gray SR, Bright NA. The delivery of endocytosed cargo to lysosomes. *Biochem Soc Trans.* 2009;37(Pt 5):1019-1021. doi: 10.1042/BST0371019 [doi].
74. Kiss AL, Botos E. Endocytosis via caveolae: Alternative pathway with distinct cellular compartments to avoid lysosomal degradation? *J Cell Mol Med.* 2009;13(7):1228-1237. doi: 10.1111/j.1582-4934.2009.00754.x [doi].
75. Agirre M, Ojeda E, Zarate J, et al. New insights into gene delivery to human neuronal precursor NT2 cells: A comparative study between lipoplexes, nioplexes, and polyplexes. *Mol Pharm.* 2015;12(11):4056-4066. doi: 10.1021/acs.molpharmaceut.5b00496 [doi].
76. Villate-Beitia I, Puras G, Zarate J, Agirre M, Ojeda E, Pedraz JL. First insights into non-invasive administration routes for non-viral gene therapy. In: D. Hashad, ed. *Gene therapy – principles and challenges*. Croatia: InTech; 2015:145.
77. Delgado D, del Pozo-Rodriguez A, Solinis MA, Rodriguez-Gascon A. Understanding the mechanism of protamine in solid lipid nanoparticle-based lipofection: The importance of the entry pathway. *Eur J Pharm Biopharm.* 2011;79(3):495-502. doi: 10.1016/j.ejpb.2011.06.005 [doi].
78. Khalil IA, Kogure K, Akita H, Harashima H. Uptake pathways and subsequent intracellular trafficking in nonviral gene delivery. *Pharmacol Rev.* 2006;58(1):32-45. doi: 58/1/32 [pii].
79. Farjo R, Skaggs J, Quiambao AB, Cooper MJ, Naash MI. Efficient non-viral ocular gene transfer with compacted DNA nanoparticles. *PLoS One.* 2006;1:e38. doi: 10.1371/journal.pone.0000038 [doi].
80. Adijanto J, Naash MI. Nanoparticle-based technologies for retinal gene therapy. *Eur J Pharm Biopharm.* 2015;95(Pt B):353-367. doi: 10.1016/j.ejpb.2014.12.028 [doi].
81. Lajunen T, Hisazumi K, Kanazawa T, et al. Topical drug delivery to retinal pigment epithelium with microfluidizer produced small liposomes. *Eur J Pharm Sci.* 2014;62:23-32. doi: 10.1016/j.ejps.2014.04.018 [doi].
82. Pringle IA, Hyde SC, Connolly MM, et al. CpG-free plasmid expression cassettes for cystic fibrosis gene therapy. *Biomaterials.* 2012;33(28):6833-6842. doi: 10.1016/j.biomaterials.2012.06.009 [doi].
83. Gill DR, Smyth SE, Goddard CA, et al. Increased persistence of lung gene expression using plasmids containing the ubiquitin C or elongation factor 1alpha promoter. *Gene Ther.* 2001;8(20):1539-1546. doi: 10.1038/sj.gt.3301561 [doi].
84. Lesina E, Dames P, Flemmer A, et al. CpG-free plasmid DNA prevents deterioration of pulmonary function in mice. *Eur J Pharm Biopharm.* 2010;74(3):427-434. doi: 10.1016/j.ejpb.2009.11.013 [doi].

85. Lesina E, Dames P, Rudolph C. The effect of CpG motifs on gene expression and clearance kinetics of aerosol administered polyethylenimine (PEI)-plasmid DNA complexes in the lung. *J Control Release*. 2010;143(2):243-250. doi: 10.1016/j.jconrel.2010.01.003 [doi].
86. Hyde SC, Pringle IA, Abdullah S, et al. CpG-free plasmids confer reduced inflammation and sustained pulmonary gene expression. *Nat Biotechnol*. 2008;26(5):549-551. doi: 10.1038/nbt1399 [doi].
87. Ahmad-Nejad P, Hacker H, Rutz M, Bauer S, Vabulas RM, Wagner H. Bacterial CpG-DNA and lipopolysaccharides activate toll-like receptors at distinct cellular compartments. *Eur J Immunol*. 2002;32(7):1958-1968. doi: 10.1002/1521-4141(200207)32:73.0.CO;2-U [doi].
88. Gracey Maniar LE, Maniar JM, Chen ZY, Lu J, Fire AZ, Kay MA. Minicircle DNA vectors achieve sustained expression reflected by active chromatin and transcriptional level. *Mol Ther*. 2013;21(1):131-138. doi: 10.1038/mt.2012.244 [doi].
89. Liu N, Wang BJ, Broughton KM, et al. PIM1-minicircle as a therapeutic treatment for myocardial infarction. *PLoS One*. 2017;12(3):e0173963. doi: 10.1371/journal.pone.0173963 [doi].
90. Tidd N, Michelsen J, Hilbert B, Quinn JC. Minicircle mediated gene delivery to canine and equine mesenchymal stem cells. *Int J Mol Sci*. 2017;18(4):10.3390/ijms18040819. doi: E819 [pii].
91. Gaspar V, de Melo-Diogo D, Costa E, et al. Minicircle DNA vectors for gene therapy: Advances and applications. *Expert Opin Biol Ther*. 2015;15(3):353-379. doi: 10.1517/14712598.2015.996544 [doi].
92. Fernandes AR CD. Part I: Minicircle vector technology limits DNA size restrictions on ex vivo gene delivery using nanoparticle vectors: Overcoming a translational barrier in neural stem cell therapy. *J Control Release*. 2016;28:238.
93. Chen ZY, He CY, Ehrhardt A, Kay MA. Minicircle DNA vectors devoid of bacterial DNA result in persistent and high-level transgene expression in vivo. *Mol Ther*. 2003;8(3):495-500. doi: S1525-0016(03)00168-0 [pii].
94. Osborn MJ, McElmurry RT, Lees CJ, et al. Minicircle DNA-based gene therapy coupled with immune modulation permits long-term expression of alpha-L-iduronidase in mice with mucopolysaccharidosis type I. *Mol Ther*. 2011;19(3):450-460. doi: 10.1038/mt.2010.249 [doi].
95. Viecelli HM, Harbottle RP, Wong SP, et al. Treatment of phenylketonuria using minicircle-based naked-DNA gene transfer to murine liver. *Hepatology*. 2014;60(3):1035-1043. doi: 10.1002/hep.27104 [doi].

96. Huang M, Chen Z, Hu S, et al. Novel minicircle vector for gene therapy in murine myocardial infarction. *Circulation*. 2009;120(11 Suppl):S230-7. doi: 10.1161/CIRCULATIONAHA.108.841155 [doi].
97. Stenler S, Andersson A, Simonson OE, et al. Gene transfer to mouse heart and skeletal muscles using a minicircle expressing human vascular endothelial growth factor. *J Cardiovasc Pharmacol*. 2009;53(1):18-23. doi: 10.1097/FJC.0b013e318194234e [doi].
98. Gratton SE, Ropp PA, Pohlhaus PD, et al. The effect of particle design on cellular internalization pathways. *Proc Natl Acad Sci U S A*. 2008;105(33):11613-11618. doi: 10.1073/pnas.0801763105 [doi].
99. Jacobs C, Kayser O, Muller RH. Nanosuspensions as a new approach for the formulation for the poorly soluble drug tarazepide. *Int J Pharm*. 2000;196(2):161-164. doi: S0378517399004123 [pii].
100. P K, B C, R R, et al. Plasmid DNA size does not affect the physicochemical properties of lipoplexes but modulates gene transfer efficiency. *Nucleic Acids Res*. 1991;27(19):3792.
101. Klausner E, Zhang Z, Wong S, Chapman R, Volin M, Harbottle RP. Corneal gene delivery: Chitosan oligomer as a carrier of CpG rich, CpG free or S/MAR plasmid DNA. *J Gene Med*. 2012;14(2):100.
102. Rezvani Amin Z, Rahimizadeh M, Eshghi H, Dehshahri A, Ramezani M. The effect of cationic charge density change on transfection efficiency of polyethylenimine. *Iran J Basic Med Sci*. 2013;16(2):150-156.
103. Conley SM, Naash MI. Nanoparticles for retinal gene therapy. *Prog Retin Eye Res*. 2010;29(5):376-397. doi: 10.1016/j.preteyeres.2010.04.004 [doi].
104. Almasieh M, Wilson AM, Morquette B, Cueva Vargas JL, Di Polo A. The molecular basis of retinal ganglion cell death in glaucoma. *Prog Retin Eye Res*. 2012;31(2):152-181. doi: 10.1016/j.preteyeres.2011.11.002 [doi].
105. Fraser JR, Laurent TC, Laurent UB. Hyaluronan: Its nature, distribution, functions and turnover. *J Intern Med*. 1997;242(1):27-33.
106. Baier Leach J, Bivens KA, Patrick CW,Jr, Schmidt CE. Photocrosslinked hyaluronic acid hydrogels: Natural, biodegradable tissue engineering scaffolds. *Biotechnol Bioeng*. 2003;82(5):578-589. doi: 10.1002/bit.10605 [doi].
107. Bhattacharai N, Gunn J, Zhang M. Chitosan-based hydrogels for controlled, localized drug delivery. *Adv Drug Deliv Rev*. 2010;62(1):83-99. doi: 10.1016/j.addr.2009.07.019 [doi].
108. Tokatlian T, Cam C, Segura T. Non-viral DNA delivery from porous hyaluronic acid hydrogels in mice. *Biomaterials*. 2014;35(2):825-835. doi: S0142-9612(13)01225-8 [pii].

109. Lei Y, Huang S, Sharif-Kashani P, Chen Y, Kavehpour P, Segura T. Incorporation of active DNA/cationic polymer polyplexes into hydrogel scaffolds. *Biomaterials*. 2010;31(34):9106-9116. doi: 10.1016/j.biomaterials.2010.08.016 [doi].
110. Taranejoo S, Chandrasekaran R, Cheng W, Hourigan K. Bioreducible PEI-functionalized glycol chitosan: A novel gene vector with reduced cytotoxicity and improved transfection efficiency. *Carbohydr Polym*. 2016;153:160.
111. Truong N, Segura T. Sustained transgene expression via hydrogel-mediated gene transfer results from multiple transfection events. *ACS Biomater. Sci. Eng.* 2018;4(3):981.
112. Monti D, Burgalassi S, Rossato MS, et al. Poloxamer 407 microspheres for orotransmucosal drug delivery. part II: In vitro/in vivo evaluation. *Int J Pharm.* 2010;400(1-2):32-36. doi: 10.1016/j.ijpharm.2010.08.018 [doi].
113. Yang C, Hu T, Cao H, et al. Facile construction of chloroquine containing PLGA-based pDNA delivery system for efficient tumor and pancreatitis targeting in vitro and in vivo. *Mol Pharm.* 2015;12(6):2167-2179. doi: 10.1021/acs.molpharmaceut.5b00155 [doi].
114. Moshayedi P, Nih LR, Llorente IL, et al. Systematic optimization of an engineered hydrogel allows for selective control of human neural stem cell survival and differentiation after transplantation in the stroke brain. *Biomaterials*. 2016;105:145-155. doi: 10.1016/j.biomaterials.2016.07.028 [doi].
115. Shepard JA, Huang A, Shikanov A, Shea LD. Balancing cell migration with matrix degradation enhances gene delivery to cells cultured three-dimensionally within hydrogels. *J Control Release*. 2010;146(1):128-135. doi: 10.1016/j.jconrel.2010.04.032 [doi].
116. Lei Y, Gojgini S, Lam J, Segura T. The spreading, migration and proliferation of mouse mesenchymal stem cells cultured inside hyaluronic acid hydrogels. *Biomaterials*. 2011;32(1):39-47. doi: 10.1016/j.biomaterials.2010.08.103 [doi].
117. Gojgini S, Tokatlian T, Segura T. Utilizing cell-matrix interactions to modulate gene transfer to stem cells inside hyaluronic acid hydrogels. *Mol Pharm.* 2011;8(5):1582-1591. doi: 10.1021/mp200171d [doi].





***Conclusions***

***Ondorioak***

***Conclusiones***



### *Conclusions*

1. The three different commercial non-viral vectors based on cationic lipids, polymers and magnetic nanoparticles presented similar physicochemical characteristics and ability to condense and protect plasmid DNA. Although the three were able to transfect central nervous system cells and the VEGF produced by transfected cells was active in all cases, magnetoplexes presented the highest transfection efficiencies in terms of both EGFP expression and VEGF production.
2. The evaluation of niosome formulations that only differed in the non-ionic tensioactive component showed that the incorporation of polysorbate 20 enhanced retinal gene delivery both *in vitro* and *in vivo* at the low cationic lipid/DNA mass ratio 2/1. The different chemical structures and HLB values of polysorbates 20, 80 and 85 seem to determine the ability of nioplexes to enter the cells, follow a particular endocytic pathway and deliver the DNA cargo into the nucleus. *In vivo*, targeted cells strongly depended on the administration route. Subretinal injection transfected the inner layers of the retina and showed clear diffusion to outer layers including the retinal pigment epithelium, while intravitreal injection transfected predominantly the ganglion cell layer.
3. The comparative study between different genetic material in nioplexes, varying in terms of size and composition, revealed that formulations containing different types of DNA molecules maintained similar physicochemical characteristics but differed in transfection efficiency. Niosomes carrying minicircle DNA were more efficient than the ones carrying DNA plasmids for retinal transfection both *in vitro* and *in vivo*, regardless of the administration route.
4. The investigation of new combinations between delivery systems and tissue-engineered scaffolds demonstrated that niosome formulations composed of 2,3-di(tetradecyloxy)propan-1-amine, Poloxamer 407, polysorbate 80 and chloroquine diphosphate salt can be successfully incorporated into hyaluronic acid hydrogels for non-viral gene delivery. Hyaluronic acid hydrogel scaffolds loaded with nioplexes presented suitable mechanical properties, little or no particle aggregation, allowed for extensive cell spreading and were able to efficiently transfect encapsulated mMSCs in 3D cultures.



### *Ondorioak*

1. Hiru bektore ez-biral komertzialek –lipoplexoak, poliplexoak eta magnetoplexoak- ezaugarri fisiko-kimiko antzekoak eta DNA eusteko, babesteko eta askatzeko pareko gaitasuna erakutsi zituzten. Gainera, hiru formulazioak gai izan ziren nerbio sistema zentraleko zeluletan VEGF genea garraiatzeko eta genea jasotako zelulek ekoiztutako VEGF proteinak aktibitate biologikoa zuela baieztago zen. Hala ere, magnetoplexoak izan ziren transfekzio-maila altuenak lortu zituzten bektore ez-biralak, bai EGFP espresioari eta baita VEGF proteinaren ekoizpenari dagokionean ere.
2. Niosoma formulazioetako tentsoaktibo ez-ionikoek transfekzio prozesuan jokatzen duten paperaren ebaluazioan ikusi zenez, Tween 20 zeramaten formulazioekin lortu ziren transfekzio-mailarik altuenak erretinako zeluletan *in vitro* zein *in vivo*. Dirudinez, surfaktante ez-ionikoen ezaugarri kimiko eta HLB balio ezberdinek nioplexoien zelulan sartzeko eta zelulaz barneko bide bat edo bestea jarraitzeko gaitasunean eragiten dute eta horrek guztiak, aldi berean, formulazioaren transfekzio efizientzian eragiten du. *In vivo* entseguetan ikusi zenez, eman-bidearen arabera erretinako zelula-geruza ezberdinetara iristea lortzen da. Erretina-azpiko injekzioaren bitartez, epitelio pigmentarioko zelulak transfektatzea lortu zen. Aldiz, bitreo-barneko injekzioaren bitartez, batez ere zelula ganglionarren geruzaraino iritsi ziren nioplexoak.
3. Tamaina eta konposizio ezberdineko material genetikoa zeramaten niosomek ezaugarri fisiko-kimiko antzekoak baina transfekzio-efizientzia ezberdinak aurkeztu zituzten. *Minicircle* DNA molekulak zeramatzenen niosoma formulazioen transfekzio-maila plasmidoak zeramatzenen bikoitza izan zen erretinako zeluletan bai *in vitro* eta baita *in vivo* ere. Beraz, tamaina txikiko eta bakteria-sekuentziarik gabeko material genetikoa erabiltzeak transfekzio eraginkortasuna hobetzen du.
4. Gene-garraiorako sistema ez-biralen eta ehun-injeniaritzaren arteko konbinaketa berrien bilaketari dagokionez, niosoma formulazioak eta azido hialuroniko hidrogelak bateragarriak direla erakutsi dugu. Lortutako emaitzetan ikusi zenez, azido hialuroniko hidrogeletan ez zegoen nioplexoren arteko agregaziorik, zelulak azalera guztian zehar hedatu ziren eta, gainera, transfekzio-maila altuak lortu ziren 3D zelula kultiboetan biziraupena kaltetu gabe.



### *Conclusiones*

1. Los tres vectores no-virales comerciales basados en lípidos catiónicos, polímeros y nanopartículas magnéticas presentaron características físico-químicas y habilidades para condensar y proteger ADN similares. A pesar de que los tres fueron capaces de transfectar células del sistema nervioso central y de que la proteína VEGF producida por las células transfectadas mantenía su actividad biológica en todos los casos, la mayor eficiencia de transfección se obtuvo con los magnetoplexos tanto en cuanto a expresión de la proteína GFP como de la proteína VEGF.
2. La evaluación de las formulaciones de niosomas que sólo diferían en su tensioactivo no-iónico reveló que la incorporación del polisorbato 20 mejora la transferencia génica en retina tanto *in vitro* como *in vivo*. Las diferencias en la estructura y valores de HLB del tensioactivo parecen determinar la habilidad de los niosomas para penetrar en las células, seguir una ruta endocítica particular y liberar el ADN en el núcleo. *In vivo*, el tipo de células transfectadas dependió de la ruta de administración, ya que a través de inyecciones intravítreas se transfectaron predominantemente células de la capa ganglionar de la retina, mientras que con las inyecciones subretinianas se pudo llegar hasta el epitelio pigmentario de la retina.
3. El estudio comparativo de los distintos tipos de material genético demostró que las características físico-químicas no variaban entre los nioplexos unidos a distintos tipos de ADN, mientras que sí se observaron diferencias significativas en cuanto a la capacidad de transfección. Las formulaciones de nioplexos que vehiculizaban material genético en forma de *minicircle* demostraron obtener mayor eficiencia de transfección que los que vehiculizaban plásmidos tanto *in vitro* como *in vivo* en células de la retina.
4. La investigación de nuevas combinaciones entre vectores no-virales e hidrogeles de ácido hialurónico concluyeron que los niosomas pueden ser incorporados de forma eficaz y sin formar agregados en geles de ácido hialurónico, y fueron liberados de manera progresiva. Además, las células fueron capaces de difundir libremente en los hidrogeles cargados con nioplexos y se obtuvo alta eficacia de transfección en cultivos 3D con excelente viabilidad celular.

